Assessment of Blended Waste Rock Material at Zinifex Century Mine

Consequences for Acid Drainage Generation

Thesis submitted by

Laura Maree McIlwaine

in February 2007

for the degree of

Master of Science

in the

Department of Chemistry,

School of Pharmacy and Molecular Sciences,

James Cook University

STATEMENT OF ACCESS

I, the undersigned author of this work, understand that James Cook University will make this thesis available for use within the University Library and, via the Australian Digital Theses network, for use elsewhere.

I understand that, as an unpublished work, a thesis has significant protection under the Copyright Act and;

I do not wish to place any further restriction on access to this work

_____ _____

Signature Date

Statement of Sources

I declare that this thesis is my own work and has not been submitted in any form for another degree or diploma at any university or other institution of tertiary education. Information derived from published or unpublished work of others has been acknowledged in the text and a list of references has been provided.

26 February 2007

Laura Maree McIlwaine **Date**

Acknowledgements

I would firstly like to thank Zinifex Century Mine Limited (ZCML) for financing this project and providing me with such a fantastic learning opportunity. Special thanks are extended to the Environmental Team (Greg Scanlan, Gavin Lee, Gaylene Taylor and Glen Ware) for enabling me to complete the project after I ceased employment with ZCML. In particular, thank you for sampling the heap leach pads and for promptly providing data and information where requested.

To the ZCML Engineering and Site Services Department and in particular Hookey Contracting, Rydans Construction and Transfield, Troy Boyles, Ian Lewis, David Neilson and Tim Lane, thank you for your efforts in constructing the heap leach pads and column leach test frame. Chongy – your precision on the backhoe and excavator is exceptional. Any other operator would have punctured the HDPE liner for sure!

To my supervisor, Dr Michael Ridd, thank you for your enthusiasm, passion, professionalism, knowledge and willingness to discuss the project, more often than not, outside work hours so you could fit in with my work schedule. Your assistance, ideas and realistic approach have been more than appreciated.

I'd like to thank the Australian Centre for Tropical Freshwater Research and Advanced Analytical Centre for the high quality of laboratory analysis they performed and the extra effort they often made in collecting samples after I'd been in the laboratory at strange hours. Thank you John Faithfull for your ideas, interest in the project and friendship and thanks to the "girls in the lab" for your friendly faces, helpful natures and putting up with the inundation of samples every week or so.

Thank you very much Dawn Wood for completing the last few sampling runs of the column leach tests after I moved to South Australia in 2005. I would not have been able to make the move without leaving the last of my labwork in your reliable hands. Thanks also for your support, belief and encouragement throughout my project. You are a true friend.

To my previous and current employer, Maunsell Australia and BHP Billiton Olympic Dam, thank you for approving unpaid leave to enable me to complete my project.

Special thanks to my proofreaders – Paul, Sonya and Murray. Your time and suggestions are very much appreciated. Thanks also Rox for your help with formatting and final compilation.

Thank you Scott "my physio" for working out the stiffness in my back, neck and wrist that was brought on by too much computer work and thanks to the Roxby Downs Leisure Centre for providing an outlet for me to stay sane during my write up!

Thank you Graeme Hawes for introducing me to the fascinating world of acid rock drainage when I was a 19 year old vacation student at the (then) Pasminco Rosebery Mine in Western Tasmania. You showed me the ARD legacy of past mining operations and sparked my desire to understand the problem to enable me to one day help manage and treat ARD and prevent similar stories from being re-told.

To my family for always being there and to my friends – near and far – for their support, belief and "study break" emails and phone calls. I am fortunate to have such a strong support network.

And lastly, thank you Paul. You weren't around when I started my MSc, but I can't even imagine how the finish would have been without you around. Thanks for putting up with my mess, late nights, neglect, unsociability and inability to even watch your cricket games. The ongoing support you have shown me throughout this project, particularly the write-up stage, has been next to none. Thank you.

Abstract

There is little doubt that acid rock drainage (ARD) is the largest and most testing long-term environmental issue facing the global minerals industry (Lawrence and Day, 1997, Munchenberg, 1998, Olson et al. 2006). The aim of this study was to assess leachate quality from different blends of waste rock at Zinifex Century Mine and determine consequences for acid drainage generation. This thesis describes the results of research undertaken to predict the risk of ARD associated with a possible change to waste rock disposal practices at the Zinifex Century Mine.

Zinifex Century Mine Limited (ZCML) comprises a zinc, lead and silver mining and milling operation at Lawn Hill in northwest Queensland, concentrate dewatering and shipping facilities at Karumba in the Gulf of Carpentaria, and a 304km slurry pipeline connecting the two operations. Similar to other mines where sulfide minerals are present, ARD may be generated at the ZCML mine site from exposed pit surfaces, ore stockpiles, removed waste rock and deposited tailings (Bates et al. 2000). To minimise the generation of ARD in the waste rock dumps, waste rock is classified into the following three classes based on competence and acid forming / consuming capabilities:

- **Class 1:** Competent rock, non-acid forming or acid-consuming material.
- **Class 2:** Non-competent, non-acid forming or acid-consuming material
- **Class 3:** Acid-forming material.

The generalised waste rock dump design for current operations comprises an outer zone of class 1 material and inner zone containing class 2 and 3 materials. Cambrian Limestone (CLS), a class 1 material, is used for its structural and acid neutralising capabilities in waste rock dump construction.

Current mine waste rock placement procedures specify that class 1 rock with greater than 5% contamination of class 3 material is to be placed within the inner zone of the waste rock dumps due to uncertainty surrounding the long-term acid producing capabilities of this rock. This procedure, as well as additional restrictions on waste rock dump design, has the potential to cause significant scheduling problems due to the limited reserve of class 1 rock available for waste rock dump rehabilitation. This is particularly the case in the latter stages of the mine life following movement of most of the waste rock to access the ore.

Due to finite reserves of CLS material and the need to develop strategies to maximise the beneficial use of available limestone reserves, as well as the belief by mine personnel that the abovementioned contamination percentage may be conservative, this project was commissioned to enable the leachate from different blends of waste rock to be assessed. The objectives of the study were to:

- Quantify blending levels of acid consuming (Cambrian Limestone) and acid forming (Hanging Wall Siltstone (HWD)) rock that will produce pH neutral leachate low in metal and salt concentrations;
- Determine the validity of current waste rock placement procedures;
- Investigate the influence of particle size on leachate quality; and
- Attempt to establish links between results from various ARD prediction tests.

Various static (acid base accounting, net acid generation tests, acid buffering characteristic curves and cyclic voltammetry) and kinetic (column leach tests (CLTs) and heap leach pads (HLPs)) ARD prediction tests were conducted on blended waste rock material from ZCML. Twenty CLTs, representing five lithology blends and three particle size distributions were assembled in a laboratory environment. Five replicate CLTs were established. Three HLPs representing three lithology blends were constructed from run of mine material at ZCML. The CLTs and HLPs were periodically watered to simulate rainfall events. In addition, the HLPs were exposed to wet season rainfall events. Results from the static and kinetic tests were compared to address the issue of scale-up.

Findings from the study were:

- Static tests conducted on blended CLS and HWD samples classified each sample as non acid forming (NAF). Results from kinetic testwork confirmed this finding, indicating that limestone blending may be effective in controlling the pH of leachate generated from waste rock, however elevated sulfate concentrations in leachate would ensue.
- Results obtained from the column leach tests were repeatable.
- Sulfate production rates were equivalent to neutralising potential depletion rates in most CLTs and HLPs. This confirmed neutralisation of the sulfuric acid produced by pyrite oxidation by calcium and magnesium carbonates.
- The calculated time to NP depletion exceeded the time to sulfide depletion in all CLTs and HLPs, however these times were misleading for columns containing armoured CLS material.
- Despite first flush events, total metal concentrations in CLT and HLP leachate generally complied with maximum limits specified in Environmental Authority No. MIM800020402 (Ecoaccess, 2004).
- Dissolved zinc concentrations were significantly greater in CLT samples with low pH values, however were not as high as thermodynamically predicted using the geochemical modelling program MINTEQA2. Dissolved zinc concentrations in HLP leachate were also not as high as thermodynamically predicted at pH values less than 7.8. This was due to the control of dissolved zinc concentrations by the rate of sphalerite oxidation at low pH values and the solubility of $Zn(OH)_2$ at high pH values.
- Dissolved lead concentrations in CLT and HLP samples were extremely small or undetectable (i.e. less than 4.8×10^{-4} µmol L^{-1}) and less than those thermodynamically predicted using MINTEQA2 due to low oxidation rates of galena resulting from surface passivation at lower pH values, and $Pb(OH)_2$ solubility controlling Pb^{2+} concentrations at neutral-alkaline pH values.
- Median dissolved zinc and copper production rates were comparable between the CLTs and HLPs, however rates were greater in the HLPs during large wet season flushes.
- Geochemical modelling confirmed the absence of gypsum precipitation in the CLT comprising the most reactive waste rock blend and smallest particle size distribution and confirmed gypsum

precipitation in HLP2 and HLP3. Sulfate production, neutralising potential depletion and oxygen consumption rates were therefore underestimated in these HLPs.

The main conclusions of the study were:

(1) Results from CLTs comprising smaller particle size distributions were most comparable with results from the HLPs. Anomalous behaviour was observed in CLTs comprising larger particle size distributions.

(2) There was no apparent benefit in leaving the HLPs unwatered for periods of time greater than one week.

(3) Oxygen consumption rates for CLT samples were significantly slower and consequently not directly comparable to those for the HLPs, despite greater flushing of the CLTs.

(4) Blending CLS and HWD material was effective in maintaining neutral pH values and regulatory-compliant total metal concentrations in drainage from CLTs and HLPs comprising blends up to 75%CLS / 25%HWD. However, sulfate concentrations in drainage from all blended samples exceeded current regulatory discharge limits.

(5) Visual inspection of material comprising the HLPs after excavation highlighted the presence of armouring layers on HWD material.

(6) The effectiveness of CLS in neutralising sulfuric acid increased with decreasing particle size.

Corresponding recommendations were:

(1) Construct CLTs from particle size distributions passing 10mm as a maximum to best emulate the particle size distributions and residence times in waste rock dumps.

(2) For future HLP testwork at ZCML, or sites of similar climatic conditions, accelerate the rate of pyrite oxidation in the HLPs by watering at weekly intervals on a continual basis in the dry season (i.e. no prolonged drought period).

(3) For future CLT testwork for sites with distinct seasonal variations, locate the CLTs in field conditions on the site under investigation, to ensure samples are exposed to similar ambient temperatures and humidity. Alternatively, where this is not possible, site temperature and humidity conditions should be simulated in a laboratory environment.

(4) To prevent a potential increase in sulfate concentrations in WRD discharge, the current 5% contamination limit of class 3 in class 1 material should not be reduced.

(5) Where there is insufficient CLS material available to cover both the dump surface and batters, priority should be given to the WRD surface, with other non-acid forming competent material used on the batters.

(6) Investigate the reduction in particle size of class 1 material placed within / on the WRDs.

Table of Contents

Abstract i
Table of Contents iv
List of Figures vii
List of Tables x
Glossary / Abbreviations xi
1 Chapter 1: Project Scope and Literature Review 1
1.1 Project Scope 1
1.1.1 Background 1
1.1.2 Project Objectives 2
1.1.3 Project Scope 2
1.1.4 Methodology 3
1.1.5 Thesis Outline 3
1.2 Literature Review 4
1.2.1 Introduction 4
1.2.2 Background to ARD Generation 5
1.2.3 ARD Prediction Techniques 9
1.2.4 Scale-Up 25
1.2.5 Summary 27
2 Chapter 2: Site Description 28
2.1 Introduction 28
2.2 Location and Regional Setting 28
2.3 Geology 29
2.3.1 Regional Geology 29
2.3.2 Ore Deposit Geology 30
2.4 Mining Process Overview 33
2.5 Waste Rock Classification 35
2.6 Waste Rock Dump Design 37
3 Chapter 3: Static Tests 39
3.1 Introduction 39
3.2 Methodology 39
3.2.1 Acid Base Analysis and NAG Testing 39
3.2.2 Cyclic Voltammetry 40
3.3 Results and Discussion 41
3.3.1 Acid-Base Analysis 41
3.3.2 Net Acid Generation Test 44
3.3.3 Acid Buffering Characteristic Curve 46
3.4 Cyclic Voltammetry 46
3.5 Static Testing Summary 47

4 Chapter 4: Column Leach Tests 48
4.1 Introduction 48
4.2 Methodology / Design 48
4.2.1 Design and Construction 48
4.2.2 Sampling, Analysis and Interpretation 50
4.2.3 Column Dismantling 55
4.2.4 Geochemical Modelling 55
4.2.5 Data Presentation 55
4.3 Column Leach Test Results and Discussion 56
4.3.1 Replication of results 56
4.3.2 pH Values 57
4.3.3 Sulfate 60
4.3.4 Metals 73
4.3.5 Column Dismantling 90
4.3.6 Geochemical Modelling of Column Leach Test Leachate 92
4.4 Column Leach Test Summary 94
5 Chapter 5: Heap Leach Pads 96
5.1 Introduction 96
5.2 Methodology / Design 96
5.2.1 Design and Construction 96
5.2.2 Sampling, Analysis and Interpretation 97
5.2.3 Heap Leach Pad Excavation 98
5.2.4 Geochemical Modelling 98
5.2.5 Data Presentation 98
5.3 Heap Leach Pad Results and Discussion 103
5.3.1 pH Values 103
5.3.2 Sulfate 105
5.3.3 Metals 117
5.3.4 Heap Leach Pad Excavation 124
5.3.5 Geochemical Modelling of Heap Leach Pad Leachate 126
5.4 Heap Leach Test Summary 128
6 Chapter 6: Scale-up 130
6.1 Introduction 130
6.2 Methodology 130
6.3 Results 131
6.3.1 pH Values 131
6.3.2 Sulfate Concentration 132
6.3.3 Oxidation Rate 135
6.3.4 Dissolved Metal Concentrations 137

6.4 Scale-Up Summary 140
7 Chapter 7: Conclusions and Recommendations 142
7.1 ARD Prediction Tests and Scale-up 142
7.1.1 General Findings 142
7.1.2 Conclusions 143
7.1.3 Recommendations 143
7.2 ARD Management at ZCML 144
7.2.1 Conclusions 144
7.2.2 Recommendations 144
7.2.3 Suggested Management Options for Sulfate Concentrations in WRD Drainage 146
8 References 150
9 Appendices 155

List of Figures

Figure 1-1: Schematic Time Dependence of Pollution in Drainage from Mine Wastes (Ritchie, 1995) 10

Figure 2-1: Location of Zinifex Century Mine (Zinifex Century Mine Limited, 2001) 28

Figure 2-2: Mean Monthly Rainfall (Lawn Hill) and Evaporation (Mount Isa) Data (Dames and Moore, 1994) 29

Figure 2-3: Century deposit and major zinc-lead-silver deposits of the Carpentaria Mount Isa zinc belt (Broadbent et al. 2002) 30

Figure 2-4: Mineralised Zone Plan (Dames and Moore, 1994) 31

Figure 2-5: Century Deposit Cross Section A-B (Dames and Moore, 1994) 32

Figure 2-6: Century Deposit Cross Section C-D (Dames and Moore, 1994) 33

Figure 2-7: Zinifex Century Mine Aerial Image July 2005 34

Figure 2-8: ZCML Conceptual Mine Waste Rock Dump Design (Bates et al. 2000) 38

Figure 4-1: Assembling Column Leach Test Filtering System 50

Figure 4-2: Column Leach Test Apparatus 50

Figure 4-3: Column Leach Test Custom Built Frame 52

Figure 4-4: Column Leach Test Replicates 57

Figure 4-5: Column Leach Test pH values 58

Figure 4-6: CLT pH Values: Time Series 58

Figure 4-7: Column Leach Test Sulfate Concentrations: Time Series 61

Figure 4-8: CLT12 Sulfate Concentrations: Time Series 62

Figure 4-9: Column Leach Test Sulfate Concentrations (note different y-axis scales) 63

Figure 4-10: Relationship between %PAF material (x-axis), Particle Size Distribution (y-axis) and Sulfate Concentration (z-axis): All Column Leach Tests (CLTs 12 and 19 excluded) 65

Figure 4-11: Relationship between Conductivity and Sulfate (note difference in y-axis scale) 66

Figure 4-12: CLT Sulfate Production and Neutralising Potential Depletion Rates (CLT12 excluded) 68

Figure 4-13: CLT12 Sulfate and Neutralising Potential Rates: Time Series 68

Figure 4-14: Relationship between Sulfate and (Calcium plus Magnesium) in Leachate (note difference in y-axis scale) 72

Figure 4-15: Relationship between sulfate concentration and the sum of calcium, magnesium and acidity/2 (note difference in y-axis scale) 73

Figure 4-16: Total Metal Concentrations: Column Leach Tests <10mm 75

Figure 4-17: CLT Dissolved Zinc Concentrations (CLTs 12 and 19 Excluded) 78

Figure 4-18: CLT12 and CLT19 Dissolved Zinc Concentrations 78

Figure 4-19: Relationship between pH and zinc (filtered): All Column Leach Tests 79

Figure 4-20: CLT Dissolved Lead Concentrations (CLT 12 Excluded) 80

Figure 4-21: CLT12 Dissolved Lead Concentrations 80
Figure 4-22: Relationship between pH and lead (filtered): All Column Leach Tests..... 81
Figure 4-23: CLT Dissolved Cadmium Concentrations (CLTs 12 and 19 Excluded) 82
Figure 4-24: CLT12 and CLT19 Dissolved Cadmium Concentrations 83
Figure 4-25: CLT Dissolved Copper Concentrations (CLTs 12 excluded) 84
Figure 4-26: CLT12 Dissolved Copper Concentrations..... 84
Figure 4-27: CLT Dissolved Iron Concentrations (CLT12 excluded)..... 86
Figure 4-28: CLT12 Dissolved Iron Concentrations 86
Figure 4-29: CLT Dissolved Aluminium Concentrations (CLTs 12 and 19 excluded) 88
Figure 4-30: CLT12 and CLT19 Dissolved Aluminium Concentrations..... 89
Figure 4-31: CLT12 Dissolved Arsenic Concentrations 89
Figure 4-32: CLT12 Armouring (scale= 300mm)..... 91
Figure 4-33: CLT19 Armouring (scale= 300mm)..... 91
Figure 4-34: CLT8 Contents at Completion of Sampling Period (scale= 300mm) 92
Figure 4-35: K-Jarosite and Gypsum Saturation Indices: CLT8..... 93
Figure 5-1: Heap Leach Pad Cross Section..... 99
Figure 5-2: Heap Leach Pad Plan View 100
Figure 5-3: Heap Leach Pad Layer Details 101
Figure 5-4: Heap Leach Pad Construction..... 102
Figure 5-5: Heap Leach Pad pH Values 104
Figure 5-6: Heap Leach Pad Sulfate Concentrations..... 105
Figure 5-7: Relationship between conductivity and sulfate: All HLPs (HLP3 datapoints marked as solid circles) 106
Figure 5-8: Relationship between (calcium plus magnesium) and sulfate: all Heap Leach Pads (HLP3 datapoints marked as solid circles)..... 107
Figure 5-9: Relationship between Sulfate Load Flushed and Time between Flush Events: all HLPs..... 108
Figure 5-10: HLP Water Inflow and Sulfate Concentration and Load 110
Figure 5-11: HLP Sulfate Production and Neutralising Potential Depletion Rate Profiles. 112
Figure 5-12: HLP Sulfate Production and Neutralising Potential Depletion Rates 113
Figure 5-13: HLP Total Metal Concentrations..... 118
Figure 5-14: HLP Dissolved Zinc Concentrations 120
Figure 5-15: Relationship between pH and dissolved zinc: all HLPs (MINTEQA2 Zinc Solubility Simulation Marked as Solid Circles)..... 120
Figure 5-16: HLP Dissolved Lead Concentrations 121

Figure 5-17: Relationship between pH and dissolved lead: all HLPS (MINTEQA2 Lead Solubility Simulation Marked as Solid Circles) 122
Figure 5-18: HLP Dissolved Metal Concentrations 123
Figure 5-19: HLP3 Excavation 124
Figure 5-20: Comparison of Weathering in HLP 1 (<1%PAF) and HLP3 (>19%PAF) (scale= 300mm) 124
Figure 5-21: HLP3 Excavation (scale= 300mm) 125
Figure 5-22: Iron Hydroxide Staining on CLS material on surface of HLP3 (scale= 300mm) 126
Figure 5-23: Discolouration of HWD at depth in HLP3 (scale= 300mm) 126
Figure 5-24: Gypsum Saturation Index: Heap Leach Pads 126
Figure 5-25: K-jarosite Saturation Index: Heap Leach Pads 127
Figure 6-1: 90% CLS / 10% HWD Blend: pH values 132
Figure 6-2: 80% CLS / 20% HWD Blend: pH values 132
Figure 6-3: 90%CLS / 10% HWD Blend: Sulfate Concentration (HLP data refers on right hand side y-axis) 132
Figure 6-4: 80%CLS / 20% HWD Blend: Sulfate Concentration (HLP data refers on right hand side y-axis) 133
Figure 6-5: HLP and CLT (<10mm) Dissolved Zinc Production Rates 138
Figure 6-6: HLP and CLT (<10mm) Dissolved Copper Production Rates 140

List of Tables

Table 1-1: Acid Consuming Minerals and their Characteristics (adapted from Steffen, Robertson and Kirsten et al. 1989) ... 8

Table 1-2: Static Testing Summary ... 12

Table 1-3: Kinetic Testing Summary ... 18

Table 1-4: Comparison of Processes in Test and Full-Scale Rock Piles (Lawrence and Day, 1997) ... 24

Table 1-5: Factors which may affect the validity of different measurement techniques ... 25

Table 2-1: Waste Rock Geochemical Classification (EGi, 1997a) ... 35

Table 2-2: Waste Rock Distribution Used in Mine Waste Schedule (EGi, 1997a) ... 35

Table 2-3: ZCML Waste Rock Class System (Bates et al. 2000) ... 37

Table 3-1: Acid-forming Characteristics of HWD and CLS Samples (EGi, 2004) ... 42

Table 3-2: Summary of Kinetic NAG Data for 100% Siltstone Size Fractions (EGi, 2004) ... 46

Table 4-1: Composition of Each Column Leach Test ... 49

Table 4-2: Parameters Analysed in CLT Leachate and Corresponding Laboratory Detection Limits ... 53

Table 4-3: Column Leach Test Sulfate Production and Neutralising Potential Depletion Rate Summary ... 69

Table 4-4: Column Leach Test Oxygen Consumption Rates ... 71

Table 4-5: Total Metal Discharge Limits (Ecoaccess, 2004) ... 74

Table 4-6: Dissolved Metal Correlation Matrix ... 76

Table 4-7: Iron Speciation in Column Leach Test Samples collected 31 January 2005 ... 87

Table 5-1: Seasonal Classification of Heap Leach Pad Sampling Periods ... 103

Table 5-2: HLP Sulfate Production and Neutralising Potential Rate Summary (per flush) ... 113

Table 5-3: HLP Sulfate Production, Neutralising Potential Depletion and Oxygen Consumption Rate Summary ... 114

Table 5-4: Concentration Profile During HLP Flow Event on 10 January 2006 ... 116

Table 5-5: Amended HLP Sulfate Production and Neutralising Potential Depletion Rate (per flush) Summary ... 116

Table 6-1: Summary of Comparative Column and Heap Leach Pad Results ... 136

Table 6-2: Oxygen Consumption Rates for HLP1 and CLT1 ... 137

Table 6-3: Median Dissolved Zinc Production Rate for each CLT and HLP ... 139

Table 6-4: Median Dissolved Copper Production Rate for each CLT and HLP ... 139

Table 7-1: Advantages and Disadvantages for ARD Management Options ... 149

Glossary / Abbreviations

Term / Acronym	Description
AAC	Advanced Analytical Centre
ABCC	Acid Buffering Characteristic Curve
AC	Acid Consuming
ACTFR	Australian Centre for Freshwater Tropical Research
Adit	Horizontal or near horizontal passage driven from the surface into the side of a mountain or hill to access mine workings or to dewater the mine (INAP, 1999).
ANC	Acid Neutralising Capacity
AP	Acid Producing
ARD	Acid Rock Drainage
Armouring	The process where acidic solutions, highly concentrated in iron and sulfur, interact with the carbonate-mineral surface forming an insoluble amorphous ferric oxyhydroxide coating on the carbonate mineral surface (Simón et al. 2004).
CANMET	Canadian National Science and Environment Research Council
CBX	Carbonate Breccia
CLS	Cambrian Limestone
CLT	see *Column Leach Test*
Column Leach Test	A *kinetic test* designed to simulate the leaching and secondary mineral precipitation and dissolution that determine drainage chemistry (INAP, 1999).
Competent	Relative to competent bed which is defined as a rock layer which, during folding, flexes without appreciable flow or internal shear (Whitten and Brooks, 1987).
Cut-off grade	The lowest grade of mineralised material in a given deposit that qualifies as *ore*. Used in the calculation of ore reserves.
Dissolved metal concentration	Operationally defined as the metal concentration in the fraction of a water sample passing through a 0.45µm membrane.
EC	see *Electrical Conductivity*
Electrical Conductivity	A measure of the ability of a water or soil solution to conduct an electric current (ANZECC and ARMCANZ, 2000).
Equilibrium Constant (K)	The equilibrium constant expresses the point of minimum free energy for a chemical reaction (Benthke, 1996).
Fault	A *fracture* or fracture zone in *rock* strata resulting from strain and with observable displacement (INAP, 1999).
Footwall	The wall or *rock* on the lower side of a vein, *ore deposit* or *fault* structure (INAP, 1999).

Term / Acronym	Description
Fracture	1. A crack, joint, *fault* or other break in *rocks*. 2. The breaking of a *mineral* other than along planes of cleavage (INAP, 1999).
Gangue	The part of an *orebody* from which a metal or metals is not extracted. Common gangue minerals include quartz, calcite, fluorite, siderite and pyrite (Whitten and Brooks, 1987).
Geochemistry	Study of the distribution and abundance of elements in *minerals*, *rocks*, *soils*, water and the atmosphere (INAP, 1999).
Hanging Wall	The wall or *rock* on the upper side of a vein, *ore deposit* or *fault* structure (INAP, 1999).
HLP	see *Heap Leach Pad*
Heap Leach Pad	Test run to show progress of *weathering* and resulting *drainage chemistry* in *mine* materials under the actual *minesite* conditions (INAP, 1999).
HWB	*Hanging Wall* Sandstone - Interbedded Black Shale (HWB)
HWD	*Hanging Wall* Siltstone
HWS	*Hanging Wall* Sandstone
IAP	see *Ion Activity Product*
ICP-MS	Inductively Coupled Plasma – Mass Spectrometry
INAP	International Network for Acid Prevention
Intrinsic Oxidation Rate	A measure of the rate of consumption of oxygen by a material under a particular set of conditions (Fague and Mostyn, 1997).
Ion Activity Product	The product of the activities of the ions in a *solubility product reaction*.
Ion-pairs	Ions that are strongly attracted to each other and act as if they are un-ionised or of lesser or different charge than anticipated (Boyd, 2000), e.g. Ca^{2+} and SO_4^{2-} form the ion pair $CaSO_4$.
IOR	see *Intrinsic Oxidation Rate*
JCU	James Cook University
Kinetic Test	A procedure for characterising the physical, chemical, or biological status of a sample through time during continued exposure to a known set of environmental conditions (Morin and Hutt, 1997). Unlike *static tests*, kinetic tests measure the performance of a *sample* over a prolonged period of time (INAP, 1999).
K_{sp}	see *Solubility Product*
Lag time	Time period to the onset of acid generation.
LBV	Lower Box Value
Leachate	Solution obtained from a leaching process (INAP, 1999).

Term / Acronym	Description
MEND	Mine Environment Neutral Drainage
Mill	A facility for milling ore in order to remove and concentrate economic metals or minerals (Morin and Hutt, 1997). Milling processes include *crushing*, *grinding*, *screening*, *concentration* and dewatering (INAP, 1999).
Mineral	A naturally occurring inorganic element or compound having an orderly internal structure and characteristic composition, crystal form and physical properties (INAP, 1999).
MINTEQA2	A geochemical modelling program sponsored by the US Environmental Protection Agency. Its primary purpose is speciation modelling, including redox, ion-exchange, and several surface complexation models (Zhu and Anderson, 2002).
MPA	Maximum Potential Acidity
NAF	Non Acid Forming
NAG	Net Acid Generation
NAPP	Net Acid Producing Potential
Neutralising Potential	The analytical bulk capacity of a sample for neutralising acidity, in units kg H_2SO_4 t^{-1} (Morin and Hutt, 1997).
NP	see *Neutralising Potential*
Open Pit	A surface depression created by the excavation of near surface ore, minerals or coal. In *open pit* mining, *overburden* covering the deposit is removed, exposed *ore* is blasted and moved to a *mill*, and *waste rock* is placed in one or more *waste rock dumps* (INAP, 1999). Also known as open cut or mine void.
Ore	Rock, sediments or soil that contains economically recoverable levels of metals or minerals (Morin and Hutt, 1997).
Orebody or Ore Deposit	A continuous well-defined mass of material containing sufficient quantities of the valuable material to make extraction economical (INAP, 1999).
Overburden	A general term referring to soil and broken rock, lying above *ore* and *waste rock*, that can usually be removed without blasting (Morin and Hutt, 1997).
PAF	Potentially Acid Forming
pH	The negative logarithm to the base 10 of the hydrogen ion activity [H+] in solution (INAP, 1999).
Primary mineral	A *mineral* that came into existence at the time the rock was formed and that retains its original composition and form (INAP, 1999)
Relative Standard Deviation	A measure of how precise the median is, expressed as a percentage. Relsd = 100*(standard deviation/│median│)
ROM	see *Run of Mine*

Term / Acronym	Description
Run of Mine	Particle size of mined material (i.e. ore or waste rock) prior to crushing or grinding.
Saturation Index (SI)	The logarithm of the ratio of *ion activity product* to *solubility product* (Zhu and Anderson, 2002).
Scale-up	The linkages between ARD prediction tests made at increasing scales of particle sizes.
Secondary mineral	A *mineral* formed by surface processes, usually at the expense of an earlier-formed *primary mineral* (INAP, 1999).
Secondary mineralisation	The processes whereby secondary minerals are formed. May include alteration, dissolution or precipitation.
SEM	Scanning Electron Microscopy
Solubility Product (K_{sp})	Equilibrium constant for a *solubility product reaction* (Zhu and Anderson, 2002).
Solubility Product Reaction	A reaction with a solid phase on one side and its constituent ions on the other (Zhu and Anderson, 2002), eg: $CaCO_{3(s)} = Ca^{2+} + CO_3^{2-}$
Static Tests	A procedure for characterising the physical, chemical, or biological status of a sample at one point in time (Morin and Hutt, 1997).
Strip ratio	Ratio of waste rock to ore mined.
TDS	Total Dissolved Salts
Test piles	see *Heap Leach Pads*
Total metal concentration	Operationally defined as the unfiltered metal concentration in a water sample.
UBV	Upper Box Value
Waste Rock	Rock with insufficient amounts of the economically valuable elements to warrant its extraction, but which has to be removed to allow physical access to the *ore* (INAP, 1999).
WRD	see *Waste Rock Dump*
Waste Rock Dump	A mined rock pile containing *waste rock* (Morin and Hutt, 1997).
XRD	X-ray Diffraction
XRF	X-ray Fluorescence
ZCML	Zinifex Century Mine Limited

1 Chapter 1: Project Scope and Literature Review

1.1 Project Scope

1.1.1 Background

Zinifex Century Mine Limited (ZCML) comprises a zinc, lead and silver mining and milling operation at Lawn Hill in northwest Queensland, concentrate dewatering and shipping facilities at Karumba in the Gulf of Carpentaria, and a 304km slurry pipeline connecting the two operations. The ZCML mine site is located 250 kilometres north-north-west of Mount Isa within the North West Queensland minerals province. An open cut method of mining using conventional drill and blast, load and haul techniques is used by ZCML from a single pit (Bates et al. 2000). Waste rock is transported to one of three main waste rock dumps (Northern, Southern or Western), short haul dumps (e.g. Stage 7 Short Haul Dump) or is deposited via in-pit dumping methods in mined out stages of the open pit. The current mining rate is approximately 82MT y^{-1} waste rock and 8MT y^{-1} ore (Lee, 2006a) with an overall strip ratio (life of mine) of approximately 11.8:1 (Bates et al. 2000). A further 470MT of waste rock are anticipated to be mined between now and when mine operations are scheduled to cease in 2016 (Lee, 2006a).

Mineralisation occurs in the upper part of the Lawn Hill Formation and is comprised of siltstone, tuffaceous siltstone, carbonaceous shale and sandstone (Dames and Moore, 1994). Pyrite (Fe_2S) occurs immediately above the mineralised sequence, and throughout the footwall carbonaceous shale forming the lower proportion of the deposit (Dames and Moore, 1994). Zinc predominantly occurs as sphalerite (ZnS) and lead as galena (PbS). Sulfides in the ZCML ore and waste rock are very fine grained and may oxidise rapidly upon exposure to generate acid rock drainage (ARD) from pit walls, marginal ore stockpiles and waste rock dumps.

The orebody is unconformably overlain by a complex folded sequence of Cambrian age limestone and dolostone (Bates et al. 2000). To minimise the generation of ARD in the waste rock dumps, they are constructed in a specific manner and waste rock is classified into the following three classes based on competence and acid forming / consuming capabilities:

- **Class 1:** Competent rock, non-acid forming or acid-consuming material.
- **Class 2:** Non-competent, non-acid forming or acid-consuming material
- **Class 3:** Acid-forming material.

The generalised waste rock dump design for current operations comprises an outer zone of class 1 material and inner zone containing class 2 and 3 materials. Cambrian Limestone (CLS), a class 1 material, is used for its structural and acid neutralising capabilities in waste rock dump construction.

Current mine waste rock placement procedures specify that class 1 rock with greater than 5% contamination of class 3 material is to be placed in the inner zone of the waste rock dumps due to uncertainty surrounding the long-term acid producing capabilities of this rock. This procedure, as well as additional restrictions on waste rock dump design, has the potential to cause significant scheduling problems due to the limited reserve of class 1 rock available for waste rock dump rehabilitation. This is particularly the case in the latter stages of the mine life following movement of most of the waste rock to access the ore.

1.1.2 Project Objectives

The aim of this study was to assess leachate quality from different blends of waste rock at Zinifex Century Mine and determine consequences for acid drainage generation. Drivers of the project included finite reserves of CLS material and the need to develop strategies to maximise the beneficial use of available limestone reserves, as well as the belief by mine personnel that the abovementioned contamination percentage may be conservative. The objectives of the study were to:

- Quantify blending levels of acid consuming (CLS) and acid forming (Hanging Wall Siltstone (HWD)) materials that will produce pH neutral leachate low in metal and salt concentrations;
- Determine the validity of current waste rock placement procedures;
- Investigate the influence of particle size on leachate quality; and
- Attempt to establish links between results from various ARD prediction tests.

Results from this study will be used to develop strategies to maximise the beneficial use of the limestone that will be mined, as well as refining site waste rock disposal procedures, rehabilitation practices and mine closure plans. Economically, results from the tests have the potential to shorten haulage distances if the percentage contamination limit of class 3 in class 1 rock is lowered, which in turn, would significantly reduce operating costs.

1.1.3 Project Scope

This study involved the assessment of leachate generated from uniformly blended waste rock materials and was not intended to predict the chemistry of drainage from the site waste rock dumps.

In assessing the leachate quality from blended waste rock material at ZCML, only the influence of particle size and percentage of potentially acid forming material in the blend were considered. The impact of factors such as oxygen availability, temperature and percentage saturation on leachate quality was not included in this study.

Both static (acid base accounting, net acid generation tests, acid buffering characteristic curves and cyclic voltammetry) and kinetic (column leach tests (CLTs) and heap lead pads (HLPs)) ARD prediction tests were used to predict the acid generation characteristics of the chosen waste rock blends.

There are various waste rock types in the ZCML deposit that are either classified as acid consuming (AC), non-acid forming (NAF), or potentially acid forming (PAF). Rather than conduct a study on all waste rock types, CLS and HWD were selected. HWD immediately above the mineralised sequence was chosen as it is one of the most reactive class 3 materials in the pit and would therefore represent a “worst case” scenario with respect to the quality of drainage produced. CLS was chosen as it is the most abundant class 1 material on site and has been identified as the preferred material to cap and batter the waste rock dumps.

1.1.4 Methodology

Bulk samples of CLS and HWD were extracted from specific locations in the ZCML open pit for use in this study. Sub samples of this material were used in the various static and kinetic tests selected.

Various static tests (acid base accounting, net acid generation tests, acid buffering characteristic curves) were conducted by Environmental Geochemistry International Pty Ltd (EGi). These results, together with those from the cyclic voltammetry tests, were compared against kinetic test results to address the issue of scale-up.

Twenty CLTs representing five lithology blends and three particle size distributions were assembled in a laboratory environment. Five replicate CLTs were established. Three HLPs representing three lithology blends were constructed from run of mine (ROM) material at ZCML. The CLTs and HLPs were periodically watered to simulate rainfall events. In addition, the HLPs were exposed to wet season rainfall events.

1.1.5 Thesis Outline

The following chapters present and discuss the findings from this study.

- Chapter 1 defines the project scope, provides a background to ARD generation and discusses and compares the different methods used for ARD prediction.
- Chapter 2 describes the ZCML mine site and includes an overview of the process, a background to waste rock classification and current waste rock dump (WRD) design procedures.
- Chapter 3 summarises the static testing results for waste rock samples used in this study.
- Chapter 4 describes the methodology, design and results obtained from the laboratory column leach tests conducted for different blends and particle sizes of waste rock from ZCML. Results for physical parameters (e.g. electrical conductivity, pH), major cations and anions (e.g. sulfate, magnesium, calcium) and total and dissolved metals are presented.
- Chapter 5 describes the methodology, design and results obtained from the field based heap leach pads conducted for three different blends of waste rock from the ZCML. Similarly to Chapter 4, results for physical parameters, major cations and anions and total and dissolved metals are presented and discussed.
- Chapter 6 discusses and compares the results from the static tests (Chapter 3), column leach tests (Chapter 4) and heap leach pads (Chapter 5). Attempts are made in this chapter to establish relationships between results from these tests to address the issue of scale-up.
- Chapter 7 discusses the implications of results from the tests for site waste rock dump design procedures and provides recommendations for future studies, improvements in testing methodology and options to improve the management of ARD at Zinifex Century Mine.

1.2 Literature Review

1.2.1 Introduction

Acid rock drainage (ARD) is defined as drainage resulting from the oxidation and leaching of sulfide-bearing rocks when exposed to air and water. Bacteria may accelerate the process and the resultant leachate is often characterised by low pH, mobilised metals, and high salinity. ARD may be transported by water (processing water, rainfall, surface water and groundwater) to receiving water bodies where it can have a deleterious and often disastrous effect. When occurring naturally, these processes usually take place very slowly in relatively competent rock and mineralisation. Alternatively, ARD emanating from fractured or finely ground mine waste where the surface area of sulfidic rocks is increased, can occur rapidly, with evidence often appearing within months.

There is little doubt that ARD is the largest and most testing long-term environmental issue facing the global minerals industry (Lawrence and Day, 1997, Munchenberg, 1998, Olson et al. 2006). ARD can arise from mining base and precious metals, coal, uranium and mineral sands, and can occur in both high rainfall and arid regions (Munchenberg, 1998). While the worst examples are a legacy of past mining practices, ARD is also a day-to-day issue facing current mining operations where sulfide minerals are present. For some mines, ARD is a high profile issue that can have a lasting, damaging effect on the company's reputation (Gauci, 2000). The consequences of inadequate ARD management are great and include major costs late in mine life and after closure (Harries, 1998). Poor ARD management may also damage a company's credibility, and ultimately harm a company's license to operate (Dowd, 2005), explore, develop and operate mines in the future (Gauci, 2000). The International Network for Acid Prevention (INAP) estimates that the total liability costs for potentially acid-generating wastes at mining sites is USD 30 million in Australia, USD 20.6 billion in the USA and up to USD 3.3 billion in Canada (Olson et al. 2006).

Prediction of whether a mining waste will generate ARD and the specific quality of the drainage is critical to planning for new mines, the efficient operation of existing mines and for closure planning (Ferguson and Firth, 2000). Accurate prediction potentially offers the most cost-effective means of reducing the impact of ARD on the environment and the associated costs by allowing advanced planning for prevention and control (Lawrence and Day, 1997).

Although a complex process, various methods and management options exist to both predict and control ARD. The various prediction methodologies in use worldwide are broadly categorised into either static or kinetic assessment procedures and vary in both suitability and efficacy. The term scale-up is used to describe the linkages between ARD prediction tests made at increasing scales of particle sizes. Accurate scale-up of laboratory based ARD predictions to field scale behaviour is critical to mine planning. Site experience has shown that often, predictive tests do not represent the observed rates of ARD generation in the field. The key to scale-up is the determination of the significance of interactions between geochemical, mineralogical and physical characteristics, as influenced by weathering. Some relationships between field and laboratory behaviour have been developed, however numerous limitations still remain. It is critical that the ability to use

small-scale controlled testing to predict large scale uncontrolled weathering is developed. There is also a need to improve the techniques available for the assessment and interpretation of geological, mineralogical and physical data, which, with geochemical data, influence (and in turn are influenced by) weathering processes (Ferguson and Firth, 2000).

A key parameter required in describing the behaviour of sulfidic mine wastes, particularly waste rock, is the rate at which the material oxidises under whatever conditions may apply to that material. Oxidation rates of sulfidic mine wastes have been measured at a range of size scales, from bench-top studies, through small and large columns, to test piles and in full-scale waste piles (Bennett et al. 2000). Bennett et al. (2000) identify and discuss systematic differences between field and laboratory measurements and identify several shortcomings in the techniques used and the application of these data in the management of sulfidic mine wastes. This report has been a major source of the information contained in this literature review.

1.2.2 Background to ARD Generation

1.2.2.1 Sulfide Oxidation

The process of sulfide oxidation to produce ARD is complex because it involves chemical, biological and electrochemical reactions and varies with environmental conditions (Parker and Robertson, 1999). The formation of ARD under well-oxygenated conditions may be summarised by the following exothermic reaction:

$$\mathbf{FeS_{2(s)} + 15/4O_{2(g)} + 7/2H_2O_{(aq)} \leftrightarrows Fe(OH)_{3(s)} + 2SO_4^{2-}{}_{(aq)} + 4H^+{}_{(aq)} + heat}$$

Equation 1-1

The various steps of ARD formation are described by Equation 1-2 to Equation 1-5. When sulfide minerals such as pyrite are exposed to the atmosphere they react with oxygen and water, producing ferrous sulfate and sulfuric acid:

$$\mathbf{FeS_2(s) + 7/2O_2 + H_2O \leftrightarrows Fe^{2+} + 2SO_4^{2-} + 2H^+}$$

Equation 1-2

If present, acid consuming minerals can react with this acid and maintain neutral pH conditions. If the surrounding environment is sufficiently oxidising, ferrous iron will rapidly oxidise to ferric iron:

$$\mathbf{Fe^{2+} + \tfrac{1}{4}O_2 + H^+ \leftrightarrows Fe^{3+} + \tfrac{1}{2}H_2O}$$

Equation 1-3

Precipitates can also form as a result of secondary reactions. For example, at pH values of approximately 3.3 and above, and in the presence of atmospheric oxygen, ferric iron precipitates as hydroxide, creating more acid and leaving little Fe^{3+} in solution:

$$\mathbf{Fe^{3+} + 3H_2O \leftrightarrows Fe(OH)_{3(s)} + 3H^+}$$

Equation 1-4

Under acidic conditions, ferric iron is, in itself, a powerful oxidising agent, which in turn may attack other sulfidic minerals, increasing the rate of sulfide oxidation and generation of oxidation products. Any ferric iron that does not precipitate from solution may replace oxygen as the dominant oxidant, thereby oxidising the additional pyrite according to:

$$\mathbf{FeS_{2(s)} + 14Fe^{3+} + 8H_2O \leftrightarrows 15Fe^{2+} + 2SO_4^{2-} + 16H^+}$$

Equation 1-5

This does not mean that oxygen is no longer required, since Equation 1-5 can only continue as long as ferric iron is available. For Equation 1-5 to continue, the ferrous iron released from FeS_2 oxidation must be converted back to the ferric state, a process requiring oxygen, as indicated by Equation 1-3.

Abiotic oxidation occurs in the absence of bacterial catalysts and biotic oxidation occurs in their presence. The oxidation rate of pyrite, and therefore the rate of the above reactions (especially Equation 1-2 and Equation 1-3), is accelerated by the bacteria Thiobacillus ferrooxidans (iron oxidising) and Thiobacillus thiooxidans (sulfur oxidising), which are associated with nearly all cases of acid drainage. These bacteria also accelerate the reaction by enhancing the rate of reduced sulfur oxidation. Maximum oxidation of pyrite occurs between a pH of 2.4 and 3.6, rapidly decreasing at increasing pH values.

The Thiobacillus ferro-oxidans bacteria are indigenous to environments containing sulfides, oxygen and low pH conditions (most active at pH 2 to 5). They are autotrophic microorganisms and obtain energy from the oxidation of iron compounds. Consequently, bacterially catalysed acid and ferric iron are produced close to the surface.

ARD can be generated at or within a number of mine site components, namely drainage from underground workings; runoff and discharges from open pits; waste rock dumps; tailings storage facilities; ore stockpiles (which have characteristics analogous to waste rock) and spent heap leach piles (Coastech Research Inc, 1991, Mitchell, 2000). Pyrite and other sulfide minerals are present in many ore deposits that are mined throughout the world. Sulfidic materials below cut-off grade are routinely consigned to waste rock dumps or tailings storage facilities. Sulfide minerals, such as those listed below, may undergo oxidation in these landforms, generating sulfate, salinity and possibly mobilising trace metals:

- Iron sulfides (eg. pyrite (FeS_2), marcasite (FeS_2) and pyrrhotite ($Fe_{1-x}S$));
- Copper sulfides (eg. chalcopyrite ($CuFeS_2$), chalcocite (Cu_2S) and bornite (Cu_5FeS_4));
- Arsenic sulfides (eg. arsenopyrite (FeAsS) and realgar (AsS)); and
- Other metal sulfides (eg. sphalerite (ZnS), galena (PbS), cinnabar (HgS) and pentlandite $(Fe,Ni)_9S_8$).

The oxidation of these sulfide minerals is influenced by:

- Water availability;
- Oxygen availability;
- Physical characteristics of the material (eg. grain size);

- Temperature;
- pH;
- Ferric/ferrous iron equilibrium; and
- Microbiological activity.

It should be noted that not all sulfide minerals are acid generating, and some minerals may need to be exposed to atmospheric conditions for a considerable period of time before acid conditions occur (Bennett et al. 2000). If conditions are not strongly oxidising (i.e. only sulfur is oxidised), oxidation of minerals composed of sulfide rather than disulfide and metals, which are not hydrolysed except at high pH, will not result in acidic conditions (Lawrence and Day, 1997). Examples include sphalerite and iron sulfide:

$$\mathbf{FeS + 2O_2 \leftrightarrows Fe^{2+} + SO_4^{2-}}$$

Equation 1-6

$$\mathbf{ZnS + 2O_2 \leftrightarrows Zn^{2+} + SO_4^{2-}}$$

Equation 1-7

1.2.2.2 pH Buffering and ARD neutralisation

The suite of geochemical reactions referred to as "acid neutralisation" minimise the impacts of acid generation by decreasing levels of acidity, increasing pH towards neutral values, and causing aqueous metals to precipitate from the leachate (Morin et al. 1991). pH buffering refers to the stable pH resulting from interaction of a leachate with a mineral (Lawrence and Day, 1997). Minerals buffer at a variety of pHs according to the relationship between mineral solubility and pH. Acidic leachates also attack other more common minerals (carbonates, hydroxides and oxides, silicates), resulting in a pH increase. The buffer pH of a mineral is not constant but depends on overall solution chemistry, the gas composition in contact with the solution and whether the system is open (i.e. having an infinite supply of reactants) or closed.

Calcite ($CaCO_3$) is the most common acid consuming mineral present in mine waste rock and, depending on the pH, consumes acid through the creation of bicarbonate (HCO_3^-) or carbonic acid (H_2CO_3):

$$\mathbf{CaCO_3 + H^+ \leftrightarrows Ca^{2+} + HCO_3^-}$$

Equation 1-8

$$\mathbf{CaCO_3 + 2H^+ \leftrightarrows Ca^{2+} + H_2CO_3}$$

Equation 1-9

Similar reactions can also be written for the dissolution of dolomite ($MgCa(CO_3)_2$):

$$\mathbf{MgCa(CO_3)_2 + 2H^+ \leftrightarrows Ca^{2+} + Mg^{2+} + 2HCO_3^-}$$

Equation 1-10

$$MgCa(CO_3)_2 + 4H^+ \leftrightarrows Ca^{2+} + Mg^{2+} + 2H_2CO_3$$

Equation 1-11

An assumption of buffering is that a particular mineral component is available in infinite amounts at a particular moment in time. As a mineral becomes exhausted, excess acidity is available and is buffered by a mineral at a lower pH. In situations where calcite is the only mineral available to buffer at higher pHs, the pH of the leachate decreases from near 7 (buffered by calcite) to near 3 (buffered by ferric hydroxide). In reality, where many different minerals are capable of buffering, the transition from near neutral pH to ferric hydroxide buffered does not occur sharply but steadily over a long period as different minerals buffer the leachate pH (Lawrence and Day, 1997). Buffer, or equilibrium, pH ranges for common acid consuming minerals are shown in Table 1-1.

Table 1-1: Acid Consuming Minerals and their Characteristics (adapted from Steffen, Robertson and Kirsten et al. 1989)

MINERAL	CHEMICAL COMPOSITION	ACID NEUTRALISING POTENTIAL*	BUFFER pH
Calcite, Aragonite	$CaCO_3$	100	5.5 – 6.9
Magnesite	$MgCO_3$	84	-
Witherite	$BaCO_3$	196	-
Dolomite	$MgCa(CO_3)_2$	92	-
Gibbsite	$Al(OH)_3$	26	4.3 – 3.7
Limonite/Goethite	FeOOH	89	3.0 – 3.7
Manganite	MnOOH	88	-
Brucite	$Mg(OH)_2$	29	-

* Acid neutralising potential is given as the mass (in grams) of the mineral required to have the same neutralisation effect as 100g of calcite.

1.2.2.3 Metal Leaching

The environmental toxicity associated with ARD is the result of not only acidic pH, but also the elevated concentrations of metals in the drainage (Morin et al. 1991). Aqueous concentrations of many metals can be correlated with pH and are typically highest at acidic pH, minimal near neutral pH, and minimal to somewhat elevated at alkaline pH (Morin et al. 1991).

Metal leaching processes in mine waste piles are complex (often more than one mechanism is involved) and are usually dependent on the mineralogy of the waste rock. Under the normal pH range of soils and water (pH 5-7), metals released by the weathering of minerals generally precipitate and become relatively immobile. However, due to the enhanced solubility of many non-sulfide minerals at acidic pH (Morin et al. 1991, Stumm and Morgan, 1996), under reduced pH conditions, metals can remain in solution and be transported off site where they may have a deleterious effect on aquatic ecosystems and other downstream water users. The mobility of the metals liberated depends on the solubility of the metal sulfate minerals (Lawrence and Day, 1997).

Factors influencing the rate of metal leaching, and the migration rate of contamination fronts, may include:

- pH conditions;
- Bacterial populations;
- Climatic conditions;
- Stored loads within dumps;
- Waste permeability;
- Availability of pore water;
- Pore water pressure; and
- Mechanisms of movement (e.g. stream flow or diffusion).

1.2.3 ARD Prediction Techniques

The time for ARD to develop can vary from a matter of days to hundreds of years (Figure 1-1). At some point in time from the initiation of acid generation, the rate will slow as reactive sulfides approach complete oxidation. At this stage, pH increases, rock becomes progressively inert and surrounding waters are increasingly less affected. Prediction of ARD can therefore be seen to be a short-term assessment of a potentially long-term phenomenon (Lawrence and Day, 1997).

The capacity to predict ARD generation accurately increases the options for planning economical, technical, and environmentally sound approaches to manage the problem. Errors in ARD prediction and the interpretation of results in the mine feasibility and design stage can lead to major liability during operation, at closure and post closure (Dowd, 2005, Morin, 2003). The thorough classification of ore and waste, effective mine design to manage PAF material during operation, and integrating closure principles into the mine design and operating plan, present opportunities for “getting it right” (Dowd, 2005). Morin (2003), Dowd (2005) and Day et al. (2003) discuss case studies where inadequate prediction or planning of the behaviour of PAF materials contributed to escalating operating or closure costs in effectively managing the issue.

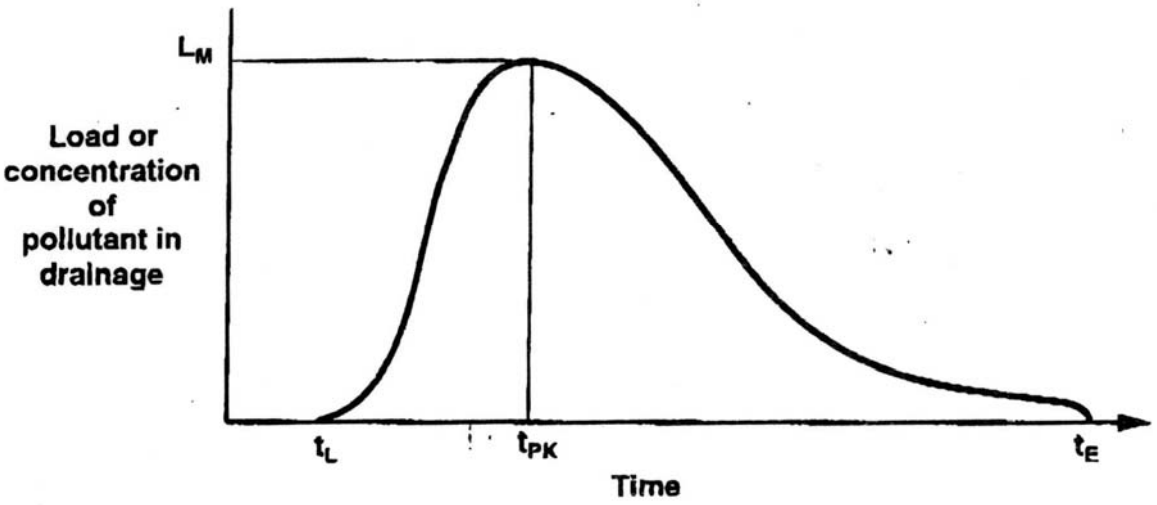

Symbol	Description	Range
t_L	Time to first appearance of acid drainage	Weeks to years
t_{PK}	Time when pollutant concentration/load reaches a maximum	Years to tens of years
t_E	Time when drainage is no longer polluted	Tens to hundreds of years
L_M	Maximum pollutant load/concentration	e.g. 100 – 100,000 mg L^{-1} SO_4

Figure 1-1: Schematic Time Dependence of Pollution in Drainage from Mine Wastes (Ritchie, 1995)

ARD predictive tests vary in scale, complexity of procedure and data interpretation, the time required to achieve a predictive result, and cost. Procedures can be broadly categorised as either static or kinetic tests, although numerous other tests are available for specific purposes or characterisation (Coastech Research Inc, 1991). Static prediction tests are simple tests that compare the balance between the acid generating components (sulfides) and acid consuming components (typically carbonates) in a sample. Kinetic prediction tests attempt to model over time the acid producing and consuming processes, including a prediction of drainage quality, in the laboratory or field (Coastech Research Inc, 1991). Thus, static tests are conducted at one point in time, and more significantly, represent one point in time, in contrast to kinetic tests that involve ongoing repetitive analysis (Morin and Hutt, 1997).

Currently, there is not any one test that can produce all the necessary information to provide a reliable assessment of the ability of a sample to generate ARD, and a combination of tests is therefore usually required (Morin and Hutt, 1997, Parker and Robertson, 1999). Although there is no globally-accepted manual outlining standardised ARD prediction tests, the Draft Acid Rock Drainage Technical Guide (Steffen, Robertson and Kirsten et al. 1989), Mine Environment Neutral Drainage (MEND) Acid Rock Drainage Prediction Manual (Coastech Research Inc, 1991) and more recently, the ARD Test Handbook (Ian Wark Research Institute and EGi, 2002) are widely accepted, off-the-shelf guides that describe in detail the various ARD predictive tests available.

In performing predictive tests, it is vital that the samples are representative of mine waste material. Sampling is defined as the operation of removing a part convenient in size for testing, from a whole which is much greater in bulk, in such a way that the proportion and distribution of the quality to be tested are the same in both the whole and the part (sample) to be tested (Coastech Research Inc, 1991). Within the mine plan area, samples should be taken from geological units defined by their physical and chemical homogeneity. Poor or inappropriate sampling leads to data that may be non-representative of the particular portion of the orebody or waste under consideration (Dobos, 2000). Coastech Research Inc (1991) provides comments and brief guidelines on sampling.

1.2.3.1 Static Tests

Static testing is usually the first step in the systematic evaluation of materials to be disturbed and generated by mining operations. Static testing comprises a wide range of simple, relatively fast and inexpensive screening tests, which confirm the reactivity of a sample. Several types of static tests define the balance between potentially acid-generating minerals (potential acidity) and acid neutralising minerals (neutralisation potential) in a sample. A sample will theoretically only generate net acidity if the potential acidity exceeds the neutralisation potential. Procedures such as the maximum potential acidity (MPA), net acid production potential (NAPP), acid neutralising capacity (ANC) and the net acid generation (NAG) test have been widely adopted as the basis for characterising wastes according to their acid generating potential (Bennett et al. 2000) and have been used in this study. Several authors including Morin and Hutt (1997), Parker and Robertson (1999), Ian Wark Research Institute and Environmental Geochemistry International Pty Ltd (2002) describe these tests in detail. Additionally the theory supporting these static tests is further described in Chapter 3: Static Tests alongside results from the static tests applied in this study.

Static tests should be viewed as a qualitative predictive method (i.e. they can only indicate whether or not there is a potential for generation of acidity at some point in time), since they provide no indication of the rates of sulfide oxidation, acid generation or acid neutralisation of a material. Additionally, they may overestimate the real, or field, neutralising potential of materials. This is because some of the neutralising minerals present may be inaccessible to ARD due to physical placement or entrainment or because of armouring by metal precipitates.

A summary of the more common static tests, and advantages and disadvantages associated with each test, is provided in Table 1-2.

Table 1-2: Static Testing Summary

ARD Prediction Test	General Principles	Advantages	Disadvantages
Mineralogy	Mineralogical factors play a dominant role in the reaction and interaction of acid generating and acid consuming components of mine waste. Chemical, mineralogical and physical analyses of waste components are usually performed as part of preliminary characterisation of the material prior to static or kinetic testing (Coastech Research Inc, 1991). Techniques commonly used to assess mineralogy include optical mineralogy, scanning electron microscopy (SEM), micro-probe, automated micro-probe point counting techniques, x-ray diffraction (XRD), and bulk elemental/oxide determinations (e.g. ICP or XRF) (Ian Wark Research Institute and EGi, 2002).	• Clarifies mineralogical assumptions commonly made in static tests such as acid-base analysis. • Provides details on the species and crystal habit of sulfur bearing and neutralising minerals indicated by other test methods (Ian Wark Research Institute and EGi, 2002). • Assists in determining the relative proportion of sulfide material in a sample, identifying the neutralising species in a sample and identifying the existence of passivating rims that inhibit sulfide oxidation (Ian Wark Research Institute and EGi, 2002).	• Minerals at levels less than 0.5-1.0% may not be detected by traditional visual, petrographic examination of thin sections. • XRD suffers from detection limits around 0.5% (Morin and Hutt, 1997). • A combination of techniques may be required for an accurate assessment.
Acid-Base Analysis	The acid-base account involves tests that evaluate the balance between acid generation processes (oxidation of sulfides) and acid neutralising processes (dissolution of alkaline carbonates, displacement of exchangeable bases, and weathering of silicates) in a sample. The values arising from the test are referred to as the maximum potential acidity (MPA) and the acid neutralising capacity (ANC). The MPA, expressed as kg H_2SO_4 t^{-1}, can be generated from the sample total sulfur content and multiplying by a stoichiometric factor of 30.6. ANC, expressed as	• Widely used and accepted method. • Fast turnaround times • Provides a simple and inexpensive screening of samples to give a preliminary yes/no predictor for acceptable or unacceptable water quality. • Determines the maximum amount of both neutralisation and acid potential available in a sample.	• Does not determine ambient rates and extent of metal leaching, acid generation, and acid neutralisation reactions (Morin and Hutt, 1997, Coastech Research Inc, 1991). • The use of the total sulfur assay may overestimate the MPA because some sulfur may occur in forms other than pyrite (Coastech Research Inc, 1991, Ian Wark Research Institute and EGi, 2002). • Calculation of MPA is based on stoichiometry of one reaction. In practice, actual stoichiometry may vary

ARD Prediction Test	General Principles	Advantages	Disadvantages
	kg H_2SO_4 t^{-1}, is obtained by reacting a sample with HCl and back-titrating the mixture with NaOH to determine the amount of unreacted HCl. The difference between the MPA and ANC is referred to as the net acid producing potential (NAPP) (Ian Wark Research Institute and EGi, 2002). A positive NAPP value classifies the waste as potentially acid forming.		significantly (Coastech Research Inc, 1991). • Method does not indicate the pH to which the sample can neutralise during extended contact with acidic water (Coastech Research Inc, 1991). • Method does not distinguish between reactive, readily available acid consuming minerals and less reactive species which might be important in the longer term (Coastech Research Inc, 1991). • Boiling procedure might overestimate neutralisation potential (Coastech Research Inc, 1991). • Does not predict drainage quality.
Net Acid Generation (NAG) Test	A sample is reacted with hydrogen peroxide (H_2O_2) to rapidly oxidise any sulfide minerals contained within the sample. Both acid generation and acid neutralisation reactions can occur simultaneously. The end result represents a direct measurement of the net amount of acid generated by the sample (i.e. NAG capacity, expressed as kg H_2SO_4 t^{-1}). The three main NAG test procedures are the Single Addition NAG Test, the Sequential NAG Test and the Kinetic NAG Test (EGi, 2004). A NAG pH less than 4.5 classifies the sample as PAF.	• Fast turnaround times • Provides a simple and inexpensive screening of samples to give a preliminary yes/no predictor for acceptable or unacceptable water quality. • Sulfur analyses not required. • Provides an indication of the form of acidity. The titration value at pH 4.5 includes acidity due to free acid as well as soluble iron and aluminium. The titration value at pH 7.0 also includes metallic ions that precipitate as hydroxides at pHs between 4.5 and 7.0 (Ian	• Does not determine ambient rates and extent of metal leaching, acid generation, and acid neutralisation reactions (Morin and Hutt, 1997, Coastech Research Inc, 1991). • Does not predict drainage quality. • Underestimates acid generation in samples with sulfur levels above 3%S (Morin and Hutt, 1997). • Carries a 5-15% error rate in results (Morin and Hutt, 1997). • Alkaline components of the sample might interfere with the efficiency of pyrite oxidation by H_2O_2 (Coastech Research Inc, 1991).

ARD Prediction Test	General Principles	Advantages	Disadvantages
		Wark Research Institute and EGi, 2002).	• As acid-neutralising minerals frequently have slow reaction rates and cannot match those of acid-generating minerals (Parker and Robertson, 1999), neutralising potential may not react the same under ambient conditions and ARD may result (Morin and Hutt, 1997).
Acid Buffering Characteristic Curve (ABCC)	The test involves slow titration of a sample with acid while continuously measuring pH. This data provides an indication of the portion of ANC within a sample that is readily available for acid neutralisation (Ian Wark Research Institute and EGi, 2002).	• Useful in assessing whether a sulfidic sample with NAPP<0 and NAGpH≥4.5 has enough readily available carbonate to render it non acid producing (Ian Wark Research Institute and EGi, 2002).	• Does not determine ambient rates and extent of metal leaching, acid generation, and acid neutralisation reactions (Morin and Hutt, 1997, Coastech Research Inc, 1991). • Does not predict drainage quality.
Cyclic Voltammetry	This electrochemical technique used involves imposing a sweep potential to the sample contained in the working carbon paste electrode in order to reach the interfacial energetic conditions that promote the electrochemical reactions. The transferred charges (electrons) associated with the electrochemical reactions are registered as a function of an imposed potential (i.e. current vs. potential, voltammograms) (Cruz et al. 2001).	• Describes the factors that influence sulfide reactivity that are not evaluated by the traditionally utilised prediction techniques (Cruz et al. 2001). • Allows reactivity evolution of waste rock material and the effect of the galvanic protection offered by associated impurities, as well as the passivation by Fe oxihydroxy coatings, to be established (Cruz et al. 2001). • Fast and relatively inexpensive.	• Does not determine ambient rates and extent of metal leaching, acid generation, and acid neutralisation reactions (Morin and Hutt, 1997, Coastech Research Inc, 1991). • Does not predict drainage quality.
Intrinsic Oxidation Rate (IOR)	The IOR is a measure of the rate of consumption of oxygen by a material under a particular set of	• The IOR only needs to be known to within an order of magnitude because the overall	• It is currently impossible to predict the functional dependence of the IOR by measuring individual

ARD Prediction Test	General Principles	Advantages	Disadvantages
	conditions (Fague and Mostyn, 1997) and is a function of several parameters including oxygen concentration, sulfide sulfur concentration, temperature, pH, sulfide mineral morphology and microbial ecology (Bennett et al. 2000). The IOR of a material is often measured for use in predictive modelling of sulfidic piles. An IOR of 10^{-8} kg(O_2)kg(material)$^{-1}$s^{-1} is considered slow and 10^{-6} kg(O_2)kg(material)$^{-1}$s^{-1} fast (Bennett et al. 2000).	oxidation rate in a WRD is comparatively insensitive to detailed changes in the IOR (Bennett et al. 2000).	material characteristics. Direct measurements of oxidation rate, either of samples in the laboratory or in-situ, are therefore generally made (Bennett et al. 2000). • Does not predict drainage quality.

1.2.3.2 Kinetic Tests

Kinetic tests are usually performed when static test results indicate the potential for ARD generation or if the results are uncertain (Coastech Research Inc, 1991). Kinetic tests provide real time data on the kinetics and rate of acid generation and acid neutralising reactions under laboratory or on-site conditions. Samples are exposed to moisture and air, in an attempt to simulate the weathering and oxidation processes over time that lead to mineral dissolution.

In most kinetic tests, water is added to a sample, the mixture is left to incubate for a period, acid producing reactions are allowed to proceed, and samples of the leachate or extracts are collected and analysed (Coastech Research Inc, 1991). Tests are often required to continue for months or years, with a limited number of samples providing information on the kinetics of overall acid generation.

Kinetic tests may be designed to quantify a range of parameters such as: sulfide oxidation rate, rate of neutralisation, sulfate and metal release rates, time periods for the onset of acid generation (lag time) and consumption of carbonates and sulfides, and the nature and concentration of predicted acid drainage. Thus the results provide information on acid generation characteristics and indicate if the rate of acid generation is significant or negligible, over what period of time it may occur, and over what time period controls would be required. They may also be used to evaluate the effectiveness of control techniques which may limit the reaction rates of oxidising material (e.g. covers, liming, layering, inundation and chemical addition such as bactericides).

The major parameters measured throughout kinetic tests may include:

- pH trends (to identify the stage of acid drainage);
- Sulfate (related to sulfide oxidation);
- Acidity or alkalinity (reflects the rate of acid production or acid neutralisation); and
- Metals (to evaluate metal solubility and leaching behaviour).

Generally, indication of the potential for ARD generation is associated with the following conditions and changes in parameters (Coastech Research Inc, 1991):

- Decrease in pH;
- Increase in electrical conductivity;
- Increase in redox potential;
- Absence or low concentrations of alkalinity;
- Increase in acidity;
- Increase in sulfate concentration; and
- Increase in dissolved metal concentrations.

There are several kinetic tests available, namely humidity cells, columns and lysimeters, the B.C. research confirmation test, shake flasks, Soxhlet extraction and test piles (Coastech Research Inc, 1991, Morin and Hutt, 1997, Parker and Robertson, 1999). A summary of the more common kinetic tests, and advantages and disadvantages associated with each test, is provided in Table 1-3.

It should be noted that one of the major weaknesses of kinetic test interpretation is the lack of long-term data. Although tests are generally conducted for several months to one or two years, the tests do not simulate the behaviour of a waste component in time frames often measured in years or tens of years. Assumptions have to be made to enable the results to be extrapolated into the future (Bennett et al. 2000).

Table 1-3: Kinetic Testing Summary

ARD Prediction Test	General Principles	Advantages	Disadvantages
Humidity cells	A humidity cell is a weathering chamber designed to provide simple control over air, temperature and moisture, while allowing for the removal of weathering products in solution for analysis. Water is added to a sample, the mixture is left to incubate for a period, acid producing reactions are allowed to proceed, and samples of the leachate or extracts are collected and analysed. The onset of ARD, mass loads, rate of acid generation and neutralisation and the concentration of metals and other species as a function of time can be determined (Coastech Research Inc, 1991).	• Standardised method exists (accepted method in Canada and U.S.A.). • Relatively simple to set up and operate. • Well characterised test materials can be utilised (Parker and Robertson, 1999). • Models the wet/dry cycles of the environment (Coastech Research Inc, 1991). • Consistent reproducible conditions permit comparison with results from other sites (Parker and Robertson, 1999). • Ambient rates and extent of metal leaching, acid generation, and acid neutralisation reactions can be determined. • Allows preliminary evaluation of ARD control options such as covers and blending to be made (Coastech Research Inc, 1991).	• Size of particles limited to fines, typically less than 10mm in diameter (Parker and Robertson, 1999). • No heterogeneity in leaching (Parker and Robertson, 1999). • Procedures do not simulate the precipitation and dissolution of secondary minerals (Parker and Robertson, 1999). • No conservation of heat generated by oxidation (Parker and Robertson, 1999). • More expensive and time consuming than static tests. • Interpretation of results is sometimes complex (Coastech Research Inc, 1991). • Rates of acidity and alkalinity release might not be comparable or readily interpreted due to the differences in the kinetics and equilibria of the reactions under laboratory and field conditions (Coastech Research Inc, 1991).
Column leach tests	As per humidity cells however greater sample volumes and particle sizes are used.	• Relatively simple to set up and operate. • Compares favourably with other prediction tests and field data for reliability (Coastech Research Inc, 1991). • Larger scale of test allows larger particle	• No standardised method exists (although is an accepted method for ARD prediction). • Interpretation of results is sometime complex (Coastech Research Inc, 1991). • Tests may require long time for completion and with relatively

ARD Prediction Test	General Principles	Advantages	Disadvantages
		sizes of waste to be evaluated. • Can be used to model saturated and unsaturated waste deposition (Coastech Research Inc, 1991). • Ambient rates and extent of metal leaching, acid generation, and acid neutralisation reactions can be determined. • Temporal variations in acid generation rates can be determined (Coastech Research Inc, 1991). • Allows preliminary evaluation of ARD control options such as covers and blending to be made (Coastech Research Inc, 1991). • For larger columns, the evaluation of changes in mineralogy and other effects of weathering with depth, and the determination of effluent quality profiles, can be made (Coastech Research Inc, 1991).	high analytical costs (Coastech Research Inc, 1991). • Rates of acidity and alkalinity release might not be comparable due to the differences in the kinetics and equilibria of the acid generating, acid consuming, and alkalinity generating reactions (Coastech Research Inc, 1991). • Often the ratio of solid sample to weekly rinse water is much higher than humidity cells so not all particle surfaces may be rinsed and the solubilities of secondary minerals may be exceeded (Morin and Hutt, 1997). • Reaction product retention may differ from field conditions. • Does not provide reliable predictions of secondary mineral reaction rates (Morin and Hutt, 1997). • Can give erroneous results due to water saturation and lack of water availability (Morin and Hutt, 1997).
Heap leach pads (test piles)	Waste rock test piles are usually established to determine the relationship between weathering rates under laboratory and field conditions.	• Regular flushing allows measurement of primary reaction rates. • Can be used to evaluate remediation options, such as capping and blending with acid	• No standardised method exists. • Secondary mineral controlled rates rather than primary mineral reaction rates are often provided due to large sample size and

ARD Prediction Test	General Principles	Advantages	Disadvantages
	Test piles of varying sizes are generally constructed from ROM material on a low permeability base to facilitate the collection and analysis of drainage flows. The piles are exposed to ambient conditions and in some cases, irrigated to simulate rainfall events.	neutralising materials (Lawrence and Day, 1997). • Larger particle sizes typically representative of mine waste. • Tests subjected to same field conditions as mine waste.	generally low water flow (Parker and Robertson, 1999). • Characterisation of the material prior to testing is difficult (Lawrence and Day, 1997). • Seasonal effects, particularly in small piles, can be severe, thereby obscuring the other features such as long term decay in release of oxidation products (Lawrence and Day, 1997). • Tests may take much longer than similar tests under laboratory conditions (Lawrence and Day, 1997) due to long residence times of water through the pile (Bennett et al. 2000). • Variations in rates that occur on time scales less than residence times cannot be obtained (Bennett et al. 2000). • The site needs to be carefully protected from damage by extreme climatic conditions and vandalism (Lawrence and Day, 1997). • Most expensive ARD prediction test due to required earthworks and analytical costs. • It cannot be assumed that test piles behave similarly to waste rock dumps.
Waste rock dumps	Oxidation rates may be estimated directly from full-scale waste rock dumps. The Australian Nuclear Science and Technology Organisation (ANSTO) has developed a method that can be	• Oxidation rates measured directly from representative mine waste in the field.	• Secondary mineralisation may control sulfate fluxes (Bennett et al. 2000). • Tests are required to be conducted for a significant period of time to coincide with the mechanics and time-scale of water

ARD Prediction Test	General Principles	Advantages	Disadvantages
	used to estimate oxidation rates in dumps and stockpiles based on monitoring changes in oxygen concentration as a function of depth and time. This method involves measuring the rate at which the oxygen concentration falls at a number of depths in a hole soon after installation. Bennett et al. (2000) describe this method.		transport in the WRD, which may be in the order of several years (Bennett et al. 2000). • Data only able to be collected after the WRD is created and therefore not available in the pre-feasibility and early stages of mine life.

The fundamental purpose of kinetic tests is to obtain reaction rates for the primary minerals in a sample from the flushes by:

$$\text{Rate (mmol kg(material)}^{-1}\text{ s}^{-1}) = \frac{\text{Concentration (mmol L}^{-1}) * \text{L water recovered}}{\text{mass sample (kg)} * \text{time between flushes (s)}}$$

Equation 1-12

Bennett et al. (2000) describe the following two methods, derived from Equation 1-2, for determining the pyritic oxidation rate of a sample of material using humidity cells and column tests:

(1) Measure the sulfate production rate and use the stoichiometry of the reaction to calculate the oxidation rate, according to:

$$\text{Oxygen consumption rate [kg(O}_2\text{) kg(material)}^{-1}\text{s}^{-1}] = 0.583 \times \text{Sulfate production rate [kg(SO}_4\text{)kg(material)}^{-1}\text{s}^{-1}]$$

Equation 1-13

This method equates the sulfate release rate to the sulfate production rate, which, in turn, relates to the pyritic oxidation rate using the stoichiometry of Equation 1-2. An important assumption in this method is that the flux of sulfate in leachate from a humidity cell or column is proportional to the sulfate production rate in the system. In systems where the infiltration or oxidation rates have changed it will take some time for the assumption to be valid (even assuming that sulfate is conservative in the system and that none is lost by precipitation). That time cannot be less than the residence time of water through the system.

The residence time is the time taken by a conservative pollutant (or tracer) to travel from the top of the system to the bottom, under the ambient, constant infiltration rate and can be determined by Equation 1-14. The water-filled volume fraction of waste rock generally falls between 0.15 and 0.25. The residence time can be considered to be a characteristic time-scale for any changes in the system to be fully represented in drainage.

$$\text{Residence time (s)} = \frac{\text{height of the system (m)} \times \text{water-filled volume fraction}}{\text{infiltration rate (m s}^{-1})}$$

Equation 1-14

(2) Measure the oxygen consumption rate in a system directly.

This method assumes that the sulfidic oxidation rate is the only oxygen consumer in the system. In suitably designed columns, this method can be used by sealing the system from the air and monitoring the decrease of oxygen contained in the known gas volume within the column. When designing such a column, it is important to incorporate a means of maintaining the gas pressure inside the column equal to the outside pressure, primarily to reduce the risk of air entering the column through any leaks in the system.

Both methods require oxygen to be freely available throughout the material at all times. Only under these conditions can the volume or mass of oxidising material be known. Columns have been known to give

erroneous results due to water saturation and consequent lack of oxygen availability (Parker and Robertson, 1999). It can be readily shown that in many systems the supply of oxygen to the reaction sites may be limited by the oxygen diffusion coefficient of the material, confining oxygen to a fraction of the total quantity of material. To ensure that oxygen is freely available in columns, Bennett et al. (2000) recommend that all columns be designed to enable pore gas oxygen consumption measurements be made to check that oxygen is not limiting oxidation. In materials with a high oxidation rate it may be necessary to maintain airflow through a column.

Sulfate flux can only be used as a measure of the rate of sulfidic oxidation if there is no significant loss of sulfate in the system through precipitation of sulfate minerals. The formation of species such as gypsum [$CaSO_4.2H_2O$] or jarosite [$KFe_3(SO_4)_2(OH)_6$] depends on the mineral composition of the material and on temperature, Eh, pH and the concentration of dissolved chemical species in pore water. Secondary minerals can form during weathering when solubility products are exceeded in the weathering solutions, so that states of mineral saturation or supersaturation are achieved. Loss of sulfate in a system due to secondary mineralisation will lead to an underestimation of oxidation rates (Bennett et al. 2000, Mehling Environmental Management Inc, 1998). An over-estimation of the oxidation rate may occur if pre-existing sulfate minerals dissolve during a test.

It must be noted that due to differences between processes in tests of different scale (see Table 1-4 for a comparison of processes in test piles and full-scale rock piles), weathering characteristics of the test samples and the resulting leachate chemistry cannot necessarily be directly used to predict on-site performance of a commercial waste rock dump. Final assessment of the data and predictions for the performance of the material, including appropriate scaling of the parameters to full-size, should include some modelling to take into account factors that are not controllable or reproduced in laboratory conditions. These include physical factors such as temperature, particle size distribution and height of dump, infiltration rates, and the degree of wetting to consider channelling. In addition, some geochemical modelling may be appropriate to be able to predict actual drainage quality from the test data (Bennett et al. 2000).

Table 1-4: Comparison of Processes in Test and Full-Scale Rock Piles (Lawrence and Day, 1997)

Process	Test piles	Waste rock dumps
Physical distribution of particles	Relatively homogeneous, lack of layering unless planned.	Extremely heterogeneous due to dumping techniques, variation in rock type and mining techniques. Layering and compacted layers probable.
Chemical composition of particles	Relatively homogeneous if planned. Readily defined by sampling.	Potentially complex due to changes in rock type during mining. Difficult to characterise due to physical heterogeneity.
Water movement	In small piles, relatively high proportion of rock particles contacted due to short distance from surface to base. Higher water to solid ratio. Retention time relatively low. Probable lack of water table(s).	Flow is complex due to internal variations in permeability. Flow is potentially concentrated in a number of small channels resulting in relatively low proportion of particles contacted by water. Water table(s) are possible both perched and at the dump base.
Effect of climatic processes	Snow melt and major rain events result in more rapid flow and expansion of flow paths into seasonally dry areas. Flushing of weathering products occurs. During dry periods, weathering products accumulate.	As per test piles.
Migration of solids	Large-scale failure unlikely. Small-scale transport of solids probable due to downward movement of water.	Large-scale failure possible. Small-scale transport of solids probable due to downward movement of water.
Gas transport	Wind advection is possibly dominant process of gas transport into and out of pile. Significant oxygen depletion within pile unlikely.	Thermal advection accepted as dominant process due to formation of temperature gradients within pile. Oxygen concentration gradients likely.
Internal reactions	Reactions comparable but fewer variables within pile due to lesser temperature and oxygen variation. Greater water flow and flushing of weathering products possibly important.	Extremely complex within various parts of the dump due to varying oxygen, temperature and water flow conditions.
Overall water chemistry	Less likely to be limited by saturation due to higher water flow. Metal concentrations potentially lower due to dilution and development of less acidic conditions, or higher due to lesser saturation control.	Water chemistry potentially controlled by saturation.

1.2.4 Scale-Up

The term scale-up is used to describe the linkages between ARD prediction tests made at increasing scales of particle size. Bennett et al. (2000) challenge the value of test piles and their usefulness in 'scaling up' from the laboratory to the field, questioning whether any information is obtained from test piles that could not be acquired from suitably-designed columns. In contrast, Mehling Environmental Management Inc. (1998) state that the extrapolation of results from field tests to full-scale piles is generally more realistic than direct extrapolations from laboratory to the field, since oxidation products are typically stored in full-scale piles. They also list larger particle sizes, more realistic blending conditions, and flushing regimes as important advantages in large scale kinetic tests. Furthermore, Coastech Research Inc (1991) state that the larger scale of field tests potentially allows a more realistic assessment of the ARD generation process and a better evaluation of control options such as limestone blending or covers than can be achieved in laboratory kinetic tests.

Bennett et al. (2000) identify and discuss a number of issues which may affect the validity of the different measurement techniques used to obtain oxidation rates at different size scales. Table 1-5 summarises each of the issues and includes recommendations from Bennett et al. (2000) on how the measurements could be improved.

Table 1-5: Factors which may affect the validity of different measurement techniques

Issue	Factors Possibly Affecting Validity	Recommendation/s
Oxygen Supply	The assumption made when deducing oxygen rate from sulfate release rates that all the material is free to oxidise. This assumption is likely to be valid in aerated humidity cells and columns, however is questionable in test piles, where diffusion cannot supply oxygen to all parts of the pile.	Programs using large columns, test piles or full size dumps should include instrumentation to enable pore gas oxygen concentrations to be determined throughout the system.
Sulfate Release	1. The assumption made when determining oxidation rates from sulfate release rates that there is no significant loss of sulfate from the system. 2. The assumption that pyrite is the only sulfidic mineral contributing to the production of sulfate.	1. Ensure the question of sulfate loss is addressed in work where conditions make secondary mineralisation likely. 2. Where sulfate precipitation is significant, measure oxygen consumption rates in columns to determine oxidation rates. If there are other sulfides oxidising at a significant rate or there is dissolution of sulfate minerals, ensure they are accounted for in relating sulfate release rate to oxidation rate.

Issue	Factors Possibly Affecting Validity	Recommendation/s
Water Residence Time	1. Long water residence times in columns and test piles have the potential to make the interpretation of some measurements impossible. 2. The sulfate flux can never be in equilibrium with conditions in the whole system in a test pile. Because the pile is subject to seasonal temperature and infiltration rate changes, sulfate fluxes cannot be used to quantify any time-dependence of periodic variations in oxidation rate which occur with a period less than the water residence time.	Ensure the water residence time is short compared with the rate of change of conditions within the system being measured so that information on rates and trends can be obtained from sulfate fluxes in leachate.
Particle Size	1. Particle size distribution is not a significant factor in determining the oxidation rate of particular material types over one to two year time-scales. 2. Laboratory measurements of the oxidation rate of samples containing a particle size distribution up to 200 mm can be taken to be representative of the oxidation rate of the material in full-sized dumps.	1. A realistic description of particle size distribution in a full-size dump is required to describe behaviour in the long term. 2. Experiments need to be run using columns containing particle size distributions up to 200mm for a period long enough to determine the dependence of IOR on sulfide sulfur content as the particles oxidise.
Temperature	The use of the Arrhenius equation to account for temperature differences between the laboratory and field, using activation energies measured in the laboratory for different sulfide minerals, may be reasonable for fine-grained materials where the sulfides may be largely liberated from the host materials, however, it seems less reasonable for run-of-mine material.	A program of work needs to be undertaken to establish the validity of the Arrhenius equation for bulk materials and to find more appropriate values of the activation energy of dominant sulfides.

Leachate composition from full-sized dumps is determined by a combination of parameters that vary in space and time. Bennett et al. (2000) list these parameters as;

- The acid generation rate in the oxidising material (governed by the IOR of the material, which has been found to vary over several orders of magnitude);
- The spatial distribution of oxidising material in the dump;
- The rate of neutralisation of the acid by gangue minerals (ranging from carbonates to silicates);
- The distribution of the acid consuming minerals in the dump;
- The evolution of oxidation in the dump as a function of space and time;
- The time it takes to completely oxidise sulfidic materials in the dump (years to hundreds of years);
- The functional form of the IOR (which depends on temp, oxygen concentration etc.); and
- The hydrology of waste rock dumps, including infiltration, residence times and flow paths.

Thus, according to Bennett et al. (2000), a test pile cannot represent a full-sized dump any better than a column when it comes to predicting the chemical composition of effluent as a function of time, or providing information such as the time for effluent from a dump to become acidic and the time over which pollutants will be generated. Bennett et al. (2000) further discuss limitations in scaling-up from laboratory experiments and test piles, including temperature and the transport of oxygen by diffusion.

1.2.5 Summary

Although there is a suite of ARD prediction techniques available, the link between results from laboratory-based tests and actual field behaviour is not clear (Ferguson and Firth, 2000). Various ARD prediction tests have been used in this study to assess the quality of leachate generated from blended waste rock material at ZCML. Results from this study will be used to improve the management of ARD at ZCML, and on a broader scale, address the issue of scale up of results between prediction tests of various particle sizes.

2 Chapter 2: Site Description

2.1 Introduction

ZCML comprises an open pit zinc, lead and silver mining and milling operation at Lawn Hill in northwest Queensland, concentrate dewatering and shipping facilities at Karumba in the Gulf of Carpentaria, and a 304km slurry pipeline connecting the two operations.

This chapter will describe the location and setting of the Zinifex Century Mine, the geology of the ore deposit and the region, mining methods employed, the classification of waste rock types and waste rock dump design.

2.2 Location and Regional Setting

The ZCML mine site is located 250km north-north-west of Mount Isa within the North West Queensland minerals province and is adjacent to Boodjamulla (Lawn Hill) National Park (Figure 2-1). The mine site is located at approximate latitude 18°44'S and longitude 138°36'E (Broadbent et al. 2002).

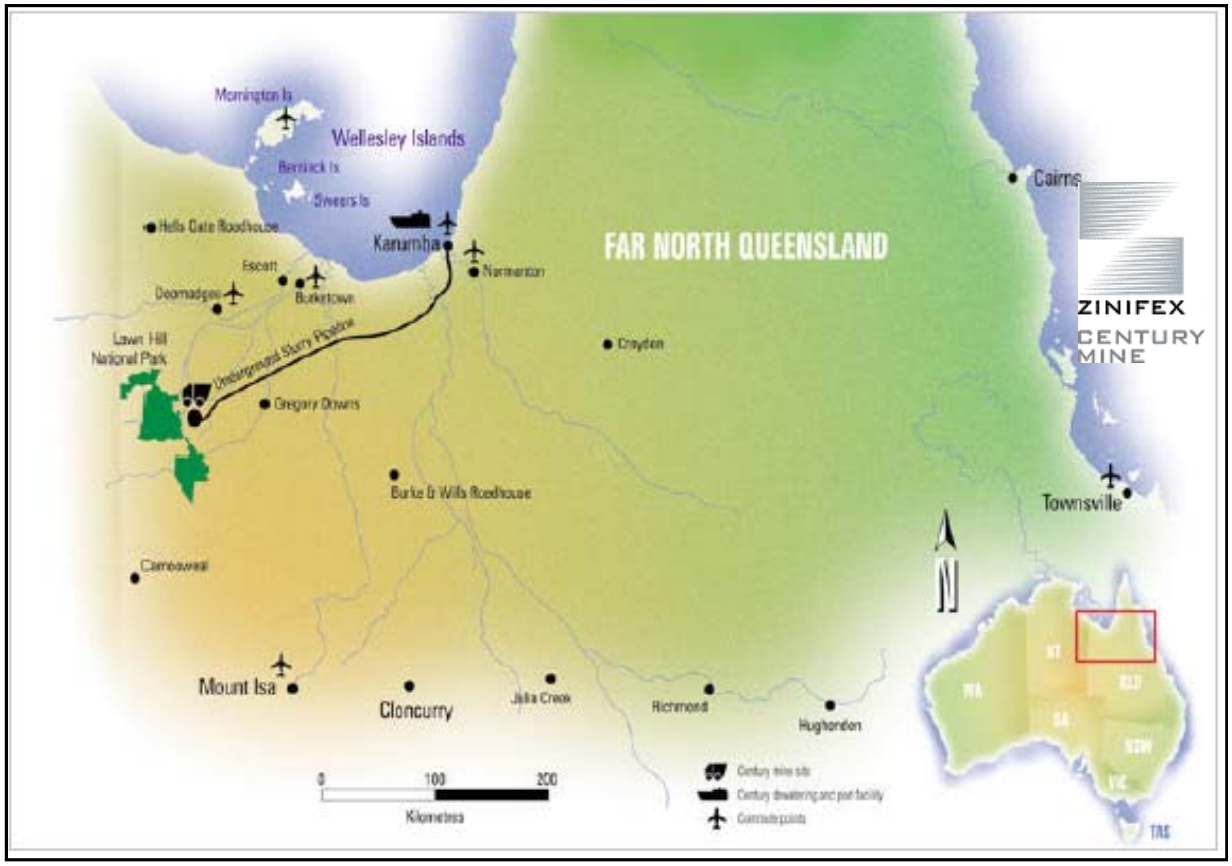

Figure 2-1: Location of Zinifex Century Mine (Zinifex Century Mine Limited, 2001)

The weather patterns at the ZCML mine site are classified as semi-arid with a distinct summer wet season and long winter dry season. The majority of the 530mm annual average rainfall occurs during January, February and March (Dames and Moore, 1994). January is typically the wettest month, with a mean long-term rainfall at Lawn Hill of 147mm, and August is the driest with a mean long-term rainfall of 1mm (Figure 2-2). Mean annual evaporation is approximately 3200mm, hence there is a considerable moisture deficit and the ground is dry for

the majority of the year. The mean daily maximum temperature at Lawn Hill ranges from 27.5°C (July) to 39.7°C (December) (Dames and Moore, 1994).

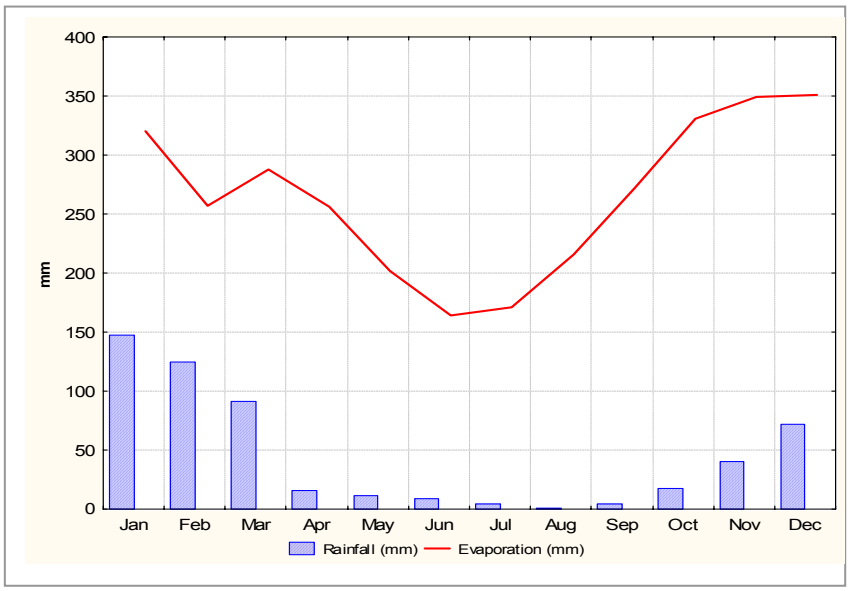

Figure 2-2: Mean Monthly Rainfall (Lawn Hill) and Evaporation (Mount Isa) Data (Dames and Moore, 1994)

Topography of the ZCML mining leases (covering approximately 23,530ha) includes low limestone hills, flat low-lying plains and outcropping Proterozoic hills primarily derived from sandstone, siltstone and shale. There are nine distinct vegetation communities found on the leases: six woodland, two grassland and one riparian, or creek line, community (Dames and Moore, 1994).

The ZCML Lawn Hill mining leases encompass five ephemeral creeks. These creeks are dry for the majority of the year, and stream water level monitoring has shown that creek flows correlate well to significant rainfall events (i.e. greater than 20mm) (Bates et al. 2000). The open pit and waste rock dumps are located in the upper reaches of the Page Creek catchment. Approximately 17km downstream to the north west of the leases, Page Creek enters the Lawn Hill Creek System. Downstream of Lawn Hill Station, Lawn Hill Creek joins the Gregory River and subsequently the Nicholson River prior to flowing into the Gulf of Carpentaria.

2.3 Geology

2.3.1 Regional Geology

The Century deposit occurs within the Mount Isa inlier, an area of more than 50,000km^2 of Middle Proterozoic sedimentary and volcanic rocks and granitoids in north-western Queensland (Broadbent et al. 2002). The Mount Isa inlier is divided into three broad tectonic units, termed the Western and Eastern fold belts, with the intervening Kalkadoon-Leichardt belt (Figure 2-3). In the Western fold belt, the Century, Mount Isa, Hilton, George Fisher, and Lady Loretta deposits are all hosted within a 5,000 to 10,000m thick pile of fine-grained clastic sedimentary rocks with minor volcanic rocks, collectively known as the McNamara Group (Broadbent et al. 2002). The siliciclastic rich rocks of the Upper McNamara group host the Century deposit. Broadbent et al.

(2002) review current understanding of the regional geology and geodynamic setting and describe the district scale stratigraphy, sedimentology and alteration of the Century deposit.

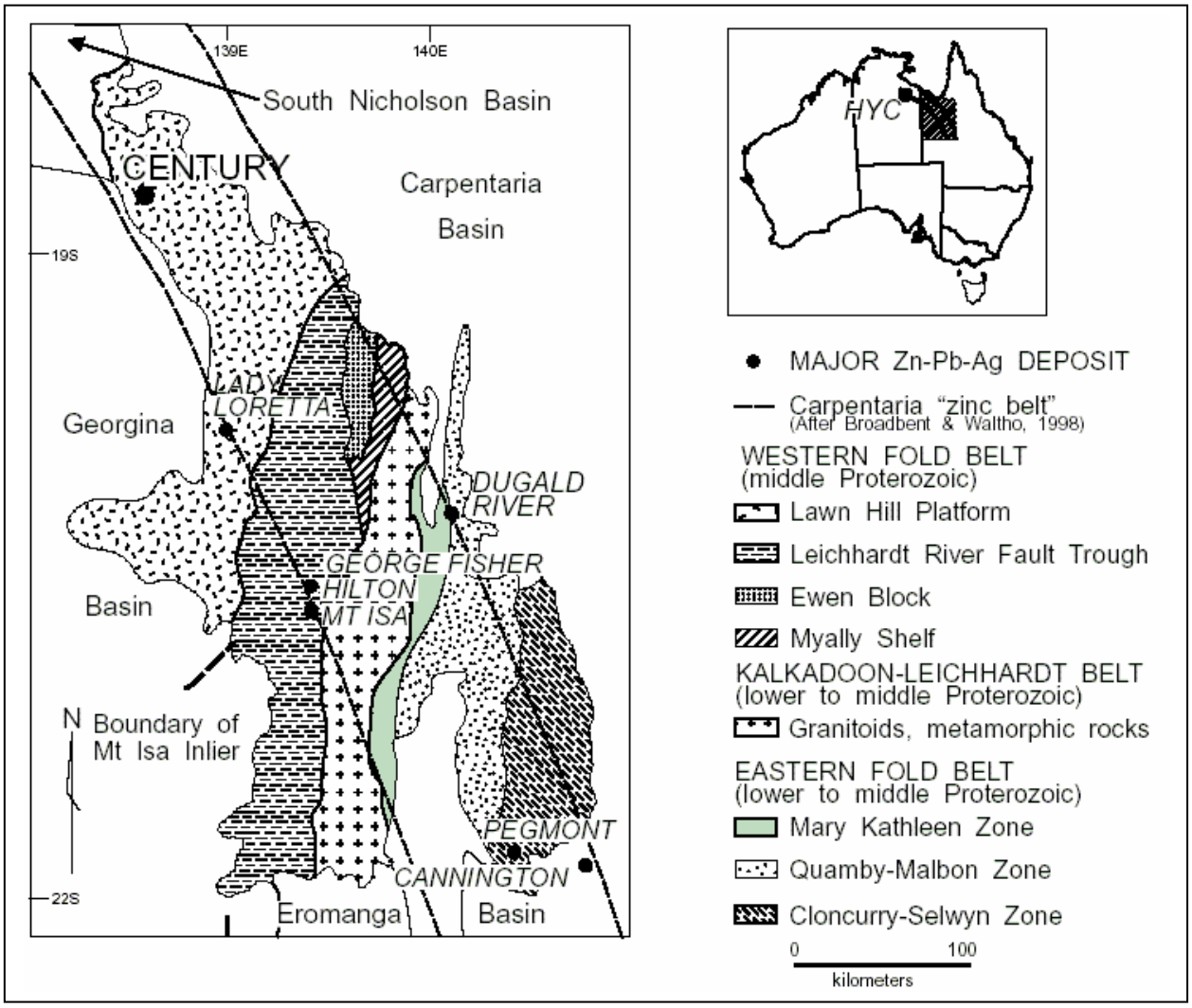

Figure 2-3: **Century deposit and major zinc-lead-silver deposits of the Carpentaria Mount Isa zinc belt (Broadbent et al. 2002)**

2.3.2 Ore Deposit Geology

Exposed Proterozoic rocks close to the Century deposit are represented by three formations of the Upper McNamara Group. These include the Riversleigh Siltstone, Termite Range Formation, and Lawn Hill Formation (Broadbent et al. 2002).

The Lawn Hill Formation conformably overlies the older Termite Range Formation, forming a north-south belt of about 6 to 11km width mainly in the western sector of the site and consisting of up to 2,300m thickness of shale, siltstone, tuff, minor sandstone and dolomite (Dames and Moore, 1994). The mineralisation forming the Century deposit occurs within the upper part of the Lawn Hill Formation. The unit is described as comprising 850m of flaggy to fissile siltstone, tuffaceous siltstone, carbonaceous shale and sandstone (Dames and Moore,

1994). The shales within the unit weather recessively leaving the sandstone and siltstone prominent on surface exposures (Dames and Moore, 1994).

Economic grade mineralisation consists of fine-grained sphalerite, galena and minor pyrite (Broadbent et al. 2002). The total resource is estimated at 167.5 million metric tons (Mt) of material grading at 8.2 percent zinc, 1.2 percent lead, and 33g t^{-1} silver, and includes a total high-grade resource of 105Mt grading 12.1 percent zinc, 1.7 percent lead, and 46g t^{-1} silver at a cut-off grade of 3.5 percent zinc (Broadbent et al. 2002). The ore mineralogy for the deposit is a simple assemblage of sphalerite, galena, and lesser pyrite associated with silica, siderite and pyrobitumen gangue (Broadbent et al. 2002). The mineralisation occurs typically as fine-grained 1mm-5mm thick laminations of alternating sulfide and carbonaceous shale layers (Broadbent et al. 2002). The fine-grain size and complex textural relationship between sphalerite, pyrobitumen and silica require a complex metallurgical process for extraction.

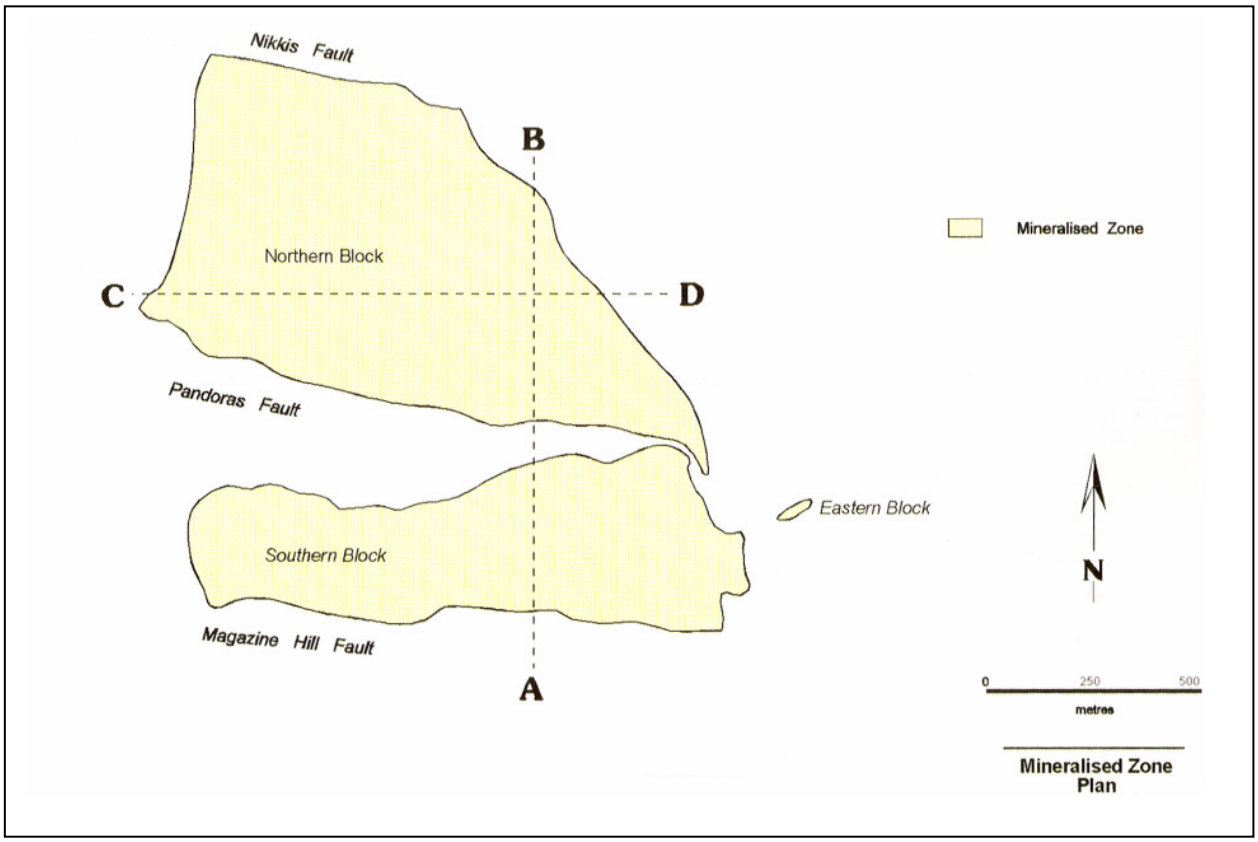

Figure 2-4: Mineralised Zone Plan (Dames and Moore, 1994)

Mineralisation has been defined in three separate blocks, referred to simply as the northern, southern and eastern blocks (Figure 2-4). The northern and southern blocks contain essentially all the currently defined resource (Dames and Moore, 1994). The extent of the mineralisation is constrained to the south by the Magazine Hill Fault, the eastern edge is defined by the Termite Range Fault and Cambrian-Proterozoic unconformity, the northern limit by Nikkis Fault and the western margin again by the limestone unconformity and erosion at the present-day land surface. Pandoras Fault, an east-west trending structure, splits the

mineralisation into the southern and northern ore blocks (Figure 2-4 and Figure 2-5). Minor pyrite occurs immediately above the mineralised sequence, and throughout the footwall carbonaceous shale forming the lower portion of the unit (Dames and Moore, 1994).

Two cross sections through the deposit are shown in Figure 2-5 and Figure 2-6. From both figures it can be seen that the host rock sequence consists of Cambrian Thorntonia Limestone cap rock (up to 100m thick), which unconformably overlies much of the deposit, and a Proterozoic sequence. The Cambrian Thorntonia Limestone consists of grey massive finely crystalline limestone and dolomite (Dames and Moore, 1994). The Proterozoic sequence comprises:

- Hangingwall Sandstone;
- Hangingwall Siltstone-shale;
- Mineralised zone hosting the stratiform zinc-lead-silver mineralisation (45m thick); and
- Footwall shale, siltstone and black carbonaceous shale.

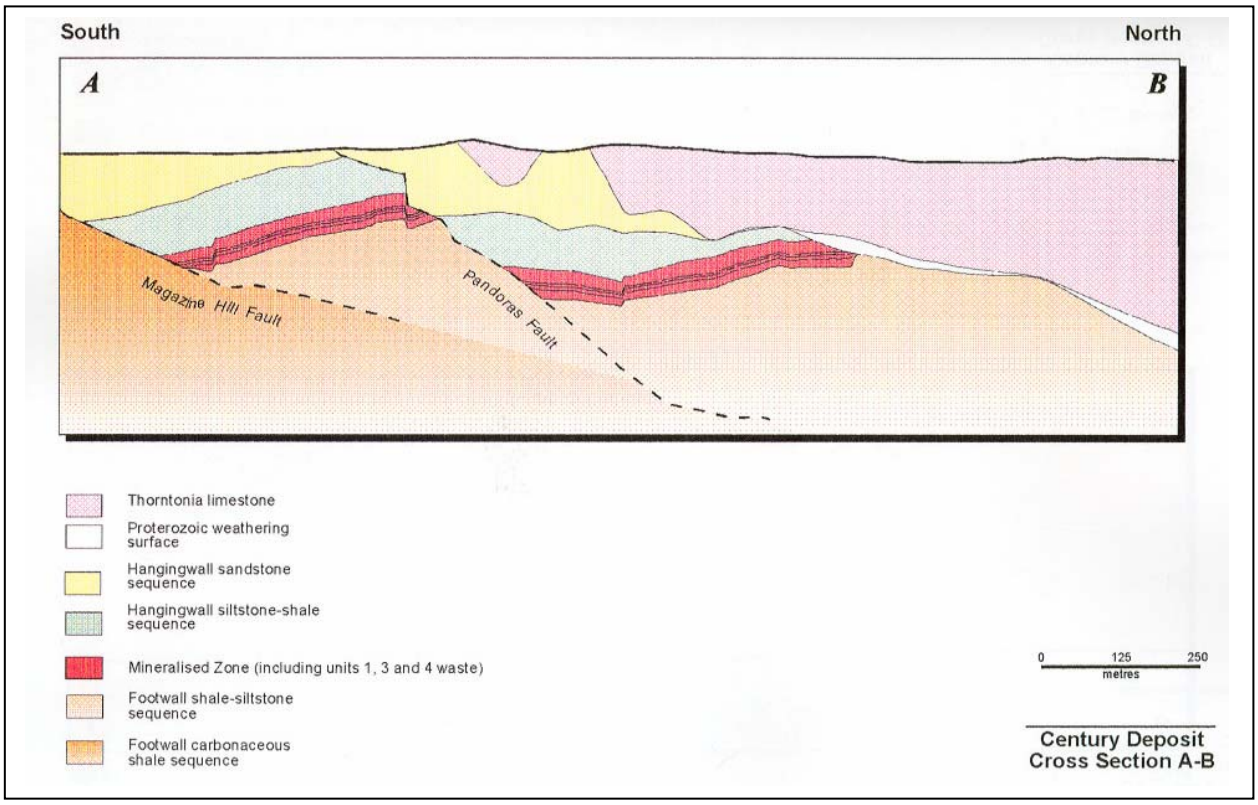

Figure 2-5: Century Deposit Cross Section A-B (Dames and Moore, 1994)

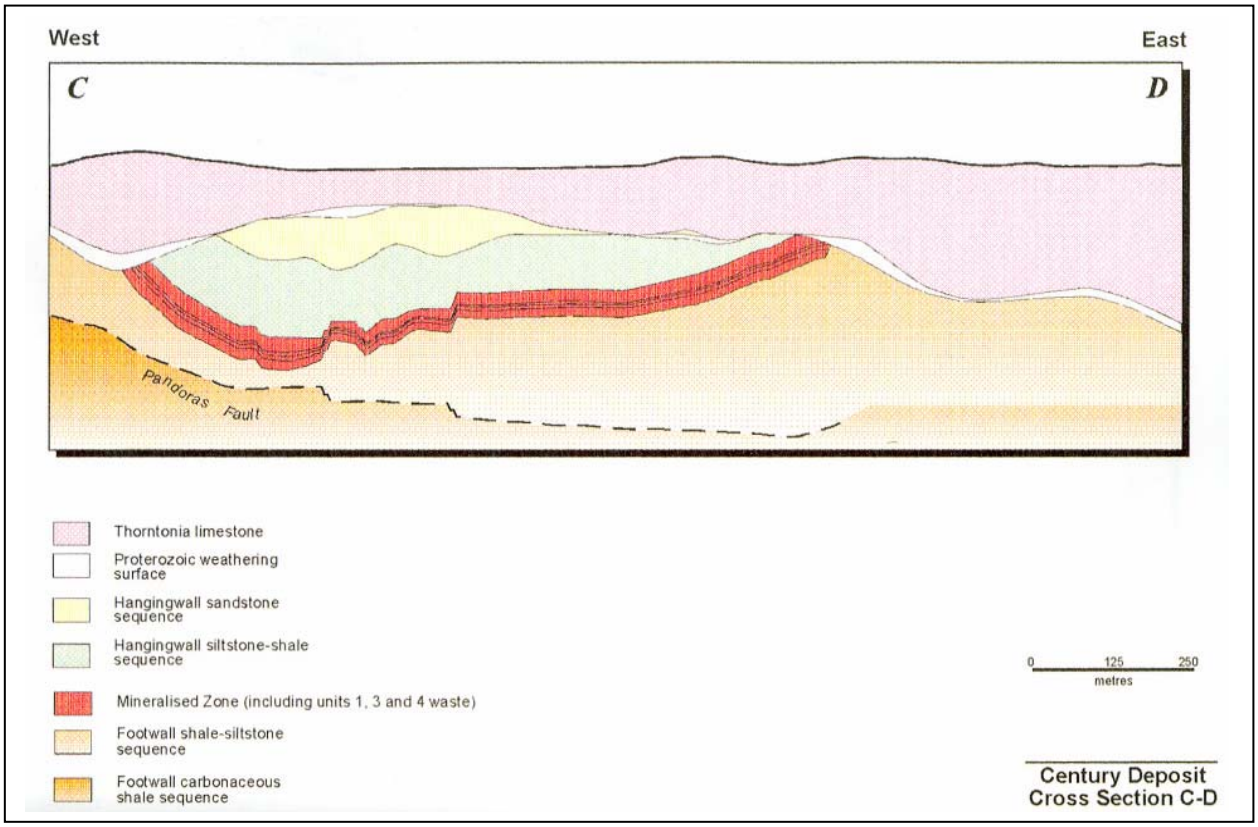

Figure 2-6: Century Deposit Cross Section C-D (Dames and Moore, 1994)

2.4 Mining Process Overview

A conventional open pit mining method, employing electric rope shovels, hydraulic excavators and haul trucks, is used by ZCML from a single pit. Pre-stripping operations commenced in April 1998. Waste rock is transported to one of three main waste rock dumps (Northern, Southern or Western), short haul dumps (e.g. Stage 7 Short Haul Dump) or is deposited via in-pit dumping methods in mined out stages of the open pit (Figure 2-7). The current mining rate is approximately 82MT y^{-1} waste rock and 8MT y^{-1} ore (Lee, 2006a) with an overall strip ratio (life of mine) of approximately 11.8:1 (Bates et al. 2000). A further 470MT of waste rock are anticipated to be mined between now and when mine operations are scheduled to cease in 2016 (Lee, 2006a).

Drainage from the WRDs and disturbed areas is diverted to sedimentation dams where it is either reused on site, evaporated during dry weather periods, pumped to the Tailings Storage Facility, or discharged to nearby ephemeral creeks during high rainfall, and hence flow, events. A network of point source and receiving water monitoring stations is installed to sample discharge and creek water quality during wet season flow events.

Approximately five million tonnes of ore is treated annually through the concentrator following a conventional crushing, grinding, and primary flotation circuit, and an ultrafine grinding and flotation circuit to separate the fine silica from the sphalerite. Batches of lead and zinc concentrate slurry are transported 304km along a 300mm underground pipeline to the port site at Karumba where it is filtered and dried prior to export shipping.


Page Creek
Western Waste
Rock Dump
Sedimentation Dam
No. 5
Northern Waste
Rock Dump
Page Creek Diversion
Open Cut
Bulk Sample Pit
ROM
Pad
Concentrator
Sedimentation Dam
No. 3
Sedimentation Dam
No. 2
Sth WRD
Seepage
Heap Leach
Pad Trials
Southern Waste
Rock Dump
ZINIFEX
CENTURY
MINE
Figure 2-7:
Zinifex Century Mine
Aerial Image
July 2005
0
200
400
600
metres

2.5 Waste Rock Classification

During the course of the mine's development, a number of studies were undertaken to characterise the ARD potential from different lithological units and aid assessment of the most suitable management options (Bates et al. 2000). Static testwork conducted by Environmental Geochemistry International Pty Ltd (EGi) classified waste rock samples from ZCML into four waste rock types (Table 2-1).

Table 2-1: Waste Rock Geochemical Classification (EGi, 1997a)

Waste Rock Type	NAG pH	NAG (kg H_2SO_4/t)	NAPP (kg H_2SO_4/t)	Description
I	≥ 4	0	< -100	Acid Neutralising or Consuming (AC)
II	≥ 4	0	≤ 0	Non Acid Forming (NAF)
III	< 4	≤ 10	0 < NAPP ≤ 10	Potentially Acid Forming - Lower Capacity (PAF-LC)
IV	< 4	> 10	> 10	Potentially Acid Forming - Higher Capacity (PAF-HC)

On the basis of the results for the test samples, a geochemical type distribution was assigned to each lithological unit within the open pit and combined with the proposed scheduled mined tonnage of that unit to estimate the total tonnes of each geochemical type on an annual basis (EGi, 1997a). The geochemical type distributions assigned to each lithological waste unit are given in Table 2-2. The assumptions inherent in the distributions are contained in EGi, 1997a.

Table 2-2: Waste Rock Distribution Used in Mine Waste Schedule (EGi, 1997a)

Major Rock Units	Percentage Distribution of Rock Type			
	Type I (AC)	Type II (NAF)	Type III (PAF - LC)	Type IV (PAF - HC)
Limestone (CLS) and Carbonate Breccia (CBX)	100%			
Weathered Sandstone and Siltstone		100%		
Hanging Wall Sandstone (HWS and HWB)		70%		30%
Hanging Wall Siltstone/Shale (HWD)		65%	17.5%	17.5%
Footwall Siltstone/Shale (UFW)			40%	60%
Ore Zone Waste (MIN)				100%[1]

[1] Note this is a conservative assumption but from an operational viewpoint it simplifies management of this type of material since no operational identification system will be required (EGi, 1997a).

In addition to the static testing program, column leach studies were conducted by EGi to provide information on the kinetics of sulfide oxidation, acid generation and metal leaching by some of the major rock units within the Century deposit. The following five laboratory scale columns prepared from drill core samples were established in June 1994 and ran for either 88 weeks (Columns 1 and 2) or 156 weeks (Columns 3, 4 and 5):

- Column 1: Hanging Wall Sandstone – Interbedded Black Shale (HWB)
- Column 2: Hanging Wall Siltstone (HWD)
- Column 3: Unit 1 Waste Rock
- Column 4: Unit 1 Waste Rock (85%) with Limestone (15%)
- Column 5: Unit 1 Waste Rock (50%) with Limestone (50%)

Summarised in EGi (1997b), the main findings from the column leach tests were:

- When first exposed to leaching, Hanging Wall Sandstone – Interbedded Black Shale, Hanging Wall Siltstone and Unit 1 Mineralised Waste initially generated leachate that was close to pH neutral. However, as leaching continued, there was significant oxidation of sulfides in each of the materials, and the pH of leachate decreased.
- HWB became the most acidic of the samples selected for column leach testwork. Leachate from HWB acidified to < pH 3.0 within 24 weeks of exposure to atmospheric conditions. The zinc concentration in the leachate also increased markedly and peaked at 1140mgL^{-1} (17.4mmol L^{-1}).
- The sample of HWD acidified to approximately pH 4.5 within 16 weeks of exposure to atmospheric conditions. The zinc concentration ranged up to 195mg L^{-1} (3.0mmol L^{-1}).
- The sample of Unit 1 Mineralised Waste acidified to approximately 3.7 within 28 weeks of exposure to atmospheric conditions. The zinc concentration in the leachate consistently exceeded 1000mg L^{-1} (15mmol L^{-1}) and ranged up to 1950mg/L (30mmol L^{-1}).
- Limestone addition to Unit 1 Mineralised Waste was effective in maintaining a pH neutral leachate. It also significantly reduced the rate of sulfate release (by approximately half) and markedly decreased the concentration of zinc in the leachate. With the addition of 15% (by weight) of limestone, the concentration of zinc typically ranged from 10 to 60mg L^{-1} (153 – 918mol L^{-1}), and with 50% limestone added, the typical range was 1 to 7mg L^{-1} (15 – 107mol L^{-1}).

Results from testing conducted by EGi in the mid-late 1990s therefore identified the potential for acidic leachate with elevated zinc concentrations to be generated from several types of ZCML waste rock. Limestone blending was found to be effective in maintaining a pH neutral leachate with lower dissolved metal concentrations, however, as will be discussed in section 2.6, limestone blending was not adopted as an ARD management tool by ZCML.

2.6 Waste Rock Dump Design

Similar to other mining operations, ARD at ZCML can potentially be produced from exposed pit surfaces, ore stockpiles, waste rock dumps and deposited tailings. In an attempt to manage ARD generation in the waste rock dumps, they are constructed in a particular manner.

Currently the only lithology that can be assumed to be suitable for placement on the outside of the dumps is CLS, as it is both non-acid forming and is a highly competent material (Bates et al. 2000). Due to the location of CLS material in the pit design (i.e. overlying the orebody) the limestone dumping strategy is limited by its timeframe of availability. This schedule limitation, the amount available and the difficulty to effectively blend NAF and PAF material in large scale dumping operations led ZCML to not use blending as a management tool (Bates et al. 2000) for ARD generation in the WRDs. The primary use of competent limestone is for the encapsulation cover construction.

For the practical application of the selective placement program for waste rock to minimise ARD generation, the "Type" classification system described in section 2.5 was modified to the "Class" system shown in Table 2-3.

Table 2-3: ZCML Waste Rock Class System (Bates et al. 2000)

Class	Description	Example
1 (I)	Competent rock, non-acid forming or acid-consuming material	Type I or II material which is competent
2 (II)	Non-competent, non-acid forming or acid-consuming material	Type I or II material which is not competent
3 (III)	Acid-forming material	Type III or IV materials

The class of a waste rock material determines where the rock is strategically placed within the dump. The generalised waste rock dump design comprises an outer zone of class 1 material and an inner zone of class 2 and 3 material (Figure 2-8). The following additional restrictions were assigned to the placement of type III and IV waste rock (Bates et al. 2000):

- Material will not be placed within 20m horizontally of the outer edge of the final dump profile; and
- Material will be buried at least 5m vertically by type I or II material (or class 1 and 2) when WRDs reach their final height.

It should be noted that assuming class 1 comprises only CLS is a conservative estimate since a proportion of the mined Hanging Wall Sandstone (HWS) is also non-acid producing and competent.

Current mining procedures specify that class 1 rock with greater than 5% contamination of class 3 material is to be placed in the inner zone of the waste rock dumps due to uncertainty surrounding the long-term acid producing capabilities of this rock. This procedure, as well as the additional restrictions on waste rock dump design, has the potential to cause significant scheduling problems, particularly in the latter stages of the mine life, due to relatively low proportions of class 1 rock available.

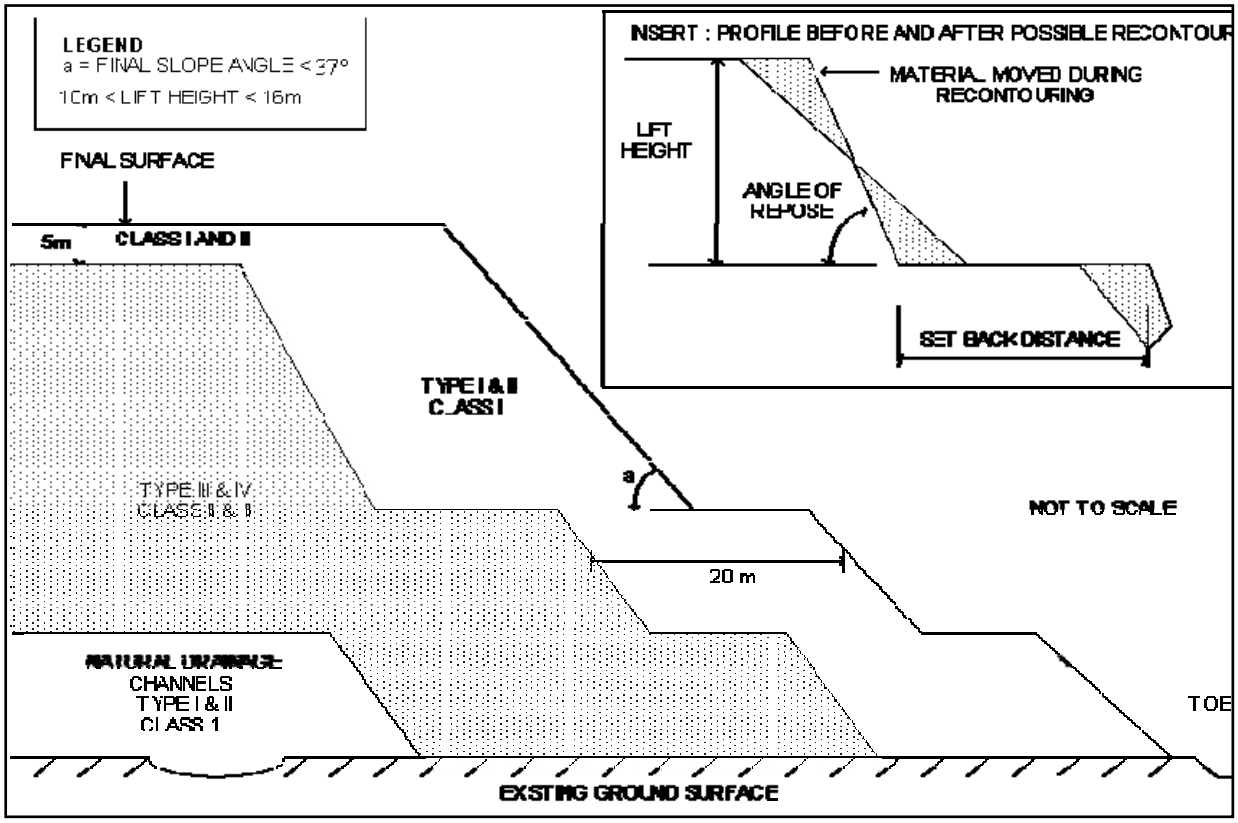

Figure 2-8: ZCML Conceptual Mine Waste Rock Dump Design (Bates et al. 2000)

3 Chapter 3: Static Tests

3.1 Introduction

Static tests are commonly used in ARD prediction to assess the balance between acid generating and acid neutralising minerals in a sample. A variety of static tests were applied to individual and blended samples of CLS and HWD to determine their reactivity. Acid base accounting, net acid generating tests and acid base characteristic curve testing was undertaken by EGi. The resultant technical memorandum is attached in Appendix 2. Cyclic voltammetry techniques were used to assess the reactivity of the HWD samples.

This chapter summarises the findings of the static testwork conducted by EGi and the cyclic voltammetry testwork conducted by the author. The results of the static testing are further discussed in Chapter 6: Scale-Up where they are compared to results from the kinetic testwork (column leach tests and heap leach pads) on the same rock type.

3.2 Methodology

Bulk samples of CLS and lower zone HWD for use in the static tests, CLTs and HLPs, were excavated from 1104-453 and 1008-335 areas of the ZCML open pit respectively in August 2002. Sub-samples were dispatched to AMDEL for crushing, sizing and mineralogical analysis prior to static testing (AMDEL, 2003 in Appendix 1).

3.2.1 Acid Base Analysis and NAG Testing

Three size fractions (<10mm, <50mm and <100mm) of CLS and HWD were dispatched to EGi for static testing. The samples were pulverised and the following lithology blends were prepared for each size fraction

- 100% CLS;
- 95% CLS / 5% HWD;
- 90% CLS / 10% HWD;
- 85% CLS / 15% HWD;
- 80% CLS / 20% HWD;
- 75% CLS / 25% HWD; and
- 100% HWD.

These samples underwent the following testing program:

- Acid Neutralising Capacity determination;

- Net Acid Generation testing*;
- Acid Buffering Characteristic Curve testing*; and
- Kinetic NAG testing*.

An explanation of the testing program commonly used by EGi for the assessment of acid forming characteristics of mine waste materials is included in Appendix 2.

3.2.2 Cyclic Voltammetry

Voltammetric techniques with carbon paste electrodes have been found to be suitable, versatile and rapid enough for multicomponent determinations, having both selectivity and sensitivity without needing several conditioning steps before analytical measurements are taken (Cisneros-Gonzalez et al. 1999). Cyclic voltammetry techniques were used to correlate the reactivity of HWD material contained within a carbon paste with the electrochemistry observed.

Prior to assessing the reactivity of HWD using cyclic voltammetry, the technique was tested on a blank sample containing 100% graphite and samples containing varying percentages of pure pyrite.

The pyrite sample was pulverised using a mortar and pestle and combined with graphite and Nujol oil to make a paste. Various pastes comprising different percentages of pyrite were prepared. The pastes were inserted into a carbon paste electrode (i.e. working electrode) and together with a mercury mercurous sulfate reference electrode and platinum mesh (i.e. auxiliary electrode) and 0.1M sodium perchlorate as the supporting electrolyte, electrochemical cells were established. A radiometer (VoltaLab PGZ301) was used to apply voltage to the samples from –300mV to 800mV and back to –300mV at a sweep rate of 10mV s^{-1}.

Similarly to the pyrite sample, a subsample of the HWD material used in the static, CLT and HLP experiments was pulverised using a mortar and pestle. A sample comprising 50% pulverised HWD and 50% powdered graphite was combined with Nujol oil to make a paste and, using the same methodology as the pyrite samples, cyclic voltammetry was used to assess the reactivity.

In order to assess the reactivity of a HWD sample after oxidation of the sulfides, hydrogen peroxide was added to a HWD subsample and reaction was allowed to proceed. Following reaction, the sample was rinsed with deionised water, filtered and dried prior to mixing with graphite and Nujol oil to make a paste. The paste was inserted into a carbon paste electrode and cyclic voltammetry techniques were applied to assess reactivity of the sample. Voltammograms for the HWD samples were assessed against those for the pyrite and blank graphite samples.

* testing on selected samples only.

3.3 Results and Discussion

Table 3-1 presents the acid forming characteristics of the HWD, CLS and blended samples as determined by the static testing conducted by EGi. These results are discussed in this section and attached in Appendix 2.

3.3.1 Acid-Base Analysis

3.3.1.1 Maximum Potential Acidity

The total sulfur content of a sample is used to determine the MPA that can be generated by a sample. The calculation for MPA assumes that all the sulfur measured in the sample occurs as pyrite (FeS_2) and that pyrite reacts under oxidising conditions to generate acid according to Equation 3-1 (EGi, 2004).

$$\mathbf{FeS_2 + 15/4O_2 + 7/2H_2O \leftrightarrows Fe(OH)_3 + 2H_2SO_4}$$

Equation 3-1

According to this reaction, the MPA of a sample containing 1%S as pyrite would be 30.6 kilograms of H_2SO_4 per tonne of material (i.e. kg H_2SO_4 t^{-1}). The MPA of a sample is therefore calculated from the total sulfur content using the following formula:

$$\mathbf{MPA\ (kg\ H_2SO_4\ t^{-1}) = (Total\ \%S) \times 30.6}$$

Equation 3-2

The use of the total sulfur assay to estimate the MPA is a conservative approach because some sulfur may occur in forms other than pyrite. Sulfate-sulfur and native sulfur, for example, are non-acid generating sulfur forms. Also, some sulfur may occur as other metal sulfides (e.g. covellite, chalcocite, sphalerite and galena) which yield less acidity than pyrite when oxidised or, in some cases, may be non-acid generating (EGi, 2004).

Total sulfur assays for the 100% CLS and 100% HWD samples were conducted by AMDEL (refer Appendix 1). EGi calculated the total sulfur contents for the blended samples based on the weight fraction of each sample included in the blend. The total sulfur contents for all samples are shown in Table 3-1.

As expected, the total sulfur contents in the 100% HWD samples passing 10mm, 50mm and 100mm were high to very high at 3.8%, 5.3% and 1.8% respectively. Total sulfur contents were lowest in the 100% CLS samples passing 10mm (0.10%), 50mm (0.09%) and 100mm (0.11%). Total sulfur contents for the blended samples increased with the proportion of HWD material in the sample.

Table 3-1: Acid-forming Characteristics of HWD and CLS Samples (EGi, 2004)

Century Sample Code		ACID-BASE ANALYSIS					NAG TEST			ARD Classification
Size Fration	Sample Description	Total %S*	MPA	ANC	NAPP	ANC/MPA Ratio	NAGpH	$NAG_{(pH4.5)}$	$NAG_{(pH7.0)}$	
			(kg H_2SO_4/t)					(kg H_2SO_4/t)		
<10 mm	Siltstone (<10 mm)	3.81	117	16	101	0.1	2.6	24	64	PAF
<50 mm	Siltstone (<50 mm)	5.34	163	12	151	0.1	2.3	48	89	PAF
<100 mm	Siltstone (<100 mm)	1.84	56	18	38	0.3	3.5	2	30	PAF
<10 mm	Limestone (<10 mm)	0.10	3	884	-881	289	-	-	-	NAF
<50 mm	Limestone (<50 mm)	0.09	3	853	-850	310	-	-	-	NAF
<100 mm	Limestone (<100 mm)	0.11	3	939	-936	279	-	-	-	NAF
<10 mm	95% Limestone/ 5% Siltstone	0.29	9	945	-936	108	-	-	-	NAF
<10 mm	90% Limestone/ 10% Siltstone	0.47	14	858	-844	60	-	-	-	NAF
<10 mm	85% Limestone/ 15% Siltstone	0.66	20	815	-795	41	-	-	-	NAF
<10 mm	80% Limestone/ 20% Siltstone	0.84	26	786	-760	31	-	-	-	NAF
<10 mm	75% Limestone/ 25% Siltstone	1.03	31	732	-701	23	8.3	0	0	NAF
<50 mm	95% Limestone/ 5% Siltstone	0.35	11	898	-887	83	-	-	-	NAF
<50 mm	90% Limestone/ 10% Siltstone	0.62	19	847	-828	45	-	-	-	NAF
<50 mm	85% Limestone/ 15% Siltstone	0.88	27	797	-770	30	-	-	-	NAF
<50 mm	80% Limestone/ 20% Siltstone	1.14	35	777	-742	22	-	-	-	NAF
<50 mm	75% Limestone/ 25% Siltstone	1.40	43	708	-665	16	8.1	0	0	NAF
<100 mm	95% Limestone/ 5% Siltstone	0.20	6	896	-890	149	-	-	-	NAF
<100 mm	90% Limestone/ 10% Siltstone	0.28	9	851	-842	98	-	-	-	NAF
<100 mm	85% Limestone/ 15% Siltstone	0.37	11	814	-803	72	-	-	-	NAF
<100 mm	80% Limestone/ 20% Siltstone	0.46	14	794	-780	57	-	-	-	NAF
<100 mm	75% Limestone/ 25% Siltstone	0.54	17	719	-702	43	7.9	0	0	NAF

KEY

* All Total S results for 100% Siltstone and 100% Limestone samples have been measured (results provided by Pasminco Century Mine). All total S results for the composite samples have been calculated from the 100% samples.

MPA = Maximum Potential Acidity (kgH_2SO_4/t)

ANC = Acid Neutralising Capacity (kgH_2SO_4/t)

NAPP = Net Acid Producing Potential (kgH_2SO_4/t)

NAF = Non-Acid Forming

PAF = Potentially Acid Forming

3.3.1.2 Acid Neutralising Capacity

The acid formed from pyrite oxidation will to some extent react with acid neutralising minerals contained within the sample. This inherent acid buffering is quantified in terms of the ANC. The following description of ANC is taken from EGi (2004).

The ANC is commonly determined by the Modified Sobek method. This method involves the addition of a known amount of standardised hydrochloric acid (HCl) to an accurately weighed sample, allowing the sample time to react (with heating), then back-titrating the mixture with standardised sodium hydroxide (NaOH) to determine the amount of unreacted HCl. The amount of acid consumed by reaction with the sample is then calculated and expressed in the same units as the MPA (i.e. kg H_2SO_4 t^{-1}).

The HWD samples had very low ANC values of 16kg H_2SO_4 t^{-1} (<10mm), 12kg H_2SO_4 t^{-1} (<50mm) and 18kg H_2SO_4 t^{-1} (<100mm) (EGi, 2004). ANC values for the CLS samples were 884kg H_2SO_4 t^{-1} (<10mm), 853kg H_2SO_4 t^{-1} (<50mm) and 939kg H_2SO_4 t^{-1} (<10mm). ANC for the blended samples increased with the percentage of CLS in the sample.

3.3.1.3 Net Acid Producing Potential

The NAPP is a theoretical calculation commonly used to indicate if a material has potential to produce acidic drainage. The following discussion of NAPP is taken from EGi (2004). Expressed in units of kg H_2SO_4 t^{-1}, the NAPP represents the balance between the capacity of a sample to generate acid (MPA) and its capacity to neutralise acid (ANC) and is calculated as follows:

$$\mathbf{NAPP = MPA - ANC}$$

Equation 3-3

If the MPA is less than the ANC, the NAPP value is negative, which indicates that the sample may have sufficient ANC to prevent acid generation. Alternatively, if the MPA exceeds the ANC, the NAPP value is positive, indicating that the material may be acid generating.

As shown in Table 3-1, the 100% HWD samples had NAPP values of 101kg H_2SO_4 t^{-1} (<10mm), 151kg H_2SO_4 t^{-1} (<50mm) and 38kg H_2SO_4 t^{-1} (<100mm). These results indicated that the HWD material might be acid generating. All the blended samples had negative NAPP values, indicating that limestone blending may be effective in controlling the pH of leachate generated from waste rock.

As noted in the technical memorandum prepared by EGi (Appendix 2), the results for the blended samples were based on well mixed, crushed and pulverised samples. The static testing results indicated the overall geochemical characteristics of the bulk sample and do not reflect the ARD characteristics of individual particle sizes, which commonly occur when limestone is mixed with other rock types for ARD control. In an operational limestone and PAF rock mix (either direct truck dumped or crusher / conveyor dumped), the limestone is typically coarse grained and segregation typically results in limestone preferentially reporting to the coarse size fractions and the PAF rock preferentially reporting to the finer fractions. Because of the higher particle surface

area of the finer fraction, it is critical that these size fractions contain an adequate amount of limestone to ensure an effective blend for ARD control. It is therefore important when scaling up the results of these types of tests to evaluate the particle size distributions of the individual material types (CLS and HWD) as well as the blends.

3.3.1.4 ANC/MPA Ratio

The ANC/MPA ratio is frequently used as a means of assessing the risk of acid generation from mine waste materials (EGi, 2004). The purpose of the ANC/MPA ratio is to provide an indication of the relative margin of safety (or lack thereof) within a material. Various ANC/MPA values are reported in the literature for indicating safe values for preventing acid generation (EGi, 2004). As a general rule, an ANC/MPA ratio of $\geq$ 2.0 indicates that there is a high probability the material will remain circum-neutral in pH and thereby should not be problematic with respect to acid drainage (EGi, 2004). It should be noted that this assumes that the rate of sulfate production is not exceeded by the rate of acid neutralisation and will therefore only be valid if the pyritic material doesn't react very quickly.

The results contained in Table 3-1 show that the ANC/MPA ratio of the three 100% HWD samples were less than the value of 1.0 and were therefore classified as having a high potential for ARD generation. The ANC/MPA ratios of the blended samples for the three different size fractions ranged from 16 (75% CLS / 25% HWD <50mm) to 149 (95% CLS / 5% HWD <100mm). The high ANC/MPA ratio of the blended samples indicated that a uniformly graded blend of siltstone and limestone is unlikely to be problematic with respect to acid rock drainage (EGi, 2004).

3.3.2 Net Acid Generation Test

The NAG test is used in association with the NAPP to classify the acid generating potential of a sample (EGi, 2004). The NAG test involves reaction of a sample with H_2O_2 to rapidly oxidise any sulfide minerals contained within the sample. During the NAG test both acid generation and acid neutralisation reactions can occur simultaneously. Therefore, the end result represents a direct measurement of the net amount of acid generated by the sample. This value is commonly referred to as the NAG capacity and is expressed in the same units as NAPP (i.e. kg H_2SO_4 t^{-1}) (EGi, 2004).

Several variations of the NAG test have been developed to accommodate the wide geochemical variability of mine waste materials. The three main NAG test procedures are the Single Addition NAG Test, the Sequential NAG Test and the Kinetic NAG Test (EGi, 2004). The Single Addition NAG Test was conducted on the 100% HWD and the 75% CLS / 25% HWD samples and the Kinetic NAG Test was conducted on the 100% HWD samples.

3.3.2.1 Single Addition NAG Test

The single addition NAG test involves the addition of 250mL of 15% H_2O_2 to a 2.5g sample. The H_2O_2 is allowed to react with the sample overnight and the following day the sample is gently heated to accelerate the

oxidation of any remaining sulfides, and then vigorously boiled for several minutes to decompose residual peroxide. When cool, the pH and acidity of the NAG liquor are measured. The acidity of the liquor is then used to estimate the net amount of acidity produced per unit weight of sample (EGi, 2004).

An indication of the form of the acidity is provided by initially titrating the NAG liquor to pH 4.5 and then continuing the titration up to pH 7.0. The titration value at pH 4.5 includes acidity due to free acid (i.e. H_2SO_4), as well as soluble iron and aluminium. The titration value at pH 7.0 also includes metallic ions that precipitate as hydroxides at pHs between 4.5 and 7.0 (EGi, 2004).

In order to confirm that all the blended samples were NAF, the 75% CLS / 25% HWD blends (i.e. the samples with the highest amount of PAF material), underwent NAG testing. The results of NAG testing are presented in Table 3-1. These results show that the three 100% HWD samples each had a NAGpH below 3.5, indicating that the HWD material was PAF. Conversely, the samples of the three blends of 75% CLS / 25% HWD material each had a NAGpH above 7.0. This indicated that the 75% CLS / 25% HWD blend was NAF and suggested that other blends containing a smaller percentage of HWD were also classified as NAF.

Titrations of the NAG liquor to pHs 4.5 and 7.0 were conducted for the 100% HWD and 75% CLS / 25% HWD samples. The 75% CLS / 25% HWD blended samples did not register any acidity in the sample. The large differences in the $NAG_{(pH4.5)}$ and $NAG_{(pH7.0)}$ values for the 100% HWD samples may be due to metallic ions such as copper or zinc, which are relatively soluble at a pH value of 4.5 (EGi, 2004). The metallic ions increase the NAG $pH_{7.0}$ values through the formation of insoluble metal hydroxides.

3.3.2.2 Kinetic NAG Test

The Kinetic NAG Test is conducted in the same manner as the Single Addition NAG Test with the exception that the temperature, pH and sometimes, electrical conductivity (EC) of the liquor are recorded. Variations in these parameters throughout the test provide an indication of the kinetics of sulfide oxidation and acid generation (EGi, 2004). This, in turn, can provide an insight into the behaviour of the material under field conditions.

Kinetic NAG testing was conducted on the three 100% HWD size fractions and the results are presented in Appendix 2 Table 2 and are replicated as Table 3-2 below. The results show that the three HWD samples were highly reactive. The pH of the NAG solution for each of the three samples started above a value of 6.0 and decreased rapidly to a pH of 2.0. The decrease in pH coincided with an increase in the temperature of the NAG solution, indicating that catalytic decomposition of H_2O_2 had occurred (EGi, 2004).

The time to pH 4.0 during the Kinetic NAG Tests were 5, 2 and 6 minutes for the <10mm, <50mm and <100mm HWD samples respectively. The rapid rate of pH drop indicated very little lag time prior to the onset of ARD generation and that materials represented by the samples are likely to develop acid conditions within one month of exposure to moist atmospheric conditions (EGi, 2004).

Table 3-2: Summary of Kinetic NAG Data for 100% Siltstone Size Fractions (EGi, 2004)

Sample Code	Initial pH	Final pH	Time to 1 pH Unit Drop (min)	Time to pH 4 (min)	Maximum Temperature (°C)	Time to Maximum Temperature (min)
<10mm Siltstone (100%)	6.4	2.0	3	5	104	30
<50mm Siltstone (100%)	7.0	2.2	<1	2	103	18
<100mm Siltstone (100%)	6.3	2.3	4	6	85	59

3.3.3 Acid Buffering Characteristic Curve

Acid Buffering Characteristic Curves were created for the 100% HWD and 100% CLS samples in order to determine the proportion of the ANC in each of the samples that was readily available for acid neutralisation (EGi, 2004).

The ABCCs for the <10mm, <50mm and <100mm 100% HWD samples are presented in Figures 1 to 3, Appendix 2. The results show that the <10mm and <50mm HWD samples had very little ability to buffer the pH of the samples above a value of 7.0. The <100mm HWD sample showed a very brief initial period of buffering where the pH remained above a value of 7.0. This buffering was equivalent to about 1.5kg H_2SO_4 t^{-1} (EGi, 2004).

The ABCCs for the <10mm, <50mm and <100mm CLS samples are presented in Figures 4 to 6, Appendix 2. The results show that all of the ANC in the three 100% CLS samples was readily available for acid neutralisation (EGi, 2004). In addition, the samples provided strong buffering of the pH above 6.0.

3.4 Cyclic Voltammetry

Results from the cyclic voltammetry testwork are contained in Appendix 3. The current density for the blank 100% graphite sample was zero (Figure A3-1). Figure A3-2 (90% graphite / 10% pyrite), Figure A3-3 (94% graphite / 6% pyrite) and Figure A3-4 (95% graphite / 5% pyrite) show that current densities increased with the increasing percentage of pyrite in the sample. As the height of the peak indicates the rate at which oxidation occurred, it could be seen that oxidation rates were faster for samples containing greater percentages of pyrite.

Figures A3-5 (50% graphite / 50% HWD) and A3-6 (50% graphite / 50% HWD after reaction with H_2O_2) highlight the difference in the reactivity of the HWD sample before and after oxidation of the sulfides with H_2O_2. The different shape of the voltammogram compared against voltammograms for the pyrite samples indicated that sulfides other than pyrite might have been oxidised in the HWD sample when exposed to the voltage applied.

These preliminary cyclic voltammetry experiments indicate that cyclic voltammetry may potentially be used to assess sulfide reactivity. However, the observation that sulfides other than pyrite contribute to the cyclic voltammetry response combined with limited availability of time, precluded further investigation of cyclic voltammetry as a predictor of ARD.

3.5 Static Testing Summary

Results from the static tests will be further discussed and compared against results from kinetic tests (column leach tests and heap leach pads) in Chapter 6: Scale-Up. Notwithstanding, the results from the geochemical static testwork conducted on pulverised samples of CLS and HWD are summarised as follows:

- Static test results for 100% HWD samples indicated that they were potentially acid forming with a high capacity to generate acid with little to no lag period. In addition, the large difference between the $NAG_{pH4.5}$ and $NAG_{pH7.0}$ values of the 100% HWD samples suggested that metallic ions such as copper or zinc might be a concern in leachate from the HWD material.
- Static testing results for 100% CLS samples indicated that they were NAF and had very high ANC values. These results suggested that the samples were readily available for acid neutralising and buffering.
- All the blended samples from the <10mm, <50mm and <100mm size fractions were classified as NAF, had strong NAPP values and high ANC/MPA ratios (EGi, 2004), indicating that limestone blending may be effective in controlling the pH of leachate generated from waste rock.
- Results obtained from cyclic voltammetry testing confirmed the reactivity of the HWD material and support further investigations in the application of cyclic voltammetry to assess waste rock reactivity.

4 Chapter 4: Column Leach Tests

4.1 Introduction

Column leach tests containing different blends of CLS and HWD were established to assess the quality of leachate generated over time and to calculate oxygen consumption rates of the waste rock blends. Twenty CLTs comprising five different waste rock blends and three particle size distributions were designed, constructed and operated in a laboratory environment for a two-year sampling period. Five replicate CLTs were established. The CLTs were periodically flushed with distilled water in an attempt to simulate rainfall events and accelerate the oxidation of pyrite under controlled conditions. Leachate from the CLTs was collected for analysis.

This chapter will present the design and methodology used for the CLTs and will discuss the quality of leachate produced from the tests, consequences for acid rock drainage generation and compliance with ZCML regulatory discharge limits.

4.2 Methodology / Design

4.2.1 Design and Construction

Twenty CLTs containing 10kg of blended waste rock material were established in an air-conditioned laboratory at ZCML for the following five lithology blends:

- 95% CLS / 5%, HWD;
- 90% CLS / 10% HWD;
- 85% CLS / 15% HWD;
- 80% CLS / 20% HWD; and
- 75% CLS / 25% HWD.

The various lithology blends were chosen to assess sulfide oxidation with increasing percentage of PAF material. Particle sizes were varied to determine if a relationship could be established between particle size and acid generation. For each blend, separate CLTs were assembled for particle size distributions passing 100mm, 50mm and 10mm. Five replicate CLTs were constructed for the mid lithology blend and particle size distribution (i.e. 85% CLS / 15% HWD < 50mm).

Table 4-1 provides a breakdown of the lithology types and particle size distribution for each CLT. Note that after the first six-month sampling period, Column 19, a replicate column, was dismantled to enable assembly of a duplicate for Column 12. To avoid confusion between these two CLTs, data from the original Column 19 has been excluded from the discussion of results. They are, however, included in Appendix 4.

Table 4-1: Composition of Each Column Leach Test

CLT no.	Lithology Blend	Particle Size
1	95% CLS / 5% HWD	<10mm
2	90% CLS / 10% HWD	<10mm
3	95% CLS / 5% HWD	<50mm
4	90% CLS / 10% HWD	<50mm
5	95% CLS / 5% HWD	<100mm
6	90% CLS / 10% HWD	<100mm
7	80% CLS / 20% HWD	<10mm
8	75% CLS / 25% HWD	<10mm
9	80% CLS / 20% HWD	<50mm
10	75% CLS / 25% HWD	<50mm
11	80% CLS / 20% HWD	<100mm
12	75% CLS / 25% HWD	<100mm
13	85% CLS / 15% HWD	<50mm
14	85% CLS / 15% HWD	<10mm
15	85% CLS / 15% HWD	<50mm
16	85% CLS / 15% HWD	<50mm
17	85% CLS / 15% HWD	<50mm
18	85% CLS / 15% HWD	<100mm
19	85% CLS / 15% HWD	<50mm
19*	75% CLS / 25% HWD	<100mm
20	85% CLS / 15% HWD	<50mm

* After the first six-month sampling period, Column 19 was dismantled to enable assembly of a duplicate for Column 12. To avoid confusion, data from the initial Column 19 have been excluded from interpretation, however are included in Appendix 4.

The CLTs were constructed from 140mm internal diameter electrical grade PVC pipe. Each column possessed an in-built filtering system of 2mm and 88μm nylon-sieve mesh (Figure 4-1). The mesh was held within the internal diameter of the column by a PVC ring. Araldite adhesive was used to secure the PVC ring to the

column and nylon sieve mesh. The CLTs were supported upright by a custom-made frame (Figure 4-3). Leachate from each CLT flowed freely through a 150mm internal diameter buchner funnel to a 1L glass collection vessel.

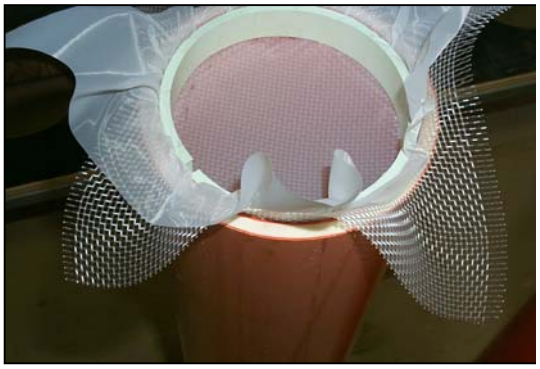

Figure 4-1: Assembling Column Leach Test Filtering System

Figure 4-2: Column Leach Test Apparatus

4.2.2 Sampling, Analysis and Interpretation

As noted in section 3.2, bulk samples of CLS and lower zone HWD for use in the static testing, CLTs and HLPs, were excavated from 1104-453 and 1008-335 areas of the ZCML open pit respectively in August 2002. Sub-samples were dispatched to AMDEL for crushing, sizing and mineralogical analysis (AMDEL, 2003 in Appendix 1) prior to use in the tests.

The CLTs were periodically flushed and left to dry in an attempt to simulate the wetting and drying cycles of waste rock in field conditions. Approximately 1L of distilled water was periodically (approximately fortnightly) flushed through the CLTs. This volume represented a typical wet season rainfall event of approximately 16mm and took up to two hours to pass through the columns. The fortnight period between flush events allowed the waste rock material to dry and oxidise between flush cycles.

Leachate was collected from each CLT and dispatched to the Australian Centre for Tropical Research (ACTFR) and the Advanced Analytical Centre (AAC) at James Cook University (JCU) for analysis of physical parameters and total and dissolved metals. Metal analysis was conducted on monthly composite samples from each CLT using Inductively Coupled Plasma – Mass Spectrometry (ICP-MS) to American Public Health Association standard method 3125 B. Samples analysed for dissolved metals were filtered at the time of sample collection using a 0.45µm filter. Parameters analysed and their respective laboratory detection limits are contained in Table 4-2. Where results were recorded as below detection limit, a value of half the laboratory detection limit was attributed to the sample.

It should be noted that in January 2004, after the first six-month sampling period, the CLTs were relocated by road transport to an air-conditioned laboratory at JCU to enable the author to continue the project following cessation of employment at ZCML. Although the relocation facilitated the delivery of samples to the laboratory immediately following flush events thereby minimising sample holding times, concentrations of most

parameters were elevated in flushes immediately following the relocations. Water quality data for the first five flushes following relocation were therefore excluded from the general dataset, however were included in mass balance calculations for the CLTs. The implication of the relocation on total metal results is discussed further in section 5.3.3.1.

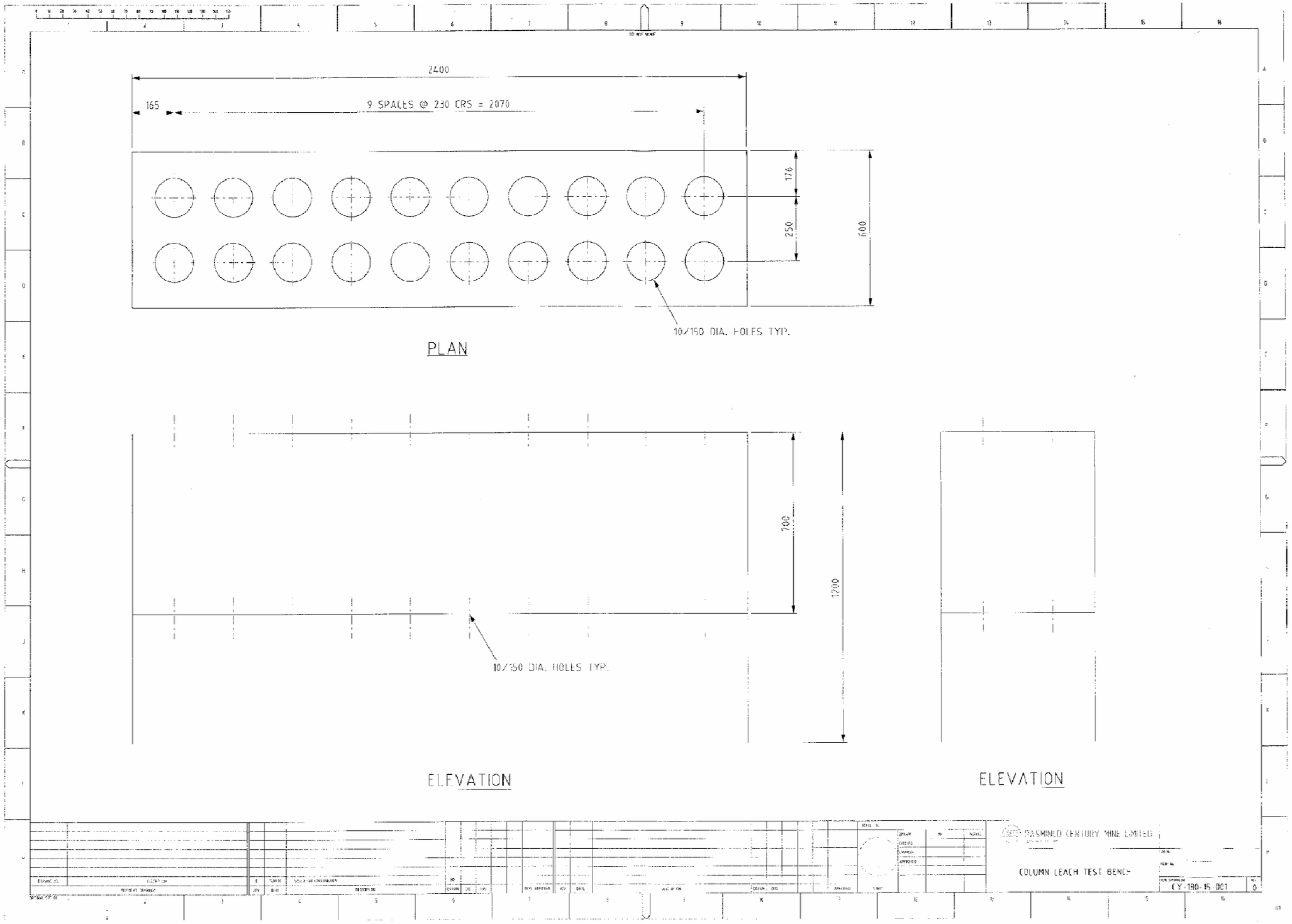

Figure 4-3: **Column Leach Test Custom Built Frame**

Table 4-2: Parameters Analysed in CLT Leachate and Corresponding Laboratory Detection Limits

Physical Parameters		Total and Dissolved Metals	
Parameter	**Detection Limit**	**Parameter**	**Detection Limit**
pH	N/A	Arsenic	1μg L^{-1}
Electrical Conductivity	N/A	Aluminium	0.5μg L^{-1}
Total Dissolved Salts (TDS)	N/A	Cadmium	0.1μg L^{-1}
Total Hardness	N/A	Cobalt	0.1μg L^{-1}
Total Alkalinity	0.1mg CaCO3 L^{-1}	Chromium	0.1μg L^{-1}
Total Acidity	5mg CaCO3 L^{-1}	Copper	0.1μg L^{-1}
Sodium	1mg L^{-1}	Iron	100μg L^{-1}
Potassium	1mg L^{-1}	Mercury	0.5μg L^{-1}
Calcium	1mg L^{-1}	Manganese	0.1μg L^{-1}
Magnesium	1mg L^{-1}	Nickel	0.1μg L^{-1}
Sulfate	1mg L^{-1}	Lead	0.1μg L^{-1}
Chloride	1mg L^{-1}	Selenium	1μg L^{-1}
Carbonate	0.1mg L^{-1}	Zinc	0.1μg L^{-1}
Bicarbonate	1mg L^{-1}		

Method IRON (3500-Fe Phenanthroline Method) (APHA, 1998) was used to determine the speciation of iron in leachate from CLTs on 31 January 2005. Because of the instability of ferrous iron, which is oxidised to the ferric form in solutions in contact with air, the determination of ferrous iron was conducted immediately following a column leach test flushing cycle.

Leachate samples were acidified with hydrochloric acid solution and mixed with phenanthroline and ammonium acetate buffer solutions prior to the measurement of colour intensity with a spectrophotometer. Values recorded were compared against a calibration curve created from standard iron solutions. Separate samples were submitted to AAC for determination of total iron concentrations. Ferric iron concentrations were determined by subtracting the ferrous iron concentration from the total iron concentration.

As discussed in section 1.2.3.2, sulfate production (or release) and neutralising potential depletion rates are often calculated in ARD kinetic testwork to enable the time to sulfide and neutralising potential depletion to be assessed (Mehling Environmental Management Inc, 1998, Morin and Hutt, 1997). Sulfate production and neutralising potential depletion rates were calculated for leachate from each CLT.

Sulfate production rates were calculated by multiplying the sample sulfate concentration by the volume of leachate recovered and dividing by the product of the total sample mass and time between flush event, i.e.:

$$\textbf{SO}_4\textbf{ production rate (mmol(SO}_4\textbf{) kg(material)}^{-1}\textbf{ s}^{-1}\textbf{) =} \frac{\textbf{SO}_4\textbf{ (mmol L}^{-1}\textbf{) * L water recovered}}{\textbf{mass sample (kg) * time between flushes (s)}}$$

Equation 4-1

Sulfate production rates are expected to be reasonable estimates of sulfide oxidation rates if oxidation products are continuously flushed from the test vessel, or corrections are made for stored oxidation products at the end of the test period (Mehling Environmental Management Inc, 1998). The estimated time to sulfide depletion in each CLT was calculated by dividing the total sulfide content (in SO_4 equivalent units) by the oxidation rate, i.e.:

$$\textbf{Estimated Time to S depletion (s) =} \frac{\textbf{(mmol S in sample- mmol S flushed from sample)}}{\textbf{(mass sample (kg) * Median SO}_4\textbf{ production rate (mmol SO}_4\textbf{ / kg (material)}^{-1}\textbf{ s}^{-1}\textbf{)}}$$

Equation 4-2

Usually the oxidation rate is calculated when the test reaches a steady state, i.e. relatively consistent sulfate loading rate over a period of greater than four weeks (Mehling Environmental Management Inc, 1998). In calculations for the column leach tests, the median sulfate production rate was calculated from the last ten flush events, when the majority of systems had reached steady state (refer Figure 4-9).

As neutralising potential (NP) in the CLTs was provided by calcium and magnesium carbonates (refer Appendix 1), and in the absence of gypsum in the original sample or as a stored oxidation product in the test vessel (confirmed by observation and geochemical modelling – see sections 4.3.5 and 4.3.6), the NP depletion rate was calculated from the calcium and magnesium concentrations in the test effluent (Mehling Environmental Management Inc, 1998). The NP depletion rate for each sample was calculated as follows:

$$\textbf{NP Depletion Rate (mmol CaCO}_3\textbf{eq kg (material)}^{-1}\textbf{ s}^{-1}\textbf{) =} \frac{\textbf{(Ca (mmol L}^{-1}\textbf{) + Mg (mmol L}^{-1}\textbf{)) * L water recovered}}{\textbf{kg sample}}$$

Equation 4-3

The estimated time to NP depletion (flushes) was calculated by dividing the total NP by the NP depletion rate, i.e.:

$$\textbf{Estimated Time to NP depletion (s) =} \frac{\textbf{(mmol NP in sample- mmol NP flushed from sample)}}{\textbf{(mass sample (kg) * Av NP depletion rate (mmol CaCO}_3\textbf{eq kg(material)}^{-1}\textbf{ s}^{-1}\textbf{))}}$$

Equation 4-4

The neutralising potential depletion rate was calculated from calcium and magnesium concentrations when they reached relatively steady values for four weeks or more (Mehling Environmental Management Inc, 1998). Neutralising potential depletion rates for the last ten flushes were used to calculate the median rate.

In accordance with Equation 1-13, the oxygen consumption rate (mmoles(O_2) kg(material)$^{-1}$ s^{-1}) for material in each CLT was calculated by multiplying the sulfate production rate by 0.583. Values were then normalised for the amount of sulfur contained in each sample to remove sulfur content as a variable that may potentially confound the interpretation of factors such as particle size on reactivity.

4.2.3 Column Dismantling

At the conclusion of the sampling period, a selection of CLTs was dismantled to enable the condition of the HWD and CLS material to be assessed. Material comprising the CLTs was inspected for precipitation of secondary minerals, including the armouring of carbonate material.

4.2.4 Geochemical Modelling

Geochemical modelling using Visual MINTEQ was used to determine the solubility phases of the different minerals present in leachate from Column 8 (75% CLS / 25% HWD, <10mm). Column 8 leachate was modelled because the waste rock blend in the CLT produced the highest sulfate production rate when the anomalous behaviour of Columns 12 and 19 (both 75%CLS / 25% HWD, <100mm) were excluded. Visual MINTEQ and its DOS-based version MINTEQA2 were also used throughout the interpretation of dissolved metal concentrations to calculate the solubility of different species. MINTEQ is a very widely used geochemical modelling program and the utility in ARD is discussed in detail in Langmuir (1997).

4.2.5 Data Presentation

Box and whisker plots are frequently used throughout this chapter to present the results from the column leach tests. In a box and whisker plot, ranges or distribution characteristics of values of a selected variable (or variables) are plotted separately for groups of cases defined by values of a categorical (grouping) variable (StatSoft, 2004). The central tendency (e.g. median or mean), and range or variation statistics (e.g. quartiles, standard errors or standard deviations) are computed for each group of cases, and the selected values are presented in the selected box plot style.

In the box and whisker plots contained within this thesis, the data are presented in a format that indicates:

- the location of the centre of the data (i.e. median), represented by the square contained in the box;
- the range of 50% of the data represented by the box. The upper box value (UBV) is the 75th percentile and the lower box value (LBV) is the 25th percentile;
- the non-outlier range (i.e. range of values that fall below the upper outlier limit (i.e. 1.5*height of the box) and above the lower outlier limit (i.e. –1.5*height of the box)), denoted by whiskers;

- outliers and extremes (i.e. atypical records, infrequent observations and datapoints which do not appear to follow the characteristic distribution of the rest of the data (StatSoft, 2004)).

A data point is deemed to be an outlier if the following conditions hold:

datapoint value > UBV + o.c.*(UBV – LBV)

or

datapoint value < LBV + o.c.*(UBV – LBV)

where:

UBV is the upper value of the box in the box plot (i.e. 75th percentile)

LBV is the lower value of the box in the box plot (i.e. 25% percentile)

o.c. is the outlier coefficient (1.5 by default).

A data point is deemed to be an extreme value if the following conditions hold:

datapoint value > UBV + 2*o.c.*(UBV – LBV)

or

datapoint value < LBV + 2*o.c.*(UBV – LBV)

Thus, extreme values are those that fall outside the three box length range from the upper and lower value of the box (StatSoft, 2004).

4.3 Column Leach Test Results and Discussion

Laboratory analysis data for the column leach tests are contained in Appendix 4 and are discussed in this section.

4.3.1 Replication of results

A number of documented column leach test studies have included the operation of duplicate (e.g. Li, 1999) or triplicate (e.g. Payant and Yanful, 1995) columns. In this project, five replicate CLTs were assembled for the 85% CLS / 15% HWD, <50mm blend to enable the repeatability of results to be assessed.

Box and whisker plots for replicate CLT leachate pH values and sulfur-normalised oxygen consumption rates are shown in Figure 4-4(a) and (b) respectively. As shown in Figure 4-4(a), median pH values for leachate sampled from CLT replicates, displayed by the square contained within the 25%-75% data range, varied from a minimum of 6.7 (Column 16) to maximum of 7.3 (Columns 15, 17 and 20). Non-outlier ranges extended from approximately 6.2 – 7.4 (Columns 13 and 16) to 6.4 – 7.8 (Columns 15, 17 and 20). Due to the contents of each CLT continually changing, statistical tests weren't conducted and instead the results were inspected for similarity. The mean of the median values was 7.1 and the variance in the range corresponded to a maximum value of ±5.3%, demonstrating a remarkable similarity in pH values between the replicate CLTs.

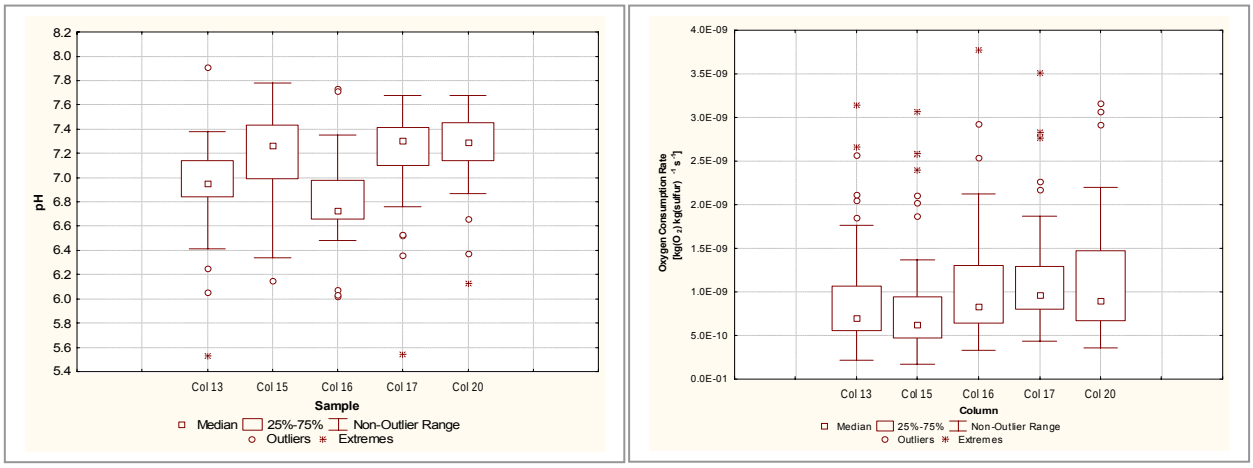

(a) pH Values (n=58) **(b) Oxygen Consumption Rate (sulfur) (n=57)**

Figure 4-4: Column Leach Test Replicates

Box and whisker plots for replicate CLT replicate sulfur-normalised oxygen consumption rates are shown in Figure 4-4(b). It should be noted that some extreme values were excluded from this plot to assist the scale. The median oxygen consumption rates (sulfur) for each replicate CLT were 7.0×10^{-10} mol(SO_4) kg(sulfur)$^{-1}$ s^{-1} (Column 13), 6.2×10^{-10} mol(SO_4) kg(sulfur)$^{-1}$ s^{-1} (Column 15), 8.3×10^{-10} mol(SO_4) kg(sulfur)$^{-1}$ s^{-1} (Column 16), 9.6×10^{-10} mol(SO_4) kg(sulfur)$^{-1}$ s^{-1} (Column 17) and 9.0×10^{-10} mol(SO_4) kg(sulfur)$^{-1}$ s^{-1} (Column 20). The non-outlier range for the five replicate CLTs was less than 2.0×10^{-9} mol(SO_4) kg(sulfur)$^{-1}$ s^{-1}. The mean of the replicate oxygen consumption rate (sulfur) median values was 8.0×10^{-10} mol(SO_4) kg(sulfur)$^{-1}$ s^{-1} and the variance in the range corresponded to a maximum value of ±22%, a good certainty.

The relative standard deviation for replicate sulfate concentrations was 19%, considerably less than the 33% relative standard deviation for cumulative acidity calculated for triplicate column leach tests in Payant and Yanful (1995). In contrast to Payant and Yanful, due to pH neutral conditions in leachate from replicate CLTs, the relative standard deviation for acidity could not be calculated. Due to the comparable pH values and oxygen consumption rates between the replicate CLTs, it was therefore concluded that each individual CLT was representative of the lithology and particle size fraction it represented.

4.3.2 pH Values

Box and whisker plots for pH values in leachate collected from all CLTs during the 24-month sampling period are shown in Figure 4-5 (entire sampling period) and Figure 4-6 (categorised into six-monthly sampling periods).

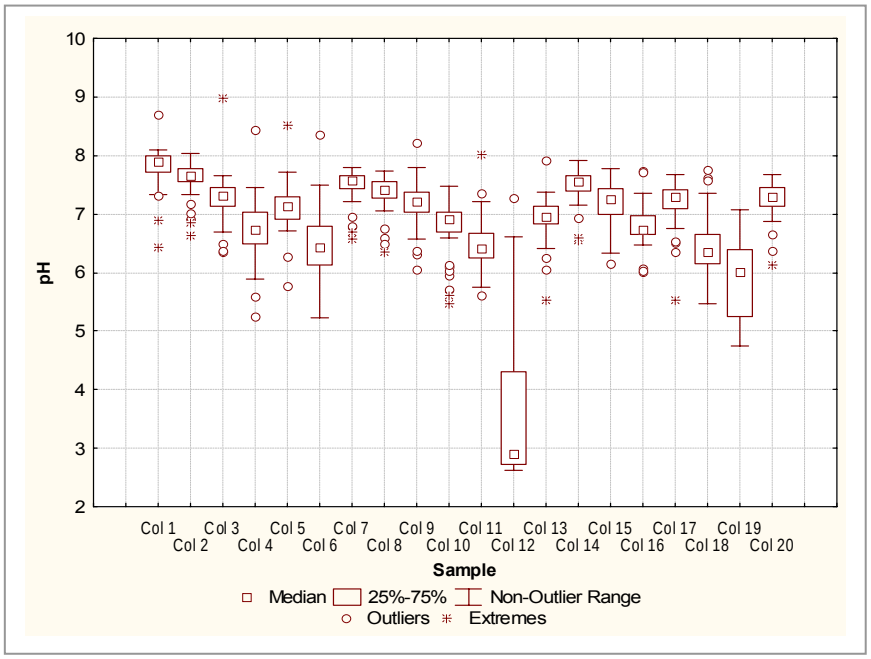

Figure 4-5: **Column Leach Test pH values**

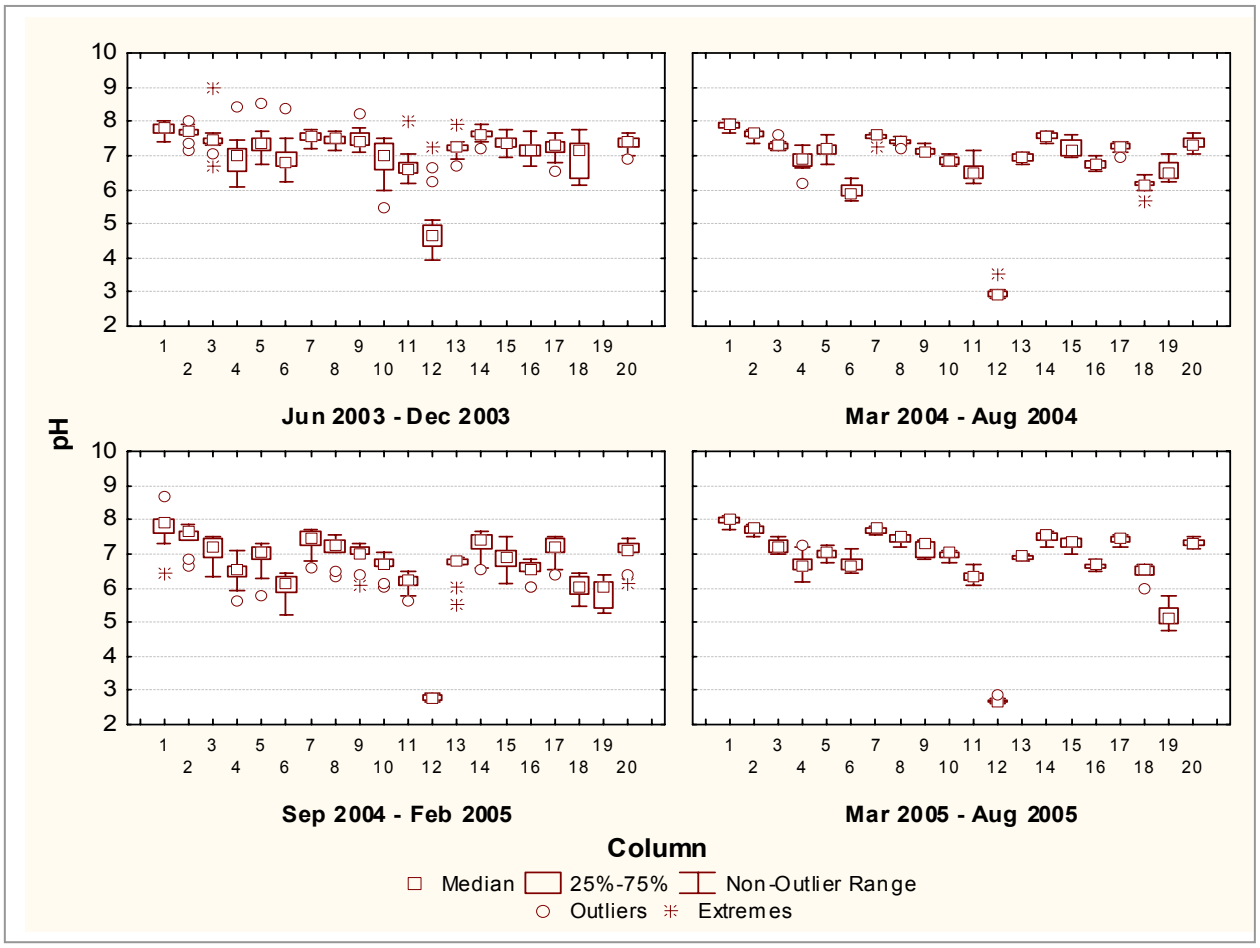

Figure 4-6: **CLT pH Values: Time Series**

It will be recalled from Table 4-1 that Columns 1, 3 and 5 contained the same waste rock blend (i.e. 95% CLS / 5%, HWD) but differed in particle size; particle size distributions increased with the number of the CLT (i.e. Column 1 contained material <10mm, Column 3 <50mm and Column 5 <100mm). The same pattern was evident in Columns 2, 4 and 6 (90%CLS / 10% HWD), Columns 7, 9 and 11 (80% CLS / 20% HWD) and Columns 8, 10 and 12 (75%CLS / 25% HWD). Evident in Figure 4-5 and Figure 4-6, pH values in leachate consistently trended down with increasing particle size in all waste rock blends. This trend is also indicated below:

increasing particle size →

columns 1 and 2 (<10mm), columns 3 and 4 (<50mm), columns 5 and 6 (<100mm)

→ **decreasing pH**

The more acidic leachates emanated from CLTs comprising waste rock with the greatest particle size of <100mm (i.e. Columns 6, 12, 18 and 19). Of particular note was the behaviour of Column 12, a mixture of 75% CLS / 25% HWD <100mm, and that of Column 19, its duplicate established after the first six months of sampling. Although the pH values in leachate collected from Column 19 didn't fall as rapidly as those in leachate from Column 12 (Figure 4-6), by the final six-monthly sampling period, its median pH value was 5.1, the lowest after Column 12 (2.7).

Despite static tests conducted on this blend indicating that the vast excess of acid consuming material would prevent the leachate from turning acidic (refer Chapter 3: Static Tests), leachate sampled from Column 12 and Column 19 had overall median pH values of less than 3.0 and 6.0 respectively. These values indicated that either armouring of the CLS material in these CLTs was occurring, or insufficient contact time of the leachate with CLS was preventing acid neutralisation.

Armouring refers to the process where acidic solutions, highly concentrated in iron and sulfur, interact with the carbonate-mineral surface forming an amorphous ferric oxyhydroxide coating on the carbonate mineral surface (Simón et al. 2004) according to:

$$\mathbf{Fe^{3+}_{(aq)} + 3OH^{-}_{(aq)} \rightarrow Fe(OH)_{3(s)}}$$

Equation 4-5

The iron hydroxide coating, which has a characteristic orange stain, is extremely insoluble (K_{sp} $Fe(OH)_3$ ~$10^{-37.1}$ (Langmuir, 1997)), inhibits the rate of carbonate dissolution and significantly diminishes the production of alkalinity (Evangelou, 1995). The description of armouring in this thesis is consistent with the literature (Langmuir, 1997 and Evangelou, 1995).

Columns 12 and 19 were dismantled at the conclusion of the sampling period to enable the extent of rock weathering and secondary mineralisation to be assessed. Shown and discussed in section 4.3.5, armouring of CLS material and weathering of the HWD material, particularly in Column 12, contributed to the low pH values in leachate.

The pH range permitted for waters discharged from ZCML, as specified in Environmental Authority No. MIM8000020402 is 6.0 – 9.0 (Ecoaccess, 2004). The pH value non-outlier range for leachate sampled from Columns 4, 6, 11, 12, 18 and 19 exceeded the lower limit of this range. With the exception of Column 4, the five other CLTs contained particle sizes of the largest size fraction (i.e. <100mm). It is therefore likely that the lower pH values in leachate samples from these CLTs may be attributed to the armouring of CLS material or water short-circuiting through the larger pore spaces.

As will be discussed in section 6.3, the sampled water quality of leachate from the heap leach pads corresponded more closely with to that of leachate sampled from column leach tests containing smaller particle sizes than those containing waste rock of greater size fractions. It is believed this was due to the substantial amount of weathering of material comprising the HLPs (see Figure 5-20), which best reflected the physical characteristics of waste rock in CLTs containing samples of particle size distributions passing 10mm (Figure 4-34). Consequently, the trend of lower pH values in larger particle sized CLTs (i.e. Columns 4, 6, 11, 12, 18 and 19) is not believed to be representative of field conditions at the Zinifex Century Mine.

4.3.3 Sulfate

4.3.3.1 Sulfate Concentration

Sulfate concentrations in leachate sampled from the 20 CLTs were explored for each six-month sampling period and are presented in Figure 4-7 and Figure 4-9. Sulfate concentrations in leachate from Column 12 (75% CLS / 25% HWD, <100mm) far exceeded those in leachate from other CLTs. Due to scale differences, sulfate concentrations in leachate from Column 12 are presented separately in Figure 4-8.

Of particular note was the increasing sulfate concentration in leachate from Column 12 throughout the 24-month sampling period (see Figure 4-8 and Figure 4-9). This behaviour was not mirrored in many other CLTs except Columns 11, 18 and 19 (the duplicate for Column 12)[2], which all contained particle size distributions passing 100mm. With the exception of outliers and extremes in datasets for several CLTs in the first six-month sampling period, which were attributed to the first flush effect of leaching surface salts, sulfate concentrations were relatively stable and appeared to have reached steady state by the second sampling period. Shown in Figure 4-9, this behaviour was primarily observed in Columns 1, 2, 3, 5, 7, 8, 9, 10, 14, 15, 16 and 20.

Excluding the behaviour exhibited by Columns 12 and 19, CLTs containing samples with smaller sized particle size distributions (e.g. Columns 7 and 8 (<10mm)) generally yielded higher sulfate concentrations in leachate than those containing samples with larger particle size distributions (e.g. Columns 4 and 10 (<50mm)). The increase in reactivity was attributed to the higher surface area to volume ratio of sulfides in CLTs comprising smaller particle size fractions. This trend was the reverse of the pH value trend discussed in section 4.3.2, where pH decreased with an increase in particle size.

[2] Note: Column 19 was established as a duplicate for Column 12 at the commencement of the second six-monthly sampling period (i.e. March 2004).

Unlike pH, which decreased with the extent of CLS armouring, sulfate concentrations were not affected by the armouring of carbonate material. Sulfate is a measure of the oxidation of pyrite to form sulfuric acid and may therefore be present in ARD during and after the neutralisation of acidity (H^+ ions). Neutralisation of H^+ by AC material does not directly affect sulfate concentration so the linkage between pH and sulfate concentration is decoupled.

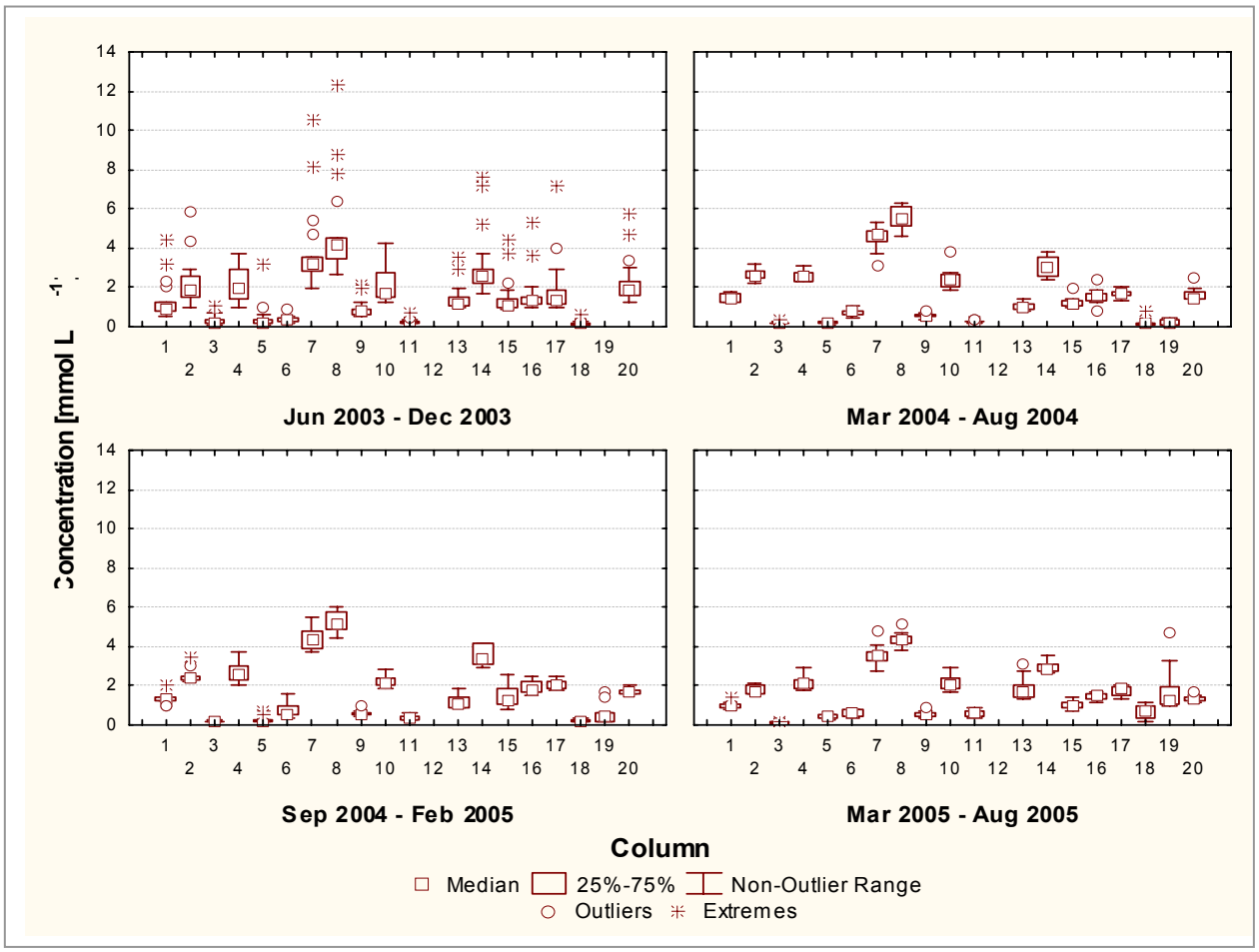

Figure 4-7: **Column Leach Test Sulfate Concentrations: Time Series**

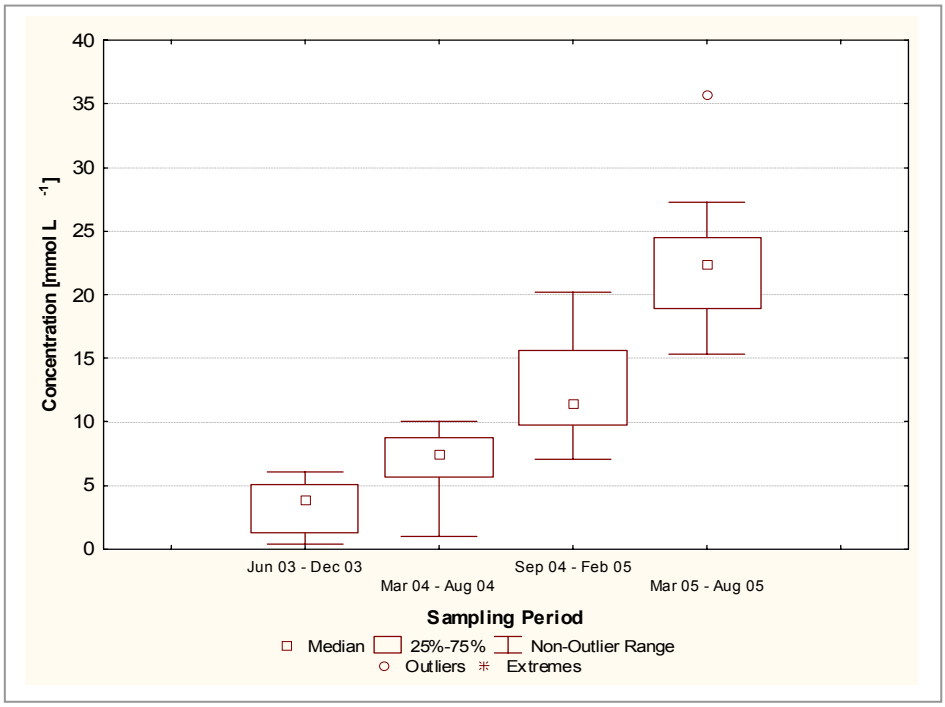

Figure 4-8: CLT12 Sulfate Concentrations: Time Series

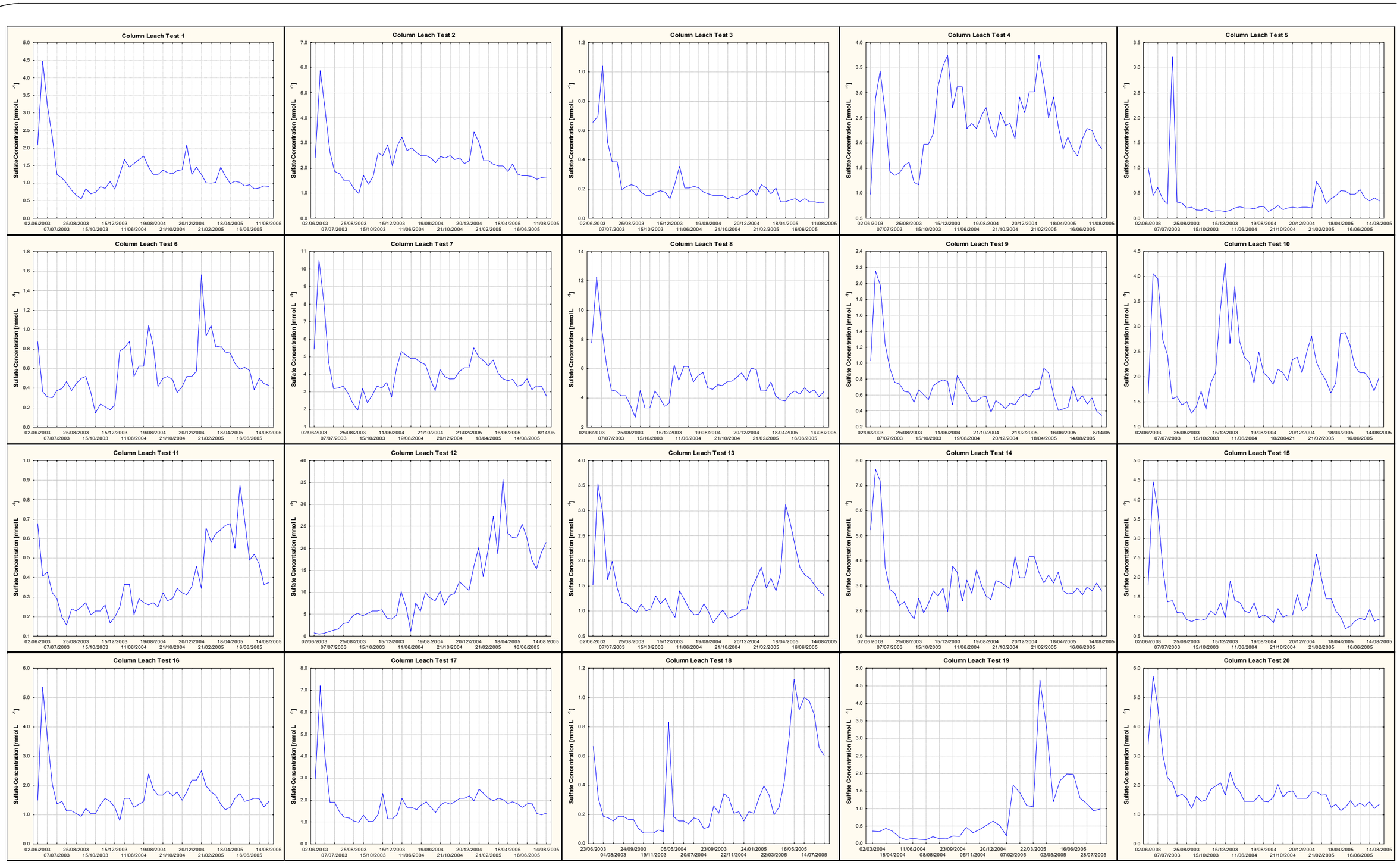

Figure 4-9: **Column Leach Test Sulfate Concentrations (note different y-axis scales)**

Sulfate concentrations in leachate from Columns 2 (90% CLS / 10% HWD, <10mm) and Column 4 (90% CLS / 10% HWD, <50mm) were identical with median values of 2.3mmol L^{-1} (Figure 4-7). In contrast, the median pH values (Figure 4-5) were 7.7 (Column 2) and 6.7 (Column 4). Column 6, comprising the same blend with a larger particle size (90% CLS / 10% HWD, <100mm), yielded leachate with a lower pH (median 6.5), however sulfate concentrations (median 0.52mmol L^{-1}) in leachate were significantly less than those measured in Columns 2 and 4. The lower average pH values and extended range in Columns 4 and 6 leachate indicated that armouring of CLS was controlling the ability of the neutralising material to maintain neutral or alkaline leachate, despite the less than or equal concentrations of sulfate in leachate.

Likewise, a similar pattern was evident in Columns 7 (80% CLS / 20% HWD, <10mm), 9 (80% CLS / 20% HWD, <50mm) and 11 (80%CLS / 20% HWD, <100mm). Median sulfate concentrations were notably higher in Column 7 (3.8mmol L^{-1}) than Column 9 (0.60mmol L^{-1}) and Column 11 (0.32mmol L^{-1}), however median pH values were lower in Column 11 (6.4) than Columns 9 (7.2) and 7 (7.6). These results indicated the presence of carbonate armouring in Columns 11 and 9 and the effective neutralisation of acid by material in Column 7.

The increasing sulfate concentrations with decreasing particle size may be a result of either the higher surface area to volume ratio of PAF material exposing more sulfide surfaces to react, or longer residence (contact) times in CLTs containing smaller sized rocks. CLTs containing larger particle sizes have the potential for water to short circuit through the column. In this instance, water can bypass certain rock types, producing either a leachate characteristic of acid consuming or acid producing rock types. Caution must be taken in interpreting this trend though, as particle size within the column may change with the weathering of pyritic material. This change was clearly demonstrated in Column 12 (refer Figure 4-32) where HWD material had significantly weathered reducing the particle size distribution of PAF material in the column.

Particle size was not the only variable to influence sulfate concentrations in leachate. As indicated in Figure 4-10, the percentage of PAF material in each CLT strongly influenced leachate sulfate concentrations. Excluding Column 12 from the dataset, leachate with the highest sulfate concentration was collected from CLTs with both the greatest percentage of PAF material and smallest particle size distribution.

Schedule C – Table 6 in Environmental Authority No. MIM8000020402 (Ecoaccess, 2004) specifies the maximum limit for sulfate in discharged mine waters as 1000mg L^{-1} (10mmol L^{-1}). This limit was exceeded in Column 12 leachate almost constantly during the third and fourth sampling periods. Sulfate concentrations in leachate from Columns 7 and 8 during the second flush event (9 June 2003) also exceeded this limit, however these results were extreme outliers and a product of the first flush events. Steady state conditions for all CLTs (except Column 12) were within the maximum discharge limit for sulfate.

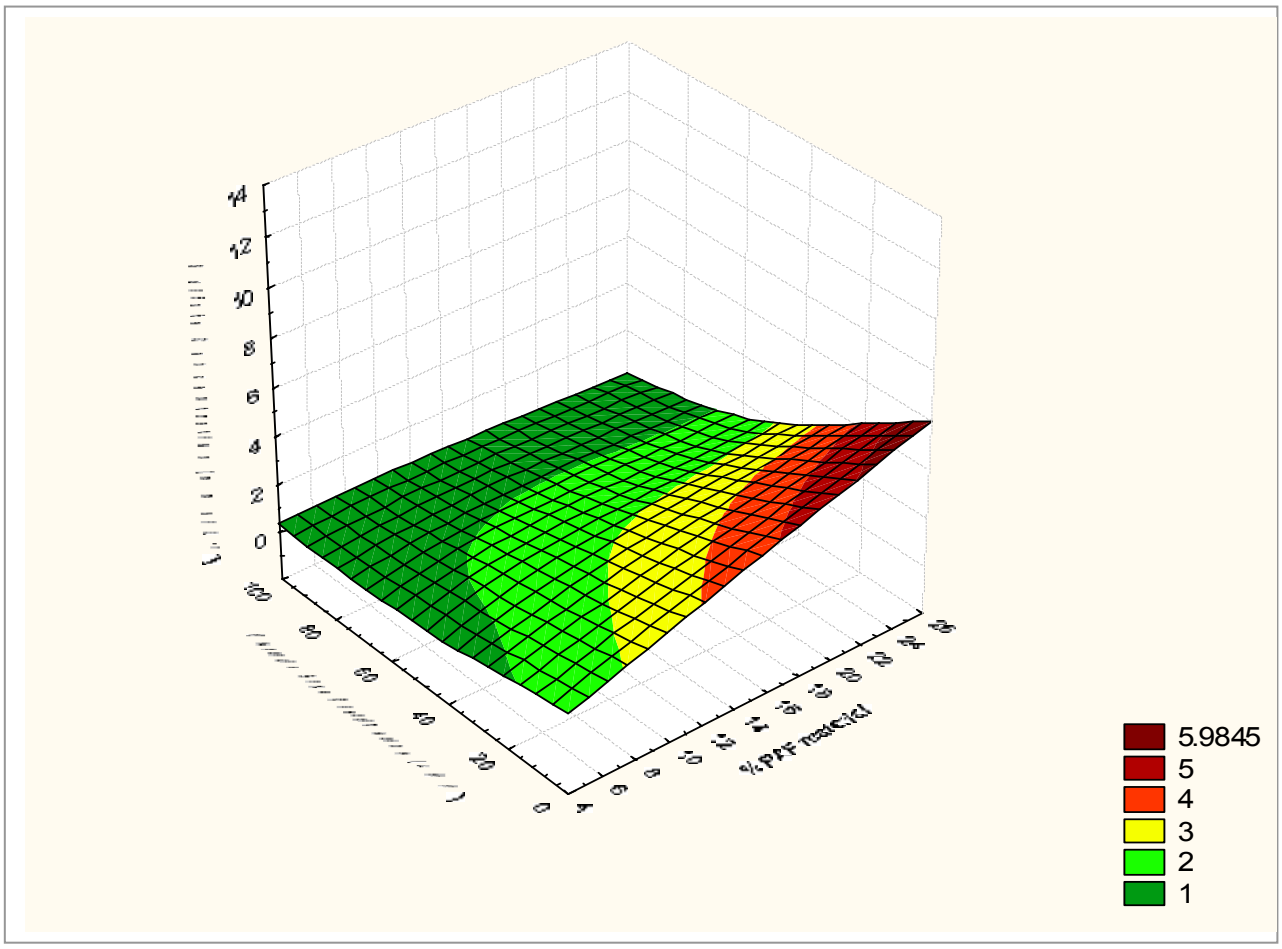

Figure 4-10: **Relationship between %PAF material (x-axis), Particle Size Distribution (y-axis) and Sulfate Concentration (z-axis): All Column Leach Tests (CLTs 12 and 19 excluded)**

4.3.3.2 Relationship between Sulfate Concentration and Electrical Conductivity

Electrical conductivity is a measure of the ability of a water or soil solution to conduct an electric current (ANZECC and ARMCANZ, 2000). EC is commonly measured in environmental monitoring and is used as an indicator of a solution's salinity and its concentration of dissolved salts (Queensland Environmental Protection Agency, 1999). The definition of electrical conductivity stems from the definition for resistivity and is the ratio of current density to the electric field causing the current (Queensland Environmental Protection Agency, 1999). The conductivity of a solution is determined by measuring the resistance of the solution inside a cell of known dimensions and is expressed in millisiemens per centimetre (mS cm^{-1}) or the SI unit millisiemens per metre (mS m^{-1}).

In ARD waters, electrical conductivity is increased by the exchange of protons between calcium and magnesium when calcium (magnesium) carbonates neutralise sulfuric acid according to Equation 1-8 through to Equation 1-11.

Figure 4-11(a) shows the relationship between electrical conductivity and sulfate concentrations in leachate sampled from all CLTs. Data points for Columns 12 and 19 (i.e. 75%CLS / 25% HWD, <100mm) have been highlighted. When a linear fit was placed on this dataset, an r^2 value of 0.9182 was obtained, indicating a small amount of scatter about the trendline. When Columns 12 and 19 were excluded from the dataset and a linear relationship fitted, the r^2 value increased to 0.9475, reflecting the reduction in scatter about the trendline (Figure 4-11(b)).

From Figure 4-11(a) it can be seen that the slope of the curve was much flatter for the highly reactive columns (Columns 12 and 19) than the remaining dataset. This may be attributed to the formation of ion-pairs at high concentrations, resulting in a decrease in the conductivity of the leachate (Boyd, 2000) due to the lower charges of the ion-pairs. Analytical methods (specific ion electrodes excluded) do not distinguish between free ions and ion-pairs (Boyd, 2000). Consequently, sulfate in solution might be distributed among SO_4^{2-}, $CaSO_4^0$, $MgSO_4^0$, KSO_4^- and $NaSO_4^-$. This effect is known to become greater as concentrations increase and it is greater for divalent and trivalent ions than for monovalent ions (Boyd, 2000).

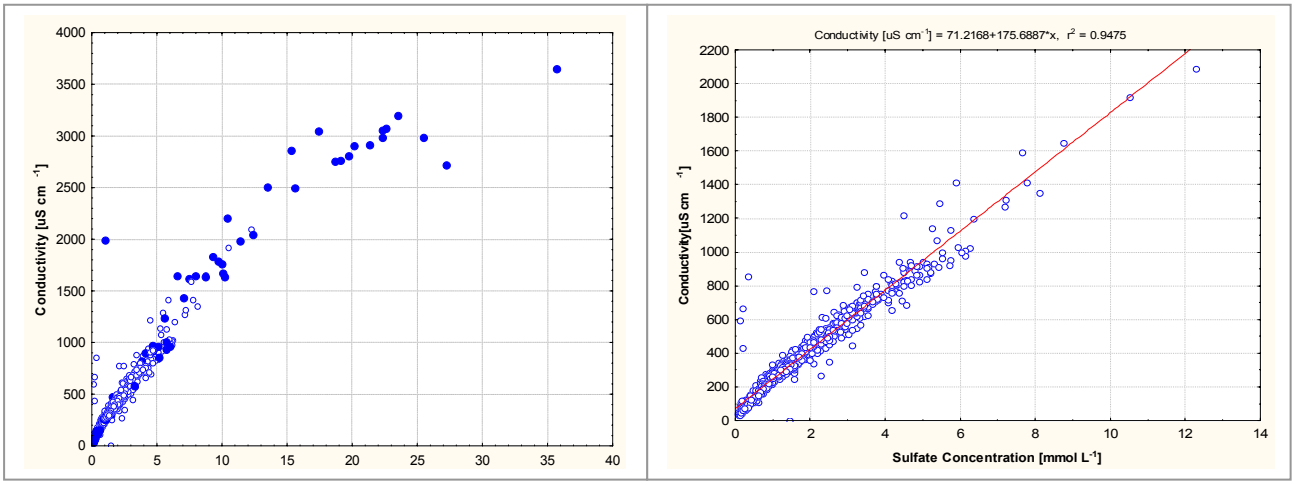

(a) All Columns (Columns 12 and 19 solid circles) **(b) All Columns (Columns 12 and 19 excluded)**

Figure 4-11: Relationship between Conductivity and Sulfate (note difference in y-axis scale)

4.3.3.3 Sulfate Production and Neutralising Potential Depletion Rates

Sulfate production and neutralising potential depletion rates were calculated for each column flush event (refer Appendix 5) and are shown as a time series plot in Figure 4-12. Note that due to scale differences, the Column 12 time series is shown separately in Figure 4-13.

With the exception of Column 12, the sulfate production and neutralising potential depletion rates were similar for each CLT. This similarity indicated that the rate of sulfate generation was matched by the rate of carbonate dissolution to result in circum-neutral pH values in leachate. Where the neutralising potential depletion rate was less than the sulfate production rate (e.g. Column 12), low pH values in leachate ensued. The gradual increase in difference between the two rates for leachate from Column 12 (Figure 4-13) indicated the occurrence of gradual armouring of CLS material in the CLT, which was confirmed at the conclusion of the sampling (section 4.3.5). Column 12's duplicate established after the first six-month sampling period, Column 19, began to display a similar trend to Column 12, albeit to a much lesser extent, by the fourth six-month sampling period (Figure 4-12). The higher values for sulfate production rate than neutralising potential depletion rate for Column 19 leachate indicated that armouring of CLS material had commenced. This armouring was confirmed when Column 19 was dismantled for evaluation at the end of the test period as shown in Figure 4-33 and discussed in section 4.3.5.

Using values obtained from the calculation of the sulfate production and neutralising potential depletion rates, the times to sulfur and neutralising potential depletion were calculated. It should be stressed that in making these calculations, it was assumed that the oxidation rate had reached steady state and would continue at the same rate until all pyrite was oxidised. Accordingly, the estimated times to sulfide and neutralising potential depletion have considerable uncertainty associated with them and should be treated as indicative. Figure 4-9 shows that sulfate concentrations in CLTs 4, 6, 11, 12, 13, 18 and 19, and hence the sulfate production rates, increased throughout the duration of the sampling program. In these cases, the sulfate production rate will be overestimated and the time to sulfur depletion underestimated. It should also be noted that each of these CLTs contained samples of larger particle size distributions (i.e. <50mm or <100mm) and were therefore not deemed to represent the behaviour of waste rock under field conditions (refer section 6.3).

Summarised in Table 4-3, the time to sulfur depletion was fastest in Column 12 (5 years) and slowest in Column 3 (230 years). The calculated time to neutralising potential depletion exceeded that for sulfur depletion in all CLTs. These results indicated that in theory, the waste rock blends contained within the CLTs should never produce ARD. In reality this is not likely to occur where armouring of CLS material renders the carbonate material ineffective (e.g. as seen for CLTs containing the larger particle sized material).

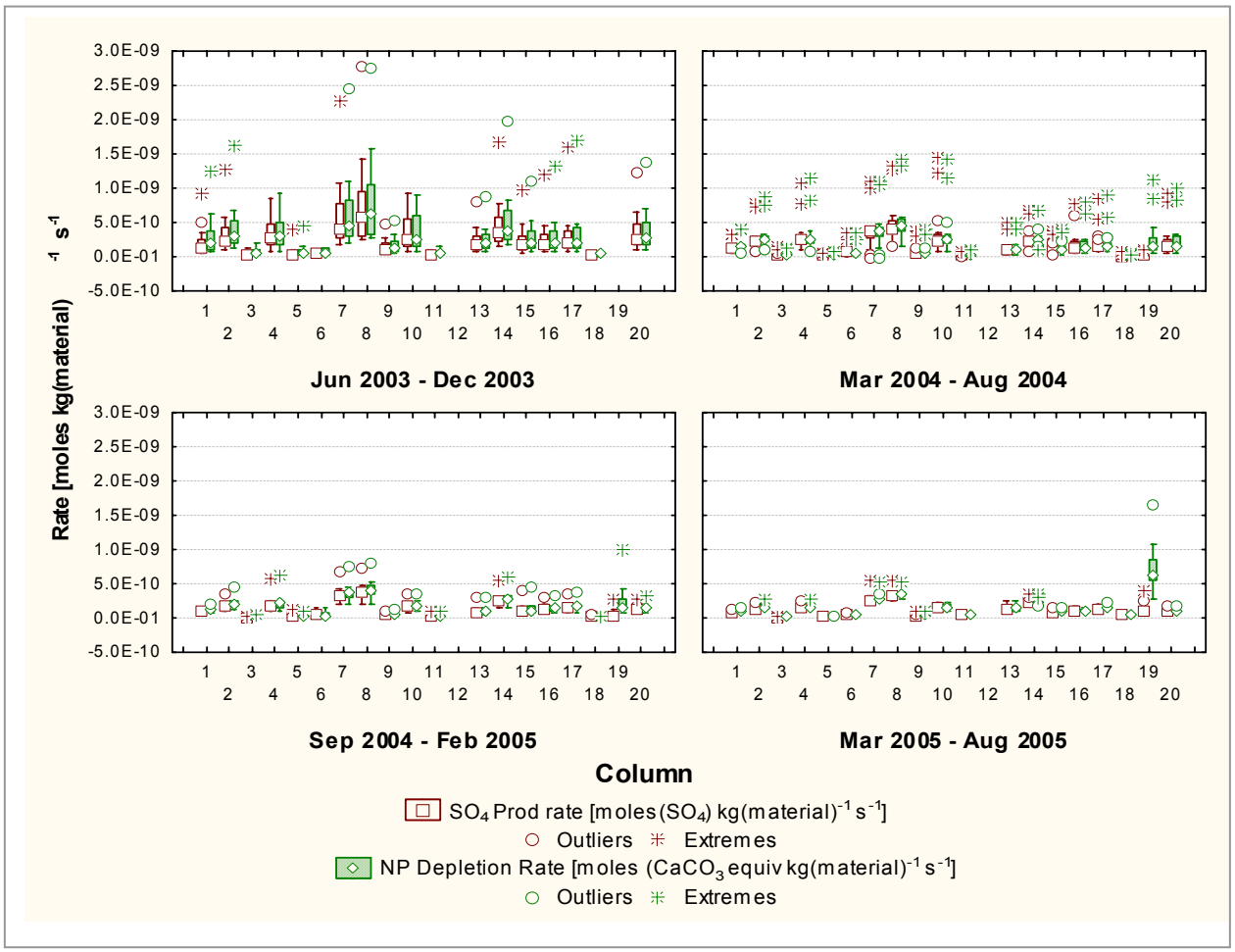

Figure 4-12: **CLT Sulfate Production and Neutralising Potential Depletion Rates (CLT12 excluded)**

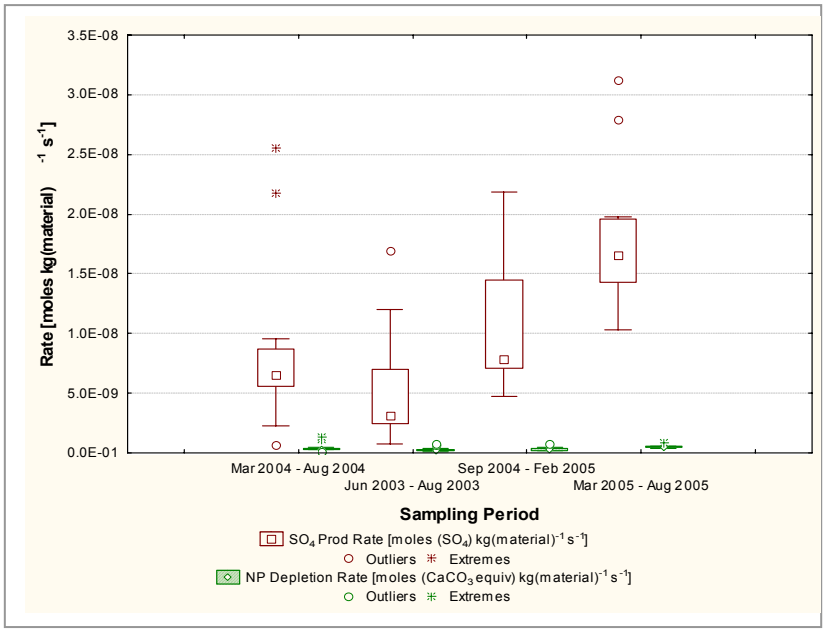

Figure 4-13: **CLT12 Sulfate and Neutralising Potential Rates: Time Series**

Table 4-3: Column Leach Test Sulfate Production and Neutralising Potential Depletion Rate Summary

CLT	% PAF	Particle Size (<mm)	% S flushed from sample	Median SO_4 Production Rate [moles(SO_4) kg(material)$^{-1}$ s^{-1}]	% NP flushed from sample	Median NP Depletion Rate [moles($CaCO_3$ eq) kg(material)$^{-1}$ s^{-1}]	Estimated Minimum Time to S Depletion (years) $^{\Phi}$	Estimated Minimum Time to NP Depletion (years)$^{\Phi}$
1	5	10	8.59	1.00E-10	0.10	1.26E-10	26	2.4E+03
2	10	10	9.51	1.98E-10	0.18	2.27E-10	21	1.3E+03
3	5	50	1.30	1.50E-11	0.02	2.53E-11	230	1.2E+04
4	10	50	7.70	2.00E-10	0.18	2.22E-10	28	1.3E+03
5	5	100	3.55	2.30E-11	0.03	3.17E-11	82	9.6E+03
6	10	100	3.94	4.85E-11	0.04	4.91E-11	55	5.9E+03
7	20	10	9.12	3.16E-10	0.31	3.42E-10	24	7.5E+02
8	25	10	9.10	3.94E-10	0.40	4.00E-10	23	6.0E+02
9	20	50	1.26	5.28E-11	0.06	6.20E-11	210	4.1E+03
10	25	50	3.41	1.98E-10	0.20	2.04E-10	68	1.2E+03
11	20	100	1.50	2.79E-11	0.03	3.17E-11	160	8.1E+03
12	25	100	34.47	7.52E-10	0.29	3.34E-10	5	7.2E+02
13	15	50	3.09	1.09E-10	0.11	1.21E-10	77	2.2E+03
14	15	10	8.99	2.39E-10	0.23	2.56E-10	25	1.1E+03
15	15	50	2.96	9.77E-11	0.11	1.10E-10	86	2.4E+03
16	15	50	3.78	1.30E-10	0.13	1.35E-10	64	2.0E+03
17	15	50	4.38	1.50E-10	0.15	1.62E-10	55	1.6E+03
18	15	100	1.46	1.84E-11	0.02	1.87E-11	200	1.5E+04
19	25	100	1.82	3.55E-11	0.02	2.28E-10	140	1.0E+03
20	15	50	4.36	1.41E-10	0.15	1.52E-10	59	1.8E+03

Φ under current flushing scenario

Oxygen consumption rates were calculated for each flush event in accordance with Equation 1-13. These values were then 'normalised' for the amount of sulfur in the CLT waste rock blend to remove sulfur content as a variable that may potentially confound the interpretation of factors such as particle size on reactivity. Oxygen consumption rates for each column leach test are summarised in Table 4-4. Again excluding the behaviour of Column 12, it could be seen that oxygen consumption rates normalised for sulfur were greatest in CLTs containing particle sizes <10mm, a result of the higher surface area to volume ratio for pyrite and adequate

contact times of leachate with the waste rock comprising the samples. From Table 4-4 it can also be seen that with the exception of Column 2 (90% CLS / 10% HWD, <10mm), oxygen consumption rates in CLTs with particle size distributions passing 10mm decreased with the decreasing percentage of PAF material in the columns (i.e. Column 8 (25% PAF) > Column 7 (20% PAF) > Column 14 (15% PAF) > Column 1 (5% PAF)). Since the sulfur-normalised oxygen consumption rate is more constant than the oxygen consumption rate without sulfur normalisation, the oxygen consumption rate is proportional to the sulfur concentration in the material.

An assumption used in calculating the sulfate production and oxygen consumption rates and time to sulfur depletion was that the rate of oxidation was constant for the duration of the period between flush events. It was suspected that this might not have been the case where water limitation prevented oxidation from continuing at the same rate for the entire period. In columns where this may have occurred, the calculated sulfate production and oxygen consumption rates will have been overestimated and time to sulfur depletion underestimated.

Table 4-4: Column Leach Test Oxygen Consumption Rates

Column Leach Test	Lithology Blend	Particle Size	Median Oxygen Consumption Rate [moles(O_2)kg(material)$^{-1}$ s^{-1}]	Median Oxygen Consumption Rate [moles(O_2)kg(S)$^{-1}$ s^{-1}]
1	95% CLS / 5% HWD	<10mm	5.60E-12	1.95E-09
2	90% CLS / 10% HWD	<10mm	1.11E-11	2.35E-09
3	95% CLS / 5% HWD	<50mm	8.42E-13	2.39E-10
4	90% CLS / 10% HWD	<50mm	1.12E-11	1.82E-09
5	95% CLS / 5% HWD	<100mm	1.29E-12	6.54E-10
6	90% CLS / 10% HWD	<100mm	2.71E-12	9.59E-10
7	80% CLS / 20% HWD	<10mm	1.77E-11	2.10E-09
8	75% CLS / 25% HWD	<10mm	2.20E-11	2.15E-09
9	80% CLS / 20% HWD	<50mm	2.96E-12	2.59E-10
10	75% CLS / 25% HWD	<50mm	1.11E-11	7.92E-10
11	80% CLS / 20% HWD	<100mm	1.56E-12	3.43E-10
12	75% CLS / 25% HWD	<100mm	4.21E-11	7.76E-09
13	85% CLS / 15% HWD	<50mm	6.11E-12	6.97E-10
14	85% CLS / 15% HWD	<10mm	1.34E-11	2.04E-09
15	85% CLS / 15% HWD	<50mm	5.47E-12	6.23E-10
16	85% CLS / 15% HWD	<50mm	7.30E-12	8.32E-10
17	85% CLS / 15% HWD	<50mm	8.41E-12	9.59E-10
18	85% CLS / 15% HWD	<100mm	1.03E-12	2.79E-10
19	85% CLS / 15% HWD	<50mm	1.99E-12	3.66E-10
20	75% CLS / 25% HWD	<100mm	7.88E-12	8.98E-10

4.3.3.4 Relationship Between Sulfate and (Calcium plus Magnesium) in Leachate

Figure 4-14(a) illustrates the relationship between sulfate concentration and the sum of calcium and magnesium ion concentrations in leachate collected from all columns during the sampling period. Datapoints for Columns 12 and 19 are highlighted as solid circles.

A slope of one was anticipated as calcium and magnesium in the dolomite were expected to react with sulfuric acid according to:

$$Ca_{(0.5)}Mg_{(0.5)}CO_3 + H_2SO_4 \leftrightarrows 1/2Ca^{2+} + 1/2\ Mg^{2+} + SO_4^{2-} + H_2O + CO_2$$

Equation 4-6

This relationship was observed (i.e. slope of 0.95 was achieved) when leachate sampled from Columns 12 and 19 were excluded from the dataset (Figure 4-14(b)). This correlation indicated that the calcium and magnesium concentrations in leachate collected from all columns except 12 and 19 arose from reaction with or dissolution of calcium/magnesium carbonates.

Sulfate concentrations were higher than the sum of calcium and magnesium ions in leachate collected from Columns 12 and 19 due to armouring of the dolomite preventing effective neutralisation of sulfuric acid. The counter ion for sulfate under these circumstances was H^+.

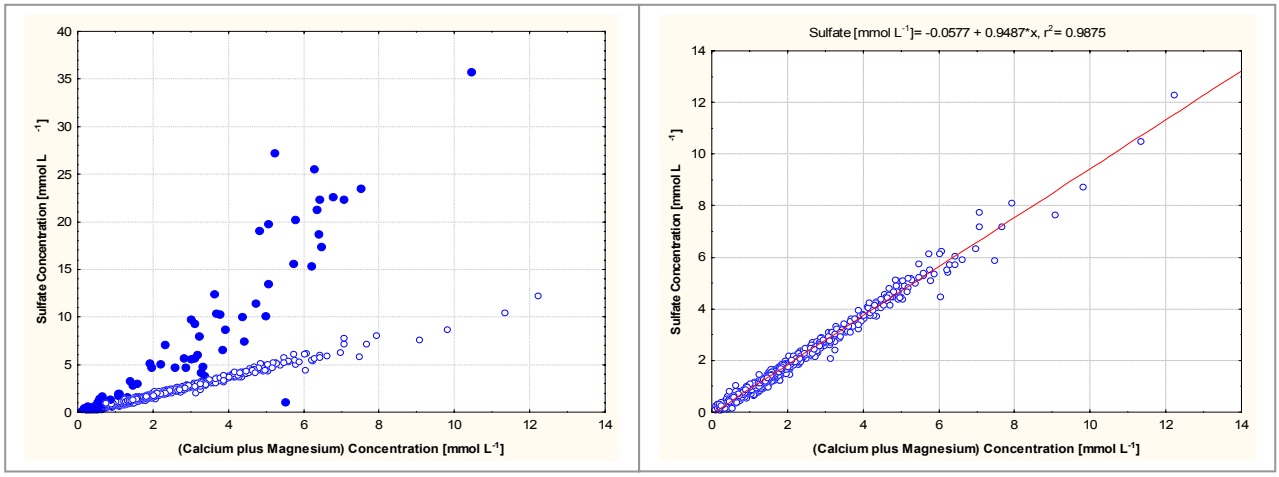

(a) All Columns (Columns 12 and 19 marked as solid circles) (b) All Columns (Columns 12 and 19 excluded)

Figure 4-14: Relationship between Sulfate and (Calcium plus Magnesium) in Leachate (note difference in y-axis scale)

From Figure 4-14(a) it can be seen that the maximum sulfate concentration recorded (36mmol L^{-1}) corresponded to a sample where the sum of calcium and magnesium concentrations was 11mmol L^{-1}. The 25mmol L^{-1} of excess sulfate ions was detected in a sample of Column 12 leachate with a pH value of 2.6. This excess is greater than can be accounted for using H^+ as the sole additional counter ion at a pH of 2.6. It was therefore concluded that Al^{3+} and Fe^{3+}, which were present at elevated concentrations in the sample,

made a significant contribution to the cation balance. Therefore, to assess the balance of ions in the sample, acidity was included to account for the contribution of Fe^{3+} and Al^{3+}.

Acidity is the capacity of a water to give or donate protons and for an acid drainage (pH 2 to 3) the total acidity might be given by (Langmuir, 1997):

$$\textbf{Acidity} = H^+ + HSO_4^- + 2Fe^{2+} + 3Fe^{3+} + 2FeOH^{2+} + 3Al^{3+}$$

Equation 4-7

Figure 4-15(a) shows this relationship for all CLTs and indicates that this method did not fully account for the discrepancy. Datapoints for Column 12 are again marked as solid circles. When Column 12 was excluded from this dataset, a linear relationship was evident (Figure 4-15(b)). This relationship indicated a balance between anions and cations in the samples.

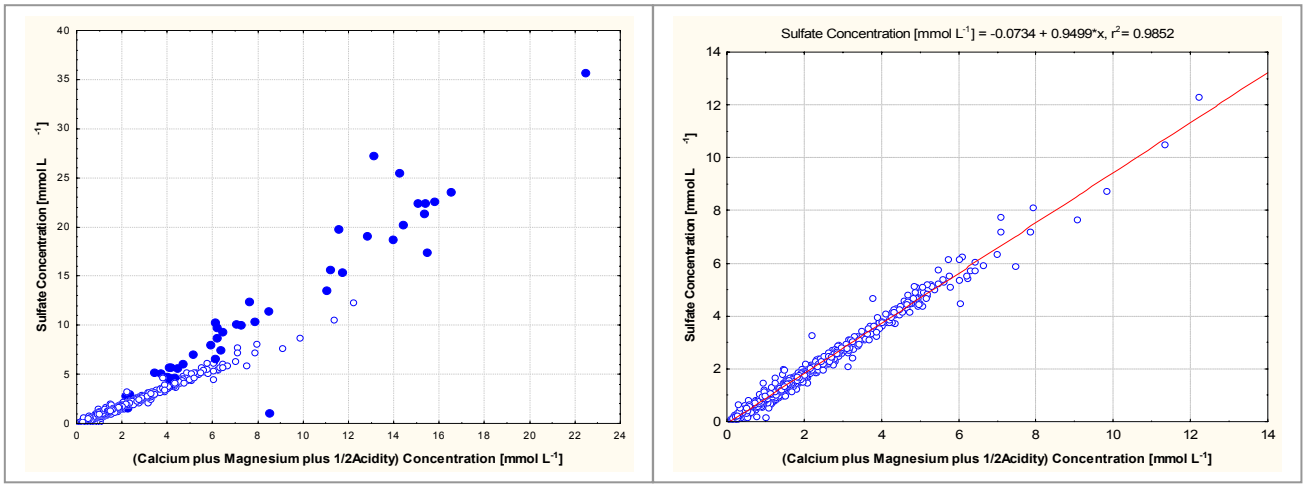

(a) All CLTs (Column 12 marked as solid circles) **(b) All CLTs (Column 12 excluded)**

Figure 4-15: Relationship between sulfate concentration and the sum of calcium, magnesium and acidity/2 (note difference in y-axis scale)

4.3.4 Metals

4.3.4.1 Total Metal Concentrations

Total metal concentrations in samples collected from the column leach tests were assessed for comparison against limits established in ZCML's Environmental Authority No. MIM8000020402 (Ecoaccess, 2004) and Table 4-5. Because dissolved metals are more geochemically predictable than total metals (total metal concentrations are driven by suspended solid concentrations) and hence provide a better understanding of the chemistry of waste rock blends, total metal data presented has been restricted to the four total metals with point source and receiving environment limits specified in MIM8000020402. Metal concentrations are presented for CLTs containing material passing 10mm only as this size fraction best represents that of the on-site waste rock dumps (i.e. columns containing larger particles sizes are not believed to facilitate effective

water contact with waste rock types). This was verified by visual observations of material comprising the column leach tests (section 4.3.5) and heap leach pads (section 5.3.4) at the conclusion of the sampling period.

Table 4-5: Total Metal Discharge Limits (Ecoaccess, 2004)

Metal	Discharge Limit [mg L^{-1}]	Discharge Limit [mol L^{-1}]
Arsenic	0.10	1.3 10^{-3} mmol L^{-1}
Zinc	40	0.61 mmol L^{-1}
Cadmium	0.01	8.9 x 10^{-8} mol L^{-1}
Lead	0.10	4.8 x 10^{-4} mmol L^{-1}

Total arsenic and total zinc concentrations in samples collected from CLTs containing waste rock passing 10mm are displayed in Figure 4-16(a) and (d) respectively. Percentages of PAF material in the CLTs are indicated in brackets with the column number in the legend. In all samples collected, both total arsenic and total zinc were in compliance with discharge limits specified in MIM8000020402 Schedule C – Table 6 (i.e. 0.10mg L^{-1} (1.3x10^{-3}mmol L^{-1}) and 40mg L^{-1} (0.61mmol L^{-1}) respectively).

Figure 4-16(b) shows total cadmium concentrations in leachate collected from CLTs with waste rock passing 10mm. It can be recalled from section 4.2 that the CLT samples were relocated from ZCML to JCU in early 2004. This process involved trucking the columns a distance of approximately 1500 kilometres on both unsealed and sealed roads, consequently disturbing the column contents. This disturbance was reflected by elevated concentrations of total arsenic, zinc, cadmium and lead in leachate samples collected immediately following the relocation. With the exception of this spike and the initial flush period, total cadmium concentrations in leachate sampled were less than the maximum limit specified in MIM800020402 Schedule C – Table 6 (i.e. 0.010mg L^{-1} or 8.9x10^{-8}mol L^{-1}).

Total lead concentrations in leachate collected from CLTs with waste rock passing 10mm are shown in Figure 4-16(c). In a similar trend to that for total cadmium, total lead exceeded the discharge limit during the initial flush and following relocation of the CLTs to JCU. Total lead concentrations complied with the maximum limit specified in MIM8000020402 Schedule C – Table 6 (0.10 mg L^{-1} or 4.8x10^{-4}mmol L^{-1}) after the CLTs reached steady state.

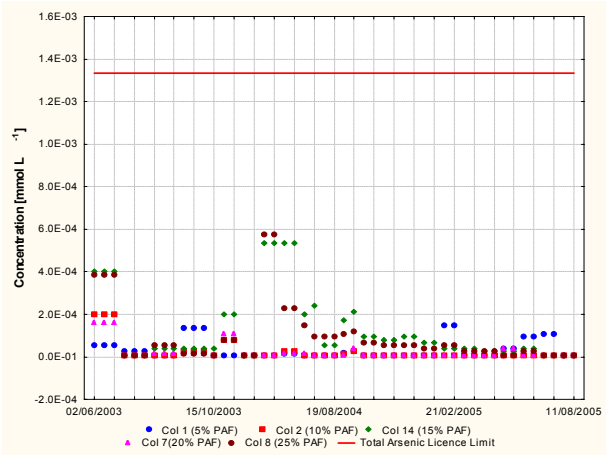

(a) Total Arsenic Concentrations

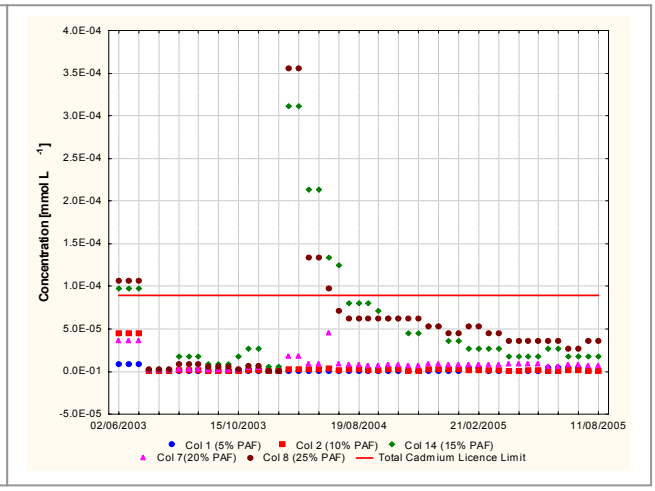

(b) Total Cadmium Concentrations

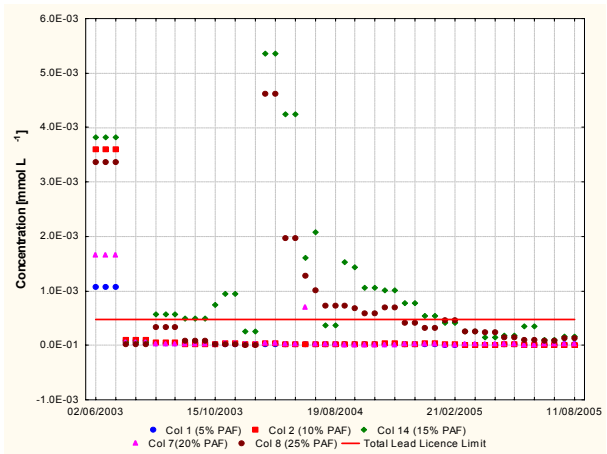

(c) Total Lead Concentrations

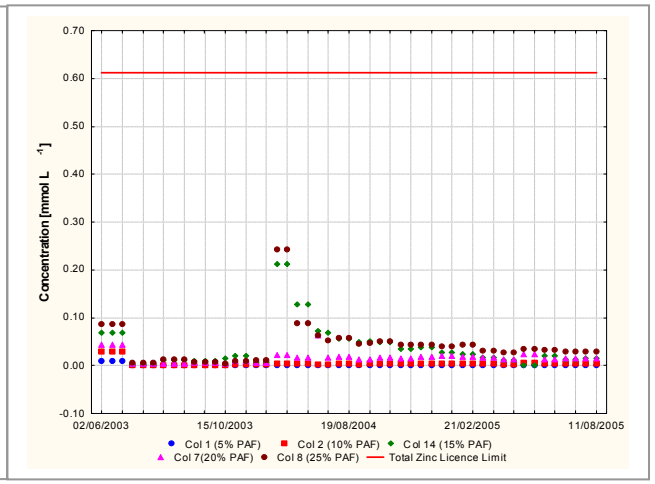

(d) Total Zinc Concentrations

Figure 4-16: Total Metal Concentrations: Column Leach Tests <10mm

4.3.4.2 Dissolved Metal Concentrations

Dissolved metal concentrations and trends in leachate collected from the column leach tests were assessed and are discussed in this section. Appendix 6 contains statistical data (i.e. median, mean, minimum, maximum, standard deviation and 10, 25, 75 and 90 percentile values) for leachate samples collected from all CLTs during the 24-month sampling period. Categorised box and whisker plots for each six-month time sampling period have been used throughout this section to enable the trends in dissolved metal concentrations over time to be assessed.

Table 4-6 shows a correlation matrix for dissolved metals where the majority of samples were greater than detection limits specified in Table 4-2. All correlations presented in Table 4-6 were significant with $p < 0.05$. Particularly strong correlations were observed between aluminium and copper, aluminium and iron, aluminium and zinc, cadmium and copper, cadmium and zinc, cobalt and nickel, copper and iron and iron and zinc.

Table 4-6: Dissolved Metal Correlation Matrix

Variable	Diss Al [mmol L^{-1}]	Diss Cd [mmol L^{-1}]	Diss Co [mmol L^{-1}]	Diss Cu [mmol L^{-1}]	Diss Fe [mmol L^{-1}]	Diss Ni [mmol L^{-1}]	Diss Zn [mmol L^{-1}]
Diss Al [mmol L^{-1}]	1.00	0.87	0.57	0.92	0.95	0.58	0.90
Diss Cd [mmol L^{-1}]		1.00	0.57	0.92	0.89	0.59	0.94
Diss Co [mmol L^{-1}]			1.00	0.51	0.56	0.93	0.65
Diss Cu [mmol L^{-1}]				1.00	0.95	0.54	0.88
Diss Fe [mmol L^{-1}]					1.00	0.57	0.90
Diss Ni [mmol L^{-1}]						1.00	0.64
Diss Zn [mmol L^{-1}]							1.00

4.3.4.2.1 Zinc

Dissolved zinc concentrations in leachate collected from the CLTs for each six-monthly sampling period are shown in Figure 4-17. Due to significant difference in scale, data for Columns 12 and 19 are displayed separately in Figure 4-18.

The highest dissolved zinc concentrations were detected in leachate from Columns 12 and 19 (both 75% CLS / 25% HWD, <100mm). The rapidly decreasing pH values in Column 12 leachate in the first six-month sampling period contributed to the high range of dissolved zinc concentrations in leachate because zinc is more soluble at lower pH values (Stumm and Morgan, 1996). pH values in samples collected during the first sampling period fell from 7.3 in June 2003 to 4.0 in November 2003.

Elevated dissolved zinc concentrations were also present in leachate sampled from Columns 18 (85% CLS, 15% HWD, <100mm) and 6 (90% CLS, 10% HWD, <100mm). As shown in Figure 4-5 and discussed in section 4.3.2, pH values in samples collected from these CLTs were typically lower than those measured in samples from other CLTs (Columns 12 and 19 excluded) as a result of armouring of CLS material and/or water short circuiting through the larger pore spaces between the rock material. The relationship between dissolved zinc concentrations and pH values in leachate is shown graphically in Figure 4-19. Datapoints for Columns 12 and 19 are highlighted as solid circles. From this graph it can be seen that dissolved zinc concentrations in CLT leachate samples increased when pH values fell.

A possible control on zinc solubility that would exhibit significant pH dependence would be the precipitation of zinc hydroxide as a secondary mineral in the CLTs. To test this possible control on dissolved Zn^{2+} concentrations in CLT leachate, the geochemical modelling program MINTEQA2 was used to calculate the solubility of $Zn(OH)_2$ in increments of 0.20 pH units from pH 8.8 to 5.0. The concentrations of Ca^{2+} (2.0×10^{-3} mol kg^{-1}), Mg^{2+} (2.7×10^{-3} mol kg^{-1}) and SO_4^{2-} (4.7×10^{-3} mol kg^{-1}) entered were typical concentrations in CLT leachate (excluding CLTs 12 and 19). NO_3^- (2.0×10^{-3} mol kg^{-1}) was used because it is a non-coordinating anion with zinc (i.e. it does not form ion-pairs with Zn^{2+}). The concentration of Zn^{2+} supplied was 1.0×10^{-3} mol kg^{-1}. The resultant modelled solubility curve is shown as solid circles in Figure 4-19. This figure demonstrates that the solubility of zinc in CLT samples was less than what was predicted on thermodynamic grounds assuming that zinc hydroxide solubility controlled dissolved Zn^{2+} concentrations. Two processes appeared to determine the solubility of Zn^{2+} in leachate solution. At low pH values (<6.0), Zn^{2+} was effectively controlled by the rate of Zn^{2+} released (i.e. the rate of sphalerite oxidation). At higher pH values (7.8), the solubility of $Zn(OH)_2$ appeared to be increasingly dominant in controlling the Zn^{2+} concentration in CLT leachate (i.e. assuming $Zn(OH)_2$ was the solubility limiting phase).

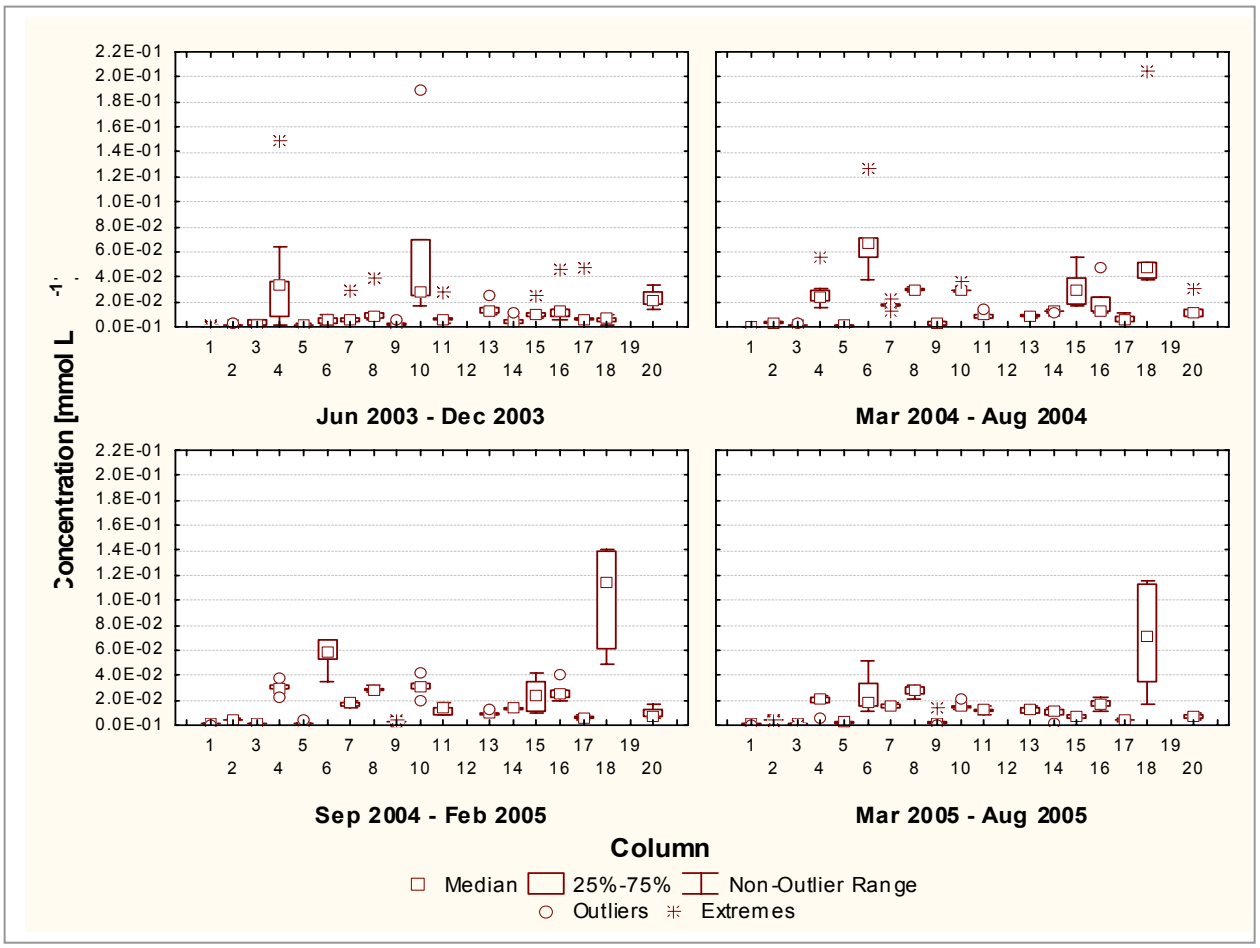

Figure 4-17: **CLT Dissolved Zinc Concentrations (CLTs 12 and 19 Excluded)**

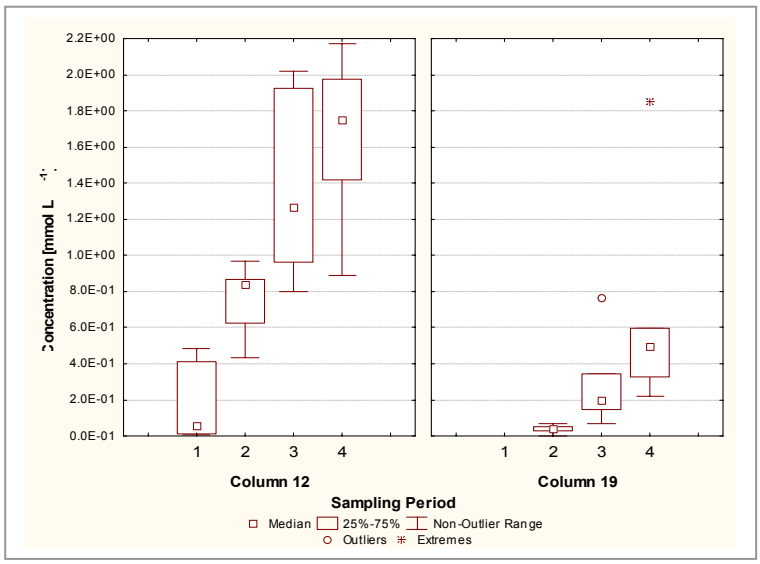

Figure 4-18: **CLT12 and CLT19 Dissolved Zinc Concentrations**

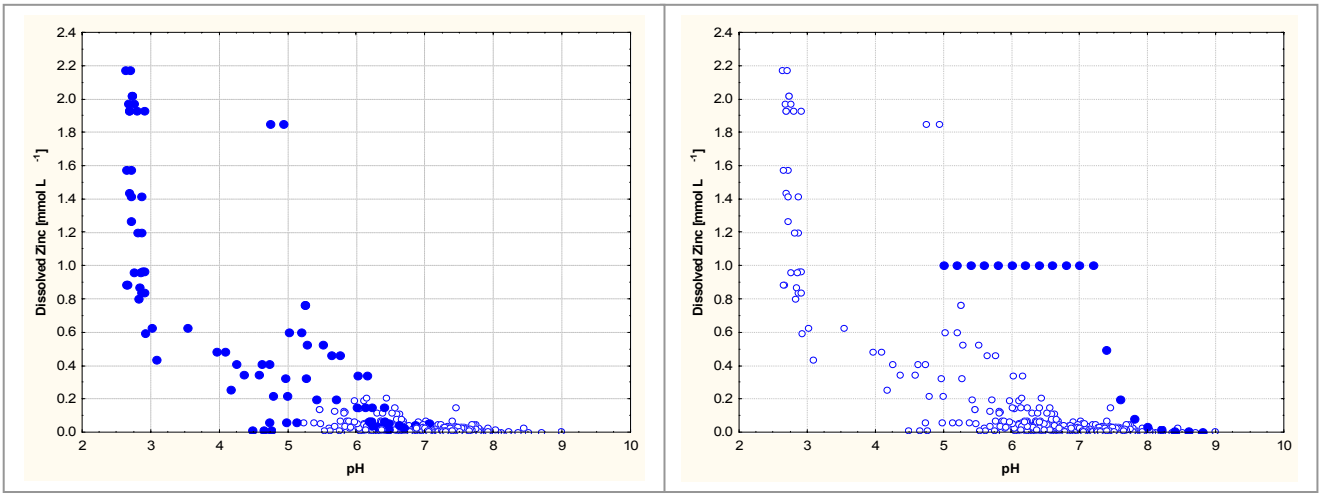

(a) CLTs 12 and 19 Marked as Solid Circles

(b) MINTEQA2 $Zn(OH)_2$Solubility Simulation Marked as Solid Circles

Figure 4-19: Relationship between pH and zinc (filtered): All Column Leach Tests

4.3.4.2.2 Lead

Dissolved lead concentrations in leachate collected from the column leach tests for each six-monthly sampling period are shown in Figure 4-20. Data for Column 12 are shown separately in Figure 4-21.

For many samples, particularly in the fourth six-month sampling period, dissolved lead concentrations in leachate sampled were extremely small or undetectable (i.e. values were less than 4.8×10^{-4} µmol L^{-1}). Despite decreasing pH values in Column 12 leachate throughout the 24-month sampling program, the median dissolved lead concentrations in leachate were similar in each sampling period. Median dissolved lead concentrations fell from 3.9×10^{-2}µmol L^{-1} in the first six-months to 2.4×10^{-2}µmol L^{-1} consistently in the second, third and fourth six-month sampling periods, despite a decrease in median pH values from 4.7 (Jun 2003 – Dec 2003) to 2.9 (Mar 2004 – Aug 2004), 2.8 (Sep 2004 – Feb 2005) and 2.7 (Mar 2005 – Aug 2005). Displaying behaviour opposite to this trend, leachate from Column 19 yielded an increase in dissolved lead concentrations (Figure 4-20) with decreasing pH (Figure 4-6) throughout the sampling period. Respective pH and dissolved lead concentrations were 6.5 and 4.8×10^{-3}µmol L^{-1} (Mar 2004 – Aug 2004), 6.0 and 1.9×10^{-2}µmol L^{-1} (Sep 2004 – Feb 2005) and 5.1 and 4.3×10^{-2}µmol L^{-1} (Mar 2005 – Aug 2005).

In other CLTs, dissolved lead was barely detectable outside the initial flushing period. By the final six-month sampling period, dissolved lead was undetectable in most samples (Figure 4-20).

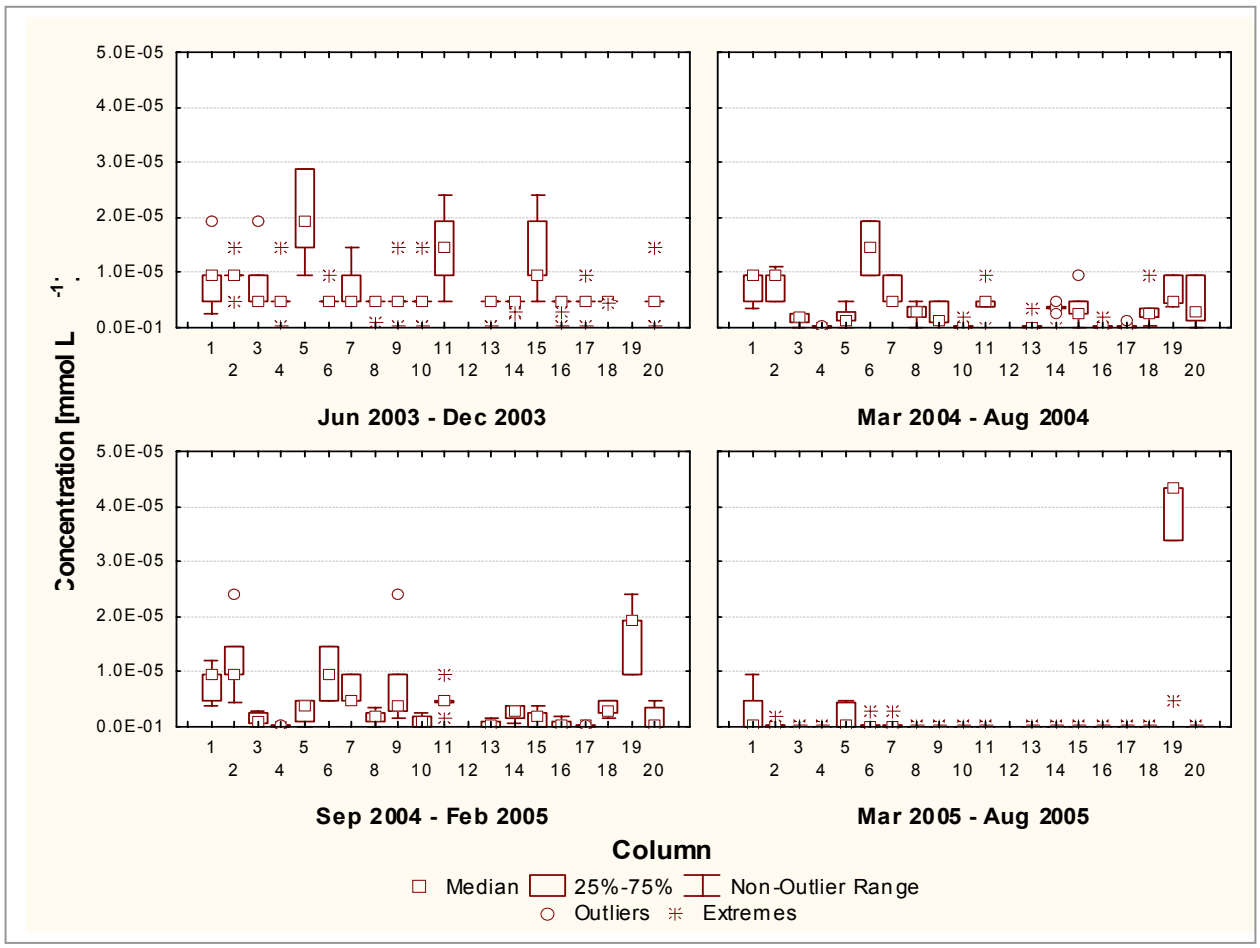

Figure 4-20: **CLT Dissolved Lead Concentrations (CLT 12 Excluded)**

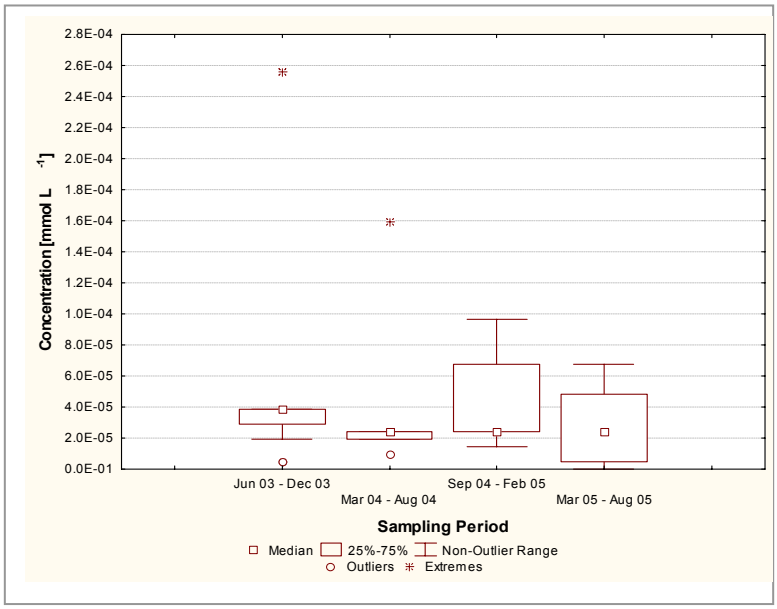

Figure 4-21: **CLT12 Dissolved Lead Concentrations**

The relationship between dissolved lead concentrations and pH values in CLT leachate is shown graphically in Figure 4-22(a). Datapoints for Columns 12 and 19 are highlighted as solid circles. From this figure it can be seen that dissolved lead concentrations in CLT leachate samples increased when pH values fell, although they were still remarkably low overall.

In an effort to determine if production of insoluble salts could account for the low lead concentrations, MINTEQA2 was used to estimate the saturation solubilities of $Pb(OH)_2$ and $PbSO_4$ in leachate waters with typical ionic compositions over a pH range of 8.7 to 3.0 in increments of 0.30 pH units. Similarly to the $Zn(OH)_2$ simulation, concentrations of Ca^{2+} (2.0 x 10^{-3} mol kg^{-1}), Mg^{2+} (2.7 x 10^{-3} mol kg^{-1}) and SO_4^{2-} (4.7 x 10^{-3} mol kg^{-1}) were entered as they were typical concentrations in CLT leachate (excluding CLTs 12 and 19). NO_3^- (2.0 x 10^{-3} mol kg^{-1}) was used because it is a non-coordinating anion with lead (i.e. it does not form ion-pairs with Pb^{2+}). The concentration of Pb^{2+} supplied was 1.0 x 10^{-3} mol kg^{-1}. The MINTEQA2 lead solubility modelling output identified that thermodynamically, aqueous lead concentrations were controlled by the solubility of $Pb(OH)_2$ in basic conditions (i.e. pH > 7.2), and by the solubility of anglesite ($PbSO_4$) in acidic conditions (i.e. pH < 6.3). The resultant modelled solubility curve is shown as solid circles in Figure 4-22(b).

It can be seen from Figure 4-22(b) that the concentration of dissolved lead in CLT samples was significantly less than thermodynamically predicted. The absence of high Pb^{2+} concentrations at low pH values indicated that the rate of supply of Pb^{2+} from the oxidation of galena (PbS) was the likely rate-limiting step. It is likely that passivation of the galena surface, possibly by elemental sulfur (Cama et al. 2005, De Giudici et al. 2005, De Giudici and Zuddas, 2001), contributed to the slow oxidation rate of galena. Low aqueous lead concentrations observed in ARD from pyrite rich ore, and with the presence of ferric iron in solution, are attributed to surface coatings on galena (Cama et al. 2005). It should be noted that the structure and composition of this surface layer is influenced by the pH of the solution (De Giudici et al. 2005) and can be confirmed using techniques such as scanning electron microscopy or x-ray diffraction.

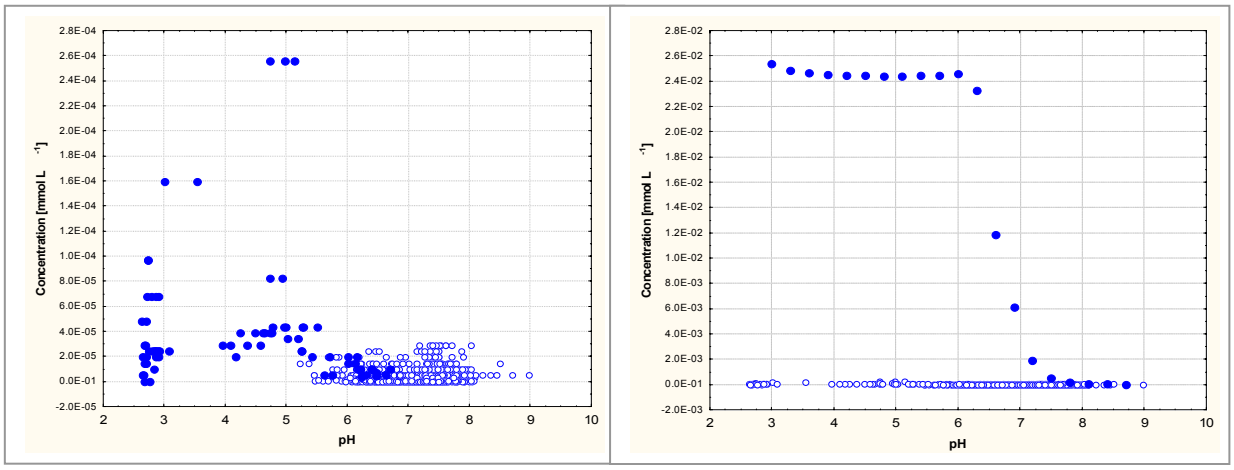

(a) CLTs 12 and 19 Marked as Solid Circles **(b) MINTEQA2 Lead Solubility Simulation Marked as Solid Circles**

Figure 4-22: Relationship between pH and lead (filtered): All Column Leach Tests

4.3.4.2.3 Cadmium

Dissolved cadmium concentrations in analysed leachate from most column leach tests were undetectable (i.e. less than 8.9×10^{-4} µmol L^{-1}) during the 24-month sampling period (Figure 4-23). Dissolved cadmium concentrations in Column 12 (Figure 4-24) and Column 19 (Figure 4-23) increased during the sampling period as pH values in leachate fell.

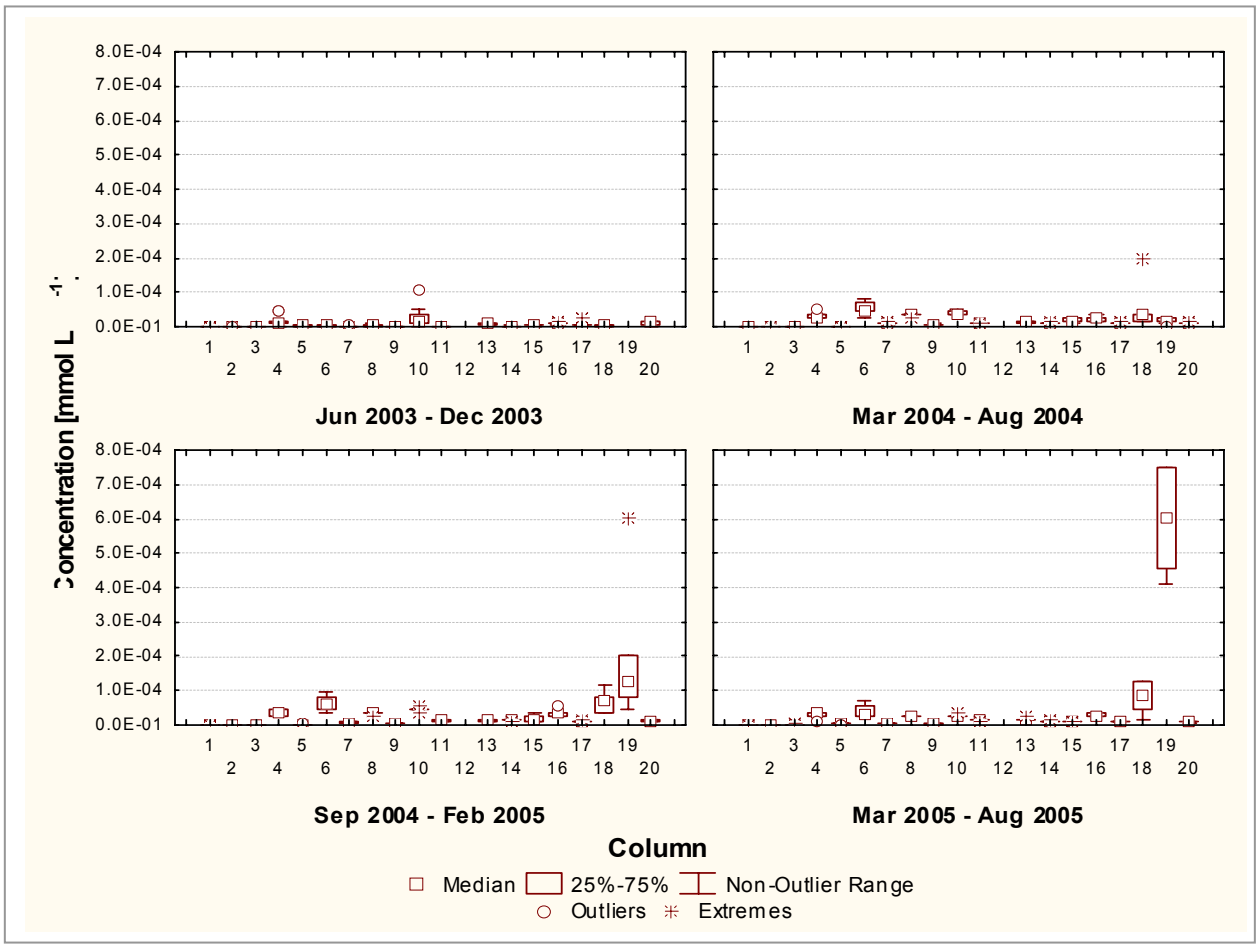

Figure 4-23: CLT Dissolved Cadmium Concentrations (CLTs 12 and 19 Excluded)

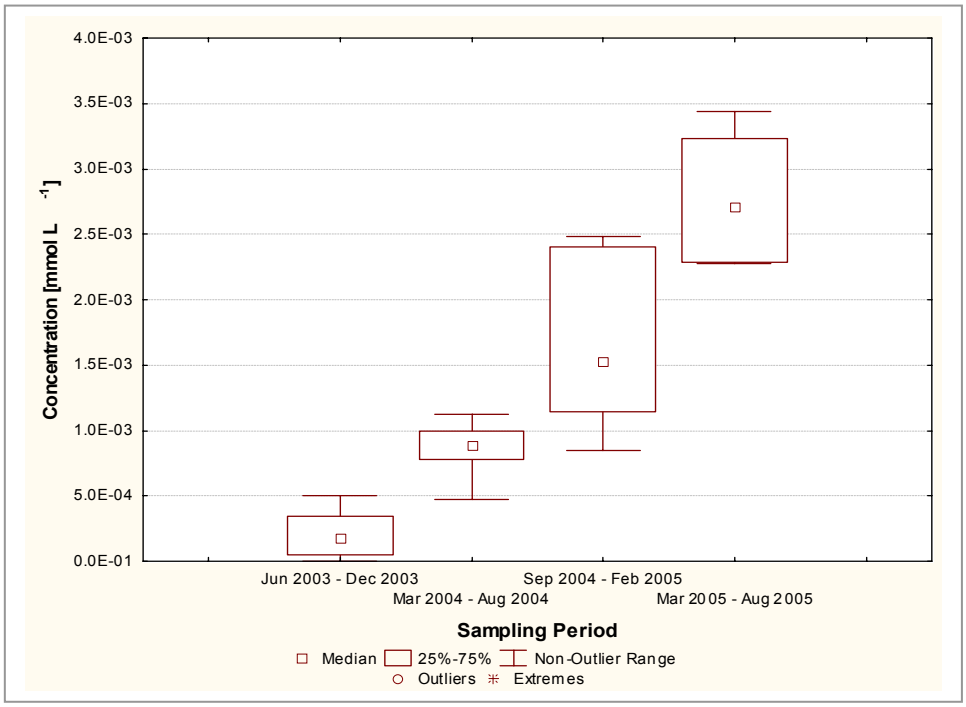

Figure 4-24: CLT12 and CLT19 Dissolved Cadmium Concentrations

4.3.4.2.4 Copper

Dissolved copper concentrations for leachate collected from the column leach tests are shown in Figure 4-25. Data for Column 12 are displayed separately in Figure 4-26 due to differences in scale. Excluding data from Columns 12 and 19, dissolved copper concentrations were highest during the first flush and lowest in the last six-month sampling period, a pattern similar to many other dissolved metals assayed. Concentrations in leachate sampled from Columns 12 and 19 increased with the decrease in pH values.

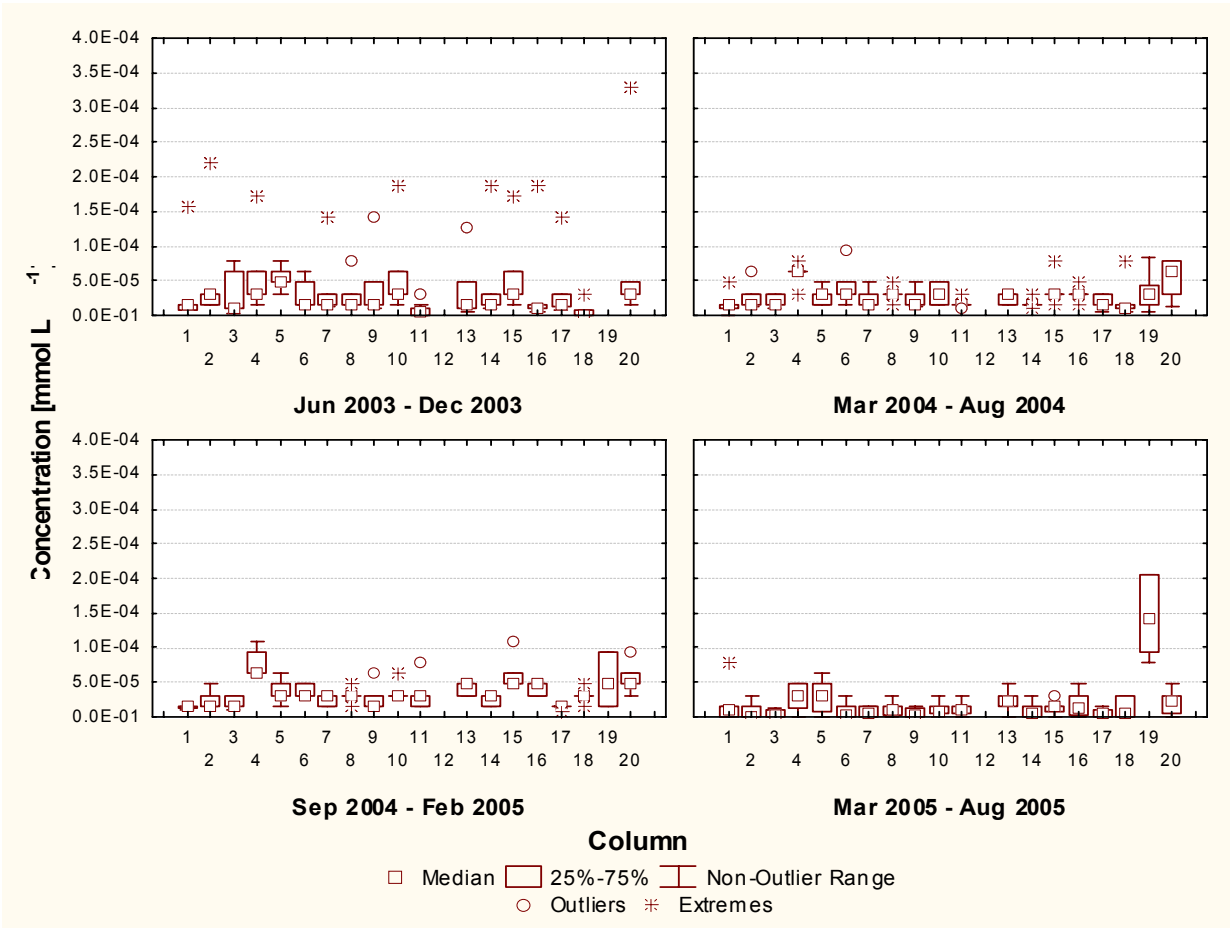

Figure 4-25: **CLT Dissolved Copper Concentrations (CLTs 12 excluded)**

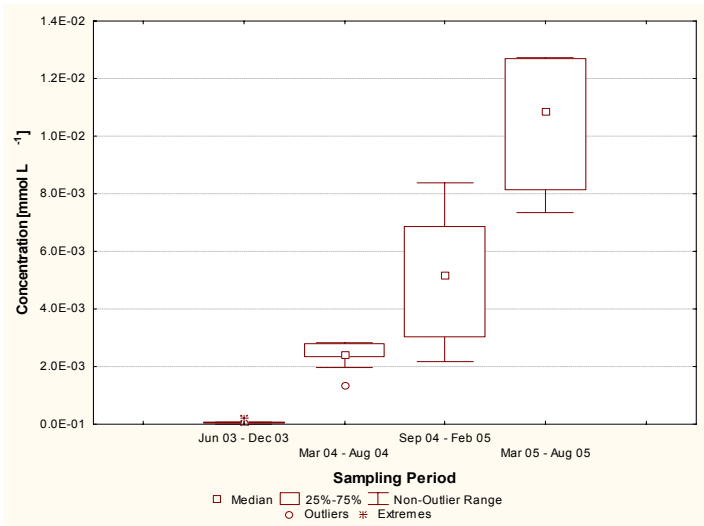

Figure 4-26: **CLT12 Dissolved Copper Concentrations**

4.3.4.2.5 Iron

Dissolved iron concentrations analysed in leachate from the column leach tests are displayed in Figure 4-27. Data for Column 12 are shown in Figure 4-28. Excluding data for Columns 12 and 19, there was no clear pattern with dissolved iron concentrations in leachate collected from CLTs comprised of different waste rock blends. In the first six-month sampling period, Column 4 (90% CLS / 10% HWD, <50mm) and Column 10 (75% CLS / 25% HWD, <50mm) returned higher ranges for dissolved iron data, despite median values being similar to those for other CLT leachate. In the second and third six-month sampling periods, Column 6 (90% CLS / 10% HWD, <100mm) produced leachate with the highest dissolved iron concentration (after Columns 12 and 19), whereas in the final six-month sampling period, it was again Column 4. In comparison with dissolved iron concentrations in Columns 12 and 19 leachate, concentrations detected (i.e. greater than 1.8µmol L^{-1}) in other CLTs were insignificant and were likely to be attributed to colloidal iron passing through the 0.45µm filters (note dissolved metal samples were passed through a 0.45µm filter prior to submission to the laboratory for analysis).

Concentrations in leachate from Column 12 steadily increased throughout the sampling period with a decrease in pH values. Concentrations in leachate from Column 19 started to increase from the third six-month sampling period when pH values decreased to a median of 6.0, however it was the fourth sampling period, when pH values fell to a median of 5.1, that dissolved iron increased to more notable concentrations. The increase in dissolved iron concentrations with decreasing pH is well documented and is attributed to the increase in iron hydroxide solubility at lower pH values (APHA, 1998, Stumm and Morgan, 1996).

Ferric iron is known to be a powerful oxidant of pyrite at lower pH values, releasing 16 moles of acidity for every mole of pyrite in accordance with Equation 1-5. To assist in the interpretation of dissolved iron results, the speciation of iron was determined colourimetrically by the method described in section 4.2. As shown in Table 4-7, iron present in column leach test samples on 31 January 2005 was predominantly in the ferric state.

It is likely the ferrous iron present in Column 12 leachate, and to a lesser extent Columns 2, 4, 6, 11, 18 and 19, was produced at lower pH values by the reaction of ferric iron with pyrite (Equation 1-5). Of note is that the majority of columns that produced leachate containing ferrous iron were of the larger size fraction (i.e. <100mm). As discussed in section 4.2.2, neutralisation reactions were not able to proceed to completeness in such columns due to carbonate armouring, short circuiting of neutralising material or insufficient contact times of leachate with neutralising material.

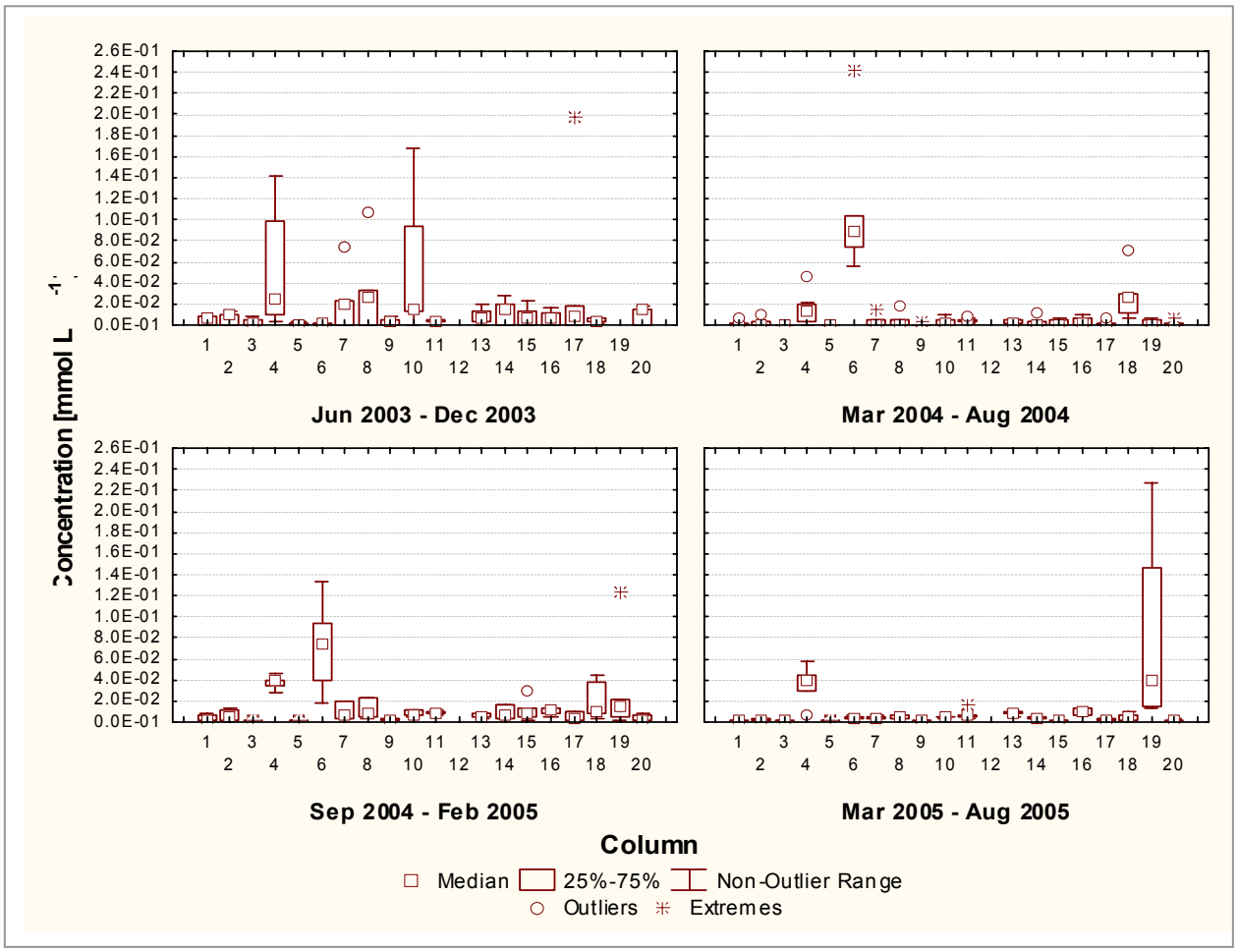

Figure 4-27: **CLT Dissolved Iron Concentrations (CLT12 excluded)**

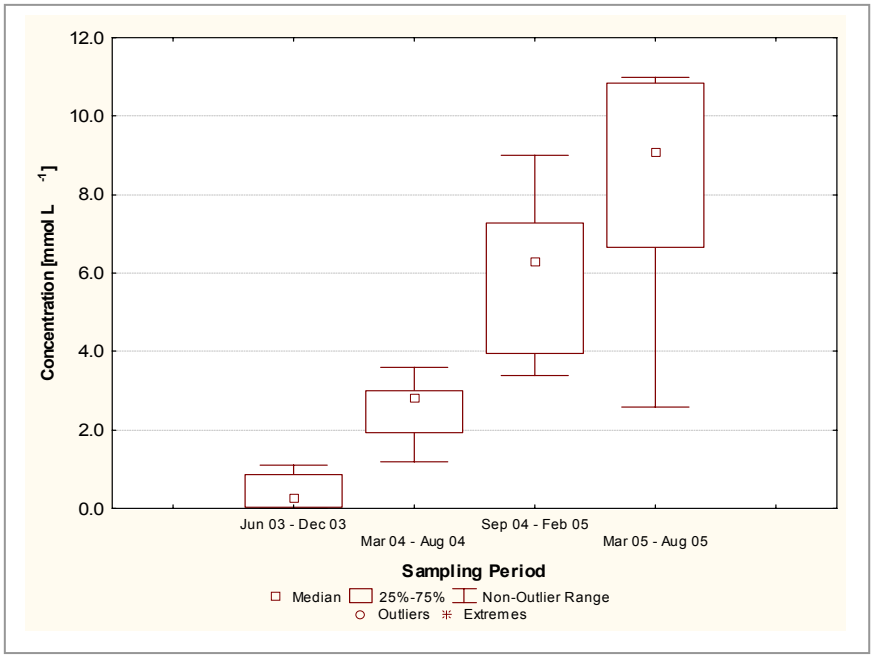

Figure 4-28: **CLT12 Dissolved Iron Concentrations**

Table 4-7: Iron Speciation in Column Leach Test Samples collected 31 January 2005

Column	Ferrous iron [μg L^{-1}][3]	Total iron [μg L^{-1}][4]	Ferric iron [μg L^{-1}][5]
1	<100	137	137
2	51	269	218
3	<100	303	303
4	417	10100	9683
5	<100	477	477
6	189	3650	3461
7	<100	459	459
8	<100	979	979
9	<100	576	576
10	<100	1620	1620
11	356	1580	1224
12	22858	966000	943142
13	<100	1300	1300
14	<100	2630	2630
15	<100	1400	1400
16	<100	1390	1390
17	<100	353	353
18	41	755	714
19	1276	10800	9524
20	<100	743	743

[3] Determined spectrophotometrically

[4] Analysed by ICP-MS

[5] Calculated by subtracting ferrous iron from total iron

4.3.4.2.6 Aluminium

Figure 4-29 provides a six-monthly period breakdown of dissolved aluminium concentrations in leachate sampled from each column leach test. Concentrations in leachate from Columns 12 and 19 are provided separately in Figure 4-30. Similar to most other dissolved metals, aluminium concentrations in samples were greater in leachate from most CLTs during the first six-month sampling period due to the influence of the first flush. It is likely that some of the measured concentrations may be colloidal, having arisen from the washing of surface clays containing aluminium from the waste rock material in the initial flushes. Following the first flushes, aluminium continued to be recorded in leachate from several CLTs, namely Columns 6, 10, 11, 12, 16 and 19. However, once again, the highest concentrations by several orders of magnitude, increasing with decreasing pH values, were recorded in Column 12 (Figure 4-30).

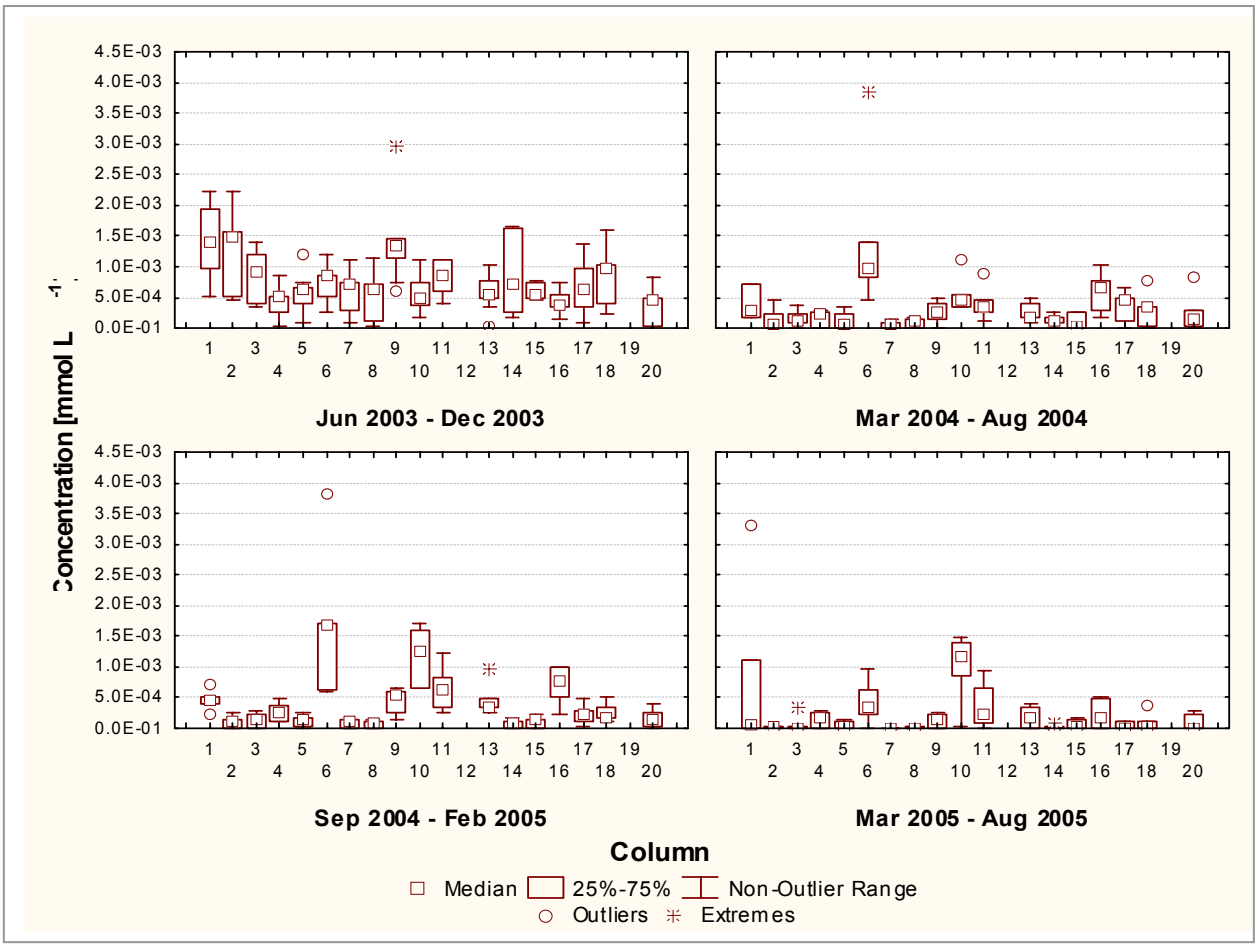

Figure 4-29: CLT Dissolved Aluminium Concentrations (CLTs 12 and 19 excluded)

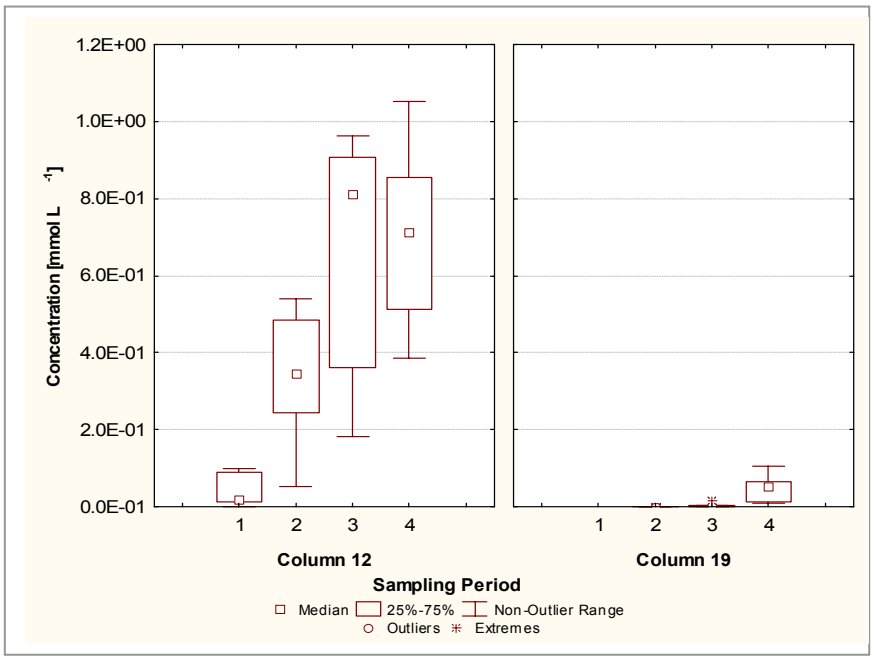

Figure 4-30: CLT12 and CLT19 Dissolved Aluminium Concentrations

4.3.4.2.7 Arsenic

Minor concentrations of dissolved arsenic were detected in leachate from several column leach tests during the first flush, however shortly afterwards, and exclusively by the fourth six-monthly sampling period, concentrations were undetectable (i.e. less than 1.3×10^{-3} µmol L^{-1}) in all CLTs except Column 12. As was the case for all dissolved metals recorded in Column 12 leachate samples except lead, dissolved arsenic concentrations increased during the sampling period as pH values in leachate decreased (Figure 4-31).

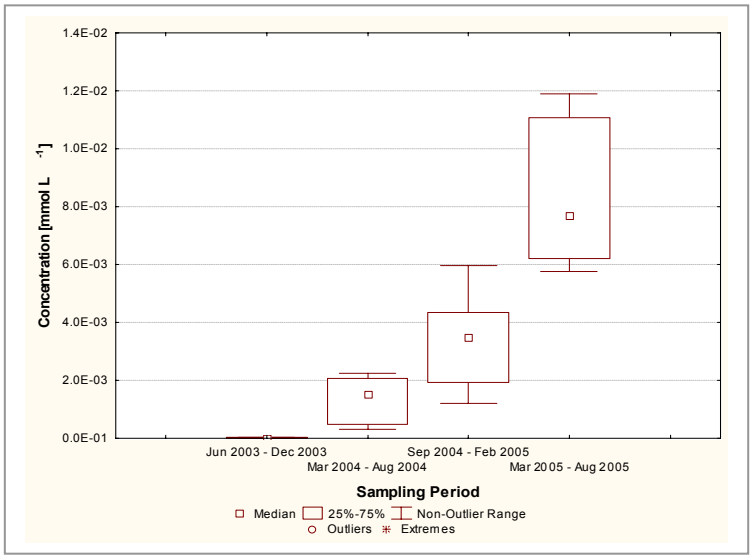

Figure 4-31: CLT12 Dissolved Arsenic Concentrations

4.3.4.2.8 CLT Dissolved Metal Concentration Summary

Dissolved zinc, lead, cadmium, copper, iron, aluminium and arsenic concentrations were detectable in leachate collected from the column leach tests. For all dissolved metals discussed with the exception of lead, concentrations increased with decreasing pH values. Concentrations of dissolved zinc, cadmium, copper, aluminium and arsenic in the CLT leachate sampled were greater than concentrations of dissolved lead. Dissolved lead concentrations were maintained at low values in leachate from all column leach tests by the passivation of galena and subsequent slow oxidation rate.

4.3.5 Column Dismantling

At the conclusion of the 24-month sampling period, a selection of columns was dismantled to enable the condition of the HWD and CLS material to be assessed. Because of the anomalous behaviour of leachate from Column 12 (75% CLS / 25% HWD <100mm), and to a lesser extent its duplicate, Column 19, these CLTs were dismantled to determine if physical characteristics were influencing the behaviour of the rock material contained within the columns.

As shown in Figure 4-32, most of the CLS located at the base and centre of Column 12 was coated with iron hydroxides. Note the presence of the 300mm scale in this figure to provide an indication of particle size. The significant weathering of HWD in the CLT during the sampling period was confirmed by the presence of flaky HWD material in the centre and base of column (Figure 4-32). This ongoing weathering of HWD material continually exposed fresh surfaces of pyritic material for oxidation and indicated that the physical nature (i.e. competence) of the pyritic material significantly influenced the drainage chemistry. The low pH values and elevated sulfate and dissolved metal concentrations in leachate from Column 12 discussed in sections 4.3.2 to 4.3.4 were therefore attributed to CLS armouring and the weathering of HWD. In addition, the larger particle size of the sample may have led to insufficient contact times with acid neutralisation material and/or the potential for water to short circuit through the column, bypassing acid neutralising or acid consuming material.

Figure 4-32: CLT12 Armouring (scale= 300mm)

The armouring of CLS material in Column 19 was minor in comparison to Column 12 (Figure 4-33). In addition, HWD material in this CLT was relatively competent, with only a small amount of weathering evident at the base of the column. The greater amount of HWD weathering in Column 12, together with the lower pH values, higher sulfate and dissolved metal concentrations, highlighted that the chemistry of leachate from the CLTs was highly dependent on the physical nature of the HWD material. The difference in severity of HWD weathering between Columns 12 and 19 also highlighted the issue of subsampling and the influence it can have on drainage chemistry from samples of larger particle sizes.

Figure 4-33: CLT19 Armouring (scale= 300mm)

In comparison Column 8, which comprised the same waste rock blend as Columns 12 and 19 but with smaller particle size (i.e. 75% CLS / 25% HWD <10mm), showed a very limited amount of armouring (Figure 4-34). This was attributed to the higher surface area of carbonate material in the CLT available to neutralise any acidic leachate produced. The HWD material in this CLT had decomposed almost completely, with decomposition further advanced towards the base of the column.

As discussed in section 4.3.2, pH values in samples collected from Column 8 were alkaline (median 7.4). The smaller particle sized sample provided sufficient contact time of leachate with the CLS to enable acid neutralisation. Additionally, the smaller pore spaces between the rocks minimised the potential for water to short circuit through the column.

Figure 4-34: CLT8 Contents at Completion of Sampling Period (scale= 300mm)

4.3.6 Geochemical Modelling of Column Leach Test Leachate

Geochemical modelling is a powerful tool for characterising environmental site contaminations and predicting environmental impacts (Zhu and Anderson, 2002). A background to geochemical modelling principles to aid interpretation of data has been provided in Appendix 9.

Rather than conduct geochemical modelling for each column leach test, Visual MINTEQ was used to model the behaviour of leachate from Column 8 to assess likely secondary mineralisation. Column 8 was chosen because the waste rock blend in the column (75% CLS / 25% HWD, <10mm) had the highest sulfate production rate when the anomalous behaviour of Columns 12 and 19 (both 75% CLS / 25% HWD, <100mm) were excluded (refer Figure 4-12). Theoretically, due to the higher reactivity in Column 8 and the subsequent higher ionic strengths, if secondary minerals were not precipitating within Column 8, they would not have been precipitating in any other column. Random modelling events for other CLTs supported this theory.

Individual models were conducted on each Column 8 leachate sample to determine the solubility phases of the different minerals present. In particular, the behaviour of gypsum and jarosite was observed, since they are secondary minerals commonly associated with ARD (Morin and Hutt, 1997). Saturation indices for gypsum and K-jarosite were recorded for each sample and are presented in Figure 4-35(a) and (b) respectively. Note the difference in the y-axis scale between the two graphs. For a number of samples, the dissolved iron

concentration was below the laboratory detection limit (i.e. less than 1.8μmol L^{-1}) and accordingly, no K-jarosite saturation indices were calculated.

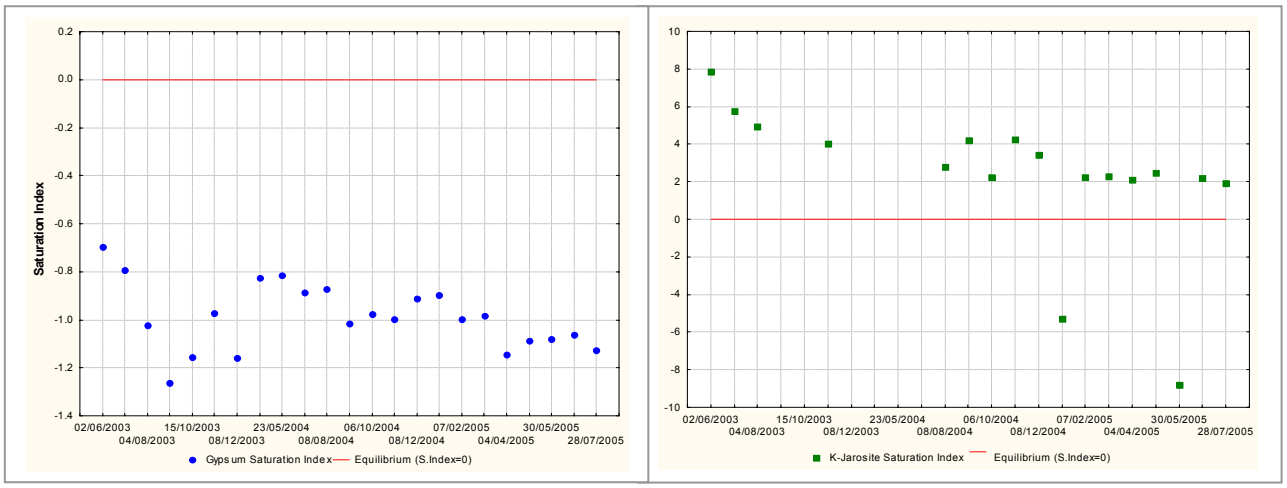

(a) Gypsum Saturation Indices **(b) K-Jarosite Saturation Indices**

Figure 4-35: K-Jarosite and Gypsum Saturation Indices: CLT8

It can be seen from Figure 4-35(a) that the saturation indices for gypsum in Column 8 leachate were consistently negative. This indicated that gypsum was theoretically not precipitating in the sample. The gypsum saturation index in Column 8 leachate ranged from –1.16 to –0.70. Since the saturation index is a logarithmic function, K_{sp}/IAP varied by $10^{-0.46}$ in leachate sampled from Column 8. In contrast, the modelled saturation indices indicated that K-jarosite ($KFe_3(OH)_6(SO_4)_2$) was often positive and therefore theoretically precipitating in Column 8 (Figure 4-35(b)). Despite these results, without better analytical data for iron (i.e. having confidence that the dissolved concentration was a true dissolved iron concentration and not colloidal iron), the saturation indices for K-jarosite could not be confirmed. Visual inspection of Column 8 contents after the sampling period (refer Figure 4-34) showed no characteristic yellow residue, indicating that jarosite was not precipitating in the column.

The conflict between the model output and the visual inspection of the column contents highlighted the limitations of geochemical models. Zhu and Anderson (2002) provide the following reasons why many of the minerals, which are calculated as supersaturated by geochemical models, may not actually be present in the system:

- Kinetic constraints may prevent minerals which are indicated to either dissolve or precipitate by the model from doing so;
- Calculated saturation indices are for pure “end-member” minerals, but the actual mineral in environmental settings can be solid solutions with complicated compositions;
- Errors in analysis may be significant (e.g. colloidal aluminium and iron hydroxides); and
- The reliability of thermodynamic data may be questionable.

These limitations were further highlighted in the Visual MINTEQ model output files for leachate from Column 8. Several iron oxyhydroxides were indicated as supersaturated, and hence precipitating, in these output files. The supersaturation of iron was not taken to be an indication of field behaviour since the iron concentration in samples was almost certainly an exaggeration of the true dissolved concentration due to the presence of colloidal iron hydroxides. Moreover, the kinetics of iron oxy-hydroxide precipitation is known to be slow; goethite and haematite have slow growth kinetics at surface temperatures (Zhu and Anderson, 2002). Despite the discussed limitations of geochemical models, the results obtained from such models can be used to understand both the controls on leachate water quality parameters and the geochemical processes occurring in samples.

4.4 Column Leach Test Summary

The results from the column leach tests are summarised as follows:

- Results obtained from the column leach tests were repeatable.
- Leachate pH values were lower in samples collected from CLTs containing waste rock passing 100mm due to carbonate armouring, HWD weathering, and water short-circuiting through the larger pore spaces (i.e. inadequate retention times).
- Excluding the behaviour exhibited by the anomalous Columns 12 and 19 (75% CLS / 25% HWD, <100mm), sulfate concentrations were greatest in CLTs comprising the highest percentage of PAF material and smaller particle sizes, due to a higher surface area to volume ratio of PAF rocks and/or longer residence times of leachate in these columns.
- CLTs containing smaller particle size distributions appeared to reach steady state sooner, possibly due to more even contact of leachate with rock surfaces (i.e. less influence of short-circuiting flows through preferential pathways).
- In all CLTs except Column 12, and Column 19 (last six-month sampling period only), the neutralising potential depletion rate mirrored the sulfate production rate. This indicated the effective neutralisation of sulfuric acid by carbonates. The difference in rates for Columns 12 and 19 was due to the armouring of CLS material.
- The calculated time to NP depletion exceeded the time to sulfide depletion in all CLTs, however these times were misleading for columns containing armoured CLS material.
- The normalisation of oxygen consumption rates for sulfur content in each sample confirmed that the oxygen consumption rates, and hence pyrite oxidation rates, were higher in CLTs containing smaller particle sized waste rock blends.
- The relationship between (calcium plus magnesium) and sulfate was linear for all column leach tests except CLTs 12 and 19. This indicated that the calcium and magnesium concentrations in leachate arose from reaction of sulfuric acid with, or dissolution of, calcium/magnesium carbonates.

- Excluding the behaviour during the first flush and immediately following relocation of the CLTs to Townsville, total metal concentrations in samples collected from CLTs complied with limits specified in Environmental Authority No. MIM800020402.
- Dissolved zinc concentrations were significantly greater in CLT samples with low pH values, however were not as high as thermodynamically predicted using the geochemical modelling program MINTEQA2. This was due to the control of dissolved zinc concentrations by the rate of sphalerite oxidation at low pH values and the solubility of $Zn(OH)_2$ at high pH values.
- Dissolved lead concentrations in CLT samples were extremely small or undetectable (i.e. less than 4.8×10^{-4} µmol L^{-1}) and less than those thermodynamically predicted using MINTEQA2 due to low oxidation rates of galena resulting from surface passivation.
- Concentrations of dissolved cadmium, copper, iron, aluminium and arsenic were low or undetectable in leachate from several CLTs however increased during the sampling period in leachate from CLT12, and to a lesser extent CLT19, corresponding to an increase in solubility with decreasing pH values.
- The dismantling of CLTs confirmed the extensive weathering of HWD material and armouring of CLS material in CLTs containing blends of larger particle sized waste rock, and the minor armouring and extensive weathering of HWD in CLTs containing smaller particle sized waste rock blends.
- Geochemical modelling confirmed the absence of gypsum precipitation in the CLT comprising the most reactive waste rock blend and smallest particle size distribution. In this CLT, iron oxyhydroxides were predicted to precipitate however visual inspection of the rock material for secondary mineralisation did not detect any iron hydroxide precipitation. The absence of iron oxyhydroxide precipitation may reflect either the slow kinetics of iron (II) oxidation and/or the likelihood that the dissolved iron concentrations in leachate were colloidal.

Results from the column leach tests will be further discussed and compared against results from the static and heap leach pad tests in Chapter 6: Scale-Up.

5 Chapter 5: Heap Leach Pads

5.1 Introduction

To assess the quality of leachate generated from blended waste rock material on a larger scale, three heap leach pads comprising different run of mine waste rock blends were designed, constructed and operated on the Southern Waste Rock Dump at Zinifex Century Mine for a two-year sampling period. The HLPs were exposed to wet season rain events and were manually flushed with potable water during the dry season in an attempt to accelerate the oxidation of pyrite under field conditions and assess the quality of water arising from the waste rock blends.

This chapter will present the design and methodology used for the heap leach pads, the quality of leachate sampled and will discuss consequences for both acid rock drainage generation and compliance with regulatory discharge limits. Comparisons of leachate quality generated from the column leach tests and heap leach pads are made in Chapter 6: Scale-Up.

5.2 Methodology / Design

5.2.1 Design and Construction

Three 10m x 10m x 3m heap leach pads were designed for the following lithology blends of ROM material:

- HLP 1: 95% CLS / 5% HWD
- HLP 2: 85% CLS / 15% HWD
- HLP 3: 75% CLS / 25% HWD

As there is no standard design for heap leach pads, the design used was adapted from Miller in Bennett et al. (2000) and is shown in Figure 5-1 (cross sectional view), Figure 5-2 (plan view) and Figure 5-3 (layer details). The bases of the HLPs were constructed from crushed limestone (Figure 5-4(a) and (b)). Crushed limestone roadbase ((Figure 5-4(c)) was used to slope each pad to a centre drain and to provide a smooth surface for the two layers of impervious PVC liner (Figure 5-4(d)). The centre-drains were welded to the PVC liner to prevent seepage through the base (Figure 5-4(e)). The centre-drain directed leachate to collection vessels for sampling via a system of sub-surface drainage (Figure 5-4(b)).

Smooth inert river pebbles were used as an immediate barrier on top of the PVC liner to prevent penetration of the PVC liner by sharp edges of CLS and HWD (Figure 5-4(f)). NAG testing was conducted on the river pebbles to confirm the rock type was not PAF or AC. In addition, these pebbles were rinsed thoroughly prior to flush events to remove sediment build up.

During the construction of the heap leach pads, waste rock material was weighed by the mine weighbridge to ensure collection of accurate record of each HLP composition. Variation in loader bucketloads lead to deviations in the heap leach pad composition, despite specified design blends. The actual compositions were:

- HLP 1: 99.60% CLS / 0.34% HWD
- HLP 2: 91.73% CLS / 8.27% HWD

- HLP 3: 80.90% CLS / 19.10% HWD

This variation lead to blends not being directly comparable with the most reactive blend established in the column leach tests (i.e. 75% CLS / 25% HWD). Instead, the most reactive HLP blend was compared to the second most reactive blend in the CLTs (i.e. 80%CLS / 20% HWD). Comparisons between the CLTs and HLPs are discussed in Chapter 6: Scale-Up.

5.2.2 Sampling, Analysis and Interpretation

As noted in section 3.2, bulk samples of CLS and lower zone HWD for use in the static testing, CLTs and HLPs, were excavated from 1104-453 and 1008-335 areas of the ZCML open pit respectively in August 2002. Sub-samples were dispatched to AMDEL for mineralogical analysis (AMDEL, 2003 in Appendix 1) to enable mass balances to be conducted for each HLP.

The sample collection system for each HLP comprised a flowmeter installed on the outlet pipe to record the volume of flow through the pad and two 200L plastic drums to contain the leachate (Figure 5-4(g) and (h)). The first drum was designed to overflow to the second, which then overflowed to ground. A composite sample of each flush event was collected from the first drum. Foot valves were installed at the base of each drum to enable the leachate to be drained at the conclusion of sampling. A sample tap-off valve was installed on the outlet pipe to enable “grab” samples of leachate to be collected if required.

In order to accelerate the oxidation of pyrite in the HLPs they were flushed regularly during the dry season by a network of sprinklers on the pad surface Figure 5-4(i). The pads were typically flushed once a week for a four-week period and then left to stand for a further four-week period. This wetting / drying cycle was designed to simulate wet and dry season flush events. Initially the dry season flush volumes were varied each week in an attempt to simulate the variation in rainfall throughout a typical wet season, however, by the 2004 dry season, these volumes were standardised for each flush (i.e. to equate to approximately 35mm rainfall) to simplify the procedure for site personnel. The HLPs were exposed to ambient rainfall during the 2003/04 and 2004/05 wet seasons.

A flowmeter was installed on the feed tank (Figure 5-4(j)) to enable the volume of water used to irrigate each HLP to be recorded. Potable water was used for the dry season flush events since raw water at the Mine is extracted from a limestone aquifer and is therefore high in carbonate concentrations. Wet season sampling occurred after rainfall events. A rain gauge located in the vicinity of the Southern Waste Rock Dump was used to record millimetres of rainfall and hence the volume of rainfall throughput.

Following each flush event, composite samples of leachate were taken from collection vessels for analysis of physical parameters and total and dissolved metals by ACTFR and AAC. Metal analysis was conducted using ICP-MS to American Public Health Association standard method 3125 B. Samples analysed for dissolved metals were filtered at the time of sample collection using a 0.45µm filter. Parameters analysed and corresponding laboratory detection limits are presented in Table 4-2. As discussed in section 4.2.2, where results were reported as below detection limits a value of half the laboratory detection limit was attributed to the

sample. Sampled analysed for dissolved metals were filtered at the time of sample collection using a 0.45µm filter.

Similarly to the column leach tests, sulfate production, neutralising potential and oxygen consumption rates were calculated for each heap leach pad. A description of how these parameters were calculated is provided in section 4.2.2. Unlike the CLTs, median rates were calculated from the entire dataset, rather than the last ten flushes because the HLP rates varied between the wet and dry seasons and steady state conditions were therefore never achieved (see Figure 5-12 and Figure 5-10).

5.2.3 Heap Leach Pad Excavation

A cross-sectional trench was excavated by a backhoe through the HLPs at the conclusion of the sampling period to assess the extent of secondary mineralisation, armouring and weathering of material comprising the pads. The HLP comprising the most reactive waste rock blend (HLP3) was excavated through to the base, a depth of approximately three metres.

5.2.4 Geochemical Modelling

The geochemical modelling program Visual MINTEQ was used to model the behaviour of HLP leachate and assess likely secondary mineralisation. Visual MINTEQ and its DOS-based version MINTEQA2 were also used throughout the interpretation of dissolved metal concentrations to calculate the solubility of different species.

5.2.5 Data Presentation

Heap leach pad results are frequently presented as box and whisker plots in this chapter. An explanation of these plot types is provided in section 4.2.5 to aid interpretation.

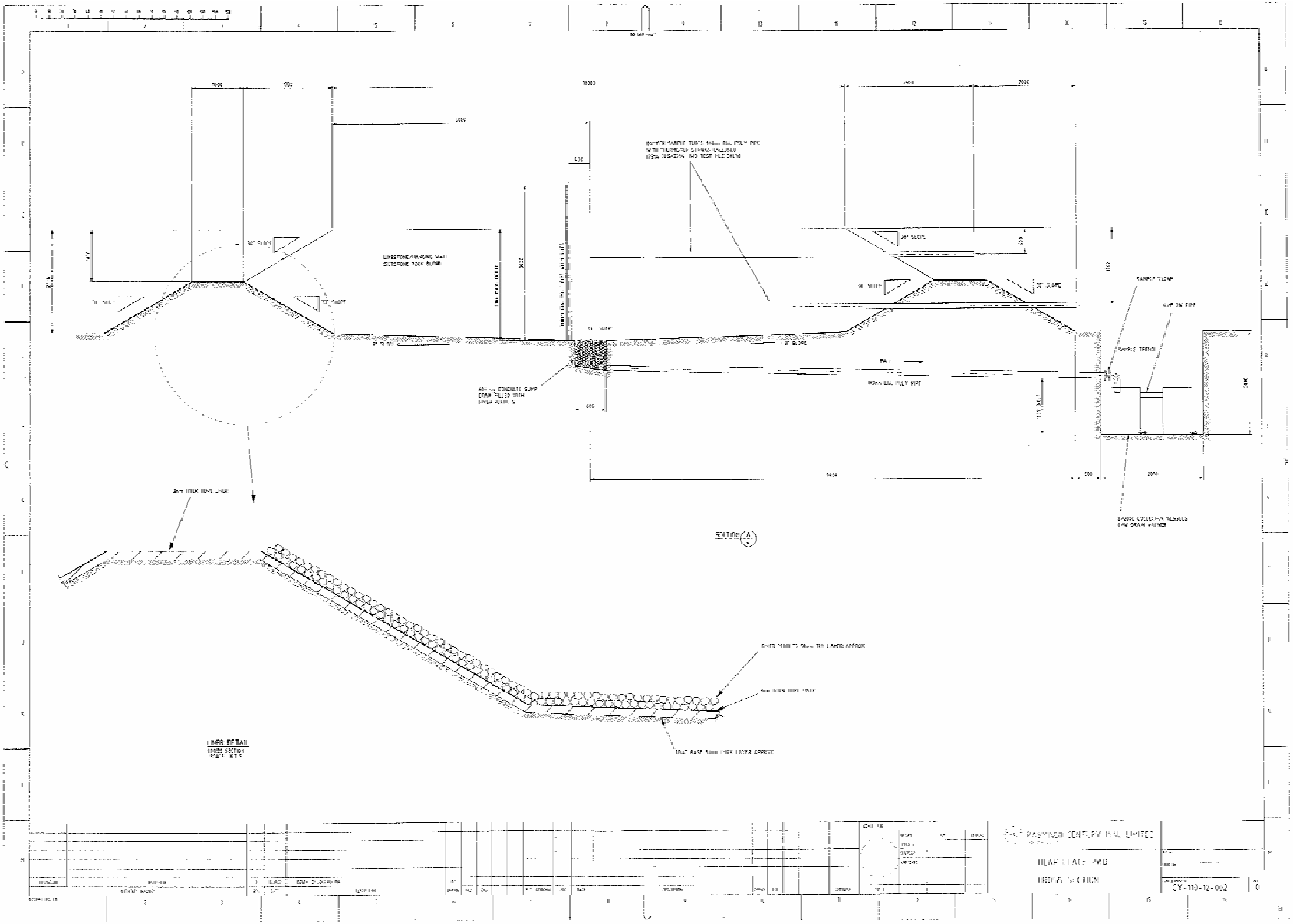

Figure 5-1: Heap Leach Pad Cross Section

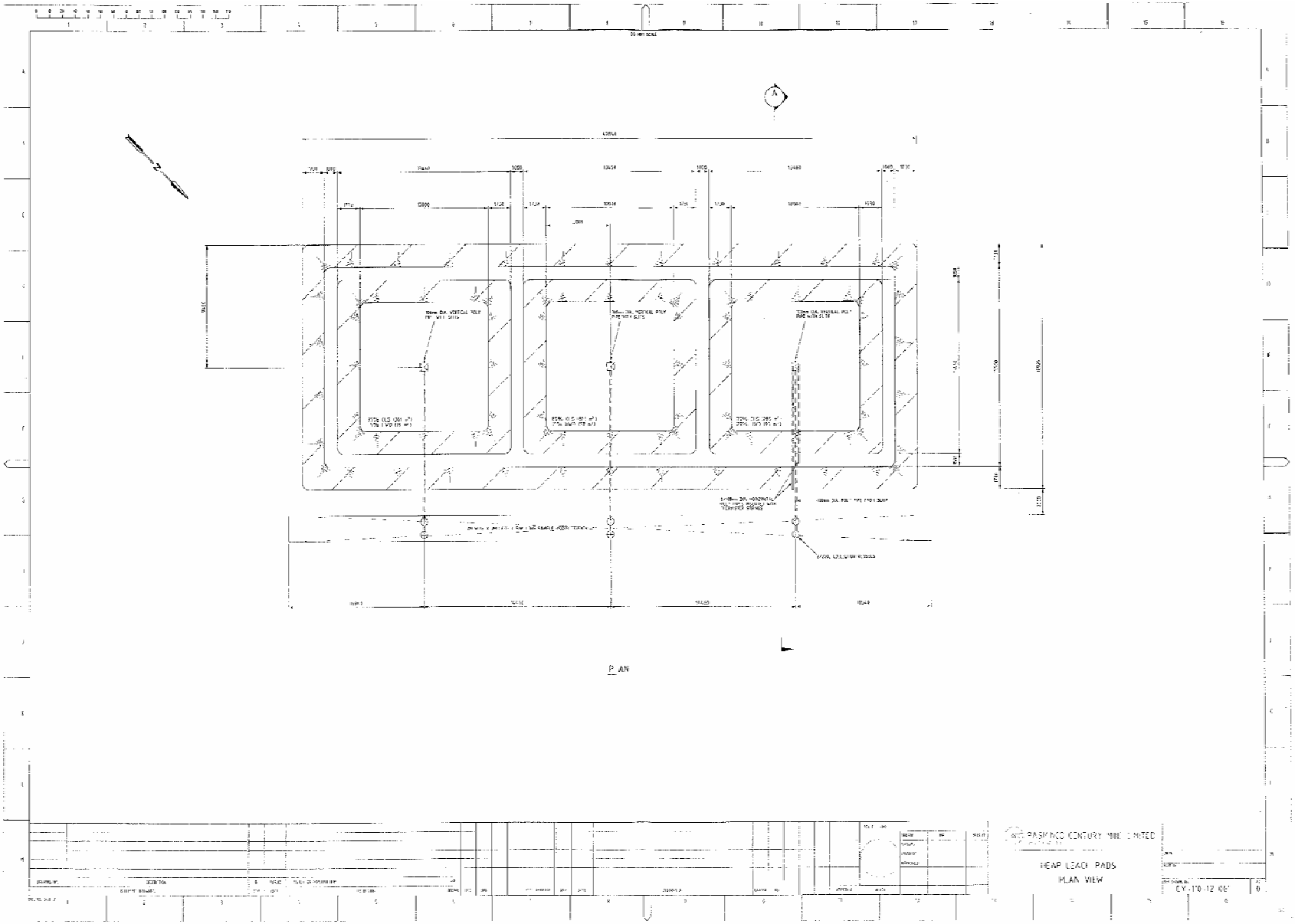

Figure 5-2: Heap Leach Pad Plan View

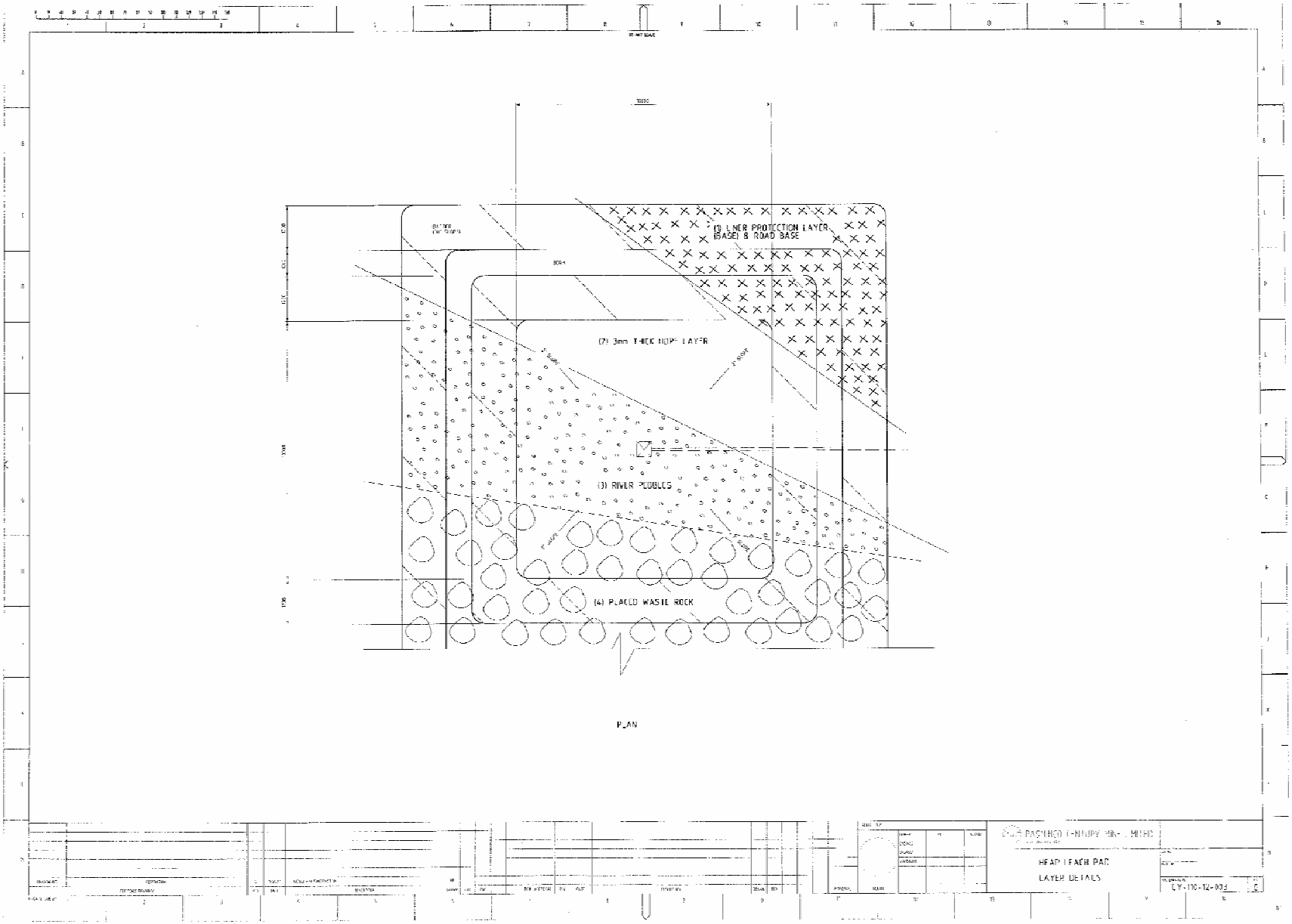

Figure 5-3: Heap Leach Pad Layer Details

	(a) HLP base		(b) Installing HLP piping
	(c) Preparing HLP base		(d) Laying HDPE liner
	(e) Centre drain		(f) Assembling Heap Leach Pads
	(g) Assembling leachate collection system		(h) Completed leachate collection system
	(i) HLP dry season watering system (Sprinklers)		(j) HLP dry season watering system (Feed Tank)

Figure 5-4: Heap Leach Pad Construction

5.3 Heap Leach Pad Results and Discussion

Laboratory analysis data for the heap leach pads are contained in Appendix 4 and are discussed in this section. Heap leach pad results were categorised into wet and dry season subsets based on rainfall data during the test period (Table 5-1). Despite the intention to accelerate the reaction during the manual dry season flushing events, the wet season subsets are considered the most realistic and similar to field conditions as flow events typically occur during the wet, not dry season (refer Figure 2-2).

Table 5-1: Seasonal Classification of Heap Leach Pad Sampling Periods

Sampling Period	Season	Rainfall (mm)	Rainfall Equivalent* (mm)
June 2003 – October 2003	Dry	-	56
November 2003 – February 2004	Wet	516	-
March 2004 – November 2004	Dry	-	399
December 2004 – March 2005	Wet	437	-
April 2005 – August 2005	Dry	-	173
TOTAL		**953**	**628**

* irrigated amount

5.3.1 pH Values

Box and whisker plots for leachate pH values in samples collected from each heap leach pad during the sampling period are shown in Figure 5-5. Samples were classified into either dry or wet season sampling events based on rainfall events (refer Table 5-1) to enable comparisons in results between each season to be obtained.

Although median leachate pH values decreased with increasing PAF material in the heap leach pads in both dry and wet season samples, all leachate samples collected during the sampling period were either of neutral or alkaline pH. This indicated that the CLS material in each HLP effectively neutralised any sulfuric acid that was produced during the flush events.

Of note is the greater pH range present in samples collected during the wet season. pH values as high as 9.5 were recorded in leachate. The differences in pH range between seasons may be attributed to the time leachate sat in the collection containers prior to sampling and the subsequent saturation of dolomite in the sample. The pH of dolomite in equilibrium with 50mmol NaCl (i.e. non-coordinating anion and cation) was calculated as pH 10 using MINTEQA2. This result indicated that due to the prolonged storage in contact with dolomite the pH was approaching that for a solution in equilibrium with dolomite.

Samples were not always collected immediately following wet season flushes due to the unpredictable timing of rainfall events and unavailability of mine environmental staff. In addition, the remote location of the mine and restricted flight schedule resulted in samples not always being dispatched to the laboratory on the same day for analysis. In contrast, because dry season sampling was conducted manually and at controlled times, samples

were collected at the time of watering and either dispatched on that day's plane or the following morning. The length of time leachate sat in the collection containers was therefore minimised.

Schedule C – Table 6 in Environmental Authority No. MIM8000020402 (Ecoaccess, 2004) specifies the discharge range for pH as 6.0 – 9.0. As shown in Figure 5-5, a small number of samples fell outside the upper limit of this range. These were either an extreme value (HLP1 dry season) or were samples collected from rainfall events which were subject to the storage constraint described above and thus are not interpreted to be a true representation of pH values in HLP leachate.

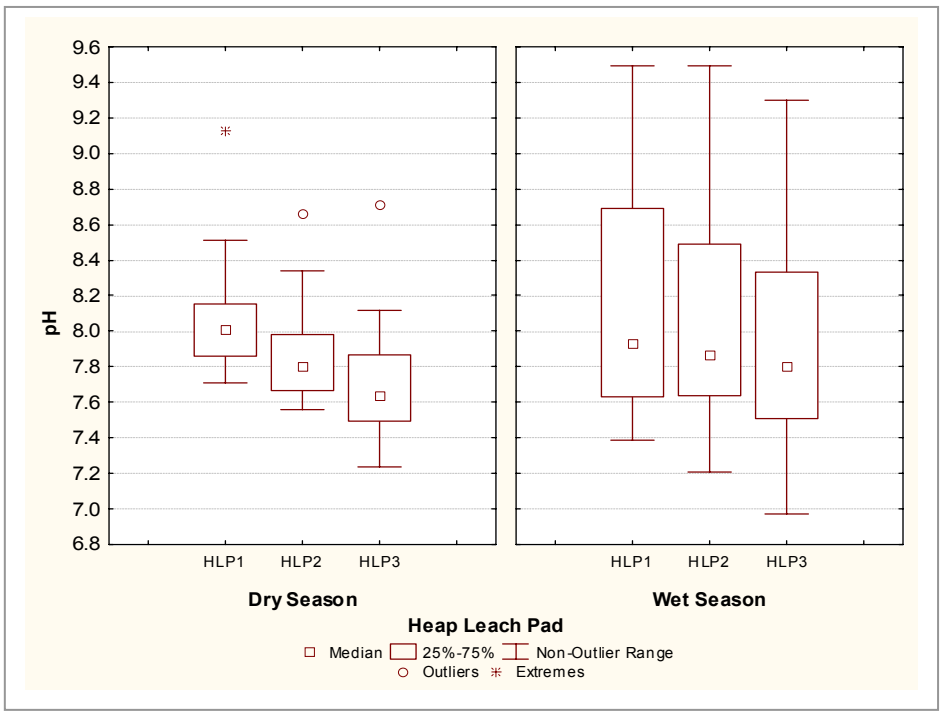

Figure 5-5: Heap Leach Pad pH Values

5.3.2 Sulfate

5.3.2.1 Sulfate Concentration

Sulfate concentrations in sampled HLP leachate for the wet and dry season sampling subsets are presented in Figure 5-6. Sulfate concentration trends for the entire sampling period are shown in Figure 5-10(a), (b) and (c). Sulfate concentrations increased with the percentage of PAF material in the heap leach pads (i.e. were highest in HLP3) and were greater in leachate collected in the wet as opposed to dry season. The median sulfate concentration in leachate from HLP3 increased from 20mmol L^{-1} in dry season to 49mmol L^{-1} in wet season flushes. It is likely the higher sulfate concentrations in samples collected during the wet season were caused by higher rates of pyrite oxidation as a result of increased ambient temperature and humidity. Humidity is an important factor in pyrite oxidation as it has been shown that pyrites weather differently depending on humidity levels. The high humidity conditions would have provided the water needed for pyrite oxidation (Borek, 1993) in between rainfall events and subsequently resulted in high sulfate concentrations in discharge from the ensuing rainfall induced flush events.

The maximum discharge limit for sulfate specified in Schedule C – Table 6 of Environmental Authority No. MIM8000020402 is 1000mg L^{-1} (10mmol L^{-1}) (Ecoaccess, 2004). Median sulfate concentrations in wet season leachate for all blends exceeded this limit. Median wet season sulfate concentrations were 20mmol L^{-1} (HLP1), 29mmol L^{-1} (HLP2) and 49mmol L^{-1} (HLP3). Although median dry season sulfate concentrations were typically half the value of wet season concentrations, the maximum discharge limit for sulfate was exceeded in leachate samples collected from each HLP in the dry season. Median dry season sulfate concentrations were 10mmol L^{-1} (HLP1), 14mmol L^{-1} (HLP2) and 21mmol L^{-1} (HLP3). It should be noted that the wet season concentrations are the most realistic dataset since they best reflect flow conditions at ZCML (i.e. concentrations during wet season flow events).

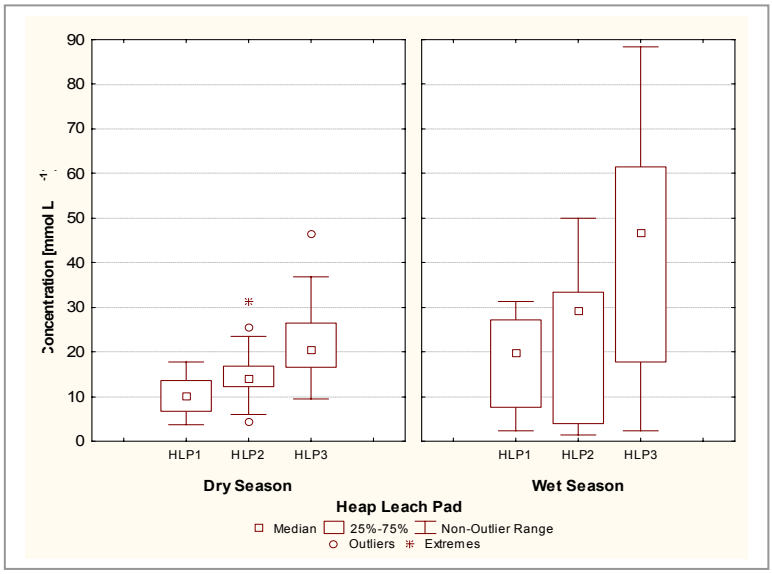

Figure 5-6: Heap Leach Pad Sulfate Concentrations

5.3.2.2 Relationship between Sulfate Concentration and Electrical Conductivity

Figure 5-7 shows the relationship between electrical conductivity and sulfate concentration for samples collected from all three HLPs with datapoints for HLP3 indicated by solid circles. HLP3 wet season drainage contained the highest conductivity and sulfate concentrations. When a linear trendline was fitted to the plot, an r^2 value of 0.9673 was achieved. This suggested that most of the conductivity in the samples was due to chemical species (calcium, magnesium and sulfate) produced from sulfide oxidation and neutralisation of the sulfuric acid formed. The flattening of the slope at high sulfate concentrations may be attributed to the formation of ion-pairs, resulting in a decrease in the conductivity of the leachate (Boyd, 2000).

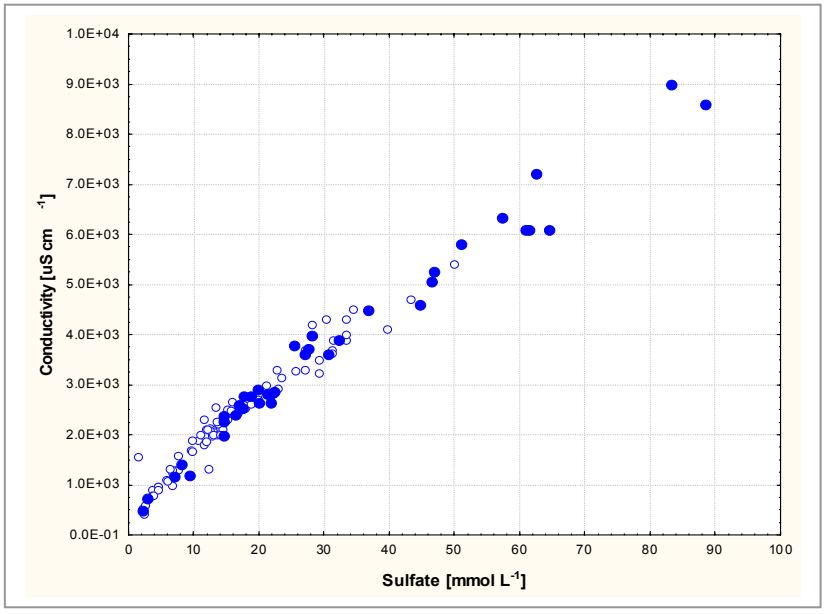

Figure 5-7: Relationship between conductivity and sulfate: All HLPs (HLP3 datapoints marked as solid circles)

5.3.2.3 Relationship between (Calcium plus Magnesium) and Sulfate Concentration

The relationship between (calcium and magnesium) and sulfate concentrations in samples collected from all three HLPs is displayed in Figure 5-8. Datapoints for HLP3 are marked as solid circles. The fit is linear, with a slope of 0.9983 and an r^2 value of 0.9888. In all heap leach pads there was good contact of the leachate with both acid producing and acid consuming rocks, providing enough time to neutralise the sulfuric acid produced. Even though sulfate concentrations were greater in wet season drainage from HLP3 (highlighted datapoints), these concentrations were matched by the sum of calcium and magnesium concentrations, indicating that acid neutralisation reactions occurred and the carbonate material was not armoured. The lack of armouring of carbonate material in HLP3 was verified by excavation of the HLP at the conclusion of sampling in August 2005 and is discussed in section 5.3.4.

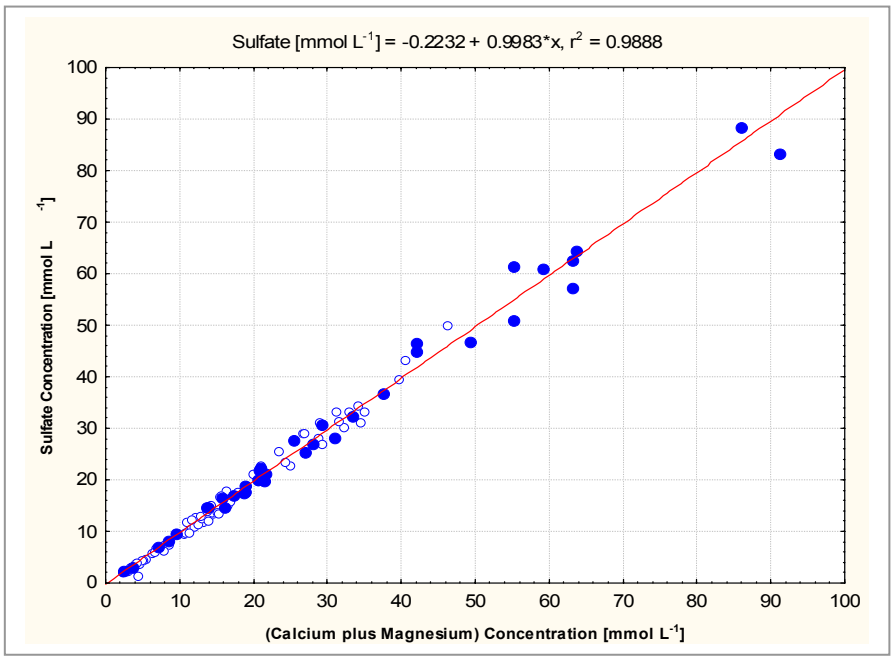

Figure 5-8: **Relationship between (calcium plus magnesium) and sulfate: all Heap Leach Pads (HLP3 datapoints marked as solid circles)**

5.3.2.4 Sulfate Production and Neutralising Potential Depletion Rates

While the calculation of the sulfate production and neutralising potential depletion rates on a time basis (i.e. moles(O_2) kg(material)$^{-1}$ s^{-1}) was considered appropriate for the column leach tests where a relatively even period of time passed between flush events, it was not believed to be valid for the heap leach pads where the time between flush events varied. Where significant periods of time passed between dry season HLP flush events, it was believed the material comprising the pads dried out and water was the limiting factor in allowing sulfide oxidation to progress at a steady rate. This is consistent with findings by Alarcón León et al. (2004) that in semi-arid/arid settings, where oxygen availability is invariably non-limiting, water availability is the rate determining factor for sulfide oxidation. During the wet season, humid conditions between flush events are believed to provide the water required to maintain a relatively constant oxidation rate (Borek, 1993). Sulfate production and neutralising potential depletion rates for the HLPs were therefore calculated on a per flush basis (i.e. moles(O_2) kg(material)$^{-1}$ flush^{-1}).

The main assumption for calculating the rates on a flush basis for the HLPs was that oxidation proceeded to completion, as constrained by water availability, between each flush event. Under this assumption, it was expected that the sulfate load from each flush event would be similar since each flush would have theoretically removed all the oxidised material contained within the pads (i.e. the sulfate load should be independent of the time between each flush event). In order to determine if there was any relationship between sulfate load from the HLPs and the time period between flush events, the two variables were plotted for each HLP (Figure 5-9). Manual dry season flushes are highlighted as solid circles in the graphs.

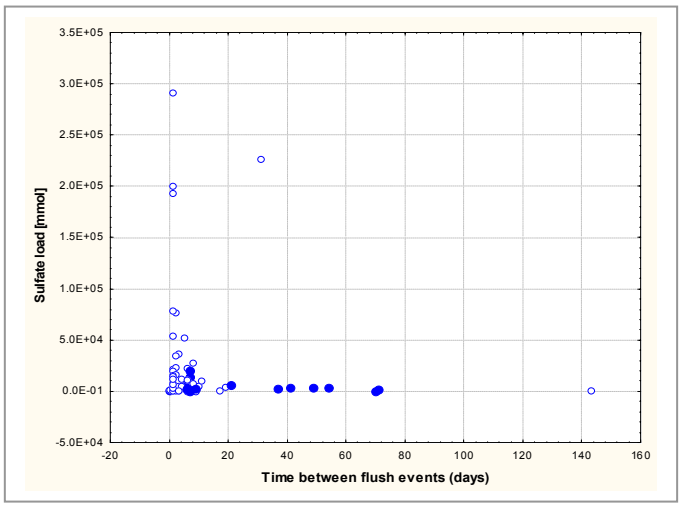

(a) Heap Leach Pad 1 (manual flushes marked as solid circles)

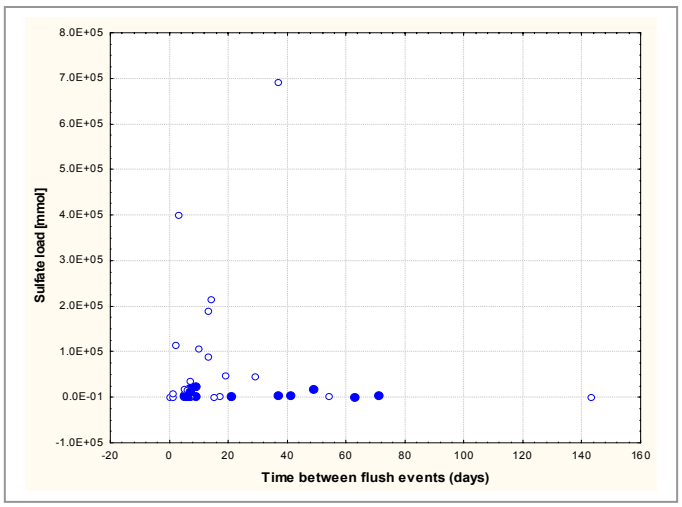

(b) Heap Leach Pad 2 (manual flushes marked as solid circles)

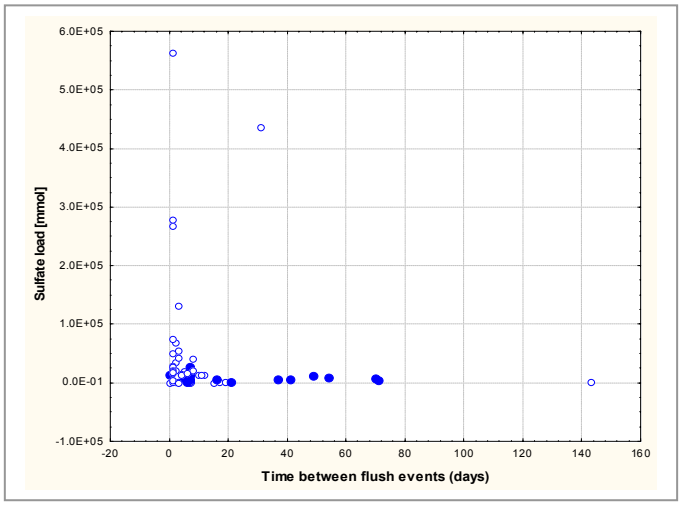

(c) Heap Leach Pad 3 (manual flushes marked as solid circles)

Figure 5-9: Relationship between Sulfate Load Flushed and Time between Flush Events: all HLPs

As shown in Figure 5-9, with the exception of one large flush event following almost forty days of 'drought' conditions, higher sulfate loads were evident where there were shorter periods of time between flush events (i.e. of periods less than two weeks). This indicated that the duration of pyrite oxidation in the HLPs was relatively short and often less than one week, thus supporting the reasoning that calculation of rates on a time basis was not appropriate for the heap leach pads because oxidation rates were not constant between flush events.

This can be further highlighted by the artificial watering events. It will be recalled that dry season watering was conducted in weekly instalments over a four-week 'flushing' period following a four-week 'drought' period. If the duration of pyrite oxidation were greater than one week, it would be expected that the load flushed from the HLPs from succeeding weeks should have monotonically increased. Inspection of sulfate loads in Figure 5-10(d), (e) and (f) suggested that this was not observed. As indicated by the datapoints for flushes during September – October 2004, sulfate concentrations in leachate did not vary between flush events where the heap leach pad was left to stand unwatered for periods between seven to twenty-eight days. If the HLP had reacted for a period greater than seven days, the sulfate concentration in the first sampling event for September 2004 would have been greater than that in the subsequent sampling events. Similar trends were observed for the sampling events in November 2004 and June 2005.

On the other hand, if the assumption that oxidation proceeded to completion between each flush event was entirely true, the sulfate load should have been constant for all significant flushes. Figure 5-10(d), (e) and (f) show that there were a number of events in the wet season where the sulfate loads were significantly higher than those for other flush events. These high sulfate loads were driven by large rainfall events and the subsequent high flows of water through the pads (Figure 5-10). These flush events were characterised by high flows, high sulfate concentrations and occurred during the wet season, when temperatures and humidity were greater between flush events thereby providing favourable conditions for pyrite oxidation (Borek, 1993). Of particular note however, is that load values recovered immediately with subsequent events yielding samples with reduced loads. This behaviour is consistent with the flushing of secondary minerals during large flush events following dry periods.

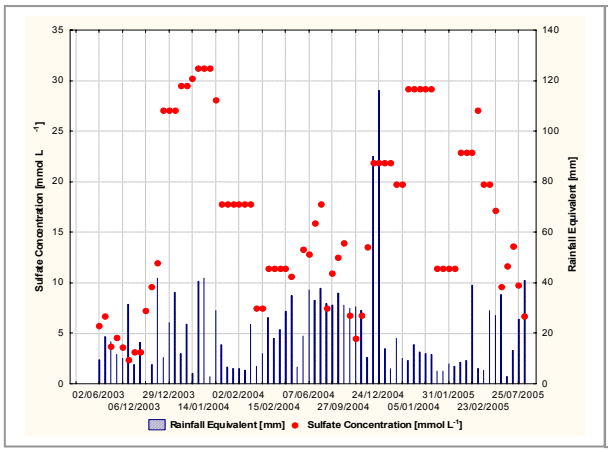

(a) HLP1 Sulfate Concentration

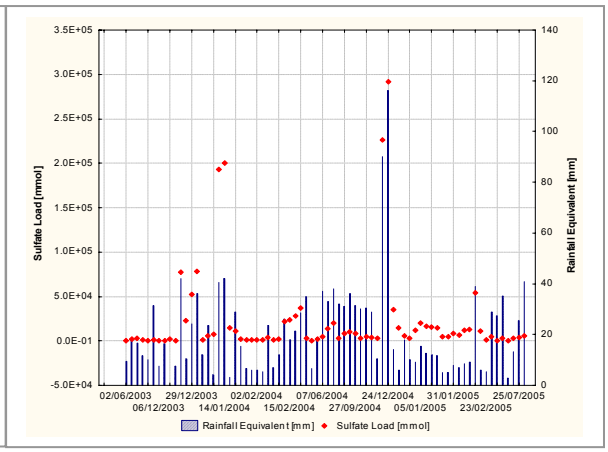

(d) HLP1 Sulfate Load

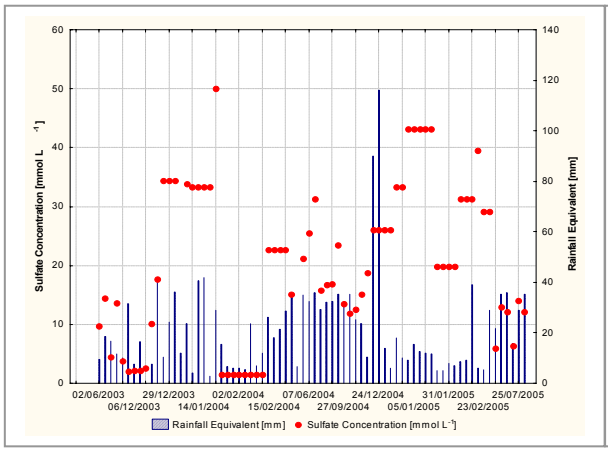

(b) HLP2 Sulfate Concentration

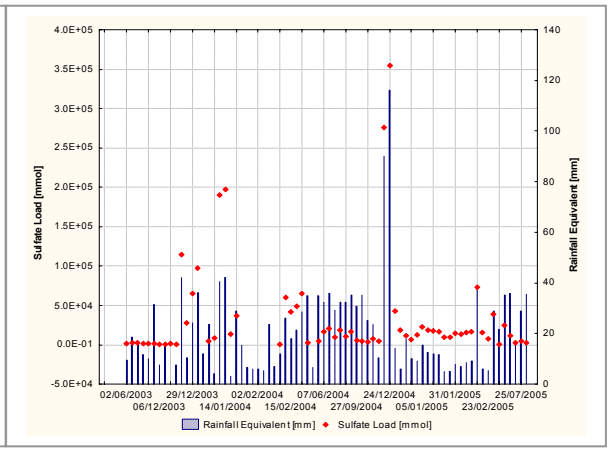

(e) HLP2 Sulfate Load

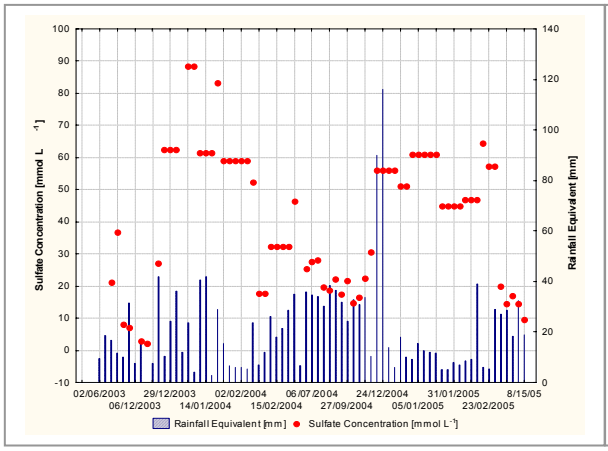

(c) HLP3 Sulfate Concentration

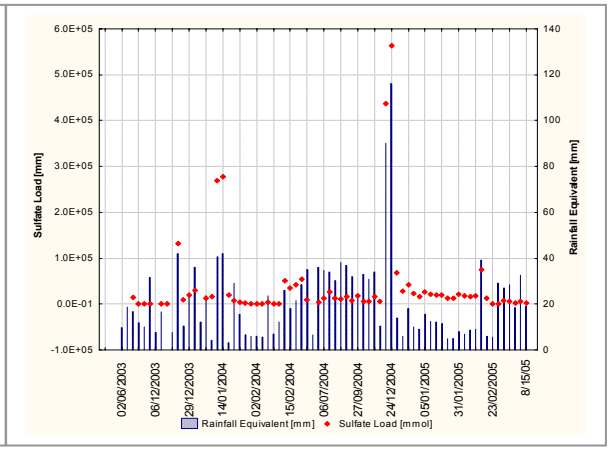

(f) HLP3 Sulfate Load

Figure 5-10: HLP Water Inflow and Sulfate Concentration and Load

Sulfate production and neutralising potential depletion rates were calculated for each heap leach pad flush event (refer Appendix 7) and are shown graphically in Figure 5-11. Rates are also presented as box and whisker plots for both wet and dry season datasets to allow comparison between the two seasons (Figure 5-12). From both figures, it can be seen that the neutralising potential depletion rates for each heap leach pad in both season datasets closely mirrored the sulfate production rate. This indicated that the acid produced by the oxidation of pyrite was neutralised by calcium and magnesium carbonates in each heap leach pad.

As with sulfate loads, sulfate production rates were highest in the wet season and were driven by a small number of significant rain events that yielded high flows through the HLPs. These values are shown as highpoints in Figure 5-11 and as outlier and extreme datapoints in Figure 5-12. It is interesting to note that the sulfate production rates recovered shortly after these high values when flow volumes reduced, even though sulfate concentrations may have been higher (refer to Figure 5-10 for comparison of sulfate concentrations and loads).

Using values obtained from the calculation of the sulfate production and neutralising potential depletion rates, an estimate of the times to sulfur and neutralising potential depletion was calculated for each HLP. From Table 5-2, it can be seen that theoretically, at the end of the sampling period (i.e. August 2005), over 97% of the sulfides in HLP1 had been flushed from the pad, leaving only a minimum of 10 flushes until sulfide depletion under similar conditions of the experiment (i.e. with manual dry season flushing events supplementing wet season rainfall and assuming a linear relationship). The estimated minimum time to sulfide depletion in HLPs 2 and 3 were 72 and 221 flushes respectively. For all HLPs, the time to neutralising potential depletion far exceeded the time to sulfide depletion. This indicated that while the carbonates in the HLPs were not armoured and were available to dissolve to neutralise sulfuric acid, acidic drainage would not be produced.

It is apparent from Table 5-2 that the median sulfate production rates for HLP2 and HLP3 were very similar, despite differing percentages of PAF material in the HLPs. As will be shown in section 5.3.5, gypsum was precipitating in both HLP2 and HLP3. This process subsequently controlled sulfate concentrations in leachate from these HLPs and as a consequence, the sulfate production and neutralising potential depletion rates are underestimated (Mehling Environmental Management Inc, 1998).

A limitation in calculating the sulfate production and neutralising potential depletion rates on a per flush basis, and in doing so assuming that oxidation proceeded to completion between flush events, is that in the event where the time between flush events was less than one week, calculated rates may be underestimated. This in turn would impact on the time to sulfide depletion, which as a result, may also be underestimated. This effect may be exacerbated by the precipitation of gypsum in HLP2 and HLP3 (refer section 5.3.5) and the resulting underestimation of the sulfate production rates for these HLPs.

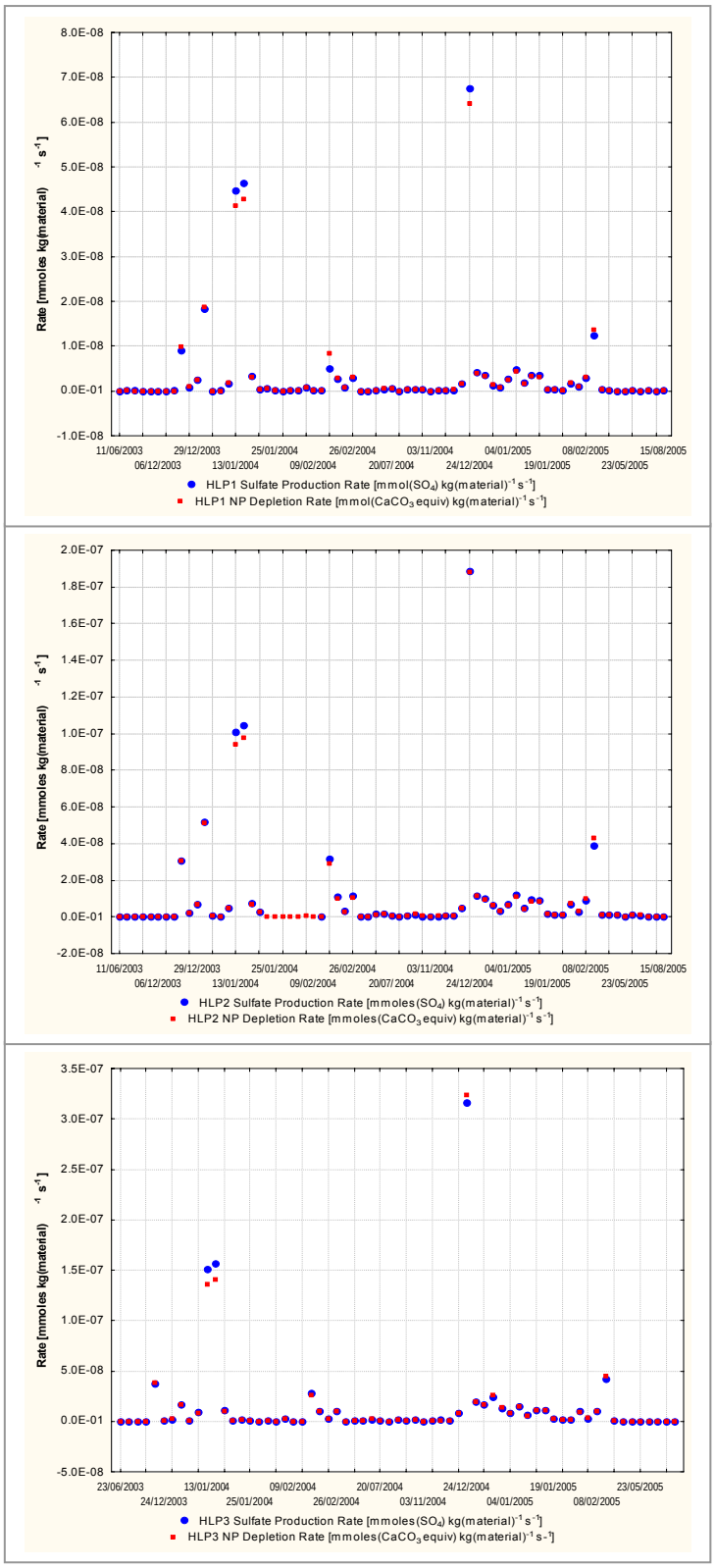

Figure 5-11: HLP Sulfate Production and Neutralising Potential Depletion Rate Profiles

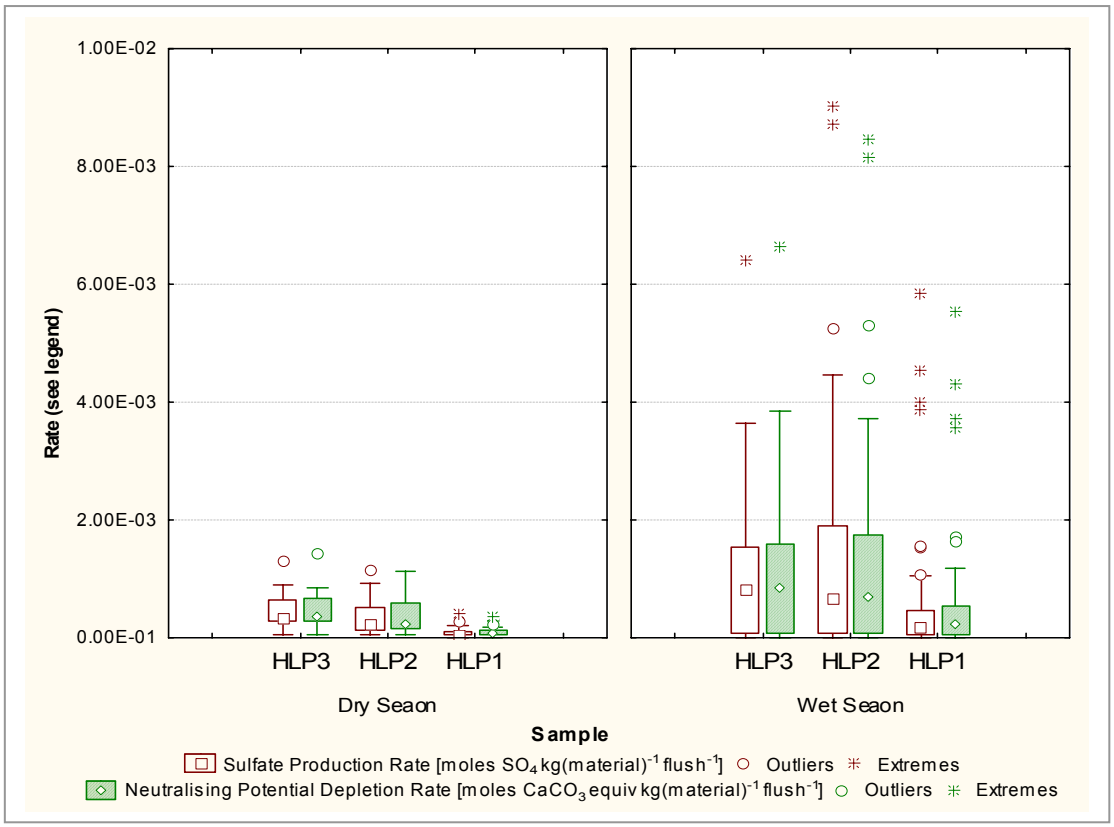

Figure 5-12: **HLP Sulfate Production and Neutralising Potential Depletion Rates**

Table 5-2: **HLP Sulfate Production and Neutralising Potential Rate Summary (per flush)**

HLP	% PAF in sample	% S flushed from sample	Median SO_4 Production Rate [moles (SO_4) kg(material)$^{-1}$ flush^{-1}]	% NP flushed from sample	Median NP Depletion Rate [moles ($CaCO_3$ eq) kg(material)$^{-1}$ flush^{-1}]	Estimated Minimum Time to S Depletion (flushes)♦	Estimated Minimum Time to NP Depletion (flushes)♦
HLP1	0.34	97	9.98E-05	0.33	1.13E-04	10	87787
HLP2	8.27	75	4.59E-04*	1.1	4.67E-04*	72	19409
HLP3	19.10	48	6.33E-04*	1.6	6.21E-04*	221	12882

*Note: these are minimum values due to gypsum precipitation in HLP2 and HLP3 (refer section 5.3.5) controlling the sulfate concentration in leachate from these HLPs.

♦ Under irrigation conditions (i.e. current flushing scenario)

To enable comparison between the column leach test and heap leach pad oxygen consumption rates, the sulfate production, neutralising potential depletion and oxygen consumption rates were calculated for the heap leach pads on a time basis, despite belief that there were significant uncertainties in this method. These rates are summarised in Table 5-3 and compared against values for similarly blended column leach tests in Chapter 6: Scale-Up. It should be noted that unlike the CLTs, HLP oxygen consumption rates were not 'normalised' for the amount of sulfur.

Table 5-3: HLP Sulfate Production, Neutralising Potential Depletion and Oxygen Consumption Rate Summary

HLP	Median SO_4 Production Rate [moles (SO_4) kg(material)$^{-1}$ s^{-1}]	Median NP Depletion Rate [moles ($CaCO_3$ eq) kg(material)$^{-1}$ s^{-1}]	Median Oxygen Consumption Rate [moles(O_2)kg(material)$^{-1}$ s^{-1}]	Estimated Minimum Time to S Depletion (years)♦	Estimated Minimum Time to NP Depletion (years)♦
HLP1	2.89E-10	3.07E-10	1.62E-11	0.11	1023
HLP2	1.01E-09*	1.01E-09*	5.63E-11*	1.0	285
HLP3	1.37E-09*	1.30E-09*	7.64E-11*	3.3	195

*Note: these are minimum values due to gypsum precipitation in HLP2 and HLP3 (refer section 5.3.5) controlling the sulfate concentration in leachate from these HLPs.

♦ Under irrigation conditions (i.e. current flushing scenario)

Similarly to the sulfate production and neutralising potential depletion rate values, the oxygen consumption rates for HLP2 and HLP3 were minimum values and almost identical for HLP2 and HLP3 because the concentration of sulfate in leachate was controlled by the solubility of gypsum and not by the intrinsic oxidation rate of the material comprising the HLPs. The effect of gypsum precipitation in the HLPs on oxygen consumption rates and the impact it had on the effective scale-up of results from the CLTs to the HLPs is discussed in Chapter 6: Scale-Up.

A potential flaw in the sampling methodology that may have affected the accuracy of calculated sulfate production rates and therefore the estimated time to sulfide depletion for both methodologies was that the mass balances and median sulfate production rates were calculated from single sulfate concentrations analysed from a composite sample for each flush event sampled. The composite sample may not have fully accounted for variation in leachate sulfate concentrations during the flow event and therefore, the median sulfate concentration may either be over or under estimated. This was considered more likely to occur during large wet season events when sulfate concentrations in the drainage were higher and the combined capacity of the collection vessels (400L) was not sufficient to capture the entire volume of leachate and therefore collection of a fully representative sample.

Although the HLPs were designed to enable a representative sample of each flush event to be taken from the first collection vessel (note: all drainage flowed through the first collection vessel and overflowed when full to the second collection vessel), there was a possibility that the sample was not a true composition of the total discharge, particularly where the collection vessels had overflowed during high flow events.

To gain an understanding of the variation in sulfate concentrations during a flow event, the sulfate concentrations throughout a wet season rainfall event were monitored. Discharge from HLP2 and HLP3 were collected at ten-minute intervals from the sample tap-off valve at the HLP discharge points during a significant rainfall event in January 2006. Samples were analysed by ACTFR for pH, sulfate, calcium and magnesium ions. Results from this flow event are displayed in Table 5-4.

From Table 5-4 it can be seen that sulfate, magnesium and calcium concentrations fell in samples collected from HLP2 and HLP3 after the initial flush and then steadily increased throughout the flush to peak at the end of the event. Concentrations typically varied by a factor of three to four from the minimum to maximum concentrations.

If samples were collected at or towards the end of the sampling period, there may be a tendency for concentrations in the sample taken from the collection vessel to be overestimated by a factor of approximately two. Given this potential bias, rates were recalculated for median sulfate, magnesium and calcium concentrations half the value than those sampled. Values for this scenario are provided in Table 5-4. Median sulfate production and neutralising potential depletion rates and oxygen consumption rates decreased with the amended lower concentrations and in turn increased the time to sulfide depletion. Even though this scenario resulted in an increase in time to sulfide depletion, the time to neutralising potential depletion was still significantly higher than the time to sulfide depletion, indicating that as long as carbonates in the HLPs were not armoured acidic drainage would not be produced in the HLPs.

Table 5-4: Concentration Profile During HLP Flow Event on 10 January 2006

Sample Time	pH	Calcium [mmol L^{-1}]	Magnesium [mmol L^{-1}]	Sulphate [mmol L^{-1}]
HLP 2				
07:24	7.53	2.07	3.78	6.77
07:34	7.48	0.95	1.65	3.44
07:44	7.33	1.47	2.34	4.89
07:54	7.23	2.12	3.50	6.97
08:04	7.15	2.79	5.06	9.58
08:14	7.44	3.37	5.02	13.53
HLP 3				
07:24	7.47	1.70	2.80	5.93
07:34	7.53	1.02	1.56	3.33
07:44	7.33	1.47	2.18	4.27
07:54	7.29	2.10	3.00	6.14
08:04	7.38	2.50	3.87	8.22
08:14	7.18	3.97	6.95	10.10

Table 5-5: Amended HLP Sulfate Production and Neutralising Potential Depletion Rate (per flush) Summary

HLP	% S flushed from sample	Median SO_4 Production Rate [moles (SO_4) kg(material)$^{-1}$ flush^{-1}]	% NP flushed from sample	Median NP Depletion Rate [moles ($CaCO_3$ eq) kg(material)$^{-1}$ flush^{-1}]	Median O_2 Consumption Rate [moles (O_2) kg(material)$^{-1}$ flush^{-1}]	Estimated Minimum Time to S Depletion (flushes)$^{\Phi}$	Estimated Minimum Time to NP Depletion (flushes)$^{\Phi}$
HLP1	49	5.15E-05	0.17	5.85E-05	2.88E-06	346	3.89E+05
HLP2	38	2.41E-04*	0.54	2.39E-04*	1.35E-05*	345	3.82E+04
HLP3	24	3.16-04*	0.78	3.09-04*	1.77E-05*	644	2.61E+04

*Note: these are minimum values due to gypsum precipitation in HLP2 and HLP3 (refer section 5.3.5) controlling the sulfate concentration in leachate from these HLPs.

$^{\Phi}$ Under irrigation conditions (i.e. current flushing scenario)

5.3.3 Metals

5.3.3.1 Total Metal Concentrations

Similar to samples collected from the column leach tests, total cadmium, total lead, total zinc and total arsenic concentrations in HLP leachate samples were compared against limits established in ZCML's Environmental Authority No. MIM8000020402 (Ecoaccess, 2004). Results for other total metals assayed are contained in Appendix 4.

Figure 5-13(a) and (d) show total arsenic and total zinc concentrations respectively in samples collected from the HLPs. Concentrations of total arsenic and total zinc were within maximum discharge limits specified in MIM8000020402 (i.e. 1.3mol L^{-1} and $6.1x10^{2}$mol L^{-1} respectively) in all samples collected from the HLPs. Concentrations increased slightly during the wet season when weathering rates increased with higher temperatures and humidity.

Total cadmium concentrations in leachate collected from the heap leach pads are shown in Figure 5-13(b). Cadmium concentrations in leachate collected from HLPs 1 and 2 were consistently below the maximum discharge limit specified in MIM8000020402 (i.e. $8.9x10^{-2}$mol L^{-1}). Although most samples collected from HLP3 complied with the total cadmium limit specified, total cadmium concentrations in sampled HLP3 leachate exceeded the licence limit during two large wet season flush events. These peaks are attributed to the high volume and intensity of the flush events and the subsequent flushing of fine solids from HLP3.

Concentrations of total lead in HLP leachate samples are shown in Figure 5-13(c). Excluding the initial flush event, total lead concentrations in samples collected from the HLPs were in compliance with the maximum specified limit (i.e. 0.48mol L^{-1}). For all the total metal concentrations sampled, concentrations increased with the increasing percentage of PAF material in the heap leach pad (i.e. were highest in HLP3 leachate).

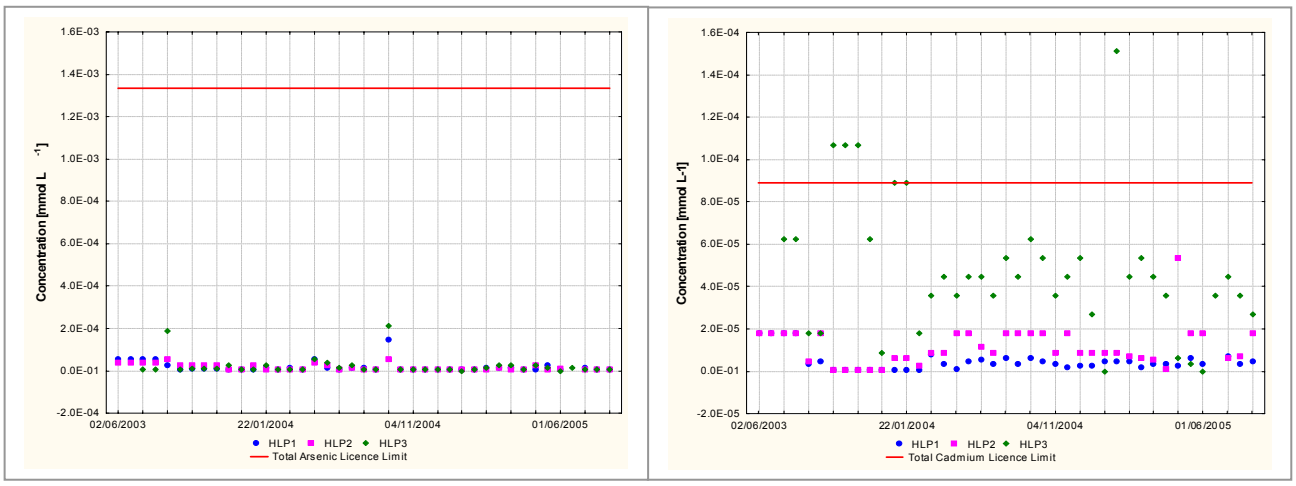

(a) Total Arsenic Concentrations **(b) Total Cadmium Concentrations**

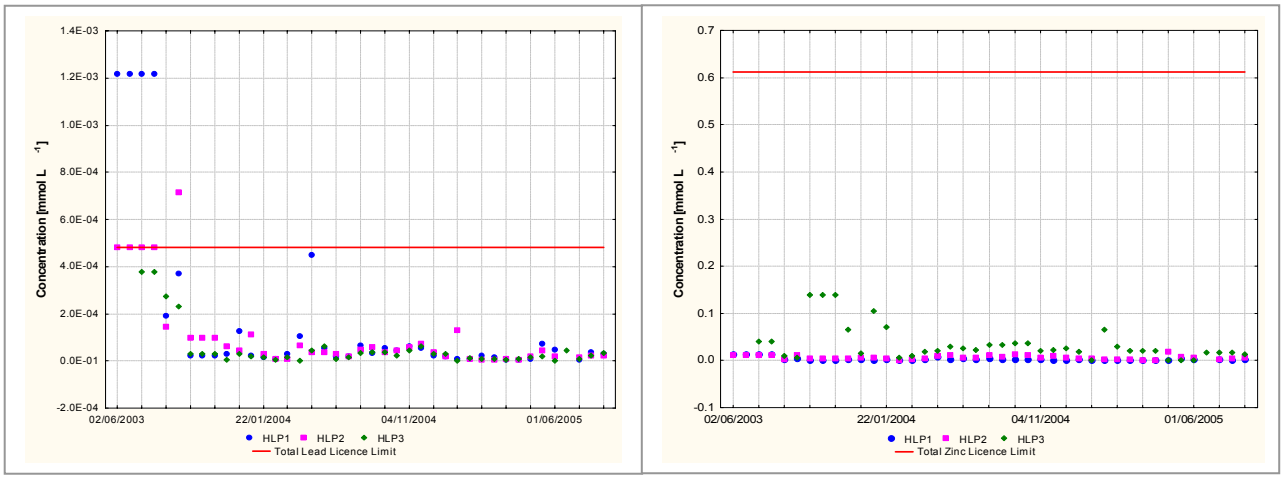

(c) Total Lead Concentrations **(d) Total Zinc Concentrations**

Figure 5-13: HLP Total Metal Concentrations

5.3.3.2 Dissolved Metal Concentrations

Appendix 8 contains statistical data (i.e. median, mean, minimum, maximum, standard deviation and 10, 25, 75 and 90 percentile values) for leachate collected from all HLPs during the two-year sampling period. Categorised box and whisker plots for the wet and dry seasons were compiled to enable the trends in dissolved metal concentrations between the different weathering conditions to be assessed.

5.3.3.2.1 Zinc

Dissolved zinc concentrations in HLP leachate for the wet and dry season sampling subsets are presented in Figure 5-14. Dissolved zinc concentrations increased with the percentage of PAF material in the HLPs (i.e. were highest in HLP3 leachate). Although the range of values for dissolved zinc was higher in samples collected during the wet season, median values were very similar, and in fact, were greater in samples collected during the dry season. Median dissolved zinc concentrations for the dry and wet season dataset respectively were 2.0×10^{-6}mol L^{-1} and 1.0×10^{-6}mol L^{-1} (HLP1), 6.0×10^{-6}mol L^{-1} and 3.0×10^{-6}mol L^{-1} (HLP2) and 2.1×10^{-5}mol L^{-1} and 1.8×10^{-5}mol L^{-1} (HLP3). The higher concentrations of dissolved zinc in wet season samples were driven by a small number of high flow events (Figure 5-14(b)).

A possible control on zinc solubility that would exhibit significant pH dependence would be the precipitation of zinc hydroxide as a secondary mineral in the HLPs. To test this possible control on dissolved Zn^{2+} concentrations in HLP leachate, the geochemical modelling program MINTEQA2 was used to calculate the solubility of $Zn(OH)_2$ in increments of 0.20 pH units from pH 8.8 to 5.0 using the concentrations specified in section 4.3.4.2.1. The resultant modelled solubility curve is shown as solid circles in Figure 5-15. This figure demonstrates that the solubility of zinc in HLP samples was less than what was predicted on thermodynamic grounds assuming that zinc hydroxide solubility controlled dissolved Zn^{2+} concentrations. Similar to CLT leachate, two processes appeared to determine the solubility of Zn^{2+} in leachate solution. At pH values below 7.8, Zn^{2+} was effectively controlled by the rate of Zn^{2+} released (i.e. the rate of sphalerite oxidation). At higher pH values (>7.8), the solubility of $Zn(OH)_2$ appeared to be increasingly dominant in controlling the Zn^{2+} concentration in HLP leachate (i.e. assuming $Zn(OH)_2$ was the solubility limiting phase).

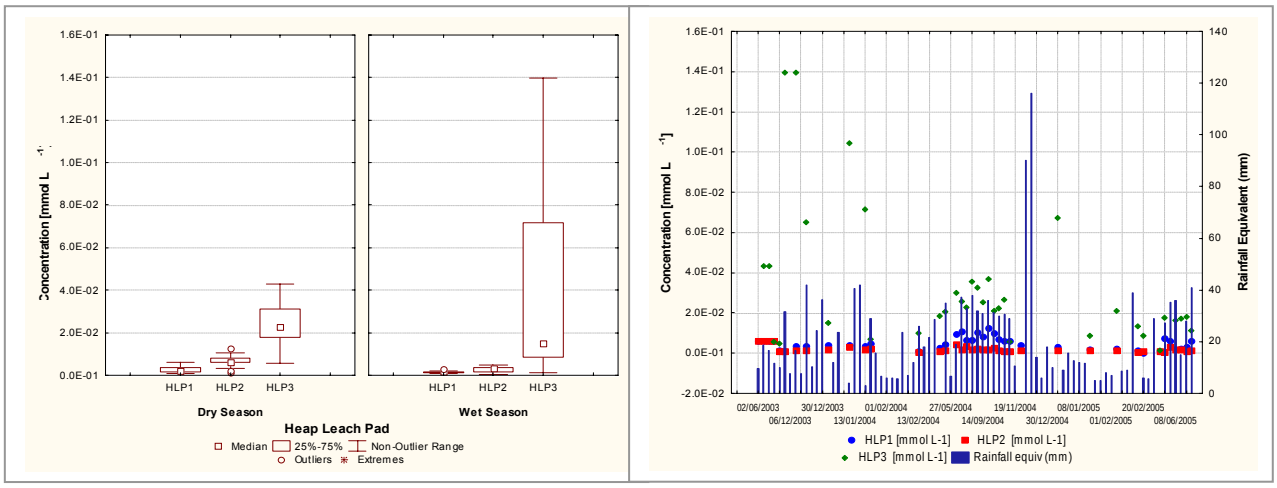

(a) Wet / Dry Season Categorised **(b) Dissolved Zinc Concentration Vs Time Profile**

Figure 5-14: HLP Dissolved Zinc Concentrations

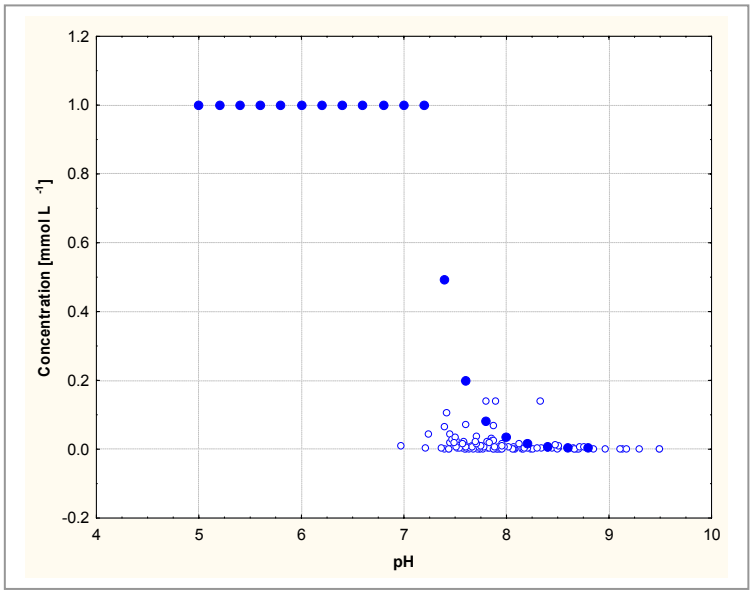

Figure 5-15: Relationship between pH and dissolved zinc: all HLPs (MINTEQA2 Zinc Solubility Simulation Marked as Solid Circles)

5.3.3.2.2 Lead

Similar to concentrations in leachate from the column leach tests, dissolved lead concentrations in drainage collected from the heap leach pads were low and in many samples undetectable (i.e. less than 4.8×10^{-4} µmolL^{-1}) (Figure 5-16). Median concentrations did not vary significantly between the different HLPs and wet season concentrations were only slightly higher than those in samples collected during the dry season.

The solubility calculation of Pb^{2+} undertaken in MINTEQA2 (Figure 5-17) showed that below pH values of 7.5, dissolved lead concentrations should be detectable in samples. As discussed in section 4.3.4.2.2, the low dissolved lead concentrations in acidic leachate from the CLTs were attributed to the formation of a surface coating on galena and the ensuing slow galena oxidation rate. Although the median pH values in all heap leach pad leachate samples collected in both wet and dry seasons were above 7.5, the lower range fell below pH 7.5 for all HLPs during the wet season (Figure 5-5). It can be seen from Figure 5-17 that dissolved lead concentrations remained very low in samples collected from the HLPs even at these slightly lower pH values. Similar to the CLT samples, dissolved lead in HLP samples was controlled by $Pb(OH)_2$ solubility at pH values above 7.2, and by the passivation of galena at pH values below this level. Despite the differences in the pH range, no real change to dissolved lead concentrations was detected between the two seasons.

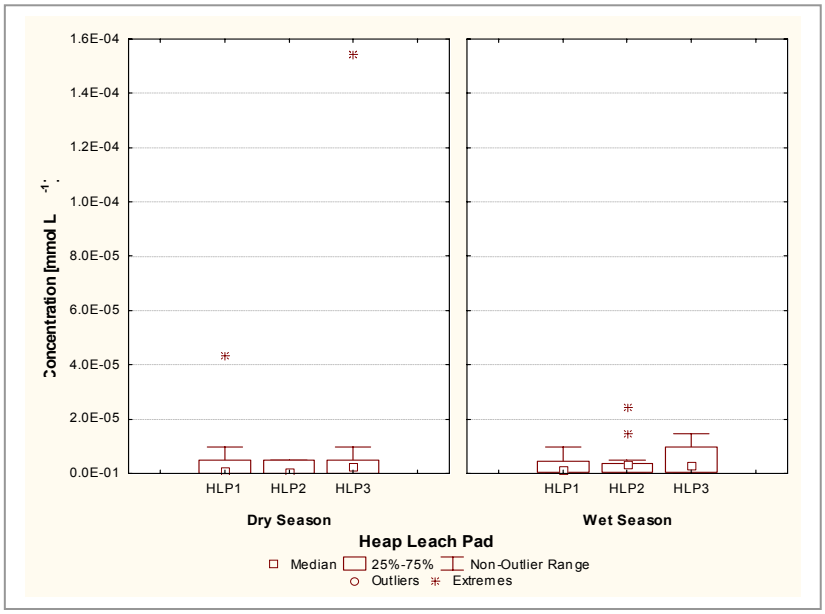

Figure 5-16: HLP Dissolved Lead Concentrations

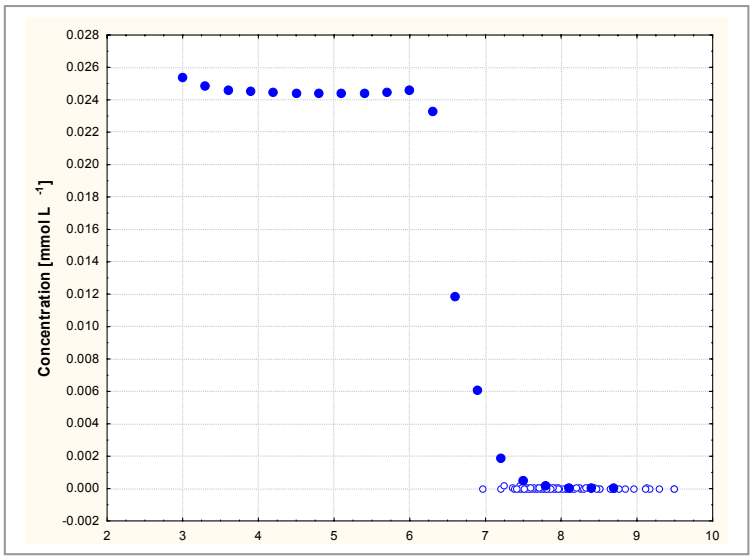

Figure 5-17: Relationship between pH and dissolved lead: all HLPS (MINTEQA2 Lead Solubility Simulation Marked as Solid Circles)

5.3.3.2.3 Arsenic

Dissolved arsenic concentrations in samples collected from the HLPs were highest in samples collected from HLP3 during the wet season flush events. Dissolved arsenic concentrations in many samples, particularly in those collected from HLPs 1 and 2, were extremely low and often undetectable (i.e. less than 1.3×10^{-3} µmol L^{-1}) and consequently have not been graphed in this section.

5.3.3.2.4 Other Dissolved Metals

Dissolved aluminium, cadmium, copper and iron concentrations in samples collected from the HLPs are shown in Figure 5-18(a) – (d) respectively. The medians and spread of dissolved cadmium, copper and iron concentration data increased with the percentage of PAF in the HLPs (i.e. higher concentrations in HLP3 samples). The range (dissolved cadmium, Figure 5-18(b)) and median (dissolved copper, Figure 5-18(c)) were typically higher in leachate samples collected during the wet season as a result of increased temperatures and humidity and therefore weathering of pyrite. Dissolved iron concentrations (Figure 5-18(d)) did not vary substantially between the wet and dry season datasets. It is likely that the dissolved iron concentrations were influenced by colloidal iron that passed through the 0.45µm filter during sampling and therefore may not be "true" dissolved iron concentrations. Likewise, there was no real pattern to the dissolved aluminium dataset. It is believed that colloidal aluminium concentrations and the issues of sample collection and handling discussed in section 5.3.1 also influenced dissolved aluminium concentrations. The influence of inaccurate dissolved iron concentrations on the accuracy of geochemical modelling is discussed in sections 4.3.6 and 5.3.5.

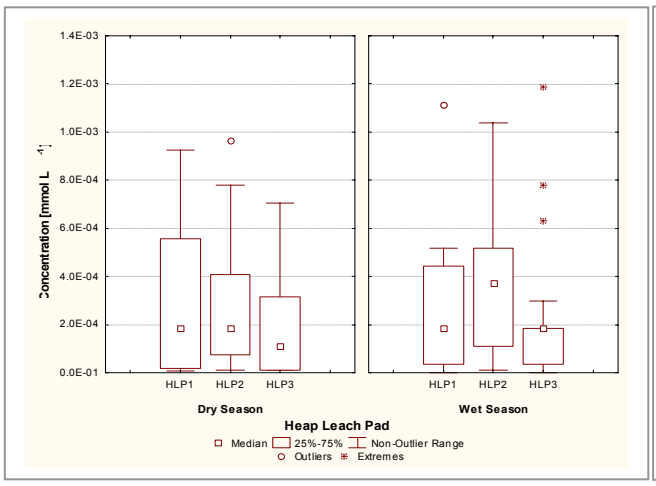

(a) HLP Dissolved Aluminium Concentrations

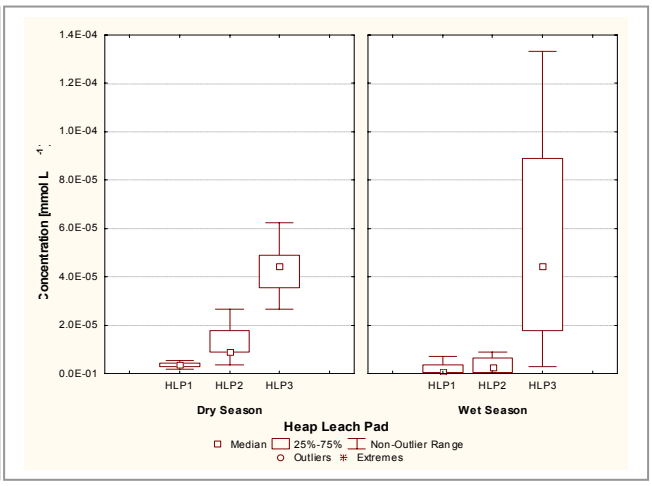

(b) HLP Dissolved Cadmium Concentrations

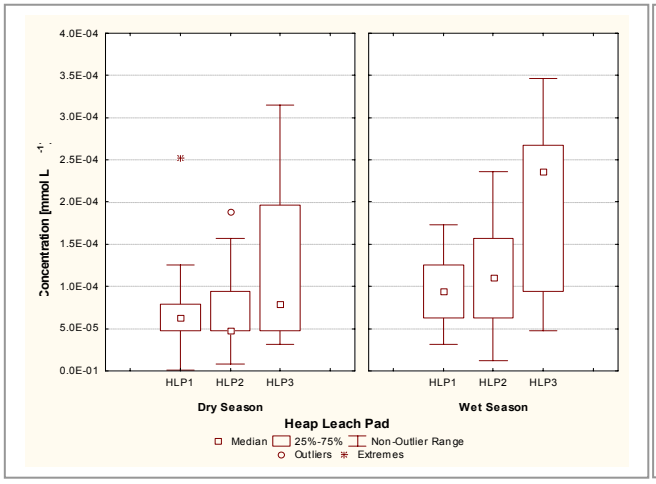

(c) HLP Dissolved Copper Concentrations

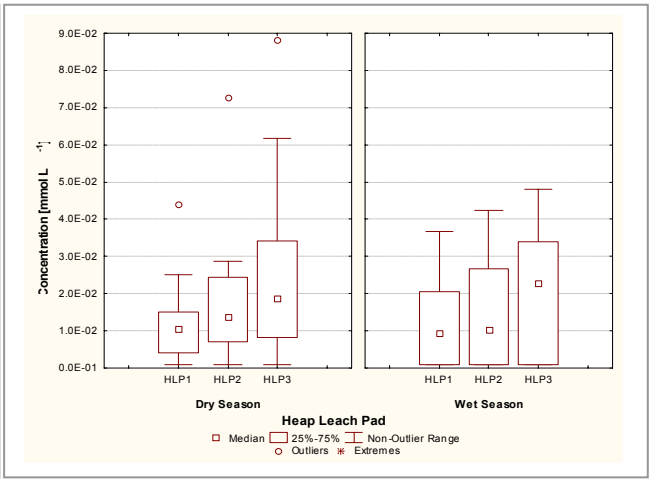

(d) HLP Dissolved Iron Concentrations

Figure 5-18: HLP Dissolved Metal Concentrations

5.3.3.2.5 HLP Dissolved Metal Concentration Summary

For all dissolved metal concentrations presented, the pH values in HLP leachate were sufficiently high that metal solubility was low and concentrations of dissolved metals were maintained in the sub-micro molar range. The lack of variability between wet and dry season datasets for dissolved iron and aluminium concentrations was attributed to the passing of colloidal iron and aluminium through the 0.45µm filter during sampling. In addition to $Pb(OH)_2$ solubility maintaining low dissolved lead concentrations at neutral to alkaline pH values, galena passivation maintained low concentrations in leachate with pH values below this level.

5.3.4 Heap Leach Pad Excavation

The HLPs were excavated at the conclusion of the sampling period (i.e. August 2005) to assess the extent of secondary mineralisation, armouring and weathering of material comprising the HLPs. A cross-sectional trench was excavated through each HLP using a backhoe (Figure 5-19).

Figure 5-19: HLP3 Excavation

Observations of the material comprising the HLPs showed that there was a significant reduction in particle size during the flushing period. The pads were constructed from ROM material, however at the end of the sampling period, much of the larger HWD material had weathered significantly to large gritty grains or gravel size. This was particularly apparent in HLP3, the test pad with the highest percentage of PAF material. Figure 5-20(a) and Figure 5-20(b) show comparative cross-sections of the excavations in HLP1 (0.34% HWD) and HLP3 (19.10% HWD) at approximately 1m depth from the surface. It is evident from this figure that the extent of weathering was greatest in the HLP containing the higher proportion of PAF material (i.e. HLP3). Note the presence of the 300mm scale in the figures to provide an indication of particle size.

(a) HLP1 Cross Section

(b) HLP3 Cross Section

Figure 5-20: Comparison of Weathering in HLP 1 (<1%PAF) and HLP3 (>19%PAF) (scale= 300mm)

In all the HLPs excavated, no significant armouring of limestone or precipitation of secondary minerals were visibly evident, although white crystals were observed in the crevices of several CLS samples. Geochemical modelling of the HLP leachate using Visual MINTEQ (section 5.3.5) indicated that these white crystals were gypsum.

Figure 5-21: HLP3 Excavation (scale= 300mm)

HLP3 was excavated to the base (Figure 5-21). The limited iron hydroxide staining on CLS material was confined mainly to the surface on CLS samples immediately beneath HWD material (Figure 5-22). There was notable discolouration of the HWD at depth caused by iron hydroxide precipitation (Figure 5-23). It is likely this occurred when high alkalinity water (caused by rainwater flowing through the carbonate material) passed over the PAF material. The formation of armouring layers on PAF material reduces the sulfide oxidation rate by isolating or substantially reducing the flux of oxygen to reactive sulfides (Miller et al. 2003b). This presence of HWD armouring in HLP3 confirmed that the practice of placing ANC material on the surface of WRDs recommended by Miller et al. (2003b), may be an effective measure for preventing carbonate armouring at ZCML, thereby allowing the beneficial use of the available limestone resource to be maximised.

Figure 5-22: **Iron Hydroxide Staining on CLS material on surface of HLP3 (scale= 300mm)**

Figure 5-23: **Discolouration of HWD at depth in HLP3 (scale= 300mm)**

5.3.5 Geochemical Modelling of Heap Leach Pad Leachate

In a similar process to that used in the modelling of leachate from Column 8 (see section 4.3.6), Visual MINTEQ was used to model the behaviour of HLP leachate and assess likely secondary mineralisation. A background to geochemical modelling principles to aid interpretation of data has been provided in Appendix 9.

Individual models were conducted on each HLP leachate sample to determine the solubility phases of the different minerals present in the sample. Saturation indices for gypsum and K-jarosite were recorded for each HLP sample and are presented in Figure 5-24 and Figure 5-25 respectively. It should be noted that given accurate analyses and thermodynamic data, saturation indices could only show which minerals could conceivably precipitate from the solution (SI>0) and which minerals absolutely could not (SI<0) (Zhu and Anderson, 2002).

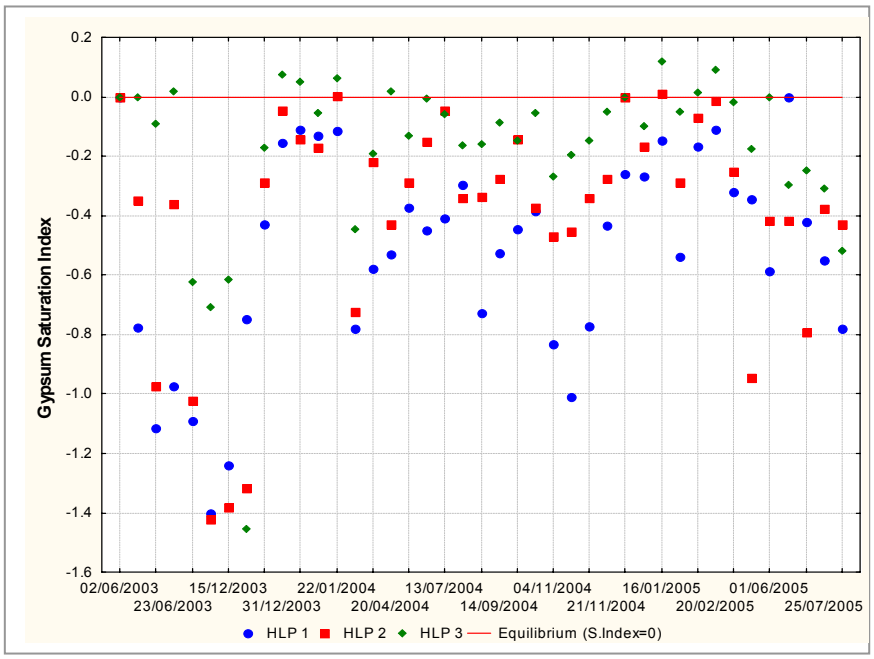

Figure 5-24: **Gypsum Saturation Index: Heap Leach Pads**

It can be seen in Figure 5-24 that for the HLP containing the highest percentage of PAF material (i.e. HLP3), and to a lesser degree the HLP containing the second most reactive blend (i.e. HLP2), the gypsum saturation index in samples fluctuated around zero. This indicated that gypsum was often precipitating in these HLPs and hence controlling sulfate and calcium concentrations in leachate. This result is consistent with rapid pyrite oxidation producing large amounts of sulfuric acid that were neutralised by calcium and magnesium carbonates, thereby saturating the leachate with calcium and sulfate and causing the precipitation of gypsum. It is evident from Figure 5-24 that gypsum saturation index values were higher in samples collected during the summer wet season months when oxidation rates, and hence sulfate production rates (refer Figure 5-12) were higher. The gypsum saturation indices in leachate samples collected from HLP1 were typically less than zero, indicating that gypsum was not precipitating in this HLP.

As shown in Figure 5-25, the modelled saturation indices indicated that K-jarosite ($KFe_3(OH)_6(SO_4)_2$) was precipitating in all HLPs. It can be recalled that the geochemical models for Column 8 leachate predicted similar behaviour (see Figure 4-35). As discussed in section 4.3.6, without having confidence that the dissolved iron concentrations represented true dissolved iron and not colloidal iron, the saturation indices for K-jarosite could not be confirmed. Visual inspection of the HLPs after the sampling period (see section 5.3.4) showed no characteristic yellow residue, indicating that jarosite was not precipitating in the HLPs.

Similar to Column 8 geochemical modelling results, several iron oxyhydroxides were indicated as supersaturated in the HLP model outputs. For reasons discussed in section 4.3.6, these results were not taken to be an indication of field behaviour.

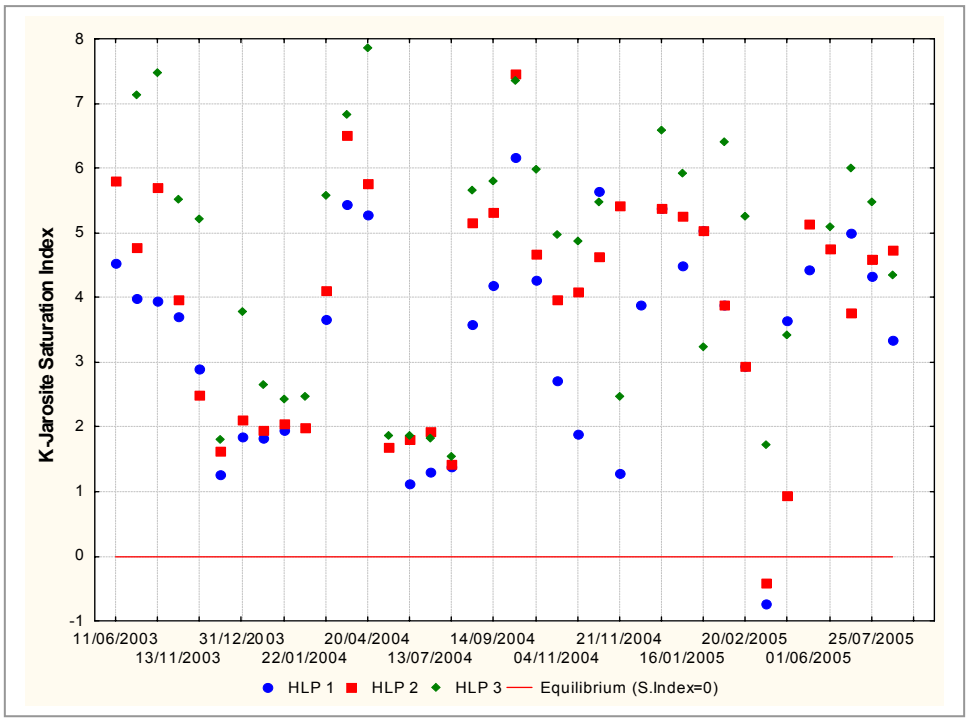

Figure 5-25: K-jarosite Saturation Index: Heap Leach Pads

5.4 Heap Leach Test Summary

Results from the heap leach pads will be further discussed and compared against results from the static and column leach tests in Chapter 6: Scale-Up, however are summarised as follows:

- pH neutral-alkaline conditions were maintained in leachate sampled from all three HLPs during the sampling period. pH values in a number of leachate samples collected during wet season sampling events were affected by prolonged storage prior to sampling and the pH values reflected that for a solution in equilibrium with dolomite.
- Sulfate concentrations in HLP leachate were greater in samples collected during the wet season due to greater ambient temperature and humidity than the dry season. These conditions lead to higher rates of pyrite oxidation, or longer durations of suitable conditions for oxidation between flush events (i.e. availability of oxygen and water). The median sulfate concentrations in leachate from each HLP in both wet and dry season datasets exceeded 10 mmol L^{-1}, the limit specified in Environmental Authority No. MIM800020402 (Ecoaccess, 2004).
- A linear relationship between (calcium plus magnesium) and sulfate existed in leachate from all three HLPs, indicating that there was good contact of the leachate with both acid producing and acid consuming rocks, and sufficient residence time to neutralise the sulfuric acid produced.
- Sulfate production rates were equivalent to neutralising potential depletion rates in each HLP. This confirmed neutralisation of the sulfuric acid produced by pyrite oxidation by calcium and magnesium carbonates in each HLP.
- For each HLP, the time to neutralising potential depletion far exceeded the estimated minimum time to sulfide depletion. This indicated that acid drainage would not be produced while carbonates in the HLPs remained unarmoured and available for pH buffering.
- Geochemical modelling and visual inspection confirmed gypsum precipitation in HLP2 and HLP3 and the subsequent controlling of sulfate concentrations in leachate. Sulfate production, neutralising potential depletion and oxygen consumption rates were therefore underestimated in these HLPs. It should be noted that due to the precipitation of gypsum in HLP2 and HLP3, sulfate concentrations in leachate from these HLPs might be high even after sulfide oxidation is complete due to dissolution of $CaSO_4$.
- Despite first flushes (total lead) and two large wet season events (total cadmium), total metal concentrations in HLP leachate complied with maximum limits specified in Environmental Authority No. MIM800020402 (Ecoaccess, 2004), i.e. 4.8×10^{-4} mmol L^{-1} and 8.9×10^{-8} mol L^{-1} for total lead and cadmium respectively.
- Total and dissolved metal concentrations increased with the percentage of PAF material in the HLPs (i.e. highest in HLP3 leachate) however were low due to pH values being sufficiently high to ensure low metal solubility. Of particular note were the extremely low dissolved lead concentrations in HLP

leachate, primarily a result of $Pb(OH)_2$ solubility controlling Pb^{2+} concentrations at neutral-alkaline pH values.

- Visual inspection of material comprising the HLPs after excavation highlighted the formation of armouring layers on the HWD material. The presence of HWD armouring suggested that the placement of acid consuming material on the surface of waste rock dumps may help maintain neutral pH conditions within the dumps and maximise available resources of carbonate material.

6 Chapter 6: Scale-up

6.1 Introduction

The term scale-up is used to describe the linkages between ARD prediction tests made at increasing scales of particle size. Field tests are generally more time consuming and expensive than laboratory tests to operate and for these reasons, conducting laboratory tests rather than field tests to predict ARD is preferred. The ability to extrapolate the results from laboratory ARD prediction tests to field behaviour of waste rock is therefore in demand. This is particularly the case for the prefeasibility and environmental impact assessment stages of mine projects where field tests may not always be practical, especially if the mine is located in a remote setting.

There is no simple solution to scale-up and successful work in this area to date has been limited. Currently the most extensive published work in this area has been conducted at the Grasberg Mine in Indonesia where good correlation has been made between column leach tests, test piles and instrumented waste rock dumps (Miller et al. 2003a). Contributing to the success of this work was the similarity in conditions between the column leach and field tests; climatic conditions at the mine facilitate the daily flushing of waste rock piles. To address the limited information and methodologies available on scale-up, INAP, INAP member companies, the Mine Environment Neutral Drainage (MEND) project in Canada, and the Canadian National Science and Environment Research Council (CANMET) have sponsored the Diavik Test Pile Research project. This project is a scale-up study involving a suite of acid drainage prediction tests and construction of a fully instrumented waste rock test pile. The aim of the project is to develop clear and concise methods to undertake scale-up calculations (INAP, 2006). The project is currently in its second year (of a five-year timeframe) and no published work on results obtained to date is available (Fleury, 2006).

In this project, measurements of acid generation potential were conducted on a range of particle sizes from pulverised material in static tests, to crushed material (<10mm to <100mm) in laboratory kinetic tests and ROM material in field test piles. In the absence of a standard method for scale-up, sulfate production, neutralising potential depletion and oxygen consumption rates for the column leach tests and heap leach pads were assessed for similarities. Results were also compared with those from static tests to determine if behaviour observed in the laboratory and field kinetic tests were predicted in the static tests conducted. This chapter will compare results from each ARD prediction test in an attempt to assess the potential for ARD generation in the specified waste rock blends sourced from Zinifex Century Mine.

6.2 Methodology

pH values, sulfate concentrations and sulfate production, neutralising potential depletion and oxygen consumption rates were compared between CLTs and HLPs of similar rock type blends (i.e. % PAF material). Columns 2 (<10mm), 4 (<50mm) and 6 (<100mm), which contained 10% HWD material, were compared with HLP 2 (8.3% HWD). Columns 7 (<10mm), 9 (<50mm) and 11 (<100mm) containing 20% HWD material in their blends were compared with HLP 3 (19% HWD).

Due to the precipitation of gypsum in HLP2 and HLP3 (refer section 5.3.5), oxygen consumption rates in these HLPs were classified as underestimated. Consequently, even though HLP1 was not constructed to its specified %PAF (refer section 5.2.1) and only contained 0.34% HWD, because gypsum was not precipitating in this HLP (refer section 5.3.5) oxygen consumption rates for HLP1 leachate were compared against those for Column 1 (95% CLS / 5% HWD, <10mm).

Due to the influence of particle size on leachate quality (in particular pH values and metal solubility) and the similarities of particle size distributions between CLTs comprising material <10mm and the HLPs, dissolved metal concentration comparisons were only conducted between CLTs comprising material <10mm and the respective HLP blend.

6.3 Results

6.3.1 pH Values

pH values in samples collected from comparable CLTs and HLPs were assessed for similarity. Figure 6-1 and Figure 6-2 show the box and whisker plots for respective pH values in blends 90% CLS / 10% HWD and 80% CLS / 20% HWD for the two-year sampling period. Median pH values in samples from CLTs containing the smallest particle size distributions (i.e. Columns 2 and 7, <10mm), were alkaline and most similar to median pH values in samples from the corresponding HLP. In both blends analysed, pH values in samples collected from the CLTs decreased with an increase in particle size.

As discussed in section 4.3.2, this may be due to either:

- Armouring of the CLS material with iron hydroxides resulting in coarser particle sizes having difficulty maintaining alkaline conditions;
- Water short-circuiting through the CLT and bypassing neutralising material; or
- Inadequate contact times with neutralising material to allow sufficient neutralisation of the leachate.

Non-outlier ranges were higher in CLTs containing larger particle sizes and reflected the decreasing pH in these CLTs during the 24-month sampling period. Non-outlier ranges were also relatively large in HLPs where pH values fluctuated between wet and dry seasons. This fluctuation is discussed in depth in section 5.3.1 and is attributed to dissolution of suspended dolomite in the leachate, an affect that was increased by the length of time the drainage remained in the leachate collection vessels prior to sample collection and laboratory analysis.

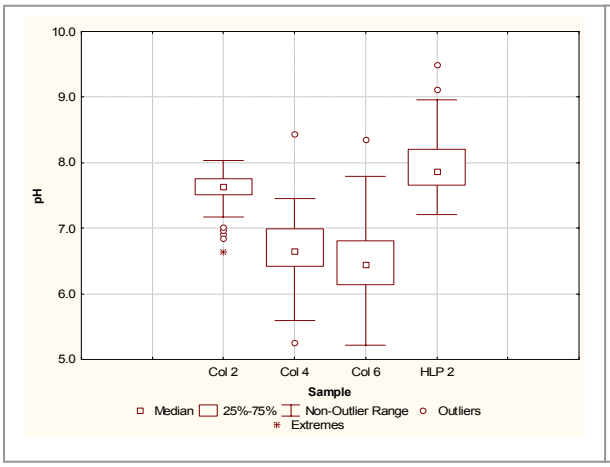

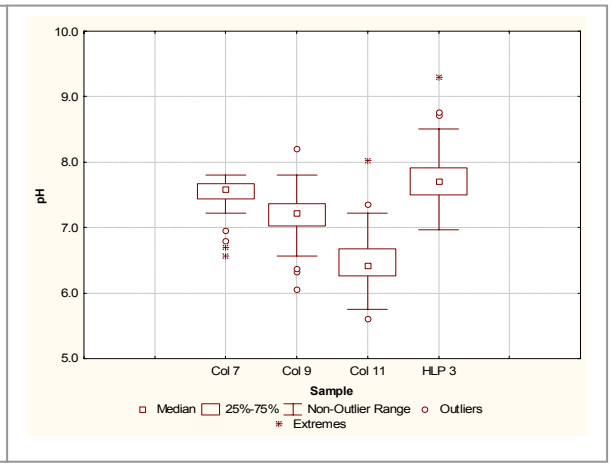

Figure 6-1: **90% CLS / 10% HWD Blend: pH values** **Figure 6-2:** **80% CLS / 20% HWD Blend: pH values**

6.3.2 Sulfate Concentration

Sulfate concentrations in samples collected from the CLTs and HLPs are discussed in sections 4.3.3.1 and 5.3.2.1 respectively. Sulfate concentrations in leachate collected from CLTs and HLPs with similar percentages of PAF material were assessed for similarity and are shown in Figure 6-3 and Figure 6-4 for blends 90% CLS / 10% HWD and 80% CLS / 20% HWD. Note that the heap leach pad data refers to the right hand side y-axis in both figures.

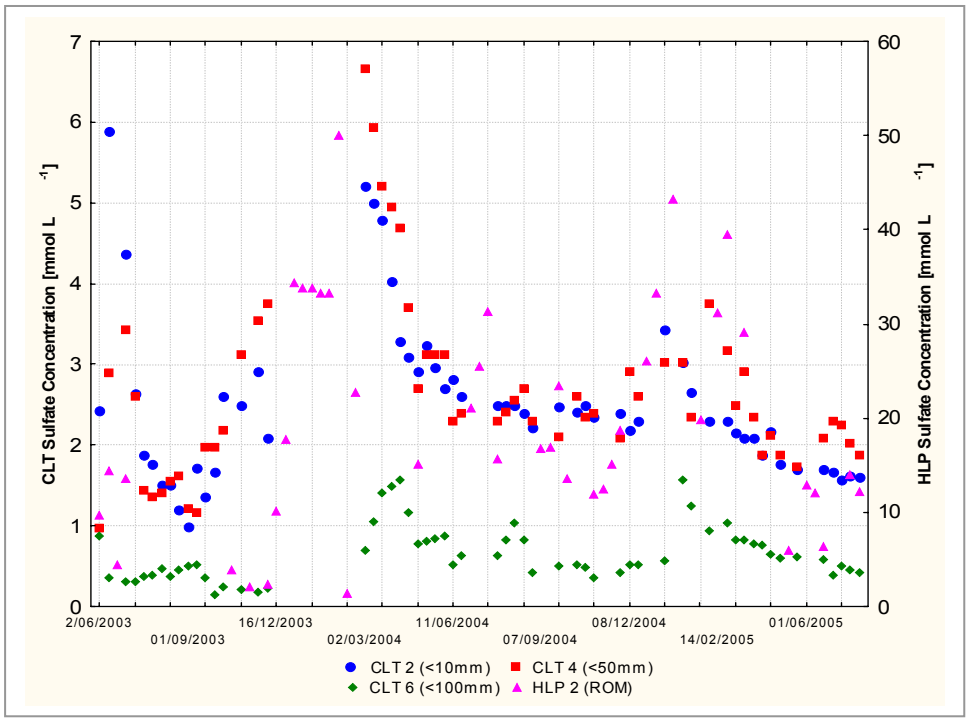

Figure 6-3: **90%CLS / 10% HWD Blend: Sulfate Concentration (HLP data refers on right hand side y-axis)**

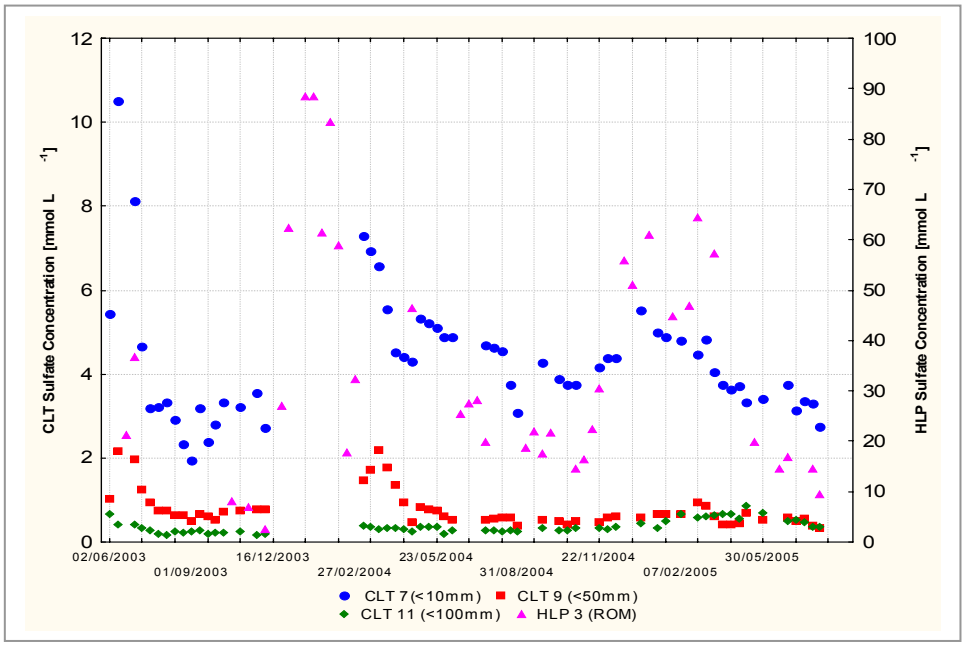

Figure 6-4: 80%CLS / 20% HWD Blend: Sulfate Concentration (HLP data refers on right hand side y-axis)

Sulfate concentrations were significantly greater in leachate samples collected from the HLPs than the CLTs. This was particularly the case during large wet season flushes. As discussed in section 4.3.3.1, it is likely the elevated wet season concentrations were due to higher temperatures and humidity that favoured the weathering of the HWD material. The rate of sulfide oxidation and therefore sulfate concentrations in discharge were lower during dry season flushes when low humidity conditions prevailed in between flush events.

Excluding the large wet season flushes, dry season sulfate concentrations in samples collected from the HLPs were most similar to those in samples from CLTs comprising material passing 10mm. This similarity is attributed to the comparable particle size distributions of the sample, contributing to similar residence (contact) times of leachate in the sample. As shown by the excavation of Column 8 (Figure 4-34) and HLP3 (Figure 5-20(b)), the material in the HLP had weathered sufficiently during the sampling period to be most similar to, and most likely smaller than, the CLTs comprising particle size distributions passing 10mm.

Despite this similarity, HLP leachate sulfate concentrations were several times greater than the corresponding CLT leachate sulfate concentration. In the 90% CLS / 10% HWD blend (Figure 6-3), HLP2 dry season sulfate concentrations (~20mmol L^{-1}) were approximately eight times greater than steady state concentrations in CLT 2 leachate (~2.5mmol L^{-1}). Similarly, for the 80% CLS / 20% HWD blend (Figure 6-4), HLP3 dry season sulfate concentrations (~24mmol L^{-1}) were six times the steady state concentrations in CLT 7 (~4.0mmol L^{-1}).

As discussed in section 5.3.2, the HLP sampling method may have contributed to the collection of inaccurate composite samples, particularly from high wet season flows. Even with the corrected (i.e. halved) dry season concentrations, typical HLP dry season sulfate concentrations were still greater than corresponding CLT passing 10mm steady state concentrations. In the 90% CLS / 10% HWD blend, corrected HLP2 dry season sulfate concentrations (~10mmol L^{-1}) were approximately four times greater than steady state concentrations in

CLT 2 leachate (~2.5mmol L^{-1}). Similarly, for the 80% CLS / 20% HWD blend, corrected HLP3 dry season sulfate concentrations (~12mmol L-1) were three times the steady state concentrations in CLT 7 (~4.0mmolL^{-1}).

As shown by the geochemical modelling of HLP leachate in section 5.3.5, sulfate concentrations in both HLP2 and HLP3 were controlled by the precipitation of gypsum. Consequently, the sulfate concentrations in leachate from HLP2 and HLP3 were considered to be minimum values. The fact that these minimum values were several times greater than those for equivalent CLT blends indicated that the two results weren't directly comparable. Discussed further in section 6.3.3, the cause of the higher sulfate concentrations in leachate from the HLPs was believed to be the increased weathering rate of pyrite under field conditions.

It can be recalled from section 5.3.2.1 that median sulfate concentrations in samples collected from each HLP exceeded the current regulatory discharge limit of 10mmol L^{-1} (Ecoaccess, 2004). While static tests classified each blended CLS and HWD sample as NAF (section 3.3), these tests were unable to predict the elevated sulfate concentrations seen in HLP drainage in particular, highlighting the inefficiencies of static tests in predicting water quality. There are a number of published case studies documenting the occurrence of ARD at particular mine sites despite static testing indicated that ARD was not likely to be produced (e.g. Ferguson and Firth, 2000, Day et al. 2003, Morin, 2003). In the case of BHP Billiton Ekati Diamond Mine, errors were made due to a lack of knowledge on the weathering behaviour of the acid neutralising material (Day et al. 2003, Morin, 2003).

6.3.3 Oxidation Rate

As the oxygen consumption rate is a function of the sulfate production rate (refer Equation 1-13), for the purpose of this thesis, both will be presented and discussed in this section.

Sulfate production rates calculated for each column leach test and heap leach pad flush event (refer sections 4.3.3 and 5.3.2) were assessed for similarity. A summary of comparative CLT and HLP blend results are shown in Table 6-1. It should be noted that unlike the median CLT sulfate production rates, which were calculated from flow data and leachate concentrations for the last ten flushes when CLT1, CLT2 and CLT7 had reached steady state (Figure 4-9), values for the HLP samples were calculated from the entire dataset due to the variability and absence of steady state conditions (see Figure 5-10 and Figure 5-11 for variations in HLP leachate sulfate concentrations throughout the sampling period). It is believed that this method prevented the vast over or underestimation of rates for the HLP samples.

As shown in Table 6-1, sulfate production, neutralising potential depletion and oxygen consumption rates were faster in the comparative heap leach pad than the column leach test samples, despite the substantially greater amount of water flushed through the CLTs. The times to sulfur and neutralising potential depletion in the HLPs were consequently less than the CLTs. These outcomes were directly attributed to the higher pyrite oxidation rate, and hence sulfate concentrations in HLP leachate as a result of increased weathering overall, and particularly, in the humid and high temperature conditions in between flush events.

It is evident from Table 6-1 that the median oxygen consumption rates were higher in the HLPs than the comparative CLTs despite the precipitation of gypsum (refer section 5.3.5) in HLP2 and HLP3 resulting in an underestimation of rates for these samples. It is also evident that the HLP oxygen consumption rates were most similar to CLTs comprising material passing 10mm, for reasons previously discussed (refer sections 6.3.1 and 6.3.2). As discussed in section 4.3.3, oxygen consumption rates in the CLTs increased with a decrease in particle size. The rate of HWD weathering in the HLPs was so significant that at the end of the two-year sampling period, the average particle size in the HLPs appeared to be less than <10mm, the smallest particle size distribution in the CLTs (refer section 5.3.4). It was therefore concluded that the oxygen consumption rates for samples in the CLTs were notably slower than, and consequently not directly comparable to those for the corresponding HLP samples. These results demonstrate the considerable influence the physical nature of waste rock material can have on leachate quality.

Table 6-1: Summary of Comparative Column and Heap Leach Pad Results

Sample	Particle Size (<mm>	Rainfall equivalent (m)	% S flushed from sample	Median SO_4 Production Rate [moles(SO_4) kg(material)$^{-1}$ s^{-1}]	% NP flushed from sample	Median NP Depletion Rate [moles($CaCO_3$ eq) kg(material)$^{-1}$ s^{-1}]	Median Oxygen Consumption Rate [moles(O_2)kg(material)$^{-1}$ s^{-1}]	Estimated Minimum Time to S Depletion (years)[†]	Estimated Minimum Time to NP Depletion (years)[†]
90% CLS / 10% HWD Blend									
CLT2	10	417	9.5	1.98E-10	0.18	2.27E-10	1.11E-11	21	1.27E+03
CLT4	50	415	7.7	2.00E-10	0.18	2.22E-10	1.12E-11	28	1.27E+03
CLT6	100	417	4.0	4.85E-11	0.04	4.91E-11	2.71E-12	55	5.87E+03
HLP2	ROM	1.6	75	1.01E-09*	1.07	1.01E-09*	5.63E-11*	1.0	285
80% CLS / 20% HWD Blend									
CLT7	10	418	9.1	3.16E-10	0.31	3.42E-10	1.77E-11	24	7.51E+02
CLT9	50	417	1.3	5.28E-11	0.06	6.20E-11	2.96E-12	211	4.07E+03
CLT11	100	418	1.5	2.79E-11	0.03	3.17E-11	1.56E-12	254	8.11E+03
HLP3	ROM	1.6	48	1.37E-09*	1.56	1.30E-09*	7.64E-11*	3.3	195

*Note: these are minimum values due to gypsum precipitation in HLP2 and HLP3 (refer section 5.3.5) controlling the sulfate concentration in leachate from these HLPs.

† Under irrigation conditions (i.e. current flushing scenario)

Even though HLP1 was not constructed to its specified %PAF (refer section 5.2) and only contained 0.34% HWD, because gypsum was not precipitating in this HLP (refer section 5.3.5) oxygen consumption rates for HLP1 leachate were compared against those for Column 1 (95% CLS / 5% HWD, <10mm) and are presented in Table 6-2.

Table 6-2: Oxygen Consumption Rates for HLP1 and CLT1

Sample	% PAF	Particle Size (<mm)	Median Oxygen Consumption Rate [moles(O_2)kg(material)$^{-1}$ s^{-1}]	Median Oxygen Consumption Rate [moles(O_2)kg(sulfur)$^{-1}$ s^{-1}]
CLT1	5.0	10	5.60E-12	1.95E-09
HLP1	0.34	ROM	1.62E-11	1.46E-08

Since gypsum was not precipitating in HLP1, the median oxygen consumption rate normalised for sulfur for HLP1 was compared against the value for CLT1. As shown in Table 6-2, the median oxygen consumption rate (sulfur) was approximately ten times greater in HLP1 than CLT1. As discussed in 5.3.2.4, the main assumption in calculating the rates on a time basis were that oxidation rates were constant between flush events. It was believed that this method was not valid for the HLPs where significant periods of time passed between flush events in the dry season and the pads dried out. In these circumstances, calculated rates would be underestimated. This result demonstrated that the weathering rate of pyrite was significantly greater under field conditions and consequently the rates for the CLTs are not directly comparable to those for the HLPs.

It is believed that the increased weathering rate of pyrite in the field samples was a direct result of higher temperatures and humidity in the field. The higher rate of weathering resulted in a decrease in the HWD particle size comprising the HLPs, which in turn, exposed more surface area of pyrite and resulted in higher concentrations of sulfate in leachate sampled. The extent of weathering in the heap leach pads was confirmed at the conclusion of the sampling period when the HLPs were excavated with a backhoe (refer section 5.3.4).

6.3.4 Dissolved Metal Concentrations

Metal concentrations in leachate from both the CLTs and HLPs have been discussed in sections 4.3.4 and 5.3.3. In order to compare metal concentrations in leachate from the two tests, dissolved zinc and dissolved copper production rates were assessed for similar waste rock blends for heap leach pads and column leach tests comprising waste rock passing 10mm. Dissolved cadmium rates were not calculated due to the large portion of results in the tests that were below the detection limit (i.e. < 0.10μg L^{-1}).

6.3.4.1 Zinc leaching

Box and whisker plots for dissolved zinc production rates for each similarly blended heap leach pad and column leach test (material passing 10mm) are shown in Figure 6-5. Median values are presented in Table 6-3. It should be noted that for scale purposes, several extreme values were excluded from the HLP dataset in

this plot. It is evident from this figure and table that median rates increased with the percentage of HWD material in the blend (i.e. HLP3 > HLP2 > HLP1 and CLT7 > CLT2 > CLT1). Median values were almost identical between comparable blended HLPs and CLTs (Table 6-3). A possible reason for the similarity may be the control of Zn^{2+} concentration in leachate by the solubility of $Zn(OH)_2$ at pHs greater than 7.8 (refer sections 4.3.4.2.1 and 5.3.3.2.1). The largest variation in rate between comparable HLPs and CLTs, although still remarkably comparable, was for HLP1 and CLT1. This difference was attributed to HLP1 containing less HWD than the specified 95% CLS / 5% HWD blend due to operational errors in construction (refer section 5.2.2). For this blend, the measured median dissolved zinc production rate was slightly higher in the corresponding column leach test.

Despite the comparable median dissolved zinc production rate values between the CLTS and HLPs, the non-outlier ranges were much higher in heap leach pad than column leach test leachate. Similar to the HLP sulfate production rates (refer section 5.3.2.4), the higher ranges and increased number of outlier and extreme values for dissolved zinc production rates in HLP leachate were driven by large wet season flush events.

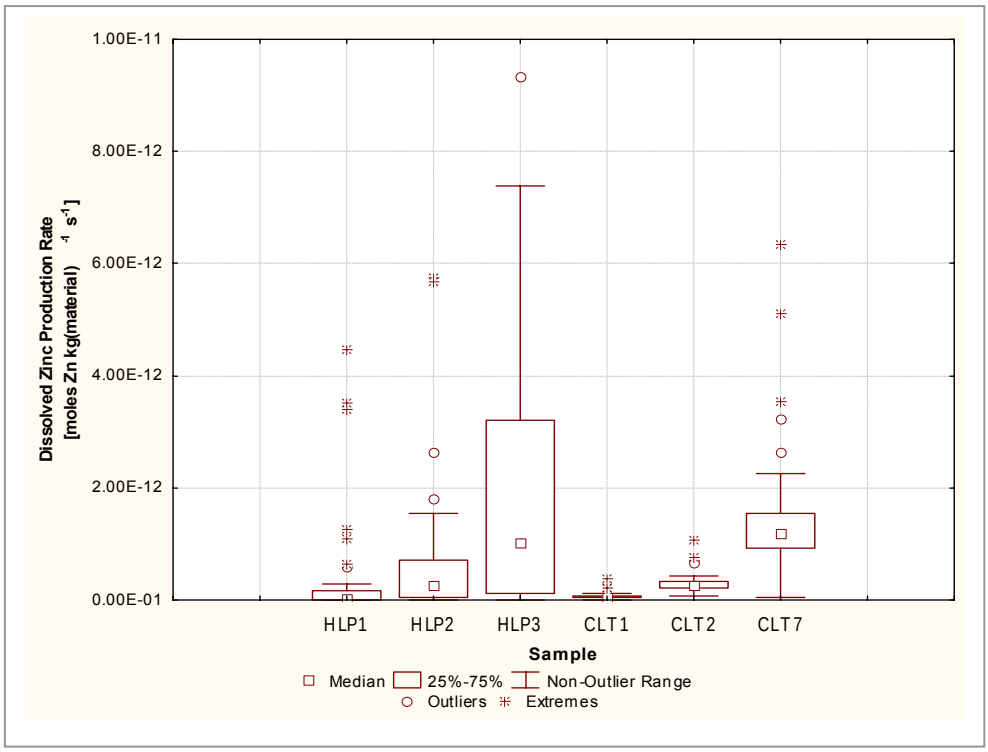

Figure 6-5: HLP and CLT (<10mm) Dissolved Zinc Production Rates

Table 6-3: Median Dissolved Zinc Production Rate for each CLT and HLP

Blend	HLP (moles(Zn) kg(material)$^{-1}$ s^{-1})	CLT (moles(Zn) kg(material)$^{-1}$ s^{-1})
95% CLS / 5% HWD	HLP1: 3.48E-14	CLT1: 5.53E-14
90% CLS / 10% HWD	HLP2: 2.56E-13	CLT2: 2.73E-13
80% CLS / 20% HWD	HLP3: 1.01E-12	CLT7: 1.19E-12

6.3.4.2 Copper Leaching

Box and whisker plots for dissolved copper production rates for each similarly blended heap leach pad and column leach test (material passing 10mm) are shown in Figure 6-6. Median values are presented in Table 6-4. It should be noted that similarly to Figure 6-5, several extreme values were excluded from the HLP dataset in this plot to improve the scale. It is evident from these data that median dissolved copper production rates increased with the percentage of HWD material in the CLT blend (i.e. CLT7 (5% HWD) > CLT2 (10% HWD) > CLT1 (20% HWD)). The median dissolved copper production rate for HLP2 was greater than HLP3, despite a higher percentage of HWD material in HLP3 and a greater range of values. This difference is believed to be insignificant due to the very small concentrations of dissolved copper observed in drainage from the samples. The higher concentrations present in HLP leachate occurred during large wet season flush events. Overall, median dissolved copper production rates were slightly higher in HLP than CLT samples but were classified as low, particularly when compared to the faster production rates for dissolved zinc.

Table 6-4: Median Dissolved Copper Production Rate for each CLT and HLP

Blend	HLP (moles(Cu) kg(material)$^{-1}$ s^{-1})	CLT (moles(Cu) kg(material)$^{-1}$ s^{-1})
95% CLS / 5% HWD	HLP1: 2.02E-15	CLT1: 1.13E-15
90% CLS / 10% HWD	HLP2: 5.36E-15	CLT2: 2.04E-15
80% CLS / 20% HWD	HLP3: 4.87E-15	CLT7: 1.61E-15

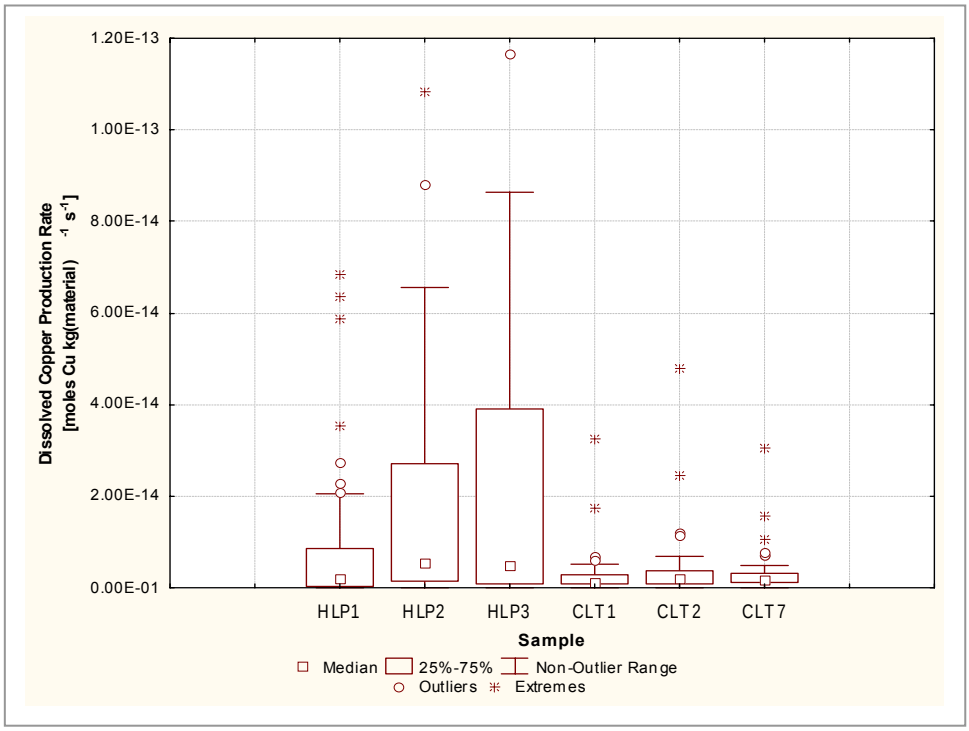

Figure 6-6: HLP and CLT (<10mm) Dissolved Copper Production Rates

6.4 Scale-Up Summary

Results from the scale-up of results between the different ARD prediction tests used on blends of CLS and HWD material are summarised as follows:

- Static tests classified each blended CLS and HWD sample as NAF. Despite pH neutral leachate, the elevated sulfate concentrations reported, particularly in HLP drainage, were not predicted by the static tests.
- Despite greater volumes of water passing through the CLTs than the HLPs, the oxygen consumption rates, and hence pyrite oxidation rates, in the HLP samples were notably higher than those measured in the CLT samples. This was the case even where gypsum was precipitating and controlling the sulfate concentrations in HLP2 and HLP3 leachate samples.
- The higher oxidation rates in the HLPs were attributed to the greater rate of pyrite weathering as a result of higher temperatures and humidity in field conditions, most notably during the wet season. This increased weathering rate of the HWD material resulted in a reduction in the particle size distribution of waste rock material comprising the HLPs.
- The rate of HWD weathering in the HLPs was so significant that at the end of the two-year sampling period, the average particle size appeared to be less than 10mm, the smallest particle size distribution in the CLTs.

- Due to the significant weathering of material comprising the HLPs, leachate chemistry from the tests was most comparable to that for the CLTs comprising rock material passing 10mm in diameter.
- Median dissolved zinc and copper production rates were comparable between the CLTs and HLPs, however rates were greater in the HLPs during large wet season flushes

The results from the CLTs and HLPs on ZCML blended waste rock have demonstrated the difficulty in scaling up results to a site with seasonally dry conditions. The results obtained from the HLPs are believed to be most representative of field conditions at ZCML due to exposure to, and the influence of, ambient temperatures and humidity on the weathering of HWD material.

Recommendations to improve the testing methodology of the CLTs to ensure the results are more comparable with those from HLPs include conducting CLTs under field conditions or in a laboratory environment where temperatures and humidity can be adjusted to simulate field conditions. This recommendation and other recommendations for future improvements to both the testing and scale-up methodologies are discussed in Chapter 7: Conclusions and Recommendations.

7 Chapter 7: Conclusions and Recommendations

This chapter has been divided into the following two sections to discuss the conclusions and recommendations relating to the broad objectives of this project:

- The ARD prediction tests used and scale-up methods applied to assess the leachate quality from blended waste rock (section 7.1); and
- Implications for the management of ARD material at ZCML (section 7.2).

7.1 ARD Prediction Tests and Scale-up

7.1.1 General Findings

Findings from the study were:

- Static tests conducted on blended CLS and HWD samples classified each sample as non acid forming (NAF). Results from kinetic testwork confirmed this finding, indicating that limestone blending may be effective in controlling the pH of leachate generated from waste rock, however elevated sulfate concentrations in leachate would ensue.
- Results obtained from the column leach tests were repeatable.
- Sulfate production rates were equivalent to neutralising potential depletion rates in most CLTs and HLPs. This confirmed neutralisation of the sulfuric acid produced by pyrite oxidation by calcium and magnesium carbonates.
- The calculated time to NP depletion exceeded the time to sulfide depletion in all CLTs and HLPs, however these times were misleading for columns containing armoured CLS material.
- Despite first flush events, total metal concentrations in CLT and HLP leachate generally complied with maximum limits specified in Environmental Authority No. MIM800020402 (Ecoaccess, 2004).
- Dissolved zinc concentrations were significantly greater in CLT samples with low pH values, however were not as high as thermodynamically predicted using the geochemical modelling program MINTEQA2. Dissolved zinc concentrations in HLP leachate were also not as high as thermodynamically predicted at pH values less than 7.8. This was due to the control of dissolved zinc concentrations by the rate of sphalerite oxidation at low pH values and the solubility of $Zn(OH)_2$ at high pH values.
- Dissolved lead concentrations in CLT and HLP samples were extremely small or undetectable (i.e. less than 4.8×10^{-4} µmol L^{-1}) and less than those thermodynamically predicted using MINTEQA2 due to low oxidation rates of galena resulting from surface passivation at lower pH values, and $Pb(OH)_2$ solubility controlling Pb^{2+} concentrations at neutral-alkaline pH values.
- Median dissolved zinc and copper production rates were comparable between the CLTs and HLPs, however rates were greater in the HLPs during large wet season flushes.
- Geochemical modelling confirmed the absence of gypsum precipitation in the CLT comprising the most reactive waste rock blend and smallest particle size distribution and confirmed gypsum

precipitation in HLP2 and HLP3. Sulfate production, neutralising potential depletion and oxygen consumption rates were therefore underestimated in these HLPs.

7.1.2 Conclusions

(1) Results from CLTs comprising smaller particle size distributions were most comparable with results from the HLPs. Anomalous behaviour was observed in column leach tests comprising larger particle size distributions.

Inadequate contact of leachate with waste rock, as well as carbonate armouring, contributed to the anomalous behaviour in CLTs comprising larger particle size distributions. Sulfate production, neutralising potential depletion and oxygen consumption rates were typically higher in CLTs comprising rock <10mm due to increased surface areas of PAF and AC material.

(2) There was no apparent benefit in leaving the ZCML heap leach pads unwatered for periods of time greater than one week.

It was demonstrated in section 5.3.2.4 that the heap leach pads reached equilibrium within approximately seven days of being watered.

(3) Oxygen consumption rates for CLT samples were significantly slower and consequently not directly comparable to those for the HLPs, despite greater flushing of the CLTs.

Due to the CLTs being conducted in an air conditioned laboratory, oxidation rates were slower than the HLPs that were conducted under field conditions at the ZCML mine site. The differences between the laboratory and field environments were thought to be the primary causes of discrepancy between CLT and HLP oxidation rates. The high ambient temperatures and humidity during the wet season increased the rate of pyrite oxidation in the HLPs, and hence weathering and a reduction in the particle size of PAF material. These results have demonstrated the difficulty in the scale-up of laboratory to field tests for sites with seasonally dry weather conditions.

7.1.3 Recommendations

(1) Construct CLTs from particle size distributions passing 10mm as a maximum to best emulate the particle size distributions and residence times in waste rock dumps.

If leachate from greater particle size distributions is to be investigated, larger columns could be used to ensure adequate contact times.

(2) For future HLP testwork at ZCML, or sites with similar climatic conditions, accelerate the rate of pyrite oxidation in the HLPs by watering at weekly intervals on a continual basis in the dry season (i.e. no prolonged drought period).

This would remove water as the rate-limiting factor in the dry season.

(3) For future CLT testwork for sites with distinct seasonal variations, conduct CLTs under field conditions at the site under investigation to ensure samples are exposed to similar ambient

temperatures and humidity. Alternatively, where this is not possible, site temperature and humidity conditions should be simulated in a laboratory environment.

This will ensure that column leach test samples are exposed to similar rates of weathering to those of heap leach pads and/or waste rock dumps.

7.2 ARD Management at ZCML

7.2.1 Conclusions

(1) Blending CLS and HWD material was effective in maintaining neutral pH values and regulatory-compliant total metal concentrations in drainage from CLTs and HLPs comprising blends up to 75%CLS / 25%HWD. However, sulfate concentrations in drainage sampled from all blended samples exceeded current regulatory discharge limits.

As long as pyrite is able to oxidise in the site waste rock dumps, sulfate will potentially be present in drainage in concentrations above the current regulatory discharge limits, despite the leachate being characterised by circum neutral pH values and low dissolved and total metal concentrations. Sulfate concentrations in WRD drainage may increase further if the current contamination percentage of class 3 in class 1 material is increased, particularly if the material is placed on WRD batters.

(2) Visual inspection of material comprising the HLPs after excavation highlighted the presence of armouring layers on HWD material.

This observation suggests that where insufficient carbonate materials are available for blending throughout the waste rock dumps, placement of acid consuming material on the surface will ensure water inflow is characterised by high alkalinity. This may help maintain neutral pH conditions within the dump, prevent armouring of CLS material, and facilitate the armouring, and hence reduced oxidation rate, of PAF material. This observation confirmed the current ZCML waste rock dump design specification that class 1 rock must be used for capping and batters (Bates et al. 2000).

Current best management practice requires the placement of a cover onto most types of mine waste including tailings, waste rock and/or spent heap leach rock at mine closure (O'Kane and Wels, 2003). The competency and acid neutralising qualities of the CLS material at ZCML have resulted in it being identified as the resource most suitable for capping and battering the waste rock dumps.

(3) The effectiveness of CLS in neutralising sulfuric acid increased with decreasing particle size.

Results from the column leach tests indicated that this was due to the higher surface area to volume ratio of acid consuming rock and less available surface for armouring.

7.2.2 Recommendations

(1) To prevent a potential increase in sulfate concentrations in WRD discharge, the current 5% contamination limit of class 3 in class 1 material should not be reduced.

The current discharge limit for point source sulfate concentrations was consistently exceeded in drainage from the HLPs (section 5.3.2.1), and occasionally in leachate from the CLTs (section 4.3.3.1). Results from this study have indicated that a weakening of the current 5% contamination limit of class 3 in class 1 material would result in a further reduction in the quality of drainage emanating from the site waste rock dumps.

A reduction in this contamination limit could only be supported if the issue of sulfate concentrations in leachate from the WRDs was addressed. Since this study has shown that the elevated sulfate concentrations cannot be prevented by waste rock blending, other options for ARD management, and in particular management of sulfate concentrations, are explored and discussed in section 7.2.3.

If sulfate concentrations in WRD drainage can be treated to within current regulatory limits, there is no evidence from the CLT and HLP results against reducing the contamination limit to 25% class 3 in class 1 material. It is recommended that due to potential errors in waste rock classification and materials handling in an operational environment, and the potential for sampling errors in this project, a "buffer" for error should be added to this limit (e.g. contamination limit should not be reduced to more than 15% class 3 in class 1 material). Prior to lowering the contamination limit, it would be wise to conduct a full scale test on a site waste rock dump batter over a period of at least two years to confirm the thesis blending findings at a larger scale. This could be conducted by establishing an 85% class 1 / 15% class 3 blend over a significant length of WRD batter (e.g. 500m) and diverting the drainage to a collection area for sampling and analysis. If established prior to the 2006/07 wet season, results from this field study would be available well before mine closure (i.e. 2016), and the latter years of the mine life when class 1 material will be scarce. It should be noted that long term mine planning schedules and mine closure designs would require amendment following any adjustment in the contamination limit.

(2) Where there is insufficient CLS material available to cover both the dump surface and batters, priority should be given to the WRD surface, with other non-acid forming competent material used on the batters.

Due to the limited resource of CLS, particularly in the latter years of mine operation, strategies must be developed at ZCML that maximise the beneficial use of the limestone that has been, and will be, mined.

One method of maximising the beneficial use of this resource is to preferentially place CLS material on the WRD surface. Any water inflow through the dump from the surface would therefore be characterised by high alkalinity, and armouring of PAF material within the WRD may result from contact with this leachate. If used on batters, the carbonate material may become armoured by acidic drainage flowing through the WRD. Competent non-acid forming material could be used on the batters as a substitute material primarily for its structural capabilities.

The current ZCML waste rock design specifies the depth of class 1 material on the WRD surface as 5m and width on the batters as 20m (Figure 2-8). Modelling and/or field trials could be undertaken to verify these limits. Further investigations on cover designs should also focus on limiting the influx of water into the WRDs, thereby minimising drainage from these structures.

(3) Investigate the reduction in particle size of class 1 material placed within / on the WRDs.

It can be recalled from Chapter 4 that the column leach test methodology used in this project involved the assessment of leachate generated from waste rock blends of five lithologies and three particle size distributions. Results presented in section 4.3.2 confirmed that neutral-alkaline conditions were best maintained in CLTs comprising smaller particle size distributions due to the larger surface area of acid consuming material available.

Due to the tendency for ZCML class 3 material to significantly weather and expose fresh pyritic surfaces for oxidation, the particle size of class 1 material in the WRDs has a significant influence on the equality of drainage emanating from the dumps. It is therefore recommended that attempts be made to actively reduce the particle size of CLS material in the ZCML waste rock dumps. This may be achieved by amending current blasting practices, or alternatively, by crushing CLS material prior to placement in the WRDs. The latter option, however, would involve higher operational costs.

7.2.3 Suggested Management Options for Sulfate Concentrations in WRD Drainage

As discussed in section 7.2.2, unless the issue of sulfate concentrations in leachate from the WRDs is addressed, the current 5% contamination limit of class 3 in class 1 material should not be reduced. Suggested site management options for sulfate concentrations in drainage from the ZCML waste rock dumps have been categorised into the four options detailed below. Although containment of ARD on site is identified as current best practice, it is recommended that ZCML conduct a risk assessment for each alternative presented to determine which option, or combination of options, may be the most suitable for the site. Advantages and disadvantages for each management option are listed in Table 7-1. It should be noted that unless drainage from the ZCML WRDs is treated for sulfate concentrations, drainage quality could potentially exceed current regulatory discharge limits. The containment and/or treatment of leachate from site WRDs are therefore identified as priority recommendations.

(1) Containment on site (i.e. zero release)

Operating a zero release policy may be achieved by:

- Storing all ARD affected water in a purpose-built ARD dam and decanting overflow to adjacent evaporation ponds;
- Evaporating water from the ARD dam and adjacent evaporation ponds during the dry season and dry periods in the wet season;
- Diverting upstream flows away from the waste rock dumps to prevent contact with material in the waste rock dumps (i.e. reduce catchment area of ARD dam and reduce basal flows through waste rock dumps);
- Having emergency storage contingency available, either in the main pit or Tailings Storage Facility.

The BHP Billiton Mt Whaleback iron ore mine is an example of best practice ARD management and containment. The site ARD Management Strategy is approved by senior management and endorsed by State Government regulatory authorities and relevant external stakeholders (Porterfield et al. 2003). An ARD

management plan has been implemented at BHP Billiton Mt Whaleback to provide a systematic approach to the efforts to manage ARD and to provide mechanisms for review, modification and improvement. The management plan is an operational document covering (Porterfield et al. 2003):

- The methods and frequency of waste rock material identification;
- Anticipated waste rock handling and movement schedules;
- Water monitoring and management;
- ARD emergency response procedures;
- Communication, employee awareness and training for handling potentially acid forming materials;
- Auditing of the plans; and
- Expansion of the practices to include all of the sites.

Containment on site is the most attractive option post mine closure where the existing storage and evaporation dams could be used, or WRD seepage could be diverted to the main pit.

(2) Restricted release during high wet season flow events (i.e. dilution)

Restricted release during high wet season flow events is currently achieved at ZCML by storing WRD seepage in sedimentation dams and releasing from the dams during high flow events. The monitoring of discharge volumes from the ZCML Southern Waste Rock Dump by site personnel has shown that flows through the WRD continue for several days following a rain event, often after flows in the nearby ephemeral creek (i.e. Page Creek) have subsided. This highlights the need for restricted release to be complemented with adequate storage volumes in sedimentation dams and availability of emergency storage contingency options to capture large amounts of drainage that may be produced during exceptionally wet years. This is currently addressed by pumping excess drainage collected in Sedimentation Dam 3 to the Tailings Storage Facility (Lee, 2006b). While this option may be viable during the mine operational phase, it is not a “walkaway” solution post mine closure.

(3) Treatment prior to discharge

Treatment of ARD from the ZCML waste rock dumps prior to discharge may result in compliance with point source regulatory limits for sulfate. There are several water treatment processes available to reduce sulfate concentrations.

Lorax Environmental was commissioned by INAP to conduct a review of the current state of the art treatment processes to reduce sulfate (with or without metals) in mine effluents (Lorax Environmental, 2003). The treatment processes meeting the review requirements (i.e. applicability to sulfate removal and availability of data on sulfate removal and costs) were arranged into the following four categories (Lorax Environmental, 2003):

- **Chemical treatment with mineral precipitation** (e.g. lime or limestone addition, addition of barium salts, the SAVMIN process and the cost-effective sulfate removal (CESR) process);

- **Membranes** (e.g. Reverse Osmosis (RO), the SPARRO process and Electrical Dialysis Reversal (EDR));
- **Ion-exchange** (e.g. the GYP-CIX process and Metal Precipitation and Ion-Exchange); and
- **Biological Sulfate Removal** (e.g. Bioreactors, Constructed Wetlands, Alkalinity Producing Systems and Permeable Reactive Barriers).

Lorax Environmental (2003) listed the four most suitable treatment processes for removal of sulfate from mine water as the limestone/lime process (as pre-treatment), the SAVMIN process, the GYP-CIX process and biological sulfate reduction in a bioreactor or permeable reactive barrier. Sulfate removal by biological sulfate reduction was noted as having the greatest potential with the following major advantages (Lorax Environmental, 2003):

- Sulfate and trace metals can be reduced to very low levels;
- The amount of waste produced is minimal;
- Capital costs are relatively low and operating costs can be drastically reduced by the development of inexpensive carbon and energy sources; and
- Trace metals in mine drainage in certain circumstances can be selectively recovered and sold for additional savings.

It should be noted that constructed wetlands and alkalinity producing systems are the least efficient sulfate removal processes (Lorax Environmental, 2003). Because the designs of constructed wetlands were originally based on the removal of other dissolved elements (e.g. Fe, Mn), new or amended designs may need to be developed if constructed wetlands are to be used specifically for sulfate removal by sulfate reduction (Lorax Environmental, 2003).

Similarly to ZCML, waste rock dumps at the Argyle Diamond Mine produce drainage characterised by neutral pH and high magnesium and sulfate concentrations. The site is currently investigating chemical treatment options for WRD seepage waters and determining the environmental effects (including ecotoxicological investigations) of magnesium sulfate-rich waters (Griebel et al. 2005). Findings from the research conducted by Argyle Diamonds may be valuable in the management of ARD at ZCML.

(4) Amending current Licence limit for sulfate to enable compliance

An application to amend the sulfate discharge limit in Schedule C – Table 6 of Environmental Authority No.MIM800020402 (Ecoaccess, 2004) to an achievable limit could be submitted to the Queensland Environmental Protection Agency. A statistical analysis on discharge water quality from sedimentation dams receiving discharge from the waste rock dumps would need to be undertaken to determine a suitable limit.

Table 7-1: Advantages and Disadvantages for ARD Management Options

ARD Management Option	Advantages	Disadvantages
(1) Containment on site	• No off-site environmental harm. • Demonstration of best practice and therefore contribution to positive relations with regulators, community and other stakeholders. • Possible manageable option post mine closure (i.e. maintain storage and evaporation dams or divert drainage to the main pit).	• High capital cost. • Land disturbance to create storage and evaporation facilities. • Availability of suitable land. Due to space constraints, the area to the west of Page Creek is the most suitable for drainage from the Southern WRD. An additional facility may be required for the Western WRD. Note: The Northern WRD may not require a designated facility due to its permeable limestone base.
(2) Restricted release during high flow events in wet season	• Able to discharge drainage off-site. • Sulfate concentrations in drainage diluted by high flow events.	• Contribute to "salting" (magnesium sulfate deposition) in ephemeral creek lines as flow through waste rock dumps delayed after peak flows in creeks. • Fine balance between volumes discharged and what creeks can handle to minimise "salting." • Possible effects on hydrology of creeks due to higher flows. • Difficult to manage during operations. • Difficult to manage post mine closure. • May contribute to negative relations with regulators, community and other stakeholders.
(3) Treatment prior to discharge	• Discharge of drainage that meets regulatory discharge limits.	• Potential high capital and operating costs. • Depending on treatment method used may not be a walk-away solution post mine closure. • Possible effects on hydrology of creeks due to higher flows.
(4) Amending Licence Limit for discharge	• Able to discharge drainage off-site.	• Contribute to "salting" (magnesium sulfate deposition) in ephemeral creek lines. • Possible effects on hydrology of creeks due to higher flows. • Regulators may not approve higher limit. • Potential to fuel negative community, regulator and stakeholder relations as not seen to be best practice.

8 References

Alarcón León, E., Rate, A.W., Hinz, C., Campbell, G.D. 2004. Weathering of sulfide minerals at circum-neutral pH in semi-arid/arid environments: influence of water content. In 'SuperSoil 2004: Proceedings of Third Australian New Zealand Soils Conference'. 5 - 9 December 2004. (Ed Dr Balwant Singh) (University of Sydney: Australia). Accessed from website http://www.regional.org.au/au/asssi/supersoil2004/s1/oral/2164_edgardoa.htm on 15 March 2006.

AMDEL, 2003. Sizing and Assaying Siltstone and Limestone Samples. Report No. N262CO03. (AMDEL Ltd: Torrensville Plaza).

ANZECC and ARMCANZ, 2000, Australian and New Zealand Guidelines for Fresh and Marine Water Quality, ANZECC and ARMCANZ.

APHA. 1998. Standard Methods for the Examination of Water and Wastewater. 20th Edition. American Public Health Association. (American Water Works Association and Water Environment Foundation: Washington, U.S.A.).

Bates, D., Bennett, S., Eaglen, P. and Taylor, P., 2000. Rehabilitation of Pasminco Century Bulk Sample Plant and Current ARD-Related Operational Details. In 'Proceedings of Fourth Australian Workshop on Acid Mine Drainage'. Townsville, Queensland. 28 February – 1 March 2000. (Eds NJ Grundon and LC Bell) pp.117-131. (Australian Centre for Minesite Rehabilitation Research: Brisbane).

Bennett, J.W., Comarmond, M.J., Jeffery, J.J. 2000. Comparison of Oxidation Rates of Sulfidic Mine Waste Measured in the Laboratory and Field. (Australian Centre for Mining Environmental Research: Brisbane).

Benthke, C.M. 1996. Geochemical Reaction Modelling - Concepts and Applications. (Oxford University Press: New York).

Borek, S.L. (1993) "Effect of Humidity on Pyrite Oxidation" *Environmental Geochemistry of Sulfide Oxidation,* Pittsburgh Research Centre, U.S. Bureau of Mines, Pittsburgh, PA, U.S.A.

Boyd, C.E. 2000. Water Quality - An Introduction. (Kluwer Academic Publishers: U.S.A.)

Broadbent, G.C., Andrews, S.J. and Kelso, I.J., 2002. A Decade of New Ideas: Geology and Exploration History of the Century Zn-Pb-Ag Deposit, Northwestern Queensland, Australia. In 'Society of Economic Geology Special Publication 9.2002', Chapter 6.

Cisneros-Gonzalez, I., Oropeza-Guzman, M.T. and Gonzalez, I, 1999. Cyclic Voltammetry Applied to the Characterisation of Galena. Hydrometallurgy (53): pp.133-144.

Cama, J., Acero, P., Ayora, C., Lobo, A. 2005. Galena surface reactivity at acidic pH and 25°C based on flow-through and in situ AFM experiments. Chemical Geology (214): pp.309-330.

Coastech Research Inc., 1991. Acid Rock Drainage Prediction Manual: A Manual of Chemical Evaluation Procedures for the Prediction of Acid Generation from Mine Wastes, MEND Project 1.16.1b. (Natural Resources Canada: Ottawa).

Cruz, R., Mendez, B.A., Monroy, M., Gonzalez, I. 2001. Cyclic Voltammetry Applied to Evaluate Reactivity in Sulfide Mining Residues. Applied Geochemistry (16): pp.1631-1640.

Dames and Moore, 1994, The Century Project Draft Impact Assessment Study Report, Australia.

Day, S., Sexsmith, K and Millard, J., 2003. Acidic Drainage from Calcareous Coarse Kimberlite Reject, Ekati Diamond MineTM, Northwest Territories, Canada. In 'Proceedings of Sixth International Conference on Acid Rock Drainage'. Cairns, Queensland. 12 – 18 July 2003. pp.587 - 600. (The Australasian Institute of Mining and Metallurgy: Melbourne).

De Giudici, G and Zuddas, P. 2001. In situ investigation of galena dissolution in oxygen saturated solution: Evolution of surface features and kinetic rate. Geochimica et Cosmochimica Acta, 65(9), pp.1381-1389.

De Giudici, G., Rossi, A., Fanfani, L., Lattanzi, P. 2005. Mechanisms of galena dissolution in oxygen-saturated solutions: Evaluation of pH effect on apparent activation energies and mineral-water interface. Geochimica et Cosmochimica Acta, 69(9), pp.2321-2331.

Dobos, S.K, 2000. Potential Problems with Geologically Uncontrolled Sampling and the Interpretation of Chemical Tests for Waste Characterisation and AMD Prediction. In 'Proceedings of Fourth Australian Workshop on Acid Mine Drainage'. Townsville, Queensland. 28 February – 1 March 2000. (Eds NJ Grundon and LC Bell) pp.25-29. (Australian Centre for Minesite Rehabilitation Research: Brisbane).

Dowd, P., 2005. The Business Case for Prevention of Acid Drainage. Paper presented at and submitted for the 'Fifth Australian Workshop on Acid Drainage'. Fremantle, Western Australia. 29 – 31 August 2005. (Australian Centre for Minerals Extension and Research: Brisbane). Note: proceedings unpublished as at 15 March 2006.

EcoAccess (2004) Environmental Authority No. MIM8000020402, Zinifex Century Mine Limited, (Queensland Environmental Protection Agency: Brisbane).

Environmental Geochemistry International Pty Ltd, 1997a. Waste Rock Geochemistry: Geochemical Characterisation, Classification and Scheduling of Waste Rock. Balmain, NSW.

Environmental Geochemistry International Pty Ltd, 1997b. Waste Rock Geochemistry: Leach Column Study of Potentially Acid Forming Waste Rock and Effect of Limestone Blending. Balmain, NSW.

Environmental Geochemistry International Pty Ltd (2004), Technical memorandum: Geochemical Characteristics of 100% Limestone, 100% Siltstone and Blended Samples. (EGi Pty Ltd: Balmain, NSW).

Evangelou, V.P., 1995, Pyrite Oxidation and Its Control. (CRC Press: Florida, U.S.A).

Fague, P.A. and Mostyn, G, 1997. Predicting Acid Rock Drainage in Waste Rock Dumps, GeoEnvironment97 Rotterdam, pp.413-421.

Fleury, A.M. 10 March 2006. Personal communication.

Ferguson, K.D. and Firth, I., 2000. The Scale-up of ARD Prediction. In 'Proceedings of Fourth Australian Workshop on Acid Mine Drainage'. Townsville, Queensland. 28 February – 1 March 2000. (Eds NJ Grundon and LC Bell) pp.35-45. (Australian Centre for Minesite Rehabilitation Research: Brisbane).

Gauci, V.P., 2000. A Corporate Perspective of Acid Mine Drainage. In 'Proceedings of Fourth Australian Workshop on Acid Mine Drainage'. Townsville, Queensland. 28 February – 1 March 2000. (Eds NJ Grundon and LC Bell) pp.1-3. (Australian Centre for Minesite Rehabilitation Research: Brisbane).

Griebel, E., Samaraweera, S and McPhail, G., 2005. Environmental Management of Secondary ARD Products at Argyle Diamonds. In abstract for presentation at the 'Fifth Australian Workshop on Acid Drainage'. Fremantle, Western Australia. 29 – 31 August 2005. (Australian Centre for Minerals Extension and Research: Brisbane). Note: proceedings unpublished as at 15 March 2006.

Gustafsson, J.P., 2003, Visual MINTEQ, Version 2.2, Stockholm, Sweden.

Harries, J. 1998. How Big a Problem? Groundwork 1 (2). pp.4-5.

Ian Wark Research Institute and Environmental Geochemistry International Pty Ltd, 2002, ARD Test Handbook, AMIRA Project P387A Prediction and Kinetic Control of Acid Mine Drainage, AMIRA International, Melbourne Australia.

INAP, 1999. Glossary of Terms Used in Metal Leaching and Acid Rock Drainage Work. Accessed from website www.inap.com.au/public_downloads/What_is_acid_drainage/Glossary(290699).PDF on 15 January 2006.

INAP, 2006. Research Projects. Accessed from website www.inap.com.au/research_projects.htm on 10 February 2006.

Langmuir, D. 1997. Aqueous Environmental Geochemistry, Prentice-Hall Inc, New Jersey, U.S.A.

Lawrence, R and Day, S. 1997. Chemical Prediction Techniques for ARD: Workshop Notes. 4th International Conference on Acid Rock Drainage, Vancouver, B.C.

Lee, G. 2006a. Personal communication 8 March 2006.

Lee, G. 2006b. Personal communication 20 March 2006.

Li, M. 1999. Hydrogeochemistry of Oxidised Waste Rock from Stratmat Site, N.B. MEND Report 2.36.2a. (Natural Resources Canada: Ottawa).

Lorax Environmental, 2003. Treatment of Sulphate in Mine Effluents. Report prepared for INAP and accessed from website www.inap.com.au/completed_research_projects.htm. on 25 February 2006.

Mehling Environmental Management Inc., 1998. Blending and Layering of Waste Rock to Delay, Mitigate or Prevent Acid Rock Drainage and Metal Leaching: A Case Study Review. MEND Project 2.37.1. (Natural Resources Canada: Ottawa).

Miller, S.D., Andrina, J and Richards, D, 2003a. Overburden Geochemistry and Acid Rock Drainage Scale-Up Investigations at the Grasberg Mine, Papua Province, Indonesia. In 'Proceedings of Sixth International

Conference on Acid Rock Drainage'. Cairns, Queensland. 12 – 18 July 2003. pp.111 - 121. (The Australasian Institute of Mining and Metallurgy: Melbourne).

Miller, S.D, Smart, R, Andrina, J, Neale, A and Richards, D, 2003b. Evaluation of Limestone Covers and Blends for Long-Term Acid Rock Drainage Control at the Grasberg Mine, Papua Province, Indonesia. In 'Proceedings of Sixth International Conference on Acid Rock Drainage'. Cairns, Queensland. 12 – 18 July 2003. pp.133 - 141. (The Australasian Institute of Mining and Metallurgy: Melbourne).

Mitchell, P. 2000. Prediction, Prevention, Control and Treatment of Acid Rock Drainage, Environmental policy in mining: corporate strategy and planning for closure. pp.117-143.

Morin, K.A., Gerencher, E., Jones, C.E. and Konasewich, D.E. 1991. Critical Literature Review of Acid Drainage from Waste Rock. MEND Project 1.11.1. (Natural Resources Canada: Ottawa).

Morin, K.A. and Hutt, N.M. 1997. Environmental Geochemistry of Minesite Drainage – Practical Theory and Case Studies. (MDAG Publishing: Vancouver).

Morin, K.A. 2003. Problems with Acid Rock Drainage Predictions at the Ekati Diamond Mine, Northwest Territories, Canada. In 'Proceedings of Sixth International Conference on Acid Rock Drainage'. Cairns, Queensland. 12 – 18 July 2003. pp.663 - 669. (The Australasian Institute of Mining and Metallurgy: Melbourne).

Munchenberg, S., 1998. Acid Test, Groundwork 1(2). pp.3.

O'Kane, M and Wels, C, 2003. Mine Waste Cover System Design – Linking Predicted Performance to Groundwater and Surface Impacts. In 'Proceedings of Sixth International Conference on Acid Rock Drainage'. Cairns, Queensland. 12 – 18 July 2003. pp.341 349. (The Australasian Institute of Mining and Metallurgy: Melbourne).

Olson, G., Clark, T and Mudder, T. 2006. "Acid Response" International Mining Volume 2 Number 3 (2006) pp.34-36.

Parker, G. and Robertson, A. 1999. Acid Drainage - A Critical Review of Acid Generation from Sulfide Oxidation: Processes, Treatment and Control. (Australian Minerals & Energy Environment Foundation: Melbourne).

Payant, S.C. and Yanful, E.K. 1995. Evaluation of Techniques for Preventing Acidic Rock Drainage. MEND Report 2.35.2b. (Natural Resources Canada: Ottawa).

Porterfield, D.C., Miller, S, and Waters, P. 2003. A Strategy for Managing Acid Rock Drainage in Arid Climates – The Mt Whaleback Story. In 'Proceedings of Sixth International Conference on Acid Rock Drainage'. Cairns, Queensland. 12 – 18 July 2003. pp.143 - 146. (The Australasian Institute of Mining and Metallurgy: Melbourne).

Ritchie, A.I.M., 1995. Application of Oxidation Rates in Rehabilitation Design. In `Proceedings of the Second Australian Acid Mine Drainage Workshop', Charters Towers, Queensland. 28-31 March 1995. (Eds. N.J.

Grundon and L.C. Bell.) pp.101-116. (Australian Centre for Minesite Rehabilitation Research: Brisbane, Australia).

Queensland Environmental Protection Agency, 1999, Water Quality Sampling Manual, 3rd edition, Queensland Environmental Protection Agency.

Scharer, J.M., Kwong, E.C.M., Nicholson, R.V., Pettit, C.M., Chambers, D.W., 1995, Factors Affecting ARD Production: Kinetics of Sulfide Oxidation. Sudbury 1995; Mining and the Environment. pp.451-458.

Sherlock, E.J., 1995. M.Sc Thesis: Evaluation of Static and Kinetic Prediction Test Data and Comparison with Field Monitoring Data. MEND Project 1.16.4. (Natural Resources Canada: Ottawa).

Simón, M., Martín, F., García, I., Bouza, B., Dorronsoro, C., Aguilar. J (2004) "Interaction of limestone grains and acidic solutions from the oxidation of pyritic tailings" Environmental Pollution 135 (2005) 65-72.

StatSoft, 2004, Statistica 7.0 Release 7, "Statistic Electronic Manual," Tulsa, U.S.A.

Steffen, Robertson and Kirsten (B.C.) Inc., in association with Norecol Environmental Consultants and Gormley Process Engineering. 1989. Draft Acid Rock Drainage Technical Guide, vols. 1 and 2. ISBN 0-7718-8893-7. Prepared for the British Columbia Acid Mine Drainage Task Force. BiTech Publishers, Richmond, British Columbia, Canada.

Stumm, W and Morgan, J.J. 1996. Aquatic Chemistry, Third Edition. (John Wiley and Sons Inc: New York).

Taylor, G. 1998. Acid Drainage: Sources, Impacts and Responses. Groundwork 1 (2). pp.4-5.

Whitten, D.G.A., Brooks, J.R.V., 1987, Dictionary of Geology. (Penguin Books: Great Britain).

ZCML, 2001. Image provided by ZCML External Affairs Department.

Zhu, C., Anderson, G, 2002, Environmental Applications of Geochemical Modelling. (Cambridge University Press: United Kingdom).

9 Appendices

Appendix 1	Sizing and Assaying Siltstone and Limestone Samples (AMDEL, 2003)
Appendix 2	Geochemical Characteristics of 100% Limestone, 100% Siltstone and Blended Samples (EGi, 2004)
Appendix 3	Results of Cyclic Voltammetry Static Testwork
Appendix 4	Column Leach Test and Heap Leach Pad Analytical Results (refer to electronic file on attached cd)
Appendix 5	Column Leach Test Water, Sulfate and Neutralising Potential Balances (refer to electronic file on attached cd)
Appendix 6	Column Leach Test Dissolved Metal Statistical Data
Appendix 7	Heap Leach Pad Water, Sulfate and Neutralising Potential Balances (refer to electronic file on attached cd)
Appendix 8	Heap Leach Pad Dissolved Metal Statistical Data
Appendix 9	Background to Geochemical Modelling Principles

DATA APPENDICES 1-8 HAVE BEEN REMOVED

Appendix 9

Background to Geochemical Modelling Principles

1. Introduction

The following background to geochemical modelling principles is taken from Zhu and Anderson (2002).

A model is an abstract object, described by a set of mathematical expressions (including data of various kinds) that are thought to represent natural processes in a particular system. Geochemical modelling programs are built, for the most part, on the fundamental laws of thermodynamics and kinetics. The "output data", or results of the model calculations, are generally quantities that are at least partially observable or experimentally verifiable. In this sense the model is capable of prediction.

A geochemical model has to be provided in the context of one part of many processes. At the minimum, for geochemical modelling to be useful, chemical reactions have to be evaluated on a real time scale and spatial coordinates. Chemical reactions therefore have to be linked to transport processes.

2. Thermodynamic Background

2.1 Systems and Equilibrium

2.1.1 Real and Model Systems

The aim of performing geochemical modelling is to understand processes in the natural system and predict the future state of the system. These real or natural systems are almost always changing, slowly or rapidly: fluids are flowing, and chemical reactions are occurring between fluids, rocks and soils.

When thermodynamic calculations are performed in order to better understand a natural geological system, strictly speaking the calculations refer not to this real system, but to a thermodynamic model of the real system. Naturally, the intention is for the thermodynamic model to mimic or represent the real system closely, because otherwise the results of the model will be useless. Nevertheless, even if the thermodynamic system is as good as possible, there are two important differences:

- The model or thermodynamic system will virtually always be incomplete and inaccurate to some degree. The reasons for this have largely to do with the choice and quality of the data used by the model, and
- Models based on thermodynamics virtually always refer to a state or states of complete equilibrium. How can these models be useful in understanding real systems, which are constantly changing?

2.1.2 Equilibrium

A system is said to be in equilibrium if none of its properties change with time (obviously eliminating virtually all environmental systems at one stroke). This definition includes *metastable equilibrium* states, which are not at their lowest possible energy levels, but are *constrained* from changing to a lower energy level; and *stable equilibrium* states, which have the lowest energy level available, and cannot change to any lower energy state. Thus, diamond is a metastable form of carbon under ordinary conditions, and graphite is the stable form.

Thermodynamics allows the calculation of energy differences between different equilibrium states, stable and metastable, for all kinds of substances. If natural systems are not in equilibrium, how can it be useful?

Local Equilibrium

Even though a natural system may not be at equilibrium overall, there may well be small parts of the system which *are* at or not very far from equilibrium. The system is then said to have areas of *local equilibrium*, and thermodynamics can be applied to these smaller parts. For example, a solution flowing through limestone may be in the process of dissolving calcite – the system is not at equilibrium. However, the calcium carbonate and other ions in the solution may well be at or not far from equilibrium among themselves. In other words, a portion of the solution, if removed from contact with the limestone, would not change – it is in a state of local equilibrium, and thermodynamics can be used to show that the solution is in fact under saturated with calcite and will dissolve calcite if in contact with it.

Because thermodynamics only applies to equilibrium states, geochemical models only apply to areas of local equilibrium. Only natural systems that have areas of local equilibrium can therefore be successfully modelled. It is in fact very difficult to determine whether natural systems do have such areas of local equilibrium, and on what scale.

2.1.3 The Role of Kinetics

Because thermodynamics deals only with equilibrium states, it can be used to show, for example, that calcite should dissolve in a certain solution, or that it should precipitate from another solution, however it cannot state *how fast* such a process will occur, or indeed if they will occur at all (metastable supersaturated solutions are well known, after all). This is a significant limitation. Many important processes may be *rate-limited* by one or more slow reactions.

2.2 Chemical Reactions

Geochemical modelling focuses on the determination of what chemical reactions are important, and determining whether that reaction is proceeding to the right, or to the left, or is at equilibrium. For example, if the modeller wishes to determine whether a particular mineral is dissolving or precipitating, they write:

solid mineral ⇆ dissolved mineral **[1]**

If this reaction proceeds to the right, the mineral is dissolving. If it proceeds to the left, the mineral is precipitating. In most cases, the dissolved form of the mineral is ionised. Using calcite as an example:

$$CaCO_{3(s)} \rightarrow Ca^{2+} + CO_3^{2-} \qquad \textbf{[2]}$$

In order to establish which way the reaction will proceed under chosen conditions, the energy per mole of each product and reactant is determined. If the products have more energy than the reactants, the reaction proceeds to the left, and vice versa. However, a special kind of energy, Gibbs Energy, is required.

2.3 Gibbs Energy

It can be shown that, because reactions are considered at a given temperature (*T*) and pressure (*P*), the appropriate energy is Gibbs energy, *G*. So for [2], if

$$G_{Ca^{2+}} + G_{CO_3^{2-}} > G_{CaCO3(s)} \qquad \textbf{[3]}$$

calcite will precipitate, and vice versa. Because the magnitudes of $G_{Ca^{2+}}$ and $G_{CO_3^{2-}}$ depend on concentration, precipitation lowers both quantities, and will proceed until

$$G_{Ca^{2+}} + G_{CO_3^{2-}} = G_{CaCO3(s)} \qquad \textbf{[4]}$$

at which point the reaction will be balanced, or at *equilibrium*.

Unfortunately, it is not possible to measure values of *G* of any substance. Only *differences* in *G* are measurable. Therefore, for a substance of interest, solid, liquid gas, or solute, the quantity $\Delta_f G°$, the difference between G of a compound substance, and the sum of the G values of its constituent elements, is measured usually by calorimetric methods, which is, each in its most stable state. For example, for calcite,

$$\Delta_f G° = G°_{CaCO_{3(s)}} - G°_{Ca} - G°_{C} - 1.5G°_{O_{2(g)}} \qquad \textbf{[5]}$$

This quantity is tabulated in databases for solids, liquids, gases, and solutes. As this quantity varies with temperature and pressure, and for solutes with concentrate as well, it must be tabulated for one specific set of conditions, call the *standard state* of the substance, which is noted by the superscript °. It is measured in joules per mole (J mol^{-1}) or calories per mole (cal mol^{-1}), where 1 cal = 4.184 J.

2.4 Activity

Activity is the difference between G^o of each product and reactant in its standard state, and G of each in the real state we are interested in. Thus, for any substance (solid, liquid, gas, solute, or ion) i, we define the activity a such that:

$$G_i - G^\circ{}_i = RT \ln a_i \quad \textbf{[6]}$$

where G is the Gibbs energy per mol of i in the system, $G^o{}_i$ is the Gibbs energy per mole of i in the standard state, and R is the *gas constant* (8.31451 J K^{-1} mol^{-1}, or 1.98722 cal K^{-1} mol^{-1}).

Standard states have been chosen such that if the system behaves ideally (i.e. obeys some simple rules such as ideal gas flow for gases and Henry's law and Raoult's law for solutes), the activity takes on very simple forms, and, if the system is not ideal, a 'fudge factor' called the *activity coefficient* can be introduced to convert the very simple form into the true activity.

For example, for aqueous solutions:

$$a_i = m_i \gamma_{H_i} \quad \textbf{[7]}$$

where a_i is the activity of any substance i and m_i is its molality. The 'fudge factor' γ_{H_i} are measures of the deviation from the ideal behaviour of substance i.

The activity of pure solids and liquids will be 1.0 (the mole fraction of a pure compound being 1.0); the activity of a solid solution component is its mol fraction; the activity of a gas is (numerically equal to) its partial pressure, and the activity of a aqueous solute is (numerically equal to) its molality. These are useful approximations for real systems, which can be improved by using the activity coefficients. Note that activities are always dimensionless.

2.5 Activity Coefficients

2.5.1 The Debye-Hückel Equation

Activity coefficients γ_H for ions can be calculated for relatively low concentrations by variations of the Debye-Hückel equation. The 'extended' Debye-Hückel equation is:

$$\log \gamma_{H\,i} = -Az_i^2 \frac{\sqrt{I}}{1 + B\text{å}\sqrt{\mathrm{I}}} \quad \textbf{[8]}$$

where A and B are temperature-dependent constants and å is an adjustable parameter corresponding to the size of the ion. The ionic strength I is defined as:

$$I = \frac{1}{2}\sum_i m_i z_i^2 \quad \textbf{[9]}$$

where m_i is the molality of ionic species *I*, and z_i is its charge.

To calculate the activity coefficients of ions, virtually all geochemical modelling programs use either a variation of the Debye-Hückel equation or the Pitzer equation. Two variations of the Debye-Hückel equation in common use are the Davies equation and the B-dot equation.

2.6 Chemical Potential

Equation [6] will often be seen in another form:

$$\mu_i - \mu^\circ{}_i = RT \ln a_i \qquad \textbf{[10]}$$

where μ_i is substituted for G_i and is the *chemical potential* of *i*. μ_i is also the Gibbs energy per mole of *i*, but its definition takes care of the fact that the magnitude of G_i varies with the concentration of *i* if *i* is a solute.

For the generalised chemical equation

$$aA + bB = cC + dD \quad \textbf{[11]}$$

to be at equilibrium, it is necessary that

$$\begin{aligned} \Delta_r G &= \Delta_r \mu \\ &= (c\mu_C + d\mu_D) - (a\mu_A + b\mu_B) \qquad \textbf{[12]} \\ &\quad \text{(products)} \qquad \text{(reactants)} \\ &= 0 \end{aligned}$$

2.7 The Equilibrium Constant

The equilibrium constant expresses the point of minimum free energy for a chemical reaction (Benthke, 1996).

Because for each reactant and product in (11) there is a relation, from (10), such that

$$\mu_i - \mu^\circ{}_i = RT \ln a_i$$

It follows from [10] that:

$$\begin{aligned} \Delta_r \mu - \Delta_r \mu^o &= \Delta_r G - \Delta_r G^o \\ &= RT \ln \frac{a_C^c a_D^d}{a_A^c a_B^d} \qquad \textbf{[13]} \\ &= RT \ln Q \end{aligned}$$

Evidently *RT* ln *Q* is a term which measures the difference between $\Delta_r G^o$, the *tabulated* or standard state Gibbs energy reaction, and $\Delta_r G$, the *real* Gibbs energy of reaction. When the activities are such that the real difference is zero $(\Delta_r G = 0)$, the reaction is at equilibrium, and *Q* is called *K*. In this case

$$\Delta G^\circ = -RT \ln K \qquad \textbf{[14]}$$

where *K* is the equilibrium constant. Equation [14] is a remarkably powerful relationship. It says that for any reaction tabulated data for substances in their arbitrary reference or standard states can be used to calculate the equilibrium relationship between product and reactant activities (concentrations) in real systems.

2.7.1 Solubility Product and Saturation Index

Equilibrium constants for various kinds of reactions have been given various names. Reactions such as [2], with a solid phase on one side and its constituent ions on the other, is called a *solubility product reaction*, and the equilibrium constant for the reaction is called the *solubility product*, K_{sp}. In this case, we have found that the K_{sp} (2) = $10^{-9.971}$.

Note that Q and K are identical in form. The difference is that the activity terms in Q are not equilibrium activities, while those in K are. Similarly, if calcite is present, $a_{CaCO_{3(s)}} = 1$ and K = K_{sp}. If Q = K_{sp}, $\Delta_r \mu$ = 0, and calcite is at equilibrium with its aqueous ions. When IAP< K_{sp}, $\Delta_r \mu$ < 0 and calcite will dissolve. The quantity $(a_{Ca^{2+}}.a_{CO_3^{2-}})$ in a real solution is called, the *Ion Activity Product (IAP)* for calcite, and similarly for any other solubility product reaction. The IAP is commonly used in geochemical modelling to predict the stability of mineral phases. The IAP/ K_{sp} ratio is called Ω, and the logarithm of the ratio is called the *Saturation Index (SI)*, so that when SI > 0 the mineral precipitates, and when SI < 0 the mineral dissolves (Table A10-1).

Table A10-1: Relationship between IAP, K_{sp}, and SI.

IAP, K_{sp}	Ω (IAP/K_{sp})	SI (=logIAP/Ksp)	Result
IAP < K_{sp}	< 1	Negative	mineral dissolves
IAP > K_{sp}	> 1	Positive	mineral precipitates
IAP = K_{sp}	1	0	equilibrium